Carbon Metabolism and Desiccation Tolerance in the Nitrogen-Fixing Rhizobia *Bradyrhizobium japonicum* and *Sinorhizobium meliloti*

by

Maria Anne Trainer

A thesis
presented to the University of Waterloo
in fulfillment of the
thesis requirement for the degree of
Doctor of Philosophy
in
Biology

Waterloo, Ontario, Canada, 2009

I hereby declare that I am the sole author of this thesis. This is a true copy of the thesis, including any required final revisions, as accepted by my examiners. I understand that my thesis may be made electronically available to the public.

Abstract

Most members of the *Rhizobiaceae* possess single copies of the poly-3-hydroxybutyrate biosynthesis genes, *phbA, phbB* and *phbC*. Analysis of the genome sequence of *Bradyrhizobium japonicum* reveals the presence of five homologues of the PHB synthase gene *phbC* as well as two homologues of the biosynthesis operon, *phbAB*. The presence of multiple, seemingly redundant homologues may suggest a functional importance. Each *B. japonicum phbC* gene was cloned and used to complement the pleiotropic phenotype of a *Sinorhizobium meliloti phbC* mutant; this mutant is unable to synthesize PHB, grow on certain PHB cycle intermediates and forms non-mucoid colonies on yeast mannitol medium. Two of the five putative *B. japonicum phbC* genes were found to complement the *S. meliloti phbC* mutant phenotype on D-3-hydroxybutyrate although none of them could fully complement the phenotype on acetoacetate. Both complementing genes were also able to restore PHB accumulation and formation of mucoid colonies on yeast mannitol agar to *phbC* mutants. In-frame deletions were constructed in three of the five *phbC* open reading frames in *B. japonicum*, as well as in both *phbAB* operons, by allelic replacement. One of the *phbC* mutants was unable to synthesize PHB under free-living conditions; one of the two *phbAB* operons was shown to be necessary and sufficient for PHB production under free-living conditions. These mutants also demonstrated an exopolysaccharide phenotype that was comparable to *S meliloti* PHB synthesis mutants. These strains were non-mucoid when grown under PHB-inducing conditions and, in contrast to wild-type *B. japonicum*, formed a compact pellet upon centrifugation. Interestingly, none of the mutants exhibited carbon-utilization phenotypes similar to those exhibited by *S. meliloti* PHB mutants. Wild-type *B. japonicum* accumulates PHB during symbiosis, and plants inoculated with the *phbC* mutants demonstrate a reproducible reduction in shoot dry mass. Analysis of bacteroid PHB accumulation in the mutant strains suggests that the *phbAB* operons of *B.*

japonicum are differently regulated relative to growth under free-living conditions; mutants of the second *phbAB* operon demonstrated a significant reduction in PHB accumulation during symbiosis. These data suggest that the first *phbAB* operon is required for PHB synthesis only under free-living conditions, but is able to partially substitute for the second operon during symbiosis. Deletion of both *phbAB* operons completely abolished PHB synthesis in bacteroids. Analysis of the upstream regions of these genes suggest the existence of putative RpoN binding sites, perhaps indicating a potential mode of regulation and highlighting the metabolic complexity that is characteristic of the *Rhizobiaceae*.

PHB metabolism in *S. meliloti* has been studied in considerable detail with two notable exceptions. No reports of the construction of either a β-ketothiolase (*phbA*) or a PHB depolymerase (*phaZ*) mutant have ever been documented. The *phaZ* gene, encoding the first enzyme of the catabolic half of the PHB cycle in *S. meliloti*, was identified and a *phaZ* mutant strain was generated by insertion mutagenesis. The *phaZ* mutant demonstrates a Fix^+ symbiotic phenotype and, unlike other PHB cycle mutants, does not demonstrate reduced rhizosphere competitiveness. Bacteroids of this strain were shown to accumulate PHB, demonstrating for the first time that *S. meliloti* is able to synthesize and accumulate PHB during symbiosis. Interestingly, there is no significant difference in shoot dry mass of plants inoculated with the *phaZ* mutant, suggesting that PHB accumulation does not occur at the expense of nitrogen fixation. The *phaZ* mutant strain was also used to demonstrate roles for PhaZ in the control of PHB accumulation and exopolysaccharide production. When grown on high-carbon media, this mutant demonstrates a mucoid phenotype characteristic of exopolysaccharide production. Subsequent analyses of a *phoA::exoF* fusion confirmed elevated transcription levels in the *phaZ* mutant background. In contrast, mutants of the PHB biosynthesis gene, *phbC*, have a characteristically dry phenotype and demonstrate reduced *exoF*

transcriptional activity. The *phaZ* mutant also demonstrates a significant increase in PHB accumulation relative to the wild-type strain. Previous work on phasin mutants in *S. meliloti* demonstrated that they lack the ability to synthesize PHB. Transduction of the *phaZ* lesion into the phasin mutant background was used to construct a *phaZ*-phasin mutant strain. Analysis of the PHB biosynthesis capacity of this strain showed that the lack of PHB synthesis exhibited by *S. meliloti* phasin mutants is due to loss of PHB biosynthesis activity and not due to an inherent instability in the PHB granules themselves.

A recent study suggested that some bacteria may possess an alternate pathway for acetate assimilation that would bypass the need for the glyoxylate cycle in organisms that do not possess the enzyme, isocitrate lyase. In these organisms, acetate is assimilated through the ethylmalonyl-CoA pathway, which has significant overlap with the anabolic half of the PHB cycle, including reliance on the PHB intermediate 3-hydroxybutyryl-CoA. The observation that *phbB* and *phbC* mutants of *S. meliloti* are unable to grow well on acetoacetate – coupled with previously unexplained data that show a class of mutants (designated *bhbA-D*) are able to grow on acetate, but not on hydroxybutyrate or acetoacetate – made it tempting to speculate that an ethylmalonyl-CoA-like pathway might be present in *S. meliloti*, and that this pathway mightoverlap with the PHB cycle at the point of 3-hydroxybutyryl-CoA. An in-frame mutation of *phbA* was constructed by crossover PCR and allelic replacement. This mutant exhibited a complete abolition of growth on acetoacetate, suggesting that PhbA represents the only exit point for carbon from the PHB cycle and that an alternative ethylmalonyl-CoA-like pathway is not present in this organism.

During symbiosis, rhizobial cells are dependent on the provision of carbon from the host plant in order to fuel cellular metabolism. This carbon is transported into the bacteroids via the dicarboxylate transport protein, DctA. Most rhizobia pos-

sess single copies of the transporter gene *dctA* and its corresponding two-component regulatory system *dctBD*. The completed genome sequence of *B. japonicum* suggests that it possesses seven copies of *dctA*. Complementation of *Sinorhizobium meliloti dct* mutants using the cosmid bank of *B. japonicum* USDA110 led to the identification a *dctA* locus and a *dctBD* operon. Interestingly, the *B. japonicum dctABD* system carried on the complementing cosmid was not able to complement the symbiotic deficiency of *S. meliloti* strains carrying individual mutations in either *dctA, dctB*, or *dctD*suggesting that the *B. japonicum dctBD* is unable to recognize either DctB/DctD or the DctB/DctD-independent regulatory elements in *S. meliloti*. All seven *B. japonicum dctA* ORFs were cloned and an analysis of their capacity to complement the free-living phenotype of a *S. meliloti dctA* mutant demonstrated that they all possess some capacity for dicarboxylate transport. Mutants of all seven *B. japonicum dctA* ORFs were constructed and an analysis of their free-living phenotypes suggested that significant functional redundancy exists in *B. japonicum* DctA function. Given the large number of potential *dctA* genes in the genome, coupled with an apparent lack of *dctBD* regulators, it is tempting to speculate that different DctA isoforms may be used during free-living and symbiotic growth and may be subject to different regulatory mechanisms than those of better-studied systems.

A comprehensive analysis of desiccation tolerance and ion sensitivity in *S. meliloti* was conducted. The results of these analyses suggest that genetic elements on both pSymA and pSymB may play a significant role in enhancing cell survival under conditions of osmotic stress. The *S. meliloti* $expR^{+}$ strains SmUW3 and SmUW6 were both shown to exhibit considerably higher desiccation tolerance than Rm1021, suggesting a role for enhanced exopolysaccharide production in facilitating survival under adverse conditions. Furthermore, scanning electron microscopy of inoculated seeds suggests that *S. meliloti* cells initiate biofilm formation upon

application to the surface of seeds. This finding has implications for the analysis of OSS and the development of desiccation assays and may explain some of the variability that is characteristic of desiccation studies.

Acknowledgements

I would like to acknowledge my supervisor, Dr. Trevor Charles. He not only provided me with the freedom to pursue the work described in this thesis, he also allowed me the time to pursue extra curricular activities. His trust in my ability to balance my PhD work with my engagement in student politics was a defining component in my professional development as a graduate student. I would like to thank all of the friends and colleagues with whom I worked at the Graduate Student Association of the University of Waterloo, especially Marek Ratajczak, Craig Sloss, Ian MacKinnon and Rose Vogt. The opportunities that I had during my tenure as Vice President (Operations and Finance) were phenomenal and I remain indebted to the Association.

I would like to extend a special thank you to the researchers at Agribiotics who helped with the on-seed survival work described in this thesis. A special thanks is extended to Jennifer Petts, Sarah Curtis and Ricardo Nordeste whose help, friendship and humour made the endless hours of on-seed survival assays bearable; I am forever indebted to Jennifer for the hours of titering she performed on my behalf. I would also like to thank Dr. Michael Kahn for agreeing to share the protocol for desiccation tolerance prior to its publication. This assay made the high-throughput analysis of *Sinorhizobium meliloti* ion sensitivities doable in a practical sense, and I remain grateful for his generosity.

In the Charles lab I would like to thank Dr. Scott Clark for teaching me everything I now know about bacterial genetics and Ricardo Nordeste for his friendship and support, especially during these past 12 months. I was also fortunate to have the assistance of some very talented undergraduate students. Kathy Lam made a significant contribution to the PhaZ, PhbA, and DctA work; Rebecca Zhou helped considerably with the early development of on-seed survival assays; and Danielle

Nash helped to get the *Bradyrhizobium japonicum dctA* clonings started. I'd also like to acknowledge Andre Masella, whose presence in the lab always made the bad days less miserable and the good ones more fun!

My parents sacrificed a great deal to give me and my sister opportunities that they could have only dreamed of. I am grateful for their encouragement and support over the years. Finally, there are a number of individuals whom I have known for only a short period of time but whose support during the final stages of this work has been significant. More than most, Chris has had to endure and tolerate a very cranky version of me over the past four months; I am most grateful for his unwavering patience, and unfailing encouragement. I also owe Chris a debt of gratitude for his assistance in constructing figures in Adobe Illustrator. Furthermore, my co-workers at the Council of Canadian Academies have been a continual source of support, humour, and perspective and I am grateful to them for their friendship, assistance and their nagging!

Financial support was provided by the Natural Sciences and Engineering Research Council of Canada, Agribiotics and EMD Crop BioSciences Inc. and is most gratefully acknowledged.

Claims of Contributions to Knowledge

- This is the first study to investigate PHB synthesis in *Bradyrhizobim japonicum*. This study reports the cloning of all five *phbC* ORF from *B. japonicum* and shows that only two of the five are capable of functionally complementing the pleiotropic phenotype of the *S. meliloti phbC* phenotype.

- Mutants in three of the five *phbC* ORFs in *B. japonicum* were constructed. All of the *B. japonicum phbC* mutants retain their capacity to synthesize PHB under free-living conditions, and none of them display similar carbon utilization phenotypes to those seen in the *S. meliloti phbC* mutant.

- Mutants of both *B. japonicum phbAB* operons were constructed and their characterization is documented herein. This study shows that *phbAB* expression in *B. japonicum* appears to be differentially regulated between free-living and symbiotic growth. This study also demonstrates a link between PHB synthesis and EPS secretion in *B. japonicum* and shows that PHB synthesis mutants of *B. japonicum* are impaired in their rhizosphere competitiveness, in a manner reminiscent of PHB synthesis mutants in *S. meliloti*.

- In order to facilitate the study of *B. japonicum* USDA110, an antibiotic-resistance and carbon utilization profile was developed.

- When tested using industry-standard methods, the *S. meliloti* pSymA mutant SmA818 is impaired in on-seed survival, suggesting a potential role for pSymA in facilitating survival under adverse conditions.

- The ability to synthesize PHB increases the survival of *S. meliloti* on-seed, implying a potential role for PHB in the long-term survival of cells under adverse storage conditions. Conversely, during the initial two weeks of desiccation,

strains that cannot synthesize PHB demonstrate higher levels of desiccation tolerance than those that can.

- The addition of trehalose to the growth medium of *S. meliloti* cells prior to inoculation on-seed improves their survival during the initial 2-4 weeks post-inoculation; the effect over longer-term storage appears to be negligible.

- *S. meliloti* cells appear to initiate biofilm formation upon application to the surface of seeds. This finding has implications for the analysis of OSS and the development of desiccation assays.

- The *S. meliloti expR*$^+$ strains SmUW3 and SmUW6 both exhibit considerably higher desiccation tolerance than Rm1021, suggesting a role for enhanced exopolysaccharide production in facilitating survival under adverse conditions.

- The *S. meliloti* mutant RmF728, which carries a large deletion in pSymB, has extremely poor desiccation tolerance relative to all other strains tested, including RmF726 which carries an overlapping deletion.

- A number of *S. meliloti* pSymB mutants exhibit significant ion sensitivities, including RmF728, RmG506, RmF514, and RmG471. Mutants possessing multiple deletions typically demonstrated the most severe ion sensitivities.

- An ion sensitivity phenotype was identified for several short-chain dehydrogenase/reductase mutants including Sma0326, SMc01698, SMb20871, and SMc00553. This is the first study to identify a phenotype that can be attributed to the particular SDR mutations in three of these strains.

- A tentative link between salt-sensitivity and poor desiccation tolerance in *S. meliloti* was identified.

- A region of the *B. japonicum* genome possessing functional copies of *dctA, dctB*, and *dctD* was identified by heterologous complementation of an *S. meliloti dctABD* mutant. The complementing cosmid was able to restore free-living growth of the *S. meliloti dctABD* mutant on succinate. The *dctABD* genes in question were identified as Blr3723, Blr3730 and Blr3731 respectively.

- The *B. japonicum dctABD* system carried on the complementing cosmid was not able to complement the symbiotic deficiency of *S. meliloti* strains carrying individual mutations in either *dctA, dctB*, or *dctD*; this suggests that the *B. japonicum dctBD* encoded by Blr3730/Blr3731 is unable to recognize either DctB/DctD or the DctB/DctD-independent regulatory elements in *S. meliloti*.

- All seven putative *B. japonicum dctA* open reading frames were cloned into the inducible expression vector pSW213. Three of the seven *dctA* ORFs demonstrated delayed but strong complementation (Blr4298, Bll1718, and Blr3723); partial complementation was seen from the other four ORFs.

- Mutants of all seven *B. japonicum dctA* open reading frames were constructed. All of these mutants demonstrated a wild-type capacity to grow on succinate as a sole carbon source, and all exhibited sensitivity to fluoroorotate. This suggests that all of the mutants still possess a functional dicarboxylate system, demonstrating redundancy in the *B. japonicum dctA* transport system.

- Analysis of the symbiotic capacity of one of the *B. japonicum dctA* mutants revealed no impairment; no significant difference in the shoot dry masses of plants inoculated with wild-type *B. japonicum* relative to those inoculated with the mutant strain was recorded.

- Construction and characterization of an *S. meliloti phaZ* mutant represented

the final step in the genetic characterization of the complete PHB cycle in *S. meliloti*.

- *phaZ* mutants of *S. meliloti* do not share the carbon-utilization deficiencies associated with other PHB cycle mutations.

- *phaZ* mutants of *S. meliloti* demonstrate a reduced capacity to survive long-term carbon starvation, highlighting the significance of PHB as a carbon source during prolonged periods of nutrient deprivation.

- *phaZ* mutants of *S. meliloti* demonstrate significant increases in PHB accumulation, relative to wild-type, under free-living conditions.

- *phaZ* mutants of *S. meliloti* exhibit a statistically significant increase in succinoglycan biosynthesis, relative to wild-type, when grown under free-living conditions.

- *phaZ* mutants of *S. meliloti* demonstrate that *S. meliloti* retains the capacity to synthesize and accumulate PHB during symbiosis. Interestingly, an analysis of shoot dry mass from plants inoculated with the *S. meliloti phaZ* mutant indicates that PHB accumulation does not occur at the expense of the *S. meliloti-M.sativa* symbiosis.

- Unlike other PHB cycle mutants, *phaZ* mutants of *S. meliloti* are not affected in their capacity to compete in the rhizosphere for nodulation.

- An in-frame *phbA* mutant of *S. meliloti* was constructed. This is the first report of the construction and characterization of a non-polar mutant *phbA* mutant in *S. meliloti*.

- *phbA* mutants of *S. meliloti* do not synthesize PHB under free-living conditions.

- *phbA* mutants of *S. meliloti* appear to be more mucoid than their wild-type counterparts. Interestingly, an analysis of their exopolysaccharide synthesis suggests that this increase in mucoidy does not translate into significantly higher secretions of EPS.

- The *S. meliloti phbA* mutant exhibits a complete abolition of growth on acetoacetate as a sole carbon source. This suggests that PhbA represents the only exit point for carbon from the PHB cycle and that an alternative ethylmalonyl-CoA-like pathway is not present in this organism.

- The *S. meliloti phbA* mutant demonstrates residual β-ketothiolase activity. Analysis of the *S. meliloti* genome sequence suggests the presence of a second β-ketothiolase.

- *S. meliloti* phasin mutants are unaffected in their capacity to establish effective nitrogen-fixing symbioses with the host plant *Medicago sativa*. This is in contrast to the pronounced reduction in symbiotic effectiveness reported for the same strain on *Medicago truncatula*.

- Construction of *phaZ*-phasin mutants shows that the lack of PHB synthesis exhibited by *S. meliloti* phasin mutants is due to loss of PHB biosynthesis activity and not due to inherent instability in the PHB granules themselves.

- *S. meliloti* Phasin-*phaZ* mutants exhibit a comparable reduction in rhizosphere competitiveness to *phbC* and *bdhA* mutants of *S. meliloti*.

- PHB cycle mutants were constructed in an $expR^+$ $nolR^+$ $pstC^+$ (SmUW3) background. An analysis of the rhizosphere competitiveness of these strains indicates that the presence of *expR* does not affect rhizosphere competitiveness; *phbC* and *bdhA* mutants remain impaired in their capacity to compete for nodulation in an $expR^+$ background.

- A comparison of SmUW24 ($expR^+$, $exoY^-$) and SmUW6 ($expR^+$, $exoY^+$) suggests that the synthesis of EPSII is not sufficient to restore nodulation competitiveness to the $exoY$ strain.

Dedication

To Helen MacPherson, who planted a seed and inspired a dream...

Contents

List of Tables

List of Figures

Glossary

- ΔG: Change in free energy of the system
- AA: Acetoacetate
- ADP: Adenosine diphosphate
- Anti-His: Antibodies raised against hexa-histidine sequence
- Ap: Ampicillin
- APS: Ammonium Persulfate
- ASA: Alternative symbiotic activation
- ATP: Adenosine triphosphate
- BNF: Biological nitrogen fixation
- bp: Base pair(s)
- BSA: Bovine serum albumin
- bu: bushel
- C_4: Molecule with a four-carbon backbone
- CDM: Cell dry mass
- CFU: Colony-forming unit
- Cm: Chloramphenicol
- Conc.: Concentration
- D3HB: D-3-hydroxybutyrate
- dH_2O: Deionized water
- DCA: Dicarboxylic acid
- DLHB: DL-3-hydroxybutyrate
- DMSO: Dimethyl sulfoxide
- DIG: Digoxygenin
- EDTA: Ethylenediaminetetraacetic acid
- EPS: Exopolysaccharide
- EtOH: Ethanol

- FOA: Fluoroorotic acid
- Gm: Gentamycin
- g: Gram
- ha: Hectare
- hr: Hour
- HCl: Hydrochloric acid
- HMW: High molecular weight
- kcal.mol^{-1}: Kilocalories per mole
- kDa: Kilodalton
- Km: Kanamycin
- l: Litre
- LB: Luria Bertani broth
- L3HB: L-3-hydroxybutyrate
- LMW: Low molecular weight
- M: Molar
- mA: Milliamp
- Mb: Mega base pair
- MCS: Multiple cloning site
- mg: Milligram
- min: Minute
- ml: Millilitre
- mM: Millimolar
- NaCl: Sodium chloride
- NaOH: Sodium hydroxide
- ng: Nanograms
- nl: Nanolitres
- nm: Nanometers

- Nm: Neomycin
- nM: Nanomolar
- Nmol: Nanomoles
- NPP: *p*-nitrophenyl phosphate
- ORF: Open reading frame
- OSS: On-seed survival
- PAGE: Polyacrylamide gel electrophoresis
- PBM: Peribacteroid membrane
- PBS: Phosphate-buffered saline
- PFU: Plaque-forming unit
- PVDF: Polyvinylidene difluoride
- r: Resistant to antibiotic
- RMM: Rhizobium minimal medium
- ROI: Return on investment
- ROS: Reactive oxygen species
- rpm: Revolutions per minute
- s: Sensitive to antibiotic
- SDM: Shoot dry mass
- SEM: Scanning electron microscopy
- SDR: Short chain dehydrogenase/reductase
- SDS: Sodium dodecyl sulphate
- Sm: Streptomycin
- Sp: Spectinomycin
- $T_{10}E_1$: 10 mM Tris, 1 mM EDTA buffer
- $T_{10}E_{25}$: 10 mM Tris, 25 mM EDTA buffer
- TAE: Tris acetate EDTA electrophoresis buffer
- TBE: Tris-borate EDTA electrophoresis buffer

- TCA: Tri-carboxylic acid cycle
- Tc: Tetracycline
- TE: Tris-HCl EDTA buffer
- TEMED: Tetramethylethylenediamine
- TEN: Tri-EDTA NaCl buffer
- Tg yr^{-1}: Teragrams per year (1 Million metric tons per year)
- TEM: Transmission electron microscopy
- Tp: Trimethoprim
- Tris: Tris buffer; Trisamine
- TY: Tryptone yeast extract medium
- U: Units
- v: Volts
- VMM: Vincent's minimal medium
- v/v: Volume per volume
- W: Watts
- wt: Wild-type
- w/v : Weight per volume
- YMA: Yeast mannitol agar
- YMB: Yeast mannitol broth
- μl: Microlitre
- μg: Microgram

Chapter 1

Introduction and Literature Review

1.1 Biological Nitrogen Fixation

Although dinitrogen constitutes approximately 80% of the atmosphere, in the molecular form it is biologically unavailable to higher organisms; this phenomenon is depicted graphically in the Nitrogen Cycle, as shown in Figure 1.1. As a result, nitrogen is typically the limiting nutrient in the growth of crop plants and thus plays a key role in establishing sustainable agricultural systems that are capable of maintaining a stable ecological environment [26, 369]. In the past, crop rotation with legumes was the main source of soil nitrogen utilized by farmers, capitalizing on biological nitrogen fixation (BNF) by the rhizobial symbionts of leguminous plants (Figure 1.3); however, as the demand for food has increased, modern agriculture has become increasingly dependent on the application of external nitrogen sources in order to maintain sufficient soil nitrogen to support high crop yields.

The population of the world is predicted to double, from 6.7 billion in 2008, to over 13.5 billion within the next sixty years [276]. In 2005, more than 3.7 billion people were considered to be malnourished [388] and the *per capita* availability of cereal grains has been declining since 1985 [364]. Continued expansion of the human

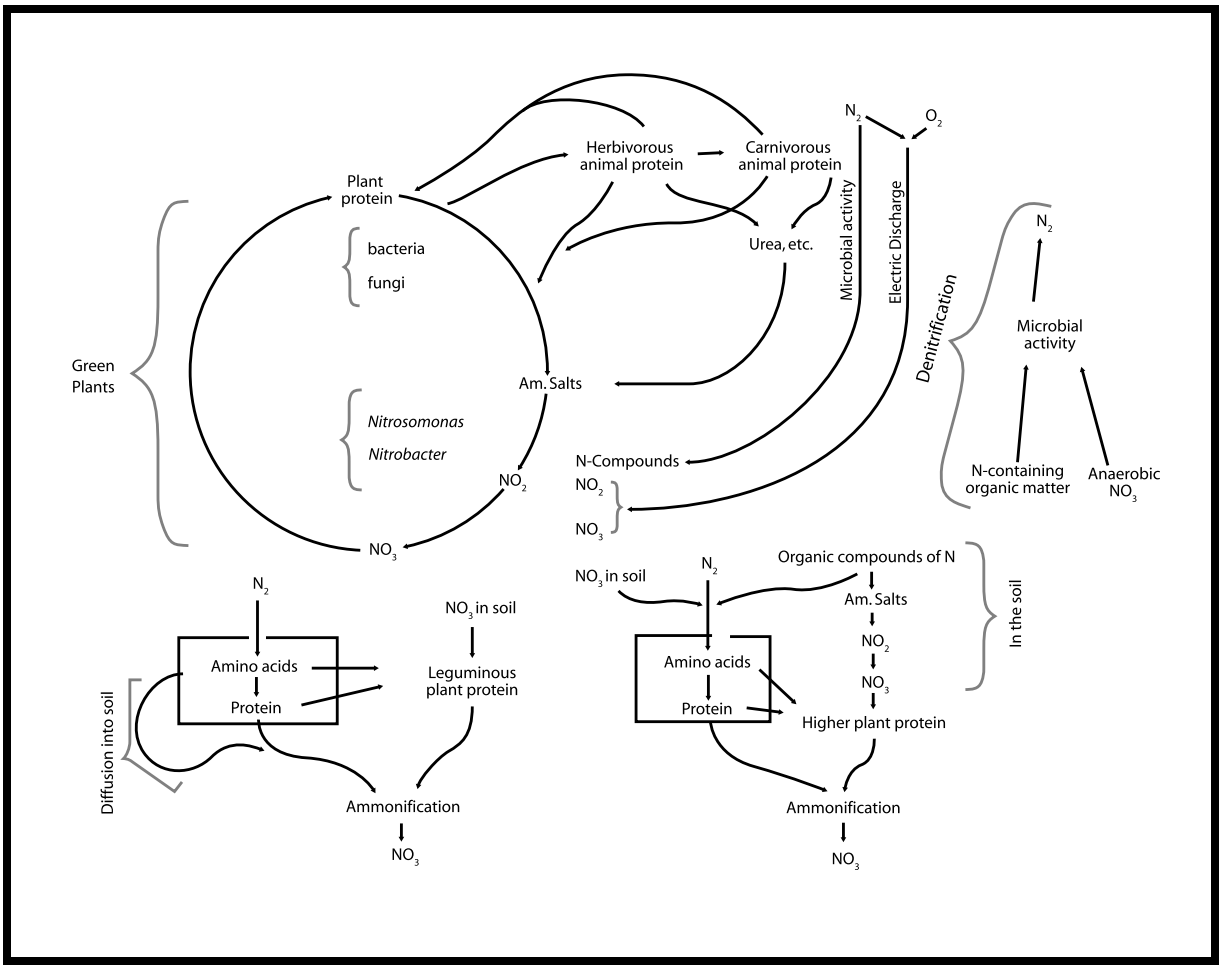

Figure 1.1: The nitrogen cycle. Modified from [284]

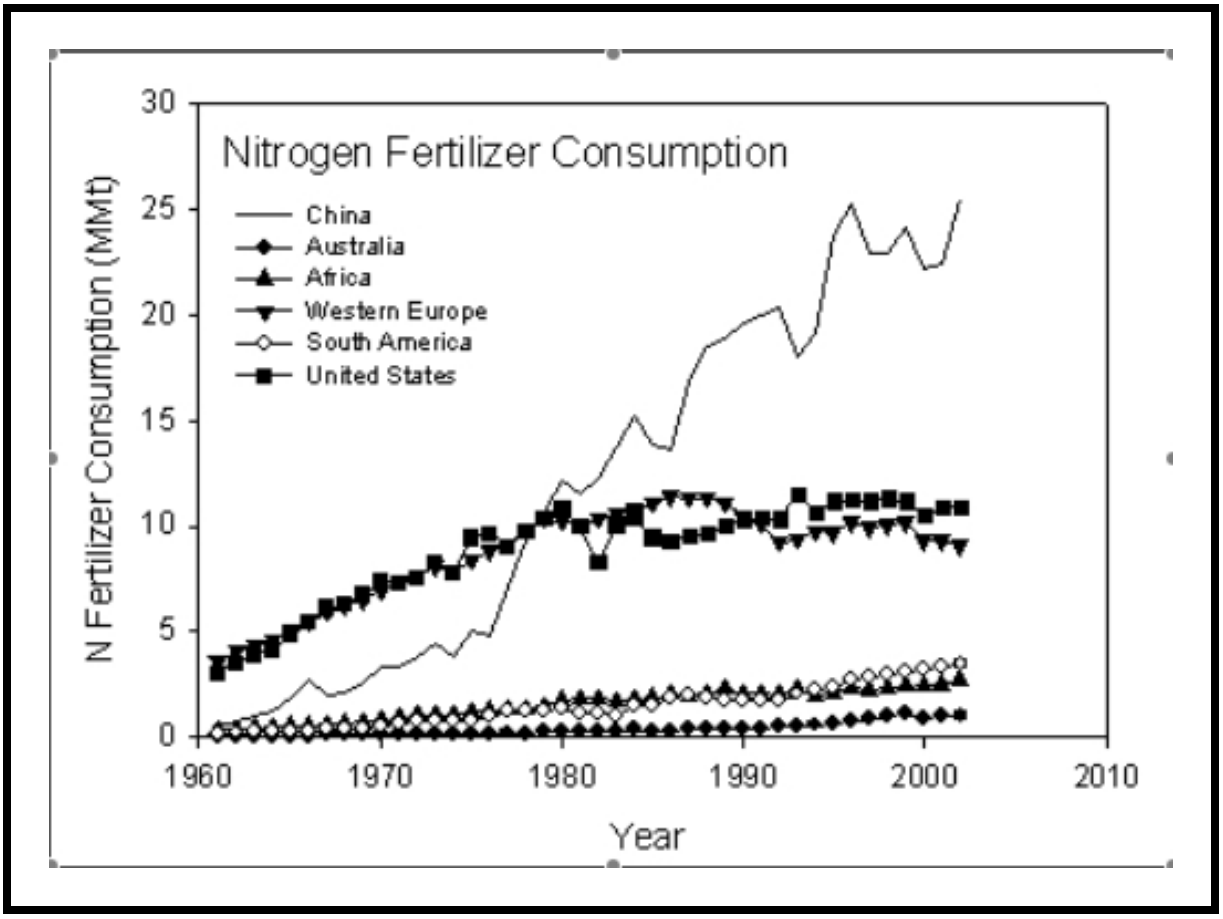

Figure 1.2: World consumption of nitrogen-based fertilizers from 1960-2002 [140]

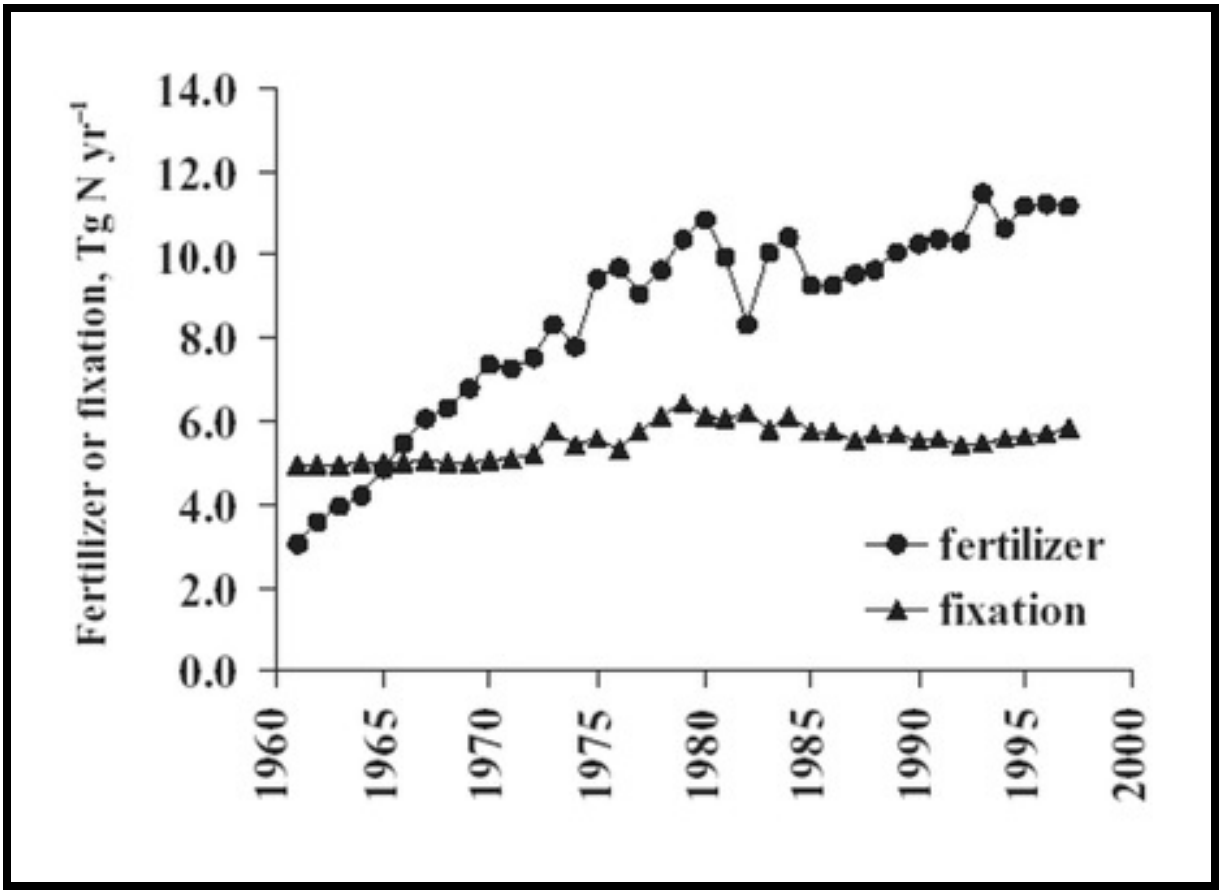

Figure 1.3: Nitrogen inputs in USA agriculture from 1961 to 1999 [105]

population will place increasing pressure on the diminishing resources necessary for food production. Increased food production necessitates the use of increased levels of fertilizers. Indeed, in 2007 world nitrogen fertilizer production exceeded 154 million tons [278]. In 2008, world nitrogen demand is expected to exceed 160 million tons per year [278], equalling the amount now produced biologically each year [105, 36]. To produce this amount of fertilizer necessitates the use of over 270 million tons of coal, or an equivalent non-renewable fossil fuel, which itself presents a major environmental risk [248], producing potent greenhouse gasses and compounds known to cause acid rain and smog [358]. BNF thus represents an environmentally responsible and safe alternative to the use of exogenously applied fertilizers. Indeed, legume crops in the US alone are responsible for the fixation of approximately 6 million tonnes of atmospheric nitrogen annually [155]. The economic value of this process exceeds $2.3 billion (US) assuming an average nitrogen fertilizer cost of $379 per tonne [363]. The use of exogenously supplied rhizobia as a means of decreasing reliance on industrially produced fertilizer has been the focus of major research efforts for several years. Rhizobia-based seed and soil inoculants are now sold world-wide, reducing the need for application of expensive fertilizer by facilitating optimal nodulation of legumes and, in turn, maximizing levels of N_2-fixation [33, 42, 67].

The use of legumes to improve soil nitrogen content has a long history, dating back to the time of the Romans; however, it was not until the advent of detailed N-balance studies that legumes were shown to accumulate N from sources other than simply soil and fertilizer. In 1886 it was shown that the ability of legumes to convert N_2 from the atmosphere into compounds that could be used by the plant was due to the presence of swellings or nodules on the legume root; more specifically it was due to the presence of particular bacteria within these nodules [144]. The first rhizobia were isolated from nodules in 1888; they were subsequntly were shown to possess the ability to reinfect their legume hosts and to fix N_2 in symbiosis [15].

1.2 The *Rhizobiaceae*

The rhizobia are the members of the Rhizobiales order of the α-proteobacteria that are capable of establishing symbiotic relationships with members of the *Leguminosae* family of flowering plants. These symbiotic relationships involve bidirectional signal exchange between the bacteria and plant partners, culminating in the formation of nitrogen-fixing root nodules. The rhizobia include the genera *Sinorhizobium, Rhizobium, Bradyrhizobium, Mesorhizobium* and *Azorhizobium*, and the range of host plants they are capable of infecting is estimated to exceed 16,000 species [126]. These include the agriculturally important plants alfalfa, pea and soybean, which yield over 300 million metric tons of crops per year, and account for over 13% of the worlds total cultivated land [109]. In symbiosis with legumes, the bacteria elicit formation of specialized, microaerophilic nodules on the roots of the host plant in which, following infection and colonization of the nodule, the bacteria undergo differentiation into a mature state known as a bacteroid, which can reduce atmospheric dinitrogen to ammonia. The bacteroids are enclosed in a plant-derived, peribacteroid membrane, through which all nutrients bound for the bacteroid must pass.

As shown in Figure 1.4, symbiosis is the result of an elaborate exchange of signals between the host and the symbiont. The rhizobia respond to the presence of plant-secreted flavonoids into the rhizosphere, the soil zone immediately surrounding the root system of the plant, by producing lipochitooligosaccharides known as Nod factors (reviewed in [69]) which in turn, activate a transduction pathway that ultimately leads to nodule formation [41]. Nod factors play a major role during early nodule development and are known to be responsible for, among other things, determining host-symbiont specificity as a result of host-specific recognition of substitutions on the lipochitooligosaccharide backbone [55]. A more extensive

discussion of the role of cell-surface factors in the symbiotic process is included in Section 1.4. During differentiation into the mature bacteroid state, the bacteria undergo significant biochemical and morphological changes in response to environmental stimuli within the nodule; these stimuli presumably include chemical signals, low oxygen concentration, pH changes, and other plant-determined conditions that are needed to facilitate the reduction of atmospheric dinitrogen to ammonia [201].

1.2.1 *Sinorhizobium meliloti*

S. meliloti is a gram negative α-proteobacterium. Primarily a soil-dwelling bacterium, *S. meliloti* can enter into effective symbioses with several genera of forage legumes including *Medicago, Melilotus and Trigonella*. The genome sequence of *S. meliloti*, completed in 2001 [104], contains three replicons: a 3.65-Mb chromosome and two megaplasmids, pSymA (1.35 Mb) and pSymB (1.68 Mb), all three of which contain genes required for symbiosis. The genome is estimated to encode 6204 proteins, approximately 60% of which have had functions ascribed on the basis of homology to proteins of known function. Furthermore, the ORFeome of *S. meliloti* was constructed in 2005 [311], and represents a phenomenally valuable tool for genetic investigations and manipulations in *S. meliloti* and related rhizobia.

In symbiosis with the host legumes *Medicago sativa* and *Medicago truncatula*, *S. meliloti* elicits the formation of indeterminate nodules; nodules that are long and cylindrical in structure, and possess a persistent apical meristem.

1.2.2 *Bradyrhizobium japonicum*

Among the *Rhizobiaceae*, *B. japonicum* is one of the most agriculturally important since it is the the symbiont of soybean. *B. japonicum* nodules are large and spherical in shape, and do not possess a persistent meristem. The genome of *B. japonicum*

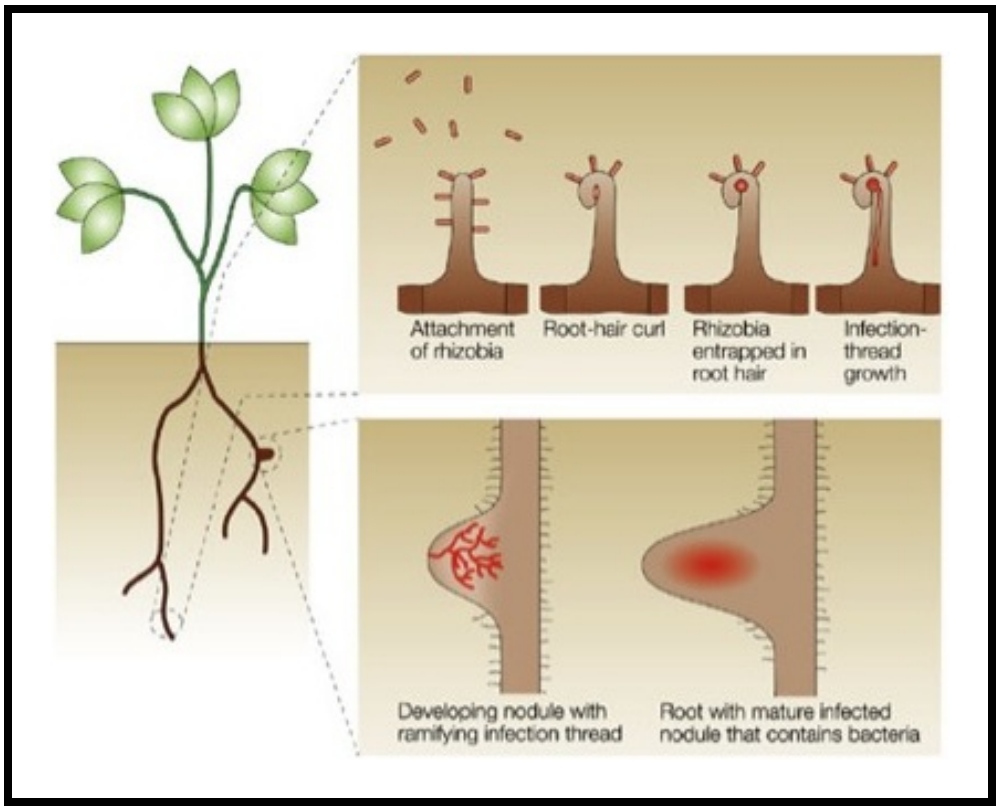

Figure 1.4: A schematic representation of the nodulation process (modified from [253])

has been sequenced and is comprised of a single circular chromosome of 9.1 Mb [178, 179]. The genome is estimated to encode 8317 proteins, approximately 52% of which have had functions ascribed on the basis of homology to proteins of known function, and 30% demonstrated homology to hypothetical genes. 34% of *B. japonicum* genes demonstrated significant similarity to genes in the related species *S. meliloti and M. loti* [104, 176, 177], and 23% appeared to be unique to *B. japonicum* [178, 179]. Although mono-partite in nature, the genome does posses a 410-kb region that contains many of the genes needed for symbiotic nitrogen fixation [123, 198, 350].

1.3 Carbon Metabolism in the *Rhizobiaceae*

The *Rhizobiaceae* can be split into two broad classes on the basis of their metabolism: fast growers and slow growers [2, 85]. Fast-growing rhizobia are typically found associated with temperate legumes and have generation times of less than six hours; these include, respectively, the common alfalfa and pea symbionts *S. meliloti* and *R. leguminosarum* (reviewed in [330]). Slow-growing rhizobia are often tropical in origin, have generation times that exceed six hours and include the soybean symbiont *B. japonicum*. While both groups are renowned for their metabolic diversity, it has been reported that the fast-growing rhizobia demonstrate a broader capacity for carbohydrate metabolism [116, 125, 300], while the slow growers can catabolize a larger variety of aromatic and hydroaromatic compounds [115, 264].

There is a considerable wealth of information in the literature regarding the diverse metabolic capacity of rhizobia however, the construction of a coherent and integrated picture of rhizobial cellular metabolism has yet to be completed. As bioinformatics tools become more powerful, attempts at developing integrative, constraint-based metabolic models will become more elegant and accurate. A recent study, using *R. etli* CFN42, documents the first attempt at a comprehensive

metabolic reconstruction of a rhizobial species [289]. This model, depicted in Figure 1.5, integrates data from the *R. etli* genome, journal publications, online databases and metabolism textbooks and represents an interesting and exciting step towards a more complete understanding of bacterial metabolic networks.

The major metabolic function of the root nodule is to take N_2 from the air and reduce it to ammonia, providing the plant with a source of fixed nitrogen. In order to fix nitrogen, the rhizobial cells must undergo a complex process of metabolic and physiological differentiation into a mature state known as the bacteroid, which is enveloped by the plant cell. The metabolism of bacteroids, which persist in the nodules low O_2 microenvironment that is compatible with the key O_2-sensitive enzymes in the nitrogen fixation process [295, 202], is overwhelmingly focused on the production of fixed nitrogen which is then transferred to the host plant. This process is fuelled by the plant host through the provision of large quantities of C_4-dicarboxylic acids such as malate or succinate [293, 99, 306].

Although bacteroid metabolism has been the subject of considerable study in recent years, and despite the wealth of recent proteomics data [308, 309], the basic questions of metabolic regulation and carbon utilization are largely unresolved. In *B. japonicum* bacteroids it is conceivable that the microaerophilic nature of the nodule may result in repression of key TCA enzymes. This would necessitate the use of alternate pathways to bypass the rate-limiting reactions in order to facilitate continued carbon oxidation, and perhaps modulate intracellular NAD(P)H levels. These pathways are shown in Figure 1.6, which depicts an overview of bacteroid metabolism in *B. japonicum*. In *S. meliloti*. previous studies have highlighted the importance of the TCA to bacteroid metabolism because citrate synthase [147], isocitrate lyase [233], succinate dehydrogenase [107], and malate dehydrogenase [82] have all been shown to be essential to symbiosis.

Figure 1.6 shows that there are a number of potential bacteroid responses to

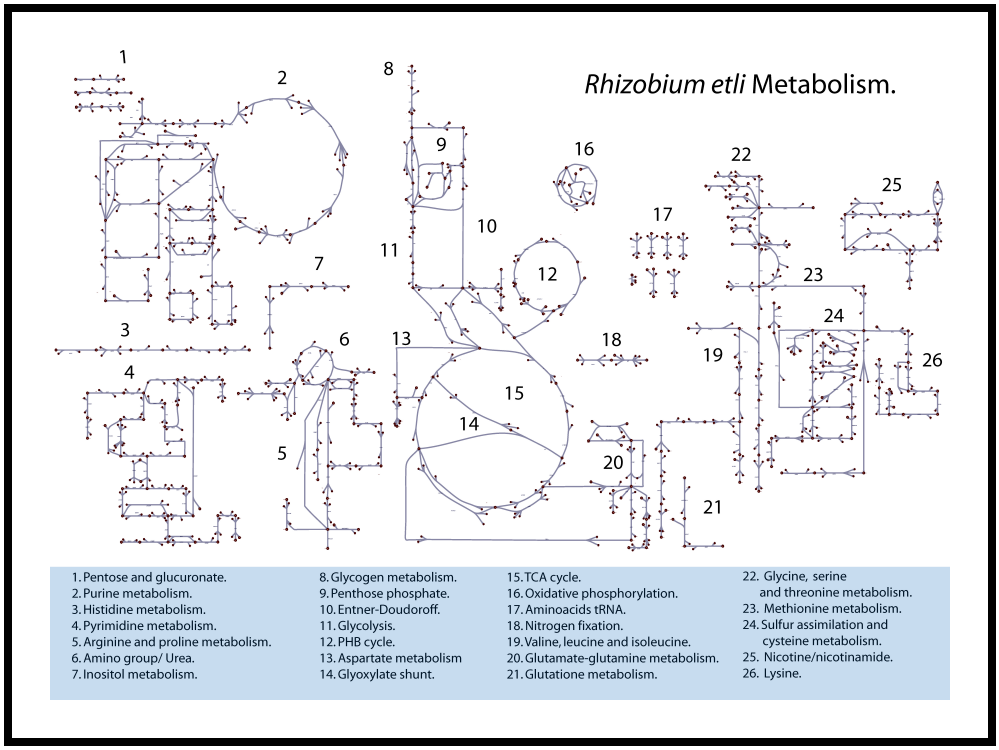

Figure 1.5: A reconstruction of carbon metabolism in *R. etli* was modelled using data from a wide variety of different sources including the *R. etli* genome sequence, journal publications, online databases and metabolism textbooks [289]

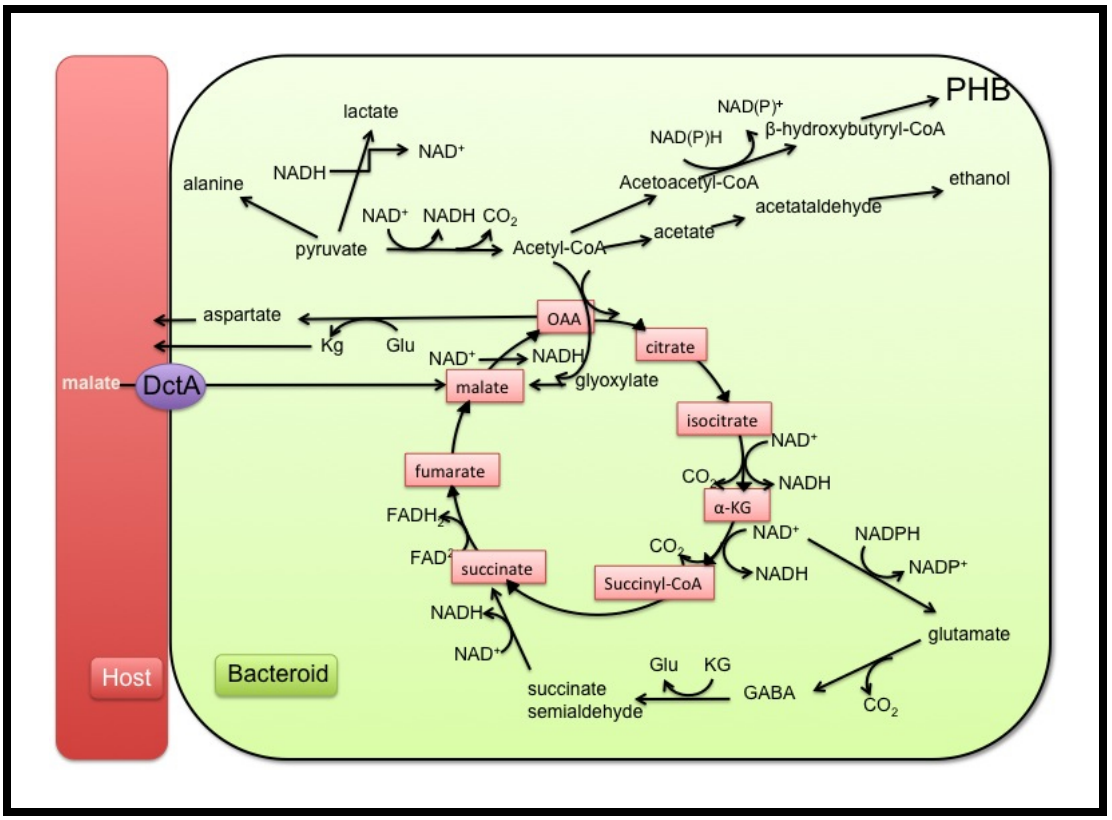

Figure 1.6: Carbon metabolism in *B. japonicum* bacteroids. The TCA has been highlighted in red. Pathways indicated include the α-ketoglutarate shunt, the γ-aminobutyrate pathway, the malate-aspartate shuttle, the modified dicarboxylic acid cycle and, the poly-β-hydroxybutyrate synthesis pathway. Modified from [232]

regulatory events. PHB metabolism is discussed in detail in Section 1.3.1; in order to facilitate a complete discussion of bacteroid metabolism, a brief overview of other pathways is included below.

1.3.0.1 Glyoxylate Shunt

The glyoxylate shunt, as indicated in Figure 1.6 and shown in more detail in Figure 1.7, represents an anapleurotic pathway that facilitates the growth of cells on C_2-substrates, allowing them to replenish TCA intermediates [59, 168]. This pathway is widespread among prokaryotes, and is encoded by the genes for isocitrate lyase (ICL) (EC 4.1.3.1) and malate synthase (MS) (EC 2.3.3.9), although data regarding its role in symbiotic nitrogen fixation remains inconclusive. Radiorespirometric analyses of *B. japonicum* indicated that up to 50% of acetyl-CoA that enters the TCA is metabolized via malate synthase [329], and ICL activity has been detected in bacteroids of senesced *B. japonicum* nodules [391]; however, isocitrate lyase activity has not been detected in bacteroids from soybean, pea, alfalfa or clover nodules [130, 168], although free-living *B. japonicum* and *S. meliloti* cells demonstrate measurable levels of ICL activity when grown on acetate under free-living conditions [79, 130, 218]. Interestingly, malate synthase activity appears to be constitutive [79, 130, 218], although activity levels appear to be higher in cowpea and soybean nodules, relative to alfalfa or pea [121, 168]. Mutational analysis of*aceA* (ICL) and *glcB* (MS) in *S. meliloti* indicated that *aceA* is essential for growth on acetate, and thus fundamental to the function of the glyoxylate shunt [282]. Interestingly, this study also showed that *glcB* is not essential for growth on acetate, which is in stark contrast to observations made in other bacteria, including *E. coli* [190, 257, 282], suggesting that other pathways for C_2-metabolism might exist in Rhizobia.

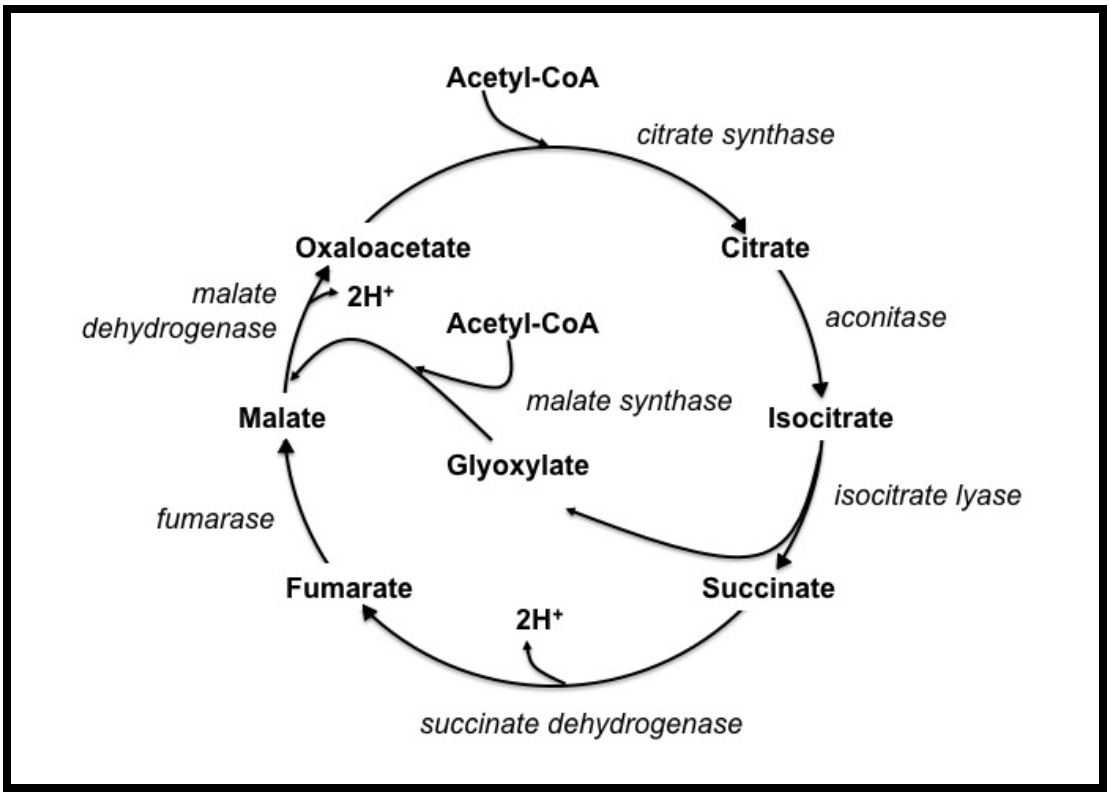

Figure 1.7: The glyoxylate shunt

1.3.0.2 Malate-Aspartate Shuttle

The malate-aspartate shuttle facilitates the oxidation of imported malate to oxaloacetate; oxaloacetate is subsequently transaminated to aspartate via a glutamate-dependent aspartate aminotransferase [175]. This would necessitate transport of glutamate across the peribacteroid membrane and into the bacteroid. The aspartate aminotransferase reaction would result in the production of aspartate and α-ketoglutarate; export of α-ketoglutarate, to compensate for malate import might facilitate the maintenance of the PBM electrochemical potential (reviewed in [232]).

In *B. japonicum* bacteroids, accumulation of oxaloacetate would result in the competitive inhibition of succinate dehydrogenase. The malate-aspartate shuttle would allow the bacteroids to metabolize oxaloacetate under conditions where the activities of citrate synthase, isocitrate dehydrogenase and α-ketoglutarate are rate-limiting relative to malate dehydrogenase. This would thus facilitate continued carbon metabolism under otherwise inhibitory conditions (reviewed in [232]).

1.3.0.3 α-Ketoglutarate-Glutamate Shunt

α-Ketoglutarate dehydrogenase activity in other gram-negative bacteria is known to be inhibited by NADH [156, 191, 329, 384] or repressed under conditions of oxygen limitation [4, 127, 160]. Given the metabolic constrains of the nodule environment, it is conceivable that a similar repression is experienced in bacteroids. Previous studies in *B. japonicum* and *R. leguminosarum* have presented data that suggest a significant portion of the carbon that enters the bacteroids is converted to glutamate [211, 305]. Glutamate dehydrogenase activity is induced by the presence of ammonium and α-ketoglutarate [101], both of which are likely to be present in the bacteroid [232]. Therefore, if α-ketoglutarate dehydrogenase activity is repressed then the accumulation of α-ketoglutarate would upregulate aspartate aminotrans-

ferase and GOGAT [386], thus providing a key link between the glutamate shunt and the malate-aspartate shuttle.

There is considerable evidence that glutamate, derived from α-ketoglutarate, can act as the transamination donor in the aspartate-aminotransferase reaction in *R. leguminosarum* bacteroids [211]. The resultant aspartate is secreted to the plant, facilitating asparagine synthesis, which is then taken up by the plant as the main nitrogen-source from the nodule (see Figure 1.11 in Section). Glutamate may also be decarboxylated to produce γ-aminobutyrate (GABA), which can be further metabolized to succinate [175], thus providing a bypass of α-ketoglutarate dehydrogenase while still removing an equivalent amount of CO_2 and producing succinate, which can then re-enter the TCA cycle.

1.3.0.4 Dicarboxylic Acid Cycle

In order to metabolize succinate or malate via the TCA cycle, bacteroids must employ an anapleurotic pathway leading to the synthesis of acetyl-CoA. While *B. japonicum* bacteroids apparently lack PEP carboxylase activity [335], it is conceivable that PEP carboxykinase or malic enzyme may be employed in the synthesis of acetyl-CoA. As shown in Figure 1.6, acetyl-CoA has four possible fates: 1. PHB synthesis; 2. TCA cycle; 3. malate synthesis; 4. reduction to ethanol. The combination of the GABA pathway and PHB synthesis provides an effective mechanism for the removal of excess carbon from the TCA cycle. For example, the GABA pathway involves a decarboxylation step, as does α-ketoglutarate dehydrogenase; employing a dicarboxylate-like pathway to channel oxaloacetate to pyruvate and then acetyl-CoA eliminates two carbon molecules. These alternative pathways thus represent potential detours around the decarboxylating steps of the TCA cycle [232].

1.3.0.5 Reductive Pathways

As shown in Figure 1.6, it is conceivable that *B. japonicum* bacteroids may synthesize acetaldehyde or ethanol to support nitrogen fixation. The potential pathway for ethanol synthesis would necessitate the upregulation of aldehyde dehydrogenase and alcohol dehydrogenase, both of which have been detected in bacteroids (reviewed in [232]).

1.3.0.6 PHB Synthesis

While most of the carbon from the plant is channelled into energy production to fuel nitrogen-reduction, it has been well-documented that in *B. japonicum* bacteroids, some carbon is diverted into the production of intracellular storage polymers composed of either glycogen or poly-β-hydroxybutyrate (PHB) that can be seen by electron-microscopy [60, 74, 122, 149, 400]. PHB and glycogen deposits are found in the cytoplasm as electron-transparent and electron-dense granules, respectively; these granules are synthesized by many bacteria when carbon is abundant and growth is limited by the shortage of another nutrient [400, 390]. PHB metabolism is discussed in more detail in the following sections.

1.3.1 Polyhydroxybutyrate Metabolism

1.3.1.1 Cellular Role of PHB

PHB is the best-characterized member of the polyhydroxyalkanoates (PHAs) [217, 326]. PHAs have generated considerable interest as potential economically competitive, environmentally benign replacements for synthetic, biologically inert polyester plastics [217]. Indeed, the potential commercial value of PHAs has generated the interest that has driven much of the research in this field.

The cellular role of PHB, although not fully understood, is known to extend further than simply acting as an intracellular carbon store that can be mobilized to provide a bacterium with a competitive advantage over other soil microbes. PHAs have been shown to protect the cell from a wide range of stresses including heat shock, UV irradiation, exposure to oxidizing agents, and osmotic shock [173]; perhaps by favouring the establishment of the bacterial cells and thus enhancing their capacity to tolerate environmental stress [174]. PHB metabolism is also tightly linked to the redox state of the cell; studies in *Azotobacter beijerinkii, Azotobacter insigni*, and *Rhizobium* ORS571 have shown that accumulation of large amounts of PHB is induced under conditions of oxygen limitation [313, 324, 328]. Under low-oxygen conditions, such as those found in the root nodule, the redox potential of the cell decreases as a result of aerobic metabolism, leading to a concurrent rise in cellular NAD(P)H levels. This leads to inhibition of both $NADP^+$-isocitrate dehydrogenase (EC 1.1.1.42) and citrate synthase (EC 2.3.3.1) which, in turn, divert acetyl-CoA and electrons away from the TCA cycle and into PHB synthesis [160, 313]. It has been suggested that in *Azotobacter*, PHB synthesis fulfills a regulatory role as an alternative electron acceptor; under conditions of oxygen limitation, NAD(P)H is channelled into PHB formation to relieve inhibition of isocitrate dehydrogenase and citrate synthase in order to allow continued operation of the TCA cycle [314, 313]. This is supported by the observation that a strain of *Azotobacter vinelandii* possessing a defective NADH oxidase synthesized massive amounts of PHB during the exponential phase of growth; in these cells PHB acts as an alternative electron sink to facilitate the regeneration of $NAD(P)^+$, and its production allows cells to maintain a wild-type level of growth [261, 262]. Although further studies are required to elucidate the mechanisms by which partitioning of acetyl-CoA between the TCA cycle and PHB synthesis is controlled, it is feasible that regulation of these pathways is probably controlled by a combination of factors,

including the acetyl-CoA/CoA ratio, the redox states of the pyridine pool, and reduced TCA cycle activity under microaerobic conditions [182].

While best-known for their ability to form nitrogen-fixing symbioses with legumes, the rhizobia are indigenous soil bacteria and as such are well-adapted to surviving in the typically oligotrophic, carbon-limiting environment of the bulk soil [368]. Carbon-rich root exudates released by plants make the rhizosphere extremely nutrient-rich relative to the bulk soil environment [368]. As rhizobia move between the rhizosphere and the bulk soil, the ability to accumulate and then degrade PHB and other carbon storage polymers would provide a competitive advantage over other bacteria. Furthermore, the recent observation that the *bdhA* gene encoding the PHB degradative enzyme 3-hydroxybutyrate dehydrogenase (BdhA, EC 1.1.1.30) in *S. meliloti* is upregulated in response to the presence of the alfalfa root exudate biotin may be significant [153]. Rapid catabolism of stored PHB to fuel cell division would allow the rhizobia to rapidly colonize the plant rhizosphere, facilitating efficient nodulation and nitrogen fixation.

1.3.1.2 PHB Metabolism

The structural similarity of PHB to polypropylene and its development as a commercial product has provided the stimulus for the isolation and study of PHA biosynthesis genes from multiple bacterial species. The PHB cycle of *S. meliloti* has been elucidated and is depicted graphically in Figure 1.8; analyses of *S. meliloti* PHB mutant phenotypes have shown that the ability to synthesize and utilize PHB, while important in competitive growth, is not essential for symbiosis [7, 390].

Synthesis of intracellular amorphous PHB storage granules from TCA cycle intermediates can act as an over-flow pathway for the TCA cycle. Two acetyl-CoA molecules are condensed by the action of a 3-ketothiolase, PhbA (PhaA; EC

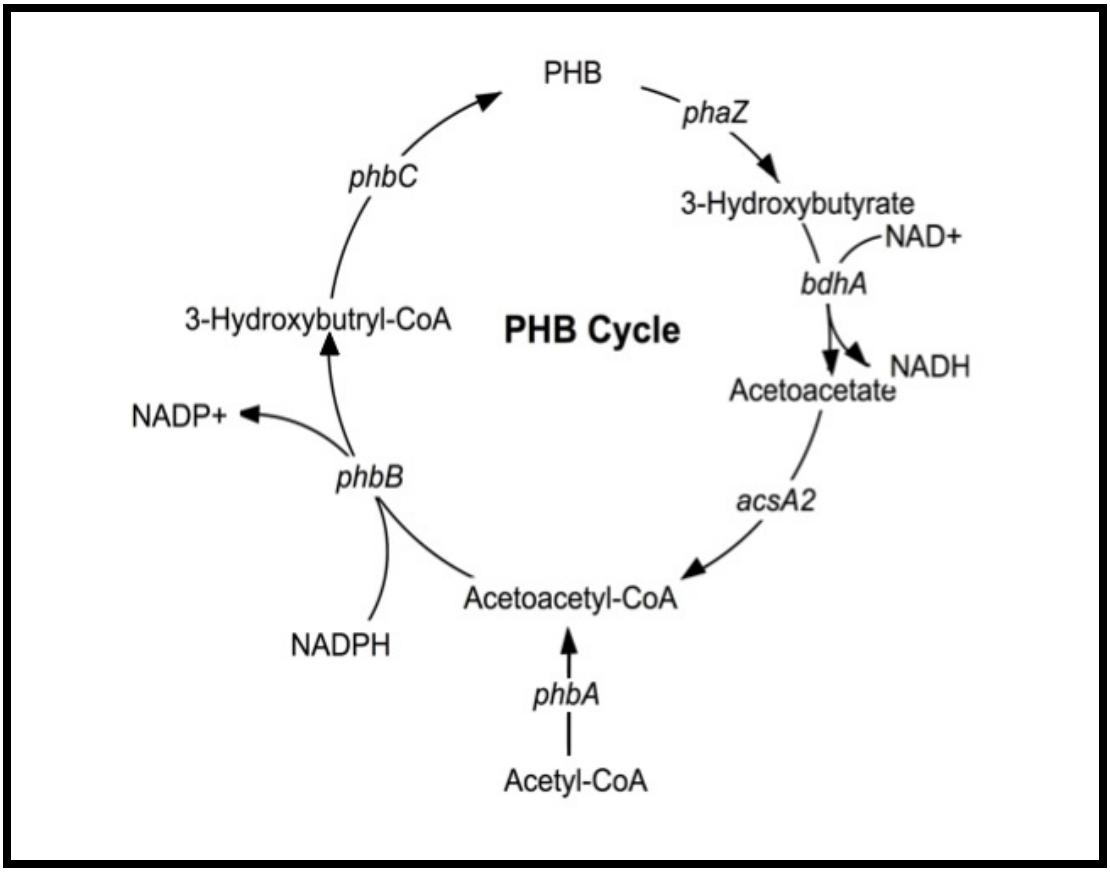

Figure 1.8: The poly-3-hydroxybutyrate cycle of *S. meliloti*

2.3.1.9) to form acetoacetyl-CoA (AA-CoA) [267]. AA-CoA is then reduced to 3-hydroxybutyryl-CoA (3-HB-CoA) by an acetoacetyl-CoA reductase, PhbB (PhaB; EC 1.1.1.36) [268]. 3-HB-CoA forms the substrate for polymerization to yield PHB through the action of PHB synthase, PhbC (PhaC; EC 2.3.1.-) [312].

Intracellularly, PHB degradation is initiated by the action of PHB depolymerase, PhaZ, (EC 3.1.1.75) which releases the D-3-hydroxybutyrate (D-3-HB) monomer [68]. D-3-HB is oxidized by the action of 3-hydroxybutyrate dehydrogenase, BdhA (EC 1.1.1.30) to acetoacetate (AA) [6], which is esterified to acetoacetyl-CoA (AA-CoA) by acetoacetyl-CoA synthetase, AcsA2, (EC 6.2.1.16) [40]. Following hydrolysis of AA-CoA by PhbA, acetyl-CoA is assimilated via the TCA cycle and glyoxylate shunt enzymes [217]. Alternatively, upon cell death and lysis, PHB granules are released into the extracellular environment where they undergo a transition into a partially crystalline polymer and can be broken down by the action of extracellular PHB depolymerases [164]. The extracellular degradative enzymes are phylogenetically unrelated to the intracellular enzymes and their substrate specificities are distinct, recognizing the amorphous and semi-crystalline forms respectively [164, 341].

1.3.1.3 Genetics and Genomics of PHB Metabolism

Analysis of the genomic organization of PHB biosynthesis genes in the α-proteobacteria has revealed that the genes encoding PHB synthases are typically not co-localized with other genes in the PHB biosynthesis pathway [285], a pattern that appears to be consistent throughout the rhizobia [104, 177, 178, 179]. This is in contrast to other PHB-accumulating bacteria in which PHB synthesis genes are often found clustered within the genome (Figure 1.10) [286]. In the β-proteobacterium *Wautersia eutropha phbC* is found clustered with *phbA* and *phbB* to form the *phbCAB* operon [312, 318] and in the γ-proteobacterium *A. vinelandii* these genes are clus-

tered to form the *phbBAC* operon [269]. In rhizobia *phbA* and *phbB* are found within an operon while *phbC* is typically found elsewhere in the genome. This pattern has been confirmed for *S. meliloti* [104], *Mesorhizobium loti* [177], and *Bradyrhizobium japonicum* [178]; although it is worth noting that *B. japonicum* possesses two copies of the *phbAB* operon and five copies of *phbC*, which are distributed throughout the genome (Figure 1.9) [7].

The PHB cycle in *S. meliloti* is the most extensively studied of the rhizobial PHB pathways. PHB biosynthetic genes were first discovered by heterologous complementation [390], heterologous hybridization [349], and mutagenesis [275]. Screening of mutants for an inability to grow on PHB cycle intermediates resulted in the identification of several genes involved in the PHB degradation cycle [6, 8, 46, 70]. The genes in the PHB degradation pathway are *phaZ* which is located on the chromosome and has yet to be experimentally characterized; *bdhA* which is located on pSymB; and *acsA2* which is located on the chromosome [40]. Mutants of several key PHB cycle enzymes have demonstrated interesting and informative phenotypes that have helped elucidate potential roles for the PHB cycle in both free-living and symbiotic growth. A summary of genes that have been shown to elicit an effect on the PHB cycle is listed in Table 1.1.

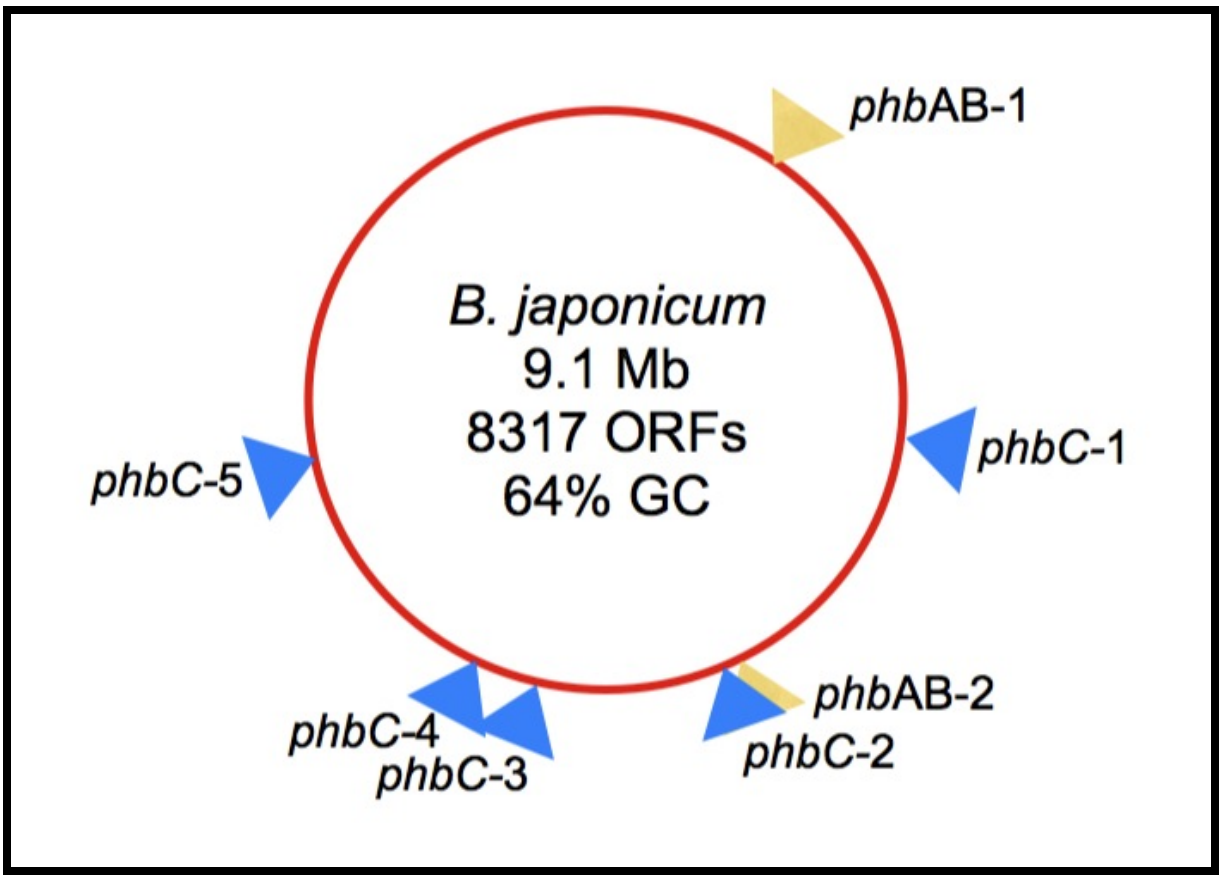

Figure 1.9: PHB synthesis genes of *B. japonicum* are distributed throughout the genome of the organism. *phbAB-1*: Bll0225/Bll0226; *phbAB-2*: Blr3724/Blr3725; *phbC-1*: Blr2885; *phbC-2*: Blr3732; *phbC-3*: Bll4360; *phbC-4*: Bll4548; *phbC-5*: Bll6073

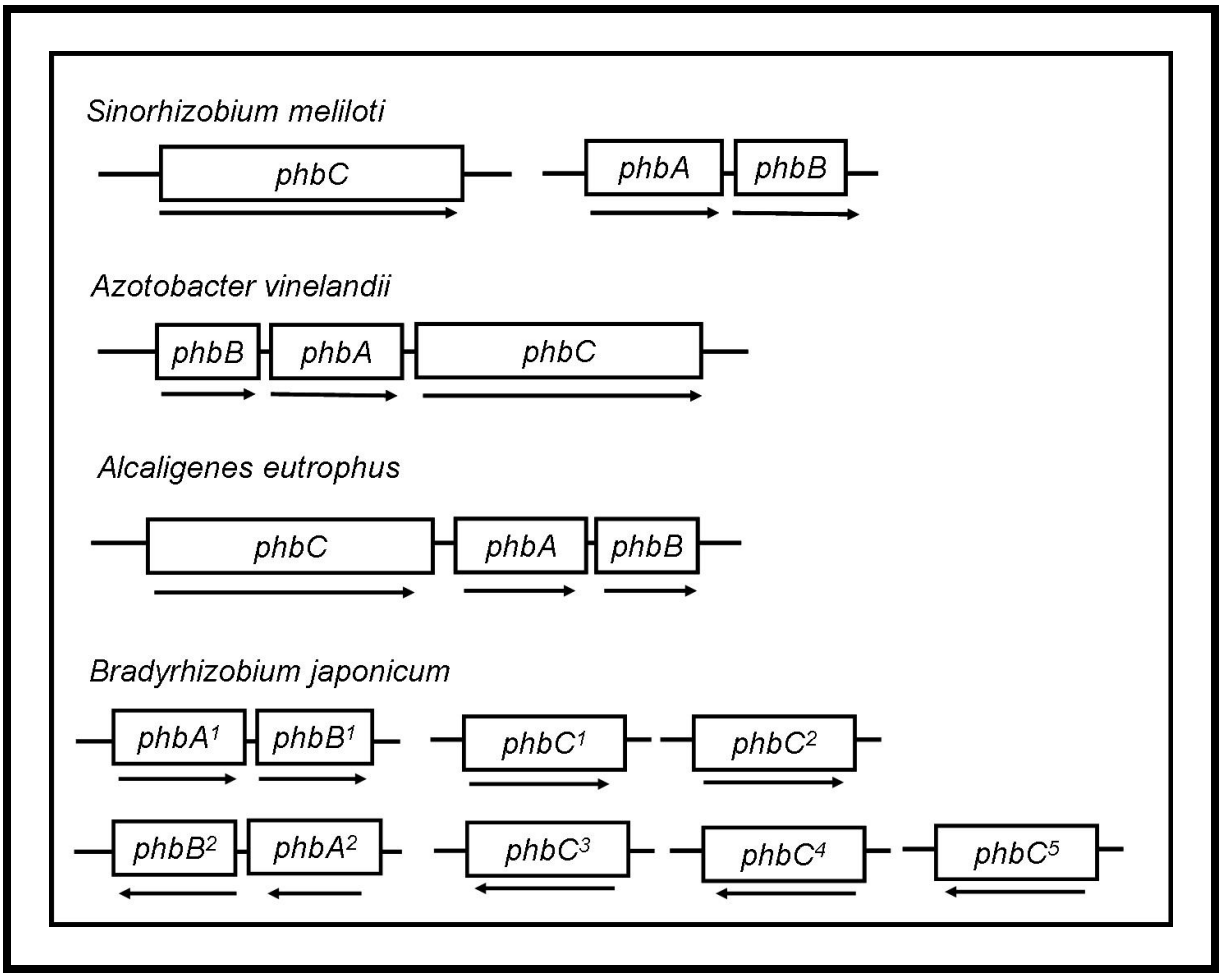

Figure 1.10: PHB synthesis genes in the Rhizobia and related organisms [351]

Table 1.1: Summary of genes that have been shown to elicit an effect upon PHB biosynthesis and/or degradation in rhizobia

Gene	Function	Organism Studied	Null Mutant Phenotype	Reference
phbC	PHB synthase	*S. meliloti, R. leguminosarum*	No PHB synthesized	reviewed in [351]
phbB	NADP-acetoacetyl-CoA Reductase	*S. meliloti*	No PHB synthesized	[7]
bdhA	3-hydroxybutyrate dehydrogenase	*S. meliloti*	No growth on D-3-HB	[46]
acsA2	acetoacetyl-CoA synthetase	*S. meliloti*	No growth on acetoacetate or D-3-HB	[46]
aniA	global carbon flux regulator	*S. meliloti, R. etli*	Reduced glycogen production and organic acid secretion, increased EPS production, global changes in protein expression	[87]
nifDK	nitrogenase structural genes	*B. japonicum*	Fix^- massive PHB accumulation	[135]
nifH	nitrogenase structural gene	*B. japonicum*	Fix^- massive PHB accumulation	[135]
aap and *bra*	amino acid permeases	*R. leguminosarum*	Double mutant produced PHB in symbiosis	[211]
bhbA	methylmalonyl-CoA mutase	*S. meliloti*	No growth on D-3-HB or AA	[45]

PhbB and PhbC are key enzymes in the anabolic arm of the PHB cycle and are encoded by genes located on the *S. meliloti* chromosome. Both *phbB* and *phbC* mutants of *S. meliloti* strain Rm1021 are deficient in the ability to produce succinoglycan, resulting in dry, non-mucoid colonies when grown under carbon-rich conditions; this phenotype is not observed in PHB degradation mutants [7]. Furthermore, the inability of these mutants to utilize the PHB cycle intermediates D-3-HB and AA as sole carbon sources [7, 40], suggests that the ability to synthesize PHB is essential for its degradation. *phbC* mutants are able to establish successful nitrogen-fixing symbioses with their host plant, and early studies implied that *phbC* mutants were essentially indistinguishable from wild-type in their symbiotic effectiveness [275, 390]. More recent studies however, have shown that plants inoculated with a *phbC* mutant strain, although appearing healthy, exhibit a delay in nodule development and a reduction in the total number of nodules formed, coupled with a significant reduction in shoot dry weight [7].

AcsA2 in *S. meliloti* is involved in the catabolic arm of the PHB cycle and is responsible for the synthesis of acetoacetyl-CoA from AA [8]; this is in contrast to *Escherichia coli* in which AA is activated by a CoA transferase [165]. *acsA2* is located on the chromosome; mutants were generated by Tn*5* mutagenesis and are unable to use either D-3-HB or AA as sole carbon sources [40, 46, 70]. Overexpression of *acsA2* in *S. meliloti* Rm1021 conferred the ability to utilize L-(+)-hydroxybutyrate (L-3-HB) as a sole carbon source, although it is worth considering that AcsA2 has a higher K_m and lower V_{max} for L-3-HB than for AA, suggesting that L-3-HB is not a natural substrate for the enzyme [8].

The *S. meliloti bdhA* gene is the first gene in an operon that also contains genes encoding subunits for xanthine oxidase and xanthine dehydrogenase [6]. Rm11107, a *bdhA* mutant of *S. meliloti*, was generated using Tn*5* mutagenesis and identified by its ability to use AA but not D-3-HB as a sole carbon source. This is in

contrast to *phbC, phbB* and *acsA2* mutants, which are all unable to grow using AA as a sole carbon source [7, 46, 70]. While neither BdhA nor PhbC is necessary for an effective symbiosis [275, 390], *S. meliloti* strains able to synthesize and degrade PHB demonstrate a measurable competitive advantage over mutants in either the anabolic or catabolic pathways of the PHB cycle during both free-living and symbiotic growth [7]. Moreover, the inability to synthesize PHB manifests a more severe defect than the inability to utilize PHB-derived D-3-HB as a source of carbon and energy [7]. This suggests that the ability of PHB to act as a redox regulator for removal of potentially growth inhibitory metabolites [80, 377] may be far more critical than its use as an internal carbon and energy store [7]. The ability to synthesize and break down PHB may confer a significant competitive advantage on *S. meliloti* during saprophytic growth. This in turn would enhance the likelihood of establishing successful symbioses upon receipt of the appropriate stimuli.

PHB cycle mutants in other species of rhizobia have also been investigated. *Rhizobium etli phaC* mutants grow poorly on pyruvate as a sole carbon source during free-living growth [43, 81]. This suggests that suppression of the TCA cycle occurs in *phaC* mutants, possibly due to the increased NADH/NAD^+ ratio, which in turn causes suppression of key metabolic enzymes including pyruvate dehydrogenase [43, 87]. This observation is similar to that reported for *R. leguminosarum* bv *viciae* (which forms indeterminate nodules on the roots of pea) but not corroborated by results from *R. leguminosarum* bv. *phaseoli* (which forms determinate nodules on the roots of bean) [212]. These data suggest that, in at least *R. etli* and *R. leguminosarum* bv. *viciae*, PHB synthesis is important for pyruvate metabolism. *R. etli phaC* mutants also accumulated up to 50-fold more glycogen in free-living growth than the wild-type strain, suggesting that carbon can be shuffled between alternative storage polymers [43].

Analysis of the genome sequence of *B. japonicum* [178] indicated the presence

of five *phbC* homologues (one of which has been shown to be able to functionally complement a *S. meliloti phbC* mutation [7]) and two *phbAB* operons encoding acetyl-CoA acetyltransferase and acetoacetyl-CoA reductase [178, 179]. The presence of so many copies of *phbC* suggests a significant role for PHB in *B. japonicum* metabolism. Although the capacity of each of these genes to encode a functional PHA synthase has not been experimentally determined, each one does contain the conserved catalytic residues found in all PHA/PHB synthases [285].

While not strictly part of the PHB cycle, the *aniA* gene encodes a transcription factor that is thought to be responsible for regulating expression of genes whose products are important in the partitioning of carbon flow in the bacterial cell [274]. In *S. meliloti*, AniA synthesis is stimulated under low-oxygen conditions, and its production results in the channelling of excess carbon into PHB and glycogen biosynthesis [274]. *aniA* mutants of *S. meliloti* exhibit a significant increase in exopolysaccharide (EPS) production under anoxic conditions but show no increase in intracellular carbon storage polymers [274]. In *R. etli* however, AniA appears to also play a significant role in controlling carbon flow under aerobic conditions [87, 274]. *aniA* mutants of *R. etli* exhibit a marked decrease in PHB accumulation, a large increase in EPS biosynthesis and a drastic alteration of global protein expression, including the disappearance of PhaB during aerobic growth [87]. *aniA* in *R. etli* was identified in a *phaC* mutant background by random Tn*5* mutagenesis; mutants restored in their ability to grow on pyruvate as a sole carbon source all possessed a single insertion that mapped to an ORF with significant homology to *aniA* of *S. meliloti* [87]. The precise role played by *aniA* in rhizobial metabolism remains to be determined but, given the significance of carbon metabolism under both free-living and symbiotic conditions, it is tempting to speculate that it will be central to multiple metabolic pathways.

1.3.1.4 PHB in the Rhizobia-Legume Symbiosis

The ability of bacterial cells to partition acetyl-CoA between the TCA cycle and PHB synthesis in order to maintain respiration at sufficiently high levels under microaerobic conditions is especially pertinent when one considers the metabolic state of the bacteroid during symbiosis. Rhizobia are obligate aerobes; however, all metabolic reactions occurring in the bacteroid must occur under the microaerobic conditions necessary to protect the O_2-labile nitrogenase enzyme that is responsible for nitrogen reduction. As a result, tight regulation of free O_2 in the root nodule is essential to ensure that, while the concentration of free O_2 is low, O_2 flux remains high enough to support the high level of respiration required for nitrogenase activity [202]. Control of free O_2 availability to the bacteroid is presumably a major factor in the control of bacteroid metabolism; it has been proposed that O_2 availability is used by the host plant as a means of sanctioning non-fixing strains of rhizobia, allowing the host plant to select against nodules that contain non-fixing rhizobia [71, 185].

The roles of PHB in the rhizobia-legume symbiosis appear to be more diverse than simply providing an alternative electron sink and data concerning the function of PHB in bacteroid metabolism is often conflicting. While most rhizobia accumulate PHB under free-living conditions [43], not all rhizobia accumulate PHB during symbiosis. The ability to accumulate PHB during symbiosis appears to be dependent on the physiology of the nodule formed by the host plant. Two major types of root nodule are formed in the rhizobia-legume symbiosis: determinate nodules which do not possess a persistent meristem and instead form a spherical-shaped structure, and indeterminate nodules which possess a persistent meristem resulting in a long, cylindrical structure [134].

1.3.1.5 Determinate Nodules

Bacteroids of determinate nodules, such as those formed by *B. japonicum* on soybean and *R. etli* on beans, accumulate high levels of PHB during the active nitrogen-fixing period of symbiosis [19, 181, 182, 391]. These PHB reserves may subsequently be mobilized for use during periods of low carbon availability, such as during periods of darkness or seed production by the host plant [18]. Bacteroids of *B. japonicum* can accumulate up to 50% of their cellular dry weight as PHB [181, 188, 238, 391], an amount which does not appear to fluctuate relative to nitrogenase activity but which does decline under extended periods of carbon stress [391]. Whole nodules of *Lupinus angustifolius* demonstrated reduced PHB levels and BdhA activity as well as a rapid reduction in nitrogen fixation when the host plants were incubated in darkness [110]. This suggests that PHB stores in determinate nodules may be mobilized in order to support nitrogen fixation under conditions of reduced carbon availability. The production of PHB and fixation of nitrogen in bacteroids, however, seem incompatible: PHB and nitrogenase potentially compete for the same energy and reductant sources and, therefore, PHB synthesis in bacteroids must compete with nitrogen-fixation for photosynthate [43, 181]. This is further supported by the observations that a *phaC* mutant of *R. etli* demonstrated higher and more prolonged nitrogenase activity relative to the wild-type strain during symbiosis [43] and Tn*5* mutants in the nitrogenase-encoding *nifD, nifK*, and *nifH* genes in *B. japonicum* all accumulated higher levels of PHB relative to the wild-type strain [135]. These data are not, however, corroborated by the observation that a *phaC* mutant of *R. leguminosarum* bv. *phaseoli* was unaffected in symbiotic efficiency on bean relative to the wild-type strain, suggesting that PHB production levels in the bacteroid may not be the sole contributor to symbiotic performance [212].

1.3.1.6 Indeterminate Nodules

Bacteroids occupying indeterminate nodules, such as *S. meliloti* on alfalfa, do not accumulate PHB during symbiosis [149, 148]; PHB synthesis does occur, but is presumably accompanied by an equivalent rate of degradation; any accumulation is insufficient to allow for the formation of granules detectable by electron microscopy [186]. These bacteria possess large numbers of PHB granules during the initial stages of invasion, which involves passage through the infection thread by means of cell division [103]. The cells then become enclosed in the plant-derived symbiosome membrane [149, 148, 170] and begin the process of differentiation into the bacteroid state. During differentiation, the PHB granules disappear and mature bacteroids are notably devoid of visible PHB granules [149, 148, 212, 370]. While the carbon source responsible for fuelling the invasion and infection process has not yet been identified, it has been speculated that PHB, while not crucial to the process [7, 390], may play some role during infection [46, 70]. Although PHB mutants are capable of nodulation and establishing effective symbioses [275, 390], it is possible that intracellular PHB stores may fuel cell division and growth during root infection and invasion. Interestingly, a recent study in *R. leguminosarum* bv. *viciae* showed that, under extraordinary conditions, PHB accumulation could occur; *R. leguminosarum* bv *viciae* carrying mutations in *aap* and *bra*, encoding broad-specificity amino acid transporters, possessed PHB granules in mature bacteroids [211]. These bacteroids were unable to cycle amino acids between the bacteroid and the host plant resulting in plants that displayed a Fix^- phenotype, even though they had nodules that appeared to possess an intermediate level of leghemoglobin and contained a functional nitrogenase [211]. Blocking the amino acid cycling pathway between the plant and the bacteroid, which appears to be essential for an effective symbiosis, prevents the synthesis of aspartate from oxaloacetate, which increases carbon flow from dicarboxylate to pyruvate, which is in turn channelled into PHB synthesis. This study

demonstrates that bacteroids of *R. leguminosarum* still retain the capacity to synthesize and store large quantities of PHB, but only when carbon supply is in excess and bacteroid metabolism is limited by the availability of a key nutrient. Further study needs to be conducted to determine if this is a behaviour that is consistent amongst all symbionts occupying indeterminate nodules.

S. meliloti possesses two malic enzymes: $NADP^+$-dependent Tme, which is present under free-living conditions, and NAD^+-dependent Dme, which is present under both free-living conditions and during symbiosis [78]. In contrast to Tme, Dme is severely inhibited by the presence of acetyl-CoA, suggesting that Dme functions in the pathway responsible for the conversion of dicarboxylate into acetyl-CoA in the bacteroid [78]. While the reason for accumulation of PHB in bacteroids of determinate nodules, but not those of indeterminate nodules, is not understood, it has been suggested that the low activity of the $NADP^+$-dependent malic enzyme Tme in bacteroids of indeterminate nodules may play a role. The bacteroid is supplied with malate and other C_4-dicarboxylates by the plant; mutations in either the dicarboxylate transport system [27, 99, 293] or the NAD^+-dependent malic enzyme Dme [77] have a severe effect on the capacity of the strain to enter into an effective symbiosis. It has been hypothesized that the synthesis of PHB in *S. meliloti* bacteroids might be inhibited because too little substrate, and too few reducing equivalents are present to shuttle acetyl-CoA into the PHB biosynthetic pathway [78]. In contrast to this, the NAD^+-malic enzyme from *B. japonicum* bacteroids demonstrated no inhibition in the presence of acetyl-CoA, suggesting that NAD^+-malic enzyme plays different physiological roles in these two species [49]. It has been suggested that both $NADP^+$- and NAD^+-dependent malic enzymes are active in *B. japonicum* bacteroids, but that the NAD^+-dependent enzyme is primarily involved in the conversion of malate to acetyl-CoA [57]. As the *B. japonicum* NAD^+-malic enzyme is not inhibited by acetyl-CoA, accumulation of acetyl-CoA that could be

channelled into PHB biosynthesis would then be possible, facilitating the formation of large PHB stores in these bacteroids.

When considering the differences between determinate and indeterminate nodules, it is also worth considering the fate of the bacteroids following nodule senescence. It is commonly believed that, following infection and differentiation, bacteroids of indeterminate nodules are terminally differentiated and are unable to return to a free-living state, while bacteroids of determinate nodules are thought to retain the capacity for free-living growth and can undergo a reverse differentiation process upon nodule senescence [132, 232, 235, 337, 357]. It is therefore tempting to speculate that PHB accumulation by bacteroids in determinate nodules and by undifferentiated cells in the infection thread of indeterminate nodules may function to give the rhizobial cells a competitive advantage when released into the soil following nodule senescence [70].

1.3.1.7 Summary of Rhizobial PHB Metabolism

The observation that, contrary to the commonly accepted paradigm, bacteroids of indeterminate nodules retain the capacity to generate PHB granules is interesting. The fact that bacteroids of *R. leguminosarum* bv. *viciae aap/bra* mutants produced PHB granules that were visible by electron microscopy provides us with some valuable insight into nodule metabolism [211]. Nodules containing bacteroids incapable of exporting fixed nitrogen will be perceived as ineffective by the plant, which will impose sanctions upon them [70]. Recent data has shown that these sanctions are likely to take the form of reduced O_2 supply to the bacteroid [185]. This might result in repression of the TCA cycle in the bacteroid but would not directly affect the supply of dicarboxylates by the plant or uptake by the bacteroid. In order to prevent build up of malate (or another C_4-dicarboxylate) due to inhibition of Dme by acetyl-CoA, the bacteroid could potentially channel the excess carbon into

PHB biosynthesis. This would have the added benefit of regenerating $NADP^+$, which would presumably accumulate when nitrogenase activity is compromised. In the absence of a functional TCA cycle however, regeneration of NAD^+ is presumably compromised and it is tempting to speculate that this might ultimately cause inhibition of Dme.

The observation that plant tissue from nodules infected by *R. leguminosarum aap/bra* mutants possesses increased levels of starch [211] suggests that, in the absence of a functional TCA cycle, channelling of dicarboxylates into PHB biosynthesis does not restore the metabolic state of the bacteroid to normal levels. Indeed, it suggests that bacteroid carbon utilization appears to still be compromised. Assuming that DctA is not feedback inhibited by a build-up of malate in the bacteroid cytoplasm, it is conceivable that the plant employs additional measures to monitor and regulate carbon demand by and supply to the bacteroid.

Carbon is transported from the sites of photosynthesis to the root nodule in the form of sucrose, which is subsequently hydrolysed by the nodule plant cells into fructose and UDP-glucose. It is from these sugars that malate (or another C_4-dicarboxylate) is synthesized and transported to the bacteroids. Malate is exported from the plant via a dicarboxylate transporter in the plant-derived peribacteroid membrane (PBM) [360, 393], and imported into the bacteroid by the bacterial transporter DctA [98, 99, 293]. The sustained uptake of malate across the PBM is dependent on subsequent uptake and metabolism by the bacteroid [359]; if bacteroid carbon metabolism is suppressed as a result of plant-enforced sanctions, it is conceivable that transport of malate across the PBM will be reduced. This would presumably cause an increase in malate levels within the root nodule tissue, which would result in down-regulation of dicarboxylate synthesis; the excess carbon would be channelled into starch biosynthesis instead. It is possible, given the apparent ability of bacteroids from determinate nodules to undergo reverse differentiation

following nodule senescence, that these symbioses have evolved to increase the provision of dicarboxylates to the bacteroid in order to fuel both cellular respiration and PHB formation. Assisting the bacteroids in PHB accumulation has the potential benefit to the host plant of seeding the soil with a population of viable rhizobia that would be available to nodulate the next generation of plants following seed formation and plant death. In indeterminate nodules, where reverse differentiation does not occur, there is no obvious benefit to either the plant or the bacteria for the bacteroids to assimilate carbon reserves; PHB is not accumulated and, indeed, NAD^+-malic enzyme has evolved to effectively switch off PHB accumulation in the nodule under normal physiological conditions. It is only when the central metabolic pathway of the bacteroid is blocked downstream of the branch point for PHB biosynthesis that bacteroids of indeterminate nodules appear to be capable of accumulating PHB. It is conceivable that, because PHB granules are osmotically inert, PHB biosynthesis is employed as a measure to maintain appropriate osmotic pressure in the bacteroid. If this is indeed the case, analysis of the ultra-structure of root nodules incubated in a N_2-reduced or N_2-free environment might be expected to reveal the presence of PHB granules in bacteroids of indeterminate nodules. Study of broad-host-range rhizobial species such as *Sinorhizobium* sp. NGR234, which are capable of symbioses involving either indeterminate and determinate nodules [280], has the potential to reveal a great deal about the differential metabolic profiles that appear to exist between bacteroids of each nodule type. Specifically, insight into the regulation of malic enzyme(s) and the effects of an *aap/bra* double mutation in a broad host range strain might reveal a great deal about nodule metabolism.

Further studies of the PBM dicarboxylate transporter are critical if we are to understand the complex relationship between host and symbiont in the rhizobia-legume symbiosis. It is worth considering that DctA and its plant-derived counterpart have different kinetic properties; in nodules of soybean infected with *B.*

japonicum, the PBM DCA transporter has a higher K_m and lower V_{max} than its bacterial counterpart [360]. It is tempting to speculate that these differences may account for the discrepancies in bacteroid PHB storage between determinate and indeterminate nodules. Studies of the transport kinetics and regulation of the PBM dicarboxylate transporters of determinate and indeterminate nodules is needed to analyse this in more detail.

1.3.2 Dicarboxylic Acid Metabolism and Transport

The specificity of carbon source utilization by bacteroids to support BNF has been under investigation since the 1960s, when it was shown that bacteroids of *B. japonicum* preferentially oxidized the TCA cycle intermediates succinate, malate and fumarate (all of which are dicarboxylates) over hexose sugars [329]. Since then, many studies have been conducted on a variety of rhizobia, which show that BNF is highly stimulated by the presence of dicarboxylates, especially succinate. C_4-dicarboxylate uptake rates by bacteroids have been shown to be 30-50 fold faster than for sugars (reviewed in [195, 387]). Interestingly, the dependence on the TCA for N_2-fixation appears to differ between fast- and slow-growing rhizobia. Mutational analyses of *B. japonicum* suggested that neither aconitase nor isocitrate dehydrogenase, both central TCA cycle enzymes, were essential to the establishment of a effective symbiosis [315, 344]. This is in contrast to *S. meliloti*, in which isocitrate dehydrogenase mutants are ineffective in symbiosis, although they are capable of eliciting the formation of bacteroid-filled nodules [233]. A similar phenomenon is documented with respect to the *sucAB* genes, which encode the 2-oxoglutarate enzyme complex and are responsible for the oxidative decarboxylation of 2-oxoglutarate to succinyl-CoA (reviewed in [387]). *B. japonicum sucA* mutants, although impaired in nodulation effectiveness, can establish N_2-fixing symbiosis with almost wild-type levels of nitrogen-fixation [128], while similar mutants of *R. leguminosarum* were unable to

form N_2-fixing nodules on pea plants [377]. It is important to remember that these experiments do not examine flux; it is thus likely, given the presence of both 2-oxoglutarate dehydrogenase and succinate semialdehyde dehydrogenase [131], that *B. japonicum* TCA cycle mutants are able to bypass the blocked points.

There have been many studies investigating the dependence of BNF on a functional dicarboxylate transport system. Prior to the isolation of the C_4-dicarboxylate transport system of *R. leguminosarum* bv. *trifolii* in 1984 [292], researchers had shown that mutants defective in the ability to transport C_4-dicarboxylates were unable to enter into effective symbioses with their respective host legumes (reviewed in [396]). Today, many examples have been documented to confirm the dependence of BNF on C_4–dicarboxylate transport and it is widely accepted that mutants are impaired in their capacity to import dicarboxylic acids (DCAs) form ineffective, non-nitrogen fixing nodules in symbiosis [11, 27, 84, 99, 117, 215, 382].

Transport of dicarboxylic acids into the bacteroids is also intimately linked to the transport of amino acids, and ultimately to a complex C/N exchange process between the host plant and the symbiont [211]. The theoretical model for this exchange is shown in Figure 1.11. This model describes how the bacteroids are believed to import glutamate from the host plant via the bacterial Aap/Bra transporters [211]. Glutamate can then act as a transamination donor to produce aspartate. Aspartate is secreted to the plant, facilitating asparagine synthesis, and allowing the bacteria to shut down ammonia assimilation [211]. It is possible that DctA functions as the aspartate carrier allowing aspartate to be exported from the bacteria.

1.3.2.1 DctA

The dicarboxylate transport system is encoded by three genes, *dctA, dctB* and *dctD* [27, 382]. *dctB* and *dctD* encode the genes for a two-component regulatory system in which the periplasmic sensor kinase (reviewed in [163]) DctB, responds to the presence of C_4–dicarboxylates in the bacterial periplasm [112, 111] modulates that activity of the response regulator DctD [133, 206], which activates transcription of *dctA* via the σ_{54}-dependent, *dctA* promoter (reviewed in [396]). The regulation of *dctA* expression is discussed in more detail in Section 1.3.2.2. DctB and DctD have been well studied both structurally and functionally and both show homology to two-component regulatory systems from many other bacteria.

Less is known about the structure and mechanism of DctA. DctA is approximately 46.5 kDa, and is a member of the glutamate transporter family, an important family of secondary transporter proteins. This structural family includes transporters found in mammalian neuronal, glial, and retinal cells, as well as bacterial nutrient uptake proteins (reviewed in [319]). The bacterial transporters catalyse the electrogenic symport of glutamate with at least two cations [347, 346, 348], while the eukaryotic proteins require the symport of two or three sodium ions and one proton and antiport of one potassium ion [5, 13, 180, 399]. The precise ion requirements of DctA in rhizobial DctA systems remain to be determined.

Homology between family members is most evident in a stretch of approximately 150 residues from the C-terminal domain. This region contains four sequence motifs (A through D), that show a high level of conservation between species. All of these motifs have been suggested to play a role in the translocation pore or substrate binding site [319]. Phylogenetic sequence analyses of these motifs have facilitated the subdivision of the glutamate transporter family into five subfamilies as follows: (i) eukaryotic glutamate transporters; (ii) bacterial glutamate transporters; (iii)

eukaryotic neutral amino acid transporters; (iv) bacterial C_4-dicarboxylate transporters (of which DctA is a member); and (v) bacterial serine transporters [319]. The precise function of these conserved motifs remains elusive. It has been speculated that motif A, by virtue of its serine-and-threonine rich nature, may be a ligand binding site. Motif C is believed to be involved in binding the carboxylate group of substrates, since it is conserved only in the glutamate, neutral amino acid and C_4-dicarboxylate carriers. Mutagenesis studies have demonstrated that motif B is involved in cation binding [319]. Motif D is located within the amphipathic membrane-spanning helix 8 and, by virtue of the substrate-specific differences in sequence, is believed to be a part of the translocation pore [228, 321]. Mutagenesis studies have demonstrated that dicarboxylate transport is affected by alterations to the conserved C-terminal domains, a region known to be important for ion and substrate selection [320, 319, 321]. Interestingly however, the residue G114 in the third transmembrane helix of *S. meliloti* also appears to be significant in substrate recognition [352, 397] and indeed, multiple sequence alignment demonstrates a high level of conservation in the region around G114, although the aligned sequences exhibit substrate-specific variation, suggesting a role in substrate recognition.

The substrate specificity of several DctA homologues has been investigated [12, 89, 229, 234, 398], and is known to include aspartate, fumarate, malate, oxaloacetate (OAA), and succinate. D-Lactate, 2-methylsuccinate, 2,2 or 2,3-dimethylsuccinate, acetoacetate, β-hydroxybutyrate, mercaptosuccinate, α-ketoglutarate, and itaconate are also potential substrates for this system [398]. In *S. meliloti*, not all substrates recognized by DctA are inducers of DctA, and not all inducers of DctA-mediated transport act as competitive inhibitors (and probably substrates) of DctA-mediated transport [398]. It is worth noting that *S. meliloti* DctA has a much lower affinity for orotate than either malate or succinate, suggesting that DctA is able to distinguish between very similar substrates based upon the relative positions of their

carboxyl groups, and that substrate specificity may be defined by very specific structural constraints [398]. DctA also has the capacity to transport orotic acid and the toxic analogue fluoroorotic acid (FOA). Strains possessing a functional DctA transport system cannot grow in the presence of FOA, facilitating an easy and powerful screen for DctA activity [398].

1.3.2.2 Regulation of *dctA* Expression

Activation of *dctA* in previously characterized systems such as *S. meliloti* and *R. leguminosarum* is outlined in Figures 1.12 and 1.13. DctB and DctD are constitutively expressed at low levels [294]. The *dctB* gene product is located in the cytoplasmic membrane and acts as a membrane-bound sensor that responds to the presence of C_4-dicarboxylates and transduces the signal across the membrane to activate its cytoplasmically located C-terminus. This results in autophosphorylation and phosphotransfer to DctD [112, 287]. Phosphorylated DctD is able to bind to two recognition sequences upstream of the *dctA* promoter at -110 and -143 bp [112, 204] and interact with the alternative sigma factor RpoN (σ54) to activate transcription of *dctA* (Figure 1.12) [199, 203, 204, 205, 294].

RpoN is associated with a wide variety of metabolic functions, including nitrogen and carbon metabolism amongst the proteobacteria [35]. Standard phenotypes of RpoN mutants in Rhizobia include the inability to transport dicarboxylic acids, and form effective symbioses with host plants [53, 242, 294, 367, 327].

Promoters activated by RpoN do not contain canonical -35 and -10 sequences, rather they possess the consensus -26 CT**GG**CACPu-N_4-TT**GC**A -12 (invariant nucleotides shown in bold) [73, 158]. RpoN-dependent transcription is modulated by activator proteins, which allow σ_{54} to activate the core RNA polymerase under different physiological conditions including the availability of dicarboxylates outside

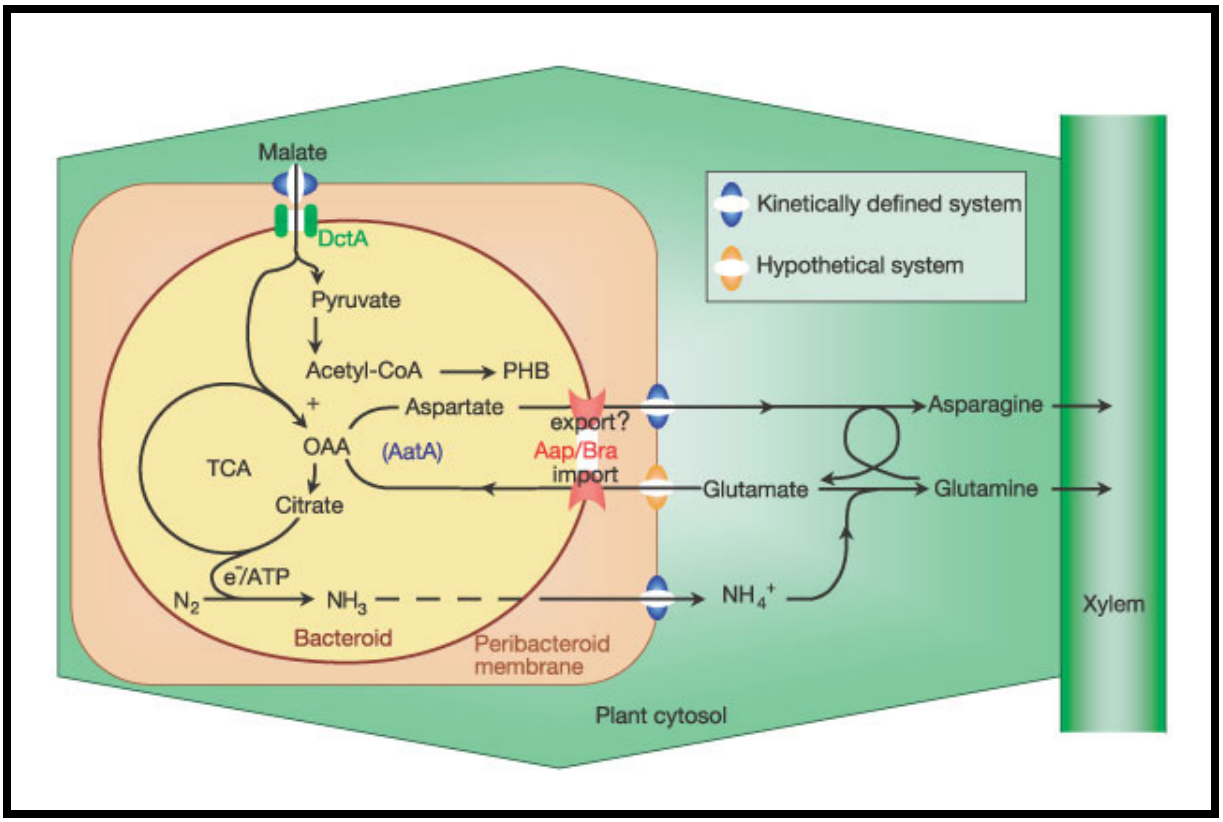

Figure 1.11: An overview of the role of amino-acid cycling in nitrogen fixation in pea nodules. Although glutamate and aspartate are shown as the amino acids most likely to cycle, others (such as alanine) may be important. The reaction catalysed by AatA also forms 2-ketoglutarate, which may be either metabolized by the bacteroid or exported back to the plant. Export via Aap/Bra is shown with a question mark to indicate that it is hypothetical [211]

of the cell [241].

1.3.3 Dicarboxylate Transport in *B. japonicum*

Most members of the *Rhizobiaceae* possess a single dicarboxylate transport system, but exceptions do exist. Both *Sinorhizobium* sp. NGR234 [366] and *Rhizobium tropici* [14] have two systems that are capable of transporting C_4-dicarboxylates, but their capacity to support symbiotic nitrogen fixation remains unknown. Furthermore, the completed genome sequence of *Mesorhizobium loti* revealed the presence of two genes with over 70% sequence identity to *S. meliloti dctA* [177, 176].

Early studies in *B. japonicum* suggested the presence of two succinate transport systems that were active under free-living conditions [157]. Analysis of the genome sequence of *B. japonicum* reveals seven genes homologous to *S. meliloti dctA*. All seven possess the eight conserved domains and three sequence motifs that are characteristic of members of the glutamate transporter family. An alignment of the encoded amino acid sequences relative to each other, and to the DctA sequence of *S. meliloti*, is shown in Figure 5.3. Interestingly, *B. japonicum* also possesses two independent, differentially regulated *rpoN* homologues [197]. Although both of these *rpoN* genes could complement the succinate- and nitrate-negative growth phenotype of the *S. meliloti rpoN* mutant, *B. japonicum* mutants of either and both homologues could grow on C_4-dicarboxylates as a carbon source, suggesting the existence of an *rpoN*-independent system for C_4-dicarboxylate uptake [197].

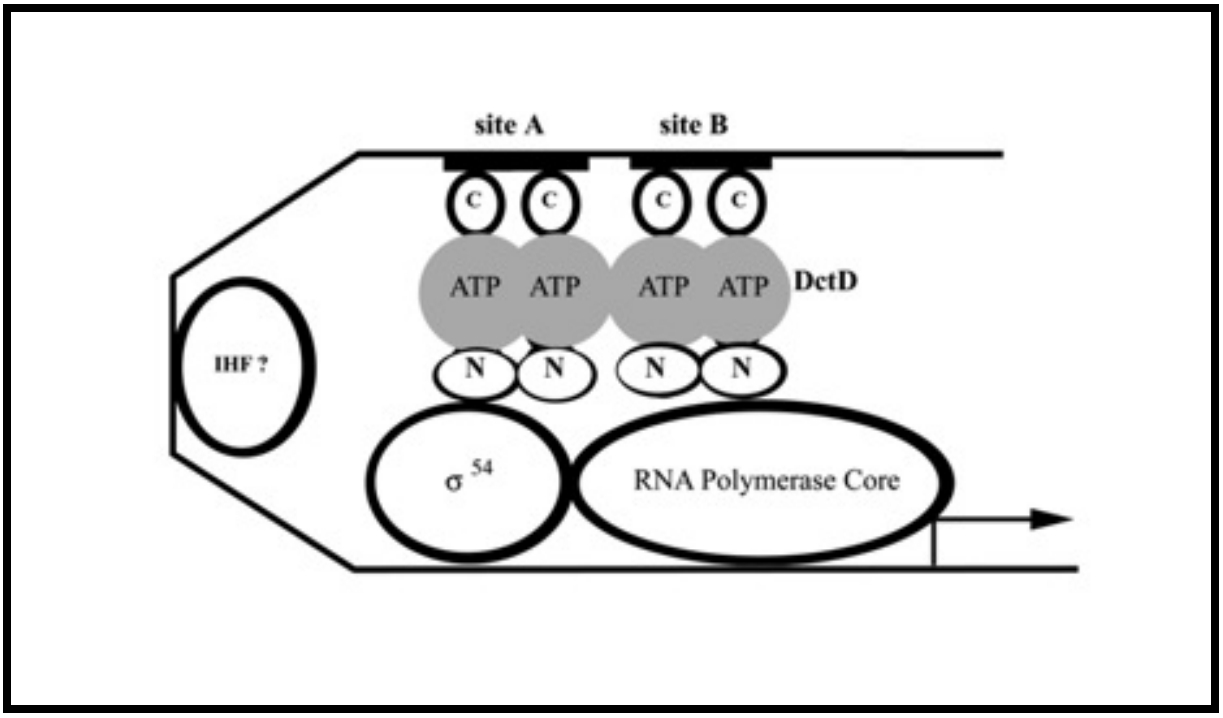

Figure 1.12: Transcriptional activation of *dctA*. DctD dimers bind to upstream activating sequences at -110 and -143. Each subunit has three domains, an amino terminus (N), an ATP binding site (ATP), and a carboxy terminus (C). These proteins interact with RpoN (σ_{54}). Depending upon the bacterial species, integration host factor (IHF) may be involved [263]

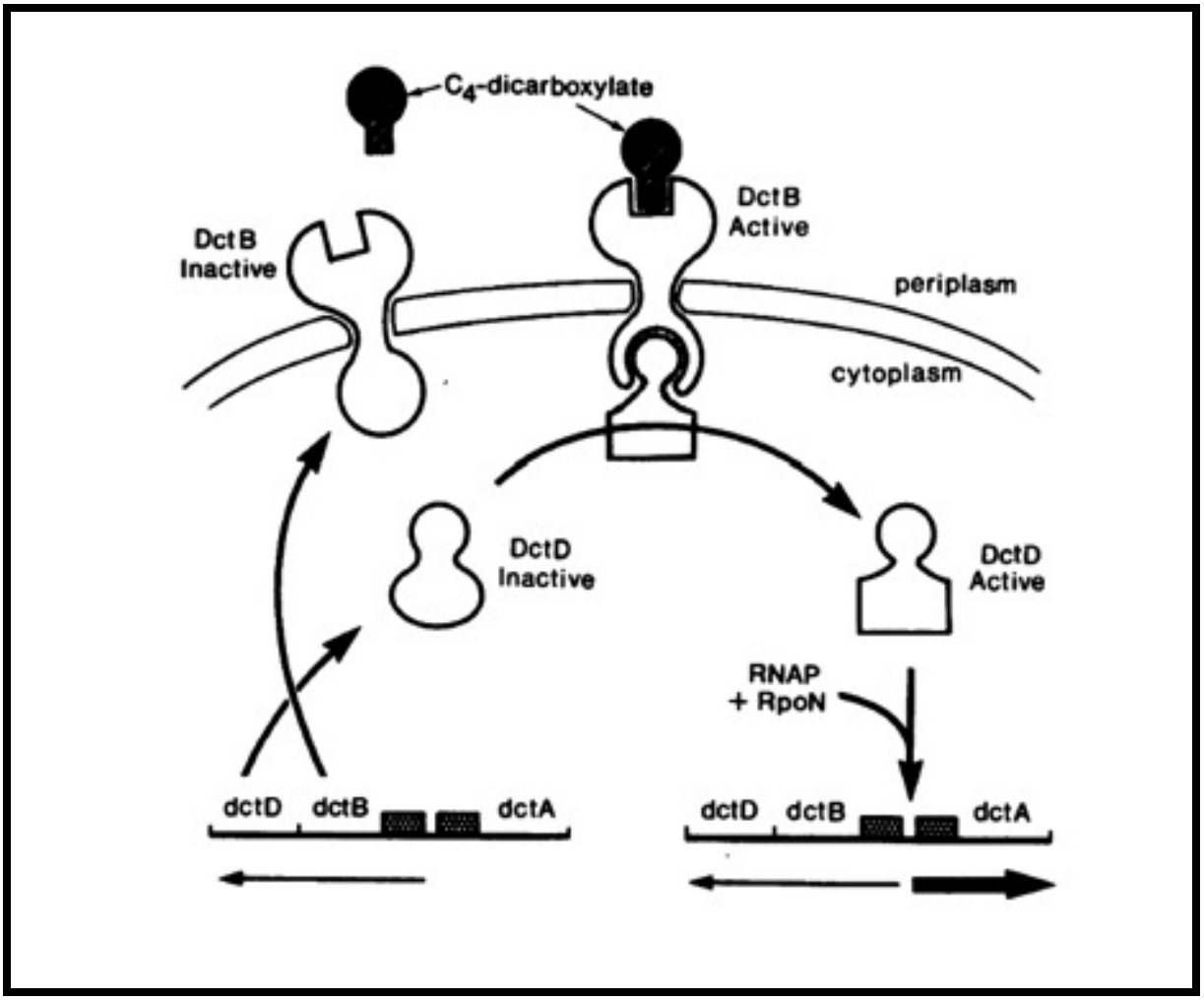

Figure 1.13: Model for the transcriptional activation of *dctA* [294]

1.4 Exopolysaccharides and the Rhizobium-Legume Symbiosis

Exopolysaccharides (EPSs) are species- and strain-specific heteropolysaccharides that are secreted into the surrounding environment. They perform a number of non-specific functions including stress-protection, surface-attachment and nutrient-gathering (reviewed in [102]) as well as a significant role in the establishment of the nitrogen-fixing symbiosis Figure 1.4. Rhizobial EPSs are structurally diverse, exhibiting considerable variability in sugar composition, linkages, repeating unit size, degree of polymerization and non-carbohydrate decoration (reviewed in [317]).

S. meliloti synthesizes two main groups of exopolysaccharides, succinoglycans (EPSI) and galactoglucans (EPSII). Succinoglycan (EPSI) is one of the most well characterized rhizobial EPS molecules. It consists of an octasaccharide repeating unit of one galactose monomer and seven glucose residues joined by β-1,3, β-1,4 and β-1,6 glycosidic linkages [288]. Galactoglucans (EPSII) are structurally distinct from succinoglycans and are synthesized only under conditions of phosphate limitation [401] or mutation of the regulatory genes *mucR* or *expR* [113, 183, 265, 402]. Galactoglucan is a polymer of disaccharide repeating subunits of an acetylated glucose and one pyruvylated galactose joined by an α-1,3 and a β-1,3 glycosidic bond [146]. Both EPSI and EPSII are synthesized in high- and low-molecular weight forms, depending on the degree of subunit polymerization. High-molecular weight (HMW) forms are typically 10^6–10^7 Da in mass, while low-molecular weight (LMW) forms exist as monomers, dimers, and trimers (reviewed in [317]).

The precise biological function of EPS in symbiosis is not well understood, however the essential role it plays is without question. The *S. meliloti* wild-type strain Rm1021 synthesizes only one symbiotically active exopolysaccharide, succinoglycan. Succinoglycan biosynthesis is controlled, through the expression of *exo* genes,

by the ExoS/ChvI two-component regulatory system [51].

Strain Rm1021 is unable to synthesize EPSII because the *expR* gene required for upregulation of symbiotically active galactoglucan is disrupted by an insertion sequence (IS) element [265]. The *expR* gene product is a LuxR homologue that is required for the activation of the *exp* genes in a cell density-dependent fashion via the ExpR/Sin quorum-sensing system [150, 265]. The ExpR/Sin quorum-sensing system is known to regulate the expression of over 200 genes under both free-living and symbiotic conditions [150]; interestingly it is also responsible modulating succinoglycan biosynthesis [118]. *S. meliloti* Rm1021 requires an active succinoglycan biosynthesis pathway in order to initiate a successful symbiosis (reviewed in [102]); however, induction of LMW EPSII is sufficient to complement the nod$^-$ phenotype of a succinoglycan biosynthesis mutant [119].

1.5 Desiccation Tolerance and On-Seed Survival of Rhizobia

The Rhizobia, like most Gram-negative bacteria, are extremely sensitive to desiccation [374]; there is significant evidence to suggest that this is the main cause of on-seed death in inoculant preparations [37, 38, 145, 222, 303, 304, 374]. It has been shown in multiple Rhizobium species that death occurs very rapidly upon application to the seed, and is concomitant with the rate of moisture loss from the surface of the seed [37, 38, 296, 303]. It has also been demonstrated that the rate of death, following application to the seeds, can be reduced by co-inoculation with a compound designed to protect the bacterium from desiccation [303]. Desiccation causes changes to occur in the cytoplasmic membrane of the cell that presumably result in leakage of cellular material beyond a critical level required for viability

[37, 38, 303, 304]. Relative humidity during storage can dramatically influence the rate of survival of the bacterium [67, 374]. A study using *R. leguminosarum* bv. *trifolii* showed that cells survived best at 100% relative humidity, and that at 60% relative humidity, no viable cells were detected after 27 hours [67]. It is possible that at high humidity levels, bacterial cells in general are metabolically able to maintain a tolerable water balance through *de novo* synthesis of compatible solutes [67]. Compatible solutes – including potassium ions, glutamate, glutamine, quaternary amines (glycine betaine), proline, and the sugars trehalose and glucosylglycerol [273] – help to maintain the water balance of the cell by means of preferential exclusion, creating an environment that facilitates the preferential hydration and consequent stabilization of cellular proteins [273]. When no water is available in the immediate environment surrounding the bacteria, the cells cannot rely on these mechanisms of preferential exclusion, and are thus more susceptible to desiccation [67].

1.5.1 The Physiological Process of Desiccation

In order to survive desiccation, bacterial cells must be able to tolerate a number of different physiological stressors including radiation, reactive oxygen species (ROS), salts and solutes and temperature fluctuations [23, 67, 273, 283, 385]. The desiccation process can be broken down into three main phases: drying (phase I), storage (phase II), and rewetting (phase III), all of which may be manipulated in several ways (reviewed in [376]) as depicted in Figure 1.14.

The rate of drying has a large impact on cell survival, with fast drying resulting in more extensive and rapid cell death [10, 38], suggesting that the physiological response to desiccation is adaptive. Water loss leads to an increase in the concentration of salts and solutes, resulting in osmotic stress. Although osmotic stress

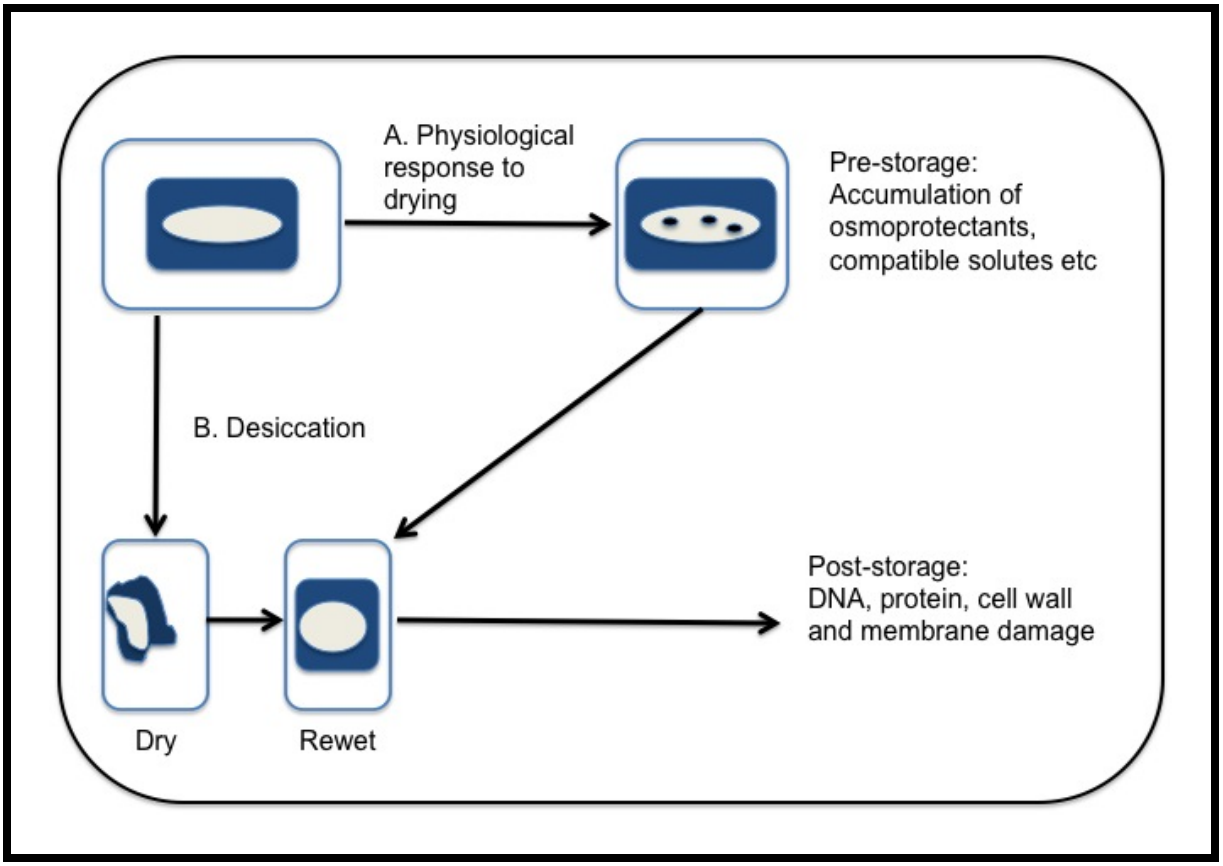

Figure 1.14: Model of two possible pathways for rhizobial response to desiccation stress and desiccation-induced damage. Pathway A depicts a response to water, osmotic, or salt stress. Pathway B outlines the cellular response to desiccation-induced stress upon rewetting (modified from [376])

and desiccation stress are different phenomena, the relationship between the two is undeniable and studies have shown that relationships between the two do exist [50]. During storage, the water phase in the bacterial cells reaches equilibrium with the surrounding gas phase so further desiccation is halted. During this time, the viable population of cells typically declines, although the rate of decline can be decreased by maintaining higher levels of relative humidity [222, 224]. Following storage, the rewetting process can have a significant effect on survival rates. After rewetting, cellular metabolism restarts and the accumulated damage is repaired. If rewetting is too rapid it can induce significant disruption to the cell envelope [37, 304], resulting in cell death; slower rehydration has been shown to considerably increase survival [194].

Some of the more well characterized determinants for survival under conditions of desiccation stress are depicted in Figure 1.14, and are discussed in more detail in subsequent sections. The response to desiccation has to occur prior to actual desiccation occurring. Cells must have sufficient time to sense and respond to a decrease in water activity [376]. The mechanisms employed by the cells upon sensing the onset of desiccation are outlined in Pathway "A" in Figure 1.15. In this pathway, desiccation induces a physiological "preceding storage" response to desiccation resulting in increased long-term survival. Pathway "B" in Figure 1.15 demonstrates an alternative pathway that is induced upon rewetting. Damage can only be repaired when the water activity is sufficiently high to support cellular metabolism. It is conceivable that some combination of these two pathways might exist in all rhizobia.

1.5.1.1 The Role of Trehalose as an Osmoprotectant

There has been significant discussion of the role of trehalose, a non-reducing disaccharide of glucose, in increasing desiccation tolerance of bacterial cells, including

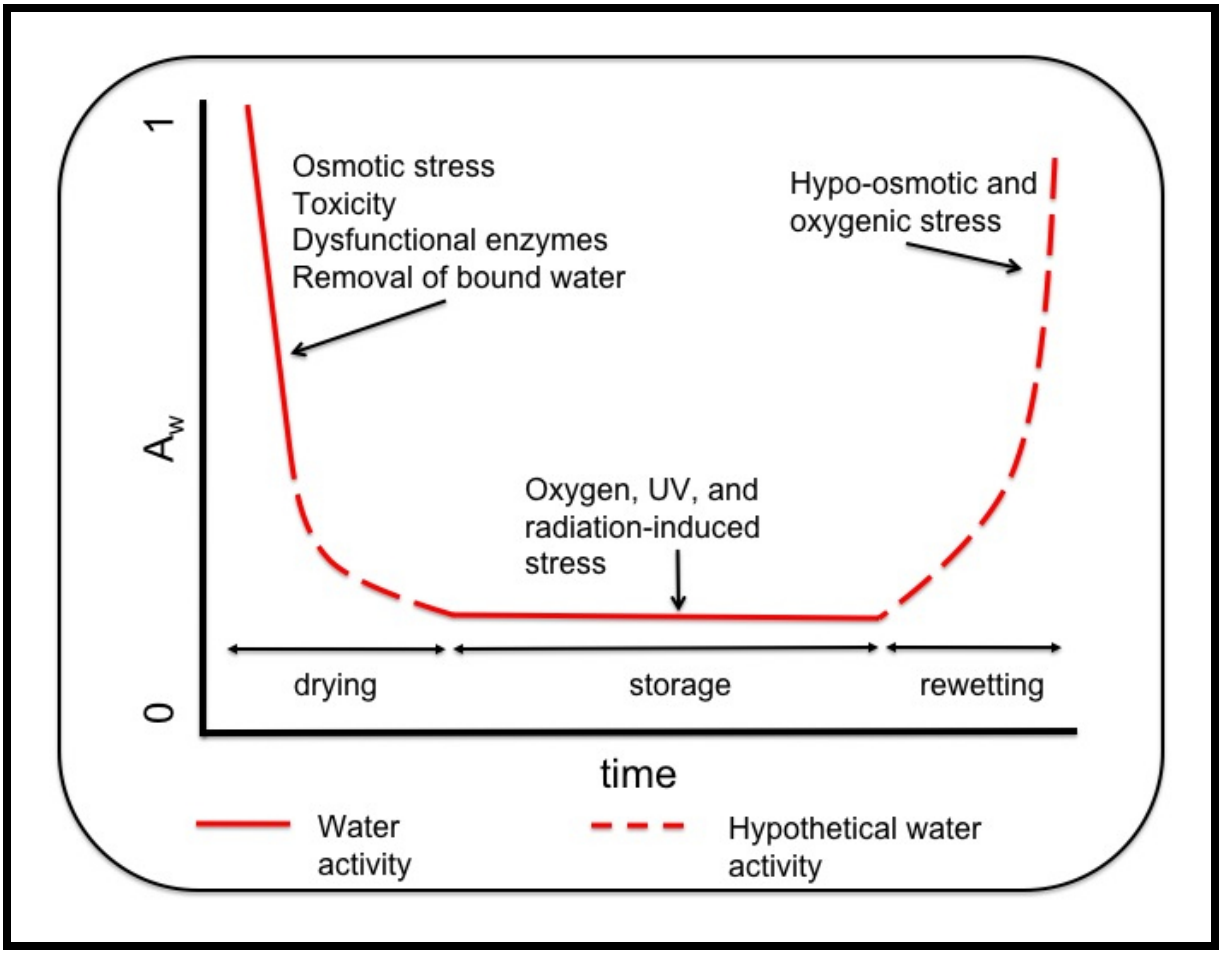

Figure 1.15: The relationship between water activity (A_w) and time during bacterial desiccation, highlighting the three main phases of drying (modified from [376])

rhizobia [62, 124, 166, 273, 332, 340]. Under low-stress conditions, *S. meliloti* can utilize trehalose as its sole carbon source [29]. Under certain high-stress conditions, including osmotic stress, *S. meliloti* synthesizes and accumulates trehalose, which can serve as a compatible solute [29, 88, 152, 166]. Upon dehydration, biological membranes typically experience significant, irreversible changes in their structural and functional integrities [61]. In organisms capable of surviving complete dehydration (the so-called anhydrobiotic organisms) trehalose can constitute up to 20% of the dry weight of the cell, and up to 95% of the cellular carbohydrate content [208, 333, 332]. In these organisms, no changes are observed in membrane integrity following dehydration and subsequent rehydration, suggesting that trehalose may play a role in protecting membranes from damage during these processes [61]. Furthermore, at physiological concentrations, trehalose is the only carbohydrate known to be able to stabilize membrane structure under conditions of sub-optimal dehydration [61]; addition of trehalose to dry phospholipid membranes elicits a response that mimics that seen upon addition of water [61]. Although the precise mechanism by which trehalose stabilizes biomolecules remains unclear, several hypotheses have been proposed to explain its protective effect [270]. The water-replacement hypothesis suggests that sugar molecules can substitute for water molecules by forming hydrogen bonds around the polar and charged groups of the phospholipid membrane, thus stabilizing the native structure of the membrane in the absence of water [62, 61, 208, 270]. In contrast, the water-entrapment hypothesis proposes that sugar molecules act to concentrate the remaining water molecules around individual cellular components, maintaining localized solvation and protecting the structural integrity of the membranes and proteins [208, 270]. It is likely that both of these proposed mechanisms might have a role to play in osmoprotection and that they are not mutually exclusive [270]. The cost of using trehalose as an additive in the formulation of inoculants is likely to be prohibitive; however, the possibility of

engineering rhizobial strains that can synthesize higher intrinsic levels of trehalose under physiological conditions may hold some promise for improving OSS rates.

1.5.1.2 The Role of Exopolysaccharides in Desiccation Tolerance

Microorganisms also respond to desiccation stress by changing the structure of the cell surface. The production of an exopolysaccharide (EPS) matrix surrounding the cell membrane may slow the rate of moisture loss under dry conditions [139, 291, 389] although data to support this argument is conflicting [37, 139]. Reducing the rate by which the cell loses moisture would increase the time available for metabolic adjustment. The EPS of a *Pseudomonas phbC* species has been shown to hold several times its own weight in water at low water potentials, presumably increasing the water availability to the bacterium, and creating a controlled microenvironment in order to increase its chances of survival [291].

Adaptations to the polysaccharide composition of *S. meliloti* cells undergoing osmotic stress and desiccation have been observed in previous studies [30, 210, 266], but again, results have been conflicting [39, 225, 259]. The mechanism by which EPS may be expected to confer protection against desiccation remain unclear, although it is reasonable to expect that the specific properties of individual polysaccharides may be a major determinant (reviewed in [273]). As discussed in Section 1.4, *S. meliloti* synthesizes two main groups of EPS, both of which can be affected by the growth conditions (reviewed in [376]).

1.5.1.3 The Role of Oxygen on Survival

Reactive oxygen species (ROS) are by-products of the electron transport chain. As rhizobia downregulate their metabolic activity in response to desiccation, they might reasonably be expected to experience ROS-induced cellular damage as a

result of free-radical production [376]. Indeed, previous studies have shown that rhizobia are sensitive to O_2 during desiccation [223, 258, 374]. Oxygen is believed to become toxic to rhizobia at relative humidities below 70% [67]; dried cells appear to have protective mechanisms against ROS so long as the relative humidity is sufficient to permit cellular metabolism [376].

1.5.2 An Introduction to Rhizobial Inoculants

The use of exogenously supplied Rhizobium as a means of decreasing reliance upon industrial fertilizers has been a topic of discussion for many years. Most legume-Rhizobium interactions are species-specific, and ensuring that the appropriate rhizobial species is able to infect and nodulate the host legume is vital. The aim of inoculation with Rhizobium is to permit maximum nodulation and N_2-fixation by providing sufficient levels of viable, effective Rhizobium of the appropriate species; to permit rapid colonization of the rhizosphere; and to facilitate nodulation as early as possible following germination [33, 42, 67]. In a successful inoculation, the bacteria become established in the rhizosphere surrounding the seed, out-compete the indigenous microflora and, upon germination of the host plant, initiate symbiosis [226, 251, 316]. The mode of delivery of viable bacterial inoculants into the soil however, has remained a central problem in the development of a widespread, commercially feasible product [32, 33, 42, 145, 226, 227, 279, 332, 342, 355]. Application of the bacteria directly on to the seed appears to be one of the most attractive methods of inoculation and has thus far proved to be the most economically viable [226, 251, 316]. Studies investigating the viability of bacteria following application to seeds however, showed very low levels of survival (Table 1.2), greatly narrowing the planting window following inoculation [34, 67]. A variety of methods are currently used to inoculate seeds but most of them require inoculation almost immediately prior to planting which, although effective, is often cumbersome and

requires the use of specialized equipment. As a result, there is a growing demand in the market for pre-inoculated seed that can be purchased from the supplier with a long planting window that would allow for greater flexibility in planting times [67].

As mentioned previously, the major limiting factor in the performance of pre-inoculated seed is the ability of the bacteria to survive following application onto the seeds. In one experiment, a 95% loss in bacterial viability was seen during the first four hours post-application to the seeds and prior to planting; of the surviving 5%, a further 83% died within the first 22 hours of planting [296]. Currently, the longest planting window is that of alfalfa seeds inoculated with *S. meliloti* which, in certain formulations, can survive on-seed for up to 24 months (Table 1.2). The superior OSS of *S. meliloti* provides a more efficient transfer of inoculant to the field, coupled with greater flexibility for planting, making it an attractive commercial product. The high OSS means that *S. meliloti* inoculants can be applied to alfalfa seeds prior to market, allowing for immediate planting by the grower and negating the need for specialized equipment for inoculant application. Furthermore, the OSS rates of *S. meliloti* provide the added convenience of delaying planting if needed (e.g. for bad weather) without having to re-inoculate the seeds.

1.5.3 Commercial Viability of Rhizobial Inoculants

In North America alone, in excess of 76 million acres are planted with soybeans and peas, and a further 5 million acres are planted with lentils [325, 362]. Currently, less than 20% of this acreage is inoculated, presenting a growth potential of up to 5-fold. Assuming a manufacturer's return of $1.25 per acre, this represents a potential profit of over $75 million if all legumes were inoculated. Studies analysing the return-on-investment (ROI) of inoculation for farmers have largely been conducted by individual inoculant companies, and unbiased data is therefore scarce. A recent

study at the Ohio State University investigating soybean yield following inoculation by a range of commercially available inoculants however, reported that the practice of inoculation was indeed profitable to the farmer [21]. This study, using 66 separate field trials and 7000 individual plots, evaluated the effects of inoculation on soybean yield over a period of ten years, and concluded that inoculation was indeed a profitable practice for the farmer with an average yield increase of 2-7 bu/acre, translating to an ROI of over 300% [21]. Given the low cost of inoculant however, even a small increase in yield of just 0.5 bu/acre is typically enough for the grower to see an ROI [21]; therefore, a potential market exists for a soybean inoculant product with an extended shelf-life that can be sold directly to the growers.

Worldwide, the potential benefits of inoculation technologies are extensive and go beyond the environmental benefits outlined in Section 1.1. In Europe, where the use of genetically modified crops is controversial, inoculation represents a technology that has the benefit of reducing reliance upon environmentally damaging fertilizers without altering the genome of the legume crop itself. The most exciting use of improved inoculants lies in the developing world however, where crop yields are typically insufficient to support the populations that depend on them. Currently, 852 million people in the world are hungry, and over 5 million children die each year as a result of starvation and/or malnutrition [361, 361]. Inoculants represent a relatively inexpensive ($2-$3 per acre, compared to $20-$30 per acre for nitrogen fertilizers) [151] and far more efficient means of introducing nitrogen into the soil than inorganic fertilizers [105, 227]. Rhizobial inoculants therefore represent a potential means of increasing crop production and promoting self-sufficiency in regions currently dependent upon outside aid.

Currently, inoculant technologies are not sufficiently robust to be used in many of the developing countries that would benefit most from them. These countries are often hot, lack properly refrigerated storage facilities, have poor infrastructure, and

lack personnel with expertise and training in modern agricultural practices [250]. To circumvent the problems presented by lack of training, and the requirement for modern machinery, inoculant would ideally be supplied on-seed; however, the lack of storage facilities and lengthy transit times to reach the farmers is prohibitive, given the rapid decline in viability of on-seed inoculants. If inoculant technologies can be improved to increase the planting window post-application to the seed, the potential benefits to developing countries would be huge.

Although improvements in the shelf-lives of liquid inoculants have been made over the past few years, no significant advances towards improving OSS of the bacteria have been reported [42]. Interestingly, most of the advances that have been made in inoculant technology have been at the nutritional level, and have focused on the composition of the inoculant formulae. Very few studies appear to have been conducted at the molecular level to investigate the genetic factors affecting OSS [42]. There appear to be significant differences between rhizobial species with respect to their OSS characteristics [222, 303], although definitive studies have not been conducted and data in the literature for individual strains is often conflicting, presumably due to differences in experimental approaches [222].

1.6 Objectives of This Study

Initially the goal of this study was to characterize the on-seed survival phenotypes of several rhizobial isolates and to identify the genetic determinants of desiccation tolerance in rhizobia in order to improve the formulations of commercial inoculants. Since earlier work by our industrial partner, Agribiotics, had identified a potential link between PHB synthesis and enhanced desiccation tolerance, we sought to better understand this relationship through mutant construction and analysis in both *S. meliloti* and *B. japonicum*. Agribiotics was sold mid-way through this project and

the company's operations were moved to the United States. As a result, the focus of the project moved away from desiccation tolerance and toward the analysis of carbon metabolism, which proved easier to study with the facilities that were at our disposal at the University of Waterloo.

Table 1.2: Planting windows for commercial inoculant products

Inoculant	Crop	Product	Planting window
Bradyrhizobium japonicum	Soybean	liquid	1-30 days
		peat	2 days
Rhizobium leguminosarum	Pea/lentil	liquid	1 day
		peat	2 days
Sinorhizobium meliloti	Alfalfa	Clay	24 months

Chapter 2

Methods and Materials

2.1 Bacterial Strains and Plasmids

A complete list of strains and plasmids used in this study is shown in Table 2.1

2.2 Bacterial Growth and Storage Conditions

All growth media recipes and appropriate antibiotic concentrations are listed in Appendix A.1.

Escherichia coli strains were routinely grown at 37°C using Luria-Bertani (LB) media [307].

Sinorhizobium meliloti strains were routinely cultured at 30°C in either LB [307] or TY [20] media. When *S. meliloti* was grown in modified M9 [243] or Rhizobium Minimal Medium (RMM) [76] the medium was supplemented with 15 mM glucose, D-3-hydroxybutyrate (D3HB), L-3-hydroxybutyrate (L3HB), DL-3-hydroxybutyrate (DLHB), acetoacetate (AA) or acetate as the carbon source. For

growth under high carbon conditions, *S. meliloti* was cultured in Yeast Mannitol (YM) medium.

Bradyrhizobium japonicum strains were routinely cultured at 30°C in Arabinose Gluconate (AG) medium. When minimal media was required, *B. japonicum* was grown in Vincent's Minimal Medium (VMM), which contains very low levels of salt. VMM was supplemented with 15 mM D3HB, AA, acetate, arabinose, mannitol, lactose or glucose. For growth under high carbon conditions, *B. japonicum* was grown in Modified AG (MAG).

Antibiotics were used in the growth media where appropriate. All antibiotics used, and their respective concentrations, are listed in Appendix A.1.2.

All bacterial cultures were stored at -80°C in glass cryovials containing 20% v/v glycerol.

To screen for the presence of intracellular PHB, 400 μl 25 mM Nile Red mixed in DMSO [323] was added to the growth medium.

2.2.1 Isolation of Spontaneous Antibiotic-Resistant Derivatives

To isolate spontaneous antibiotic-resistant derivatives of particular strains, the strain of interest was grown to late-log phase. 1 ml of the original culture was harvested by centrifugation, resuspended in 100 μl 0.85% NaCl and the full volume was subsequently plated on media containing the antibiotic in question. Following incubation, colonies that grew up on the selective were restreaked three times on the selective medium.

Table 2.1: Bacterial strains, plasmids and phage constructed and/or used in this study

Strain or Plasmid	Relevant Characteristics	Reference
E. coli		
DH5α	F' *endA1 hsdR17* ($r_K m_+$) *supE44* thi^{-1} *recA1 gyrA* Nal^R *relA1* Δ(*lacIZYA-argF) U169 deoR* (ϕ80*dlac*Δ(*lacZ*)M15)	[136]
MT607	*pro-82 thi-1 hsdR17 supE44 recA56*	[96]
MT616	MT607 pRK600	[96]
HB101	*supE44 hsdS20 recA13 ara-14 proA2 lacY1 galK2 rpsL20 xyl-5 mtl-1* r^- m^-	[136]
BL21 (λDE3)	F^- *ompT* $hsdS_B$ (r_{B-}, m_{B-}) *dcm gal* λDE3	[64, 334]
B. japonicum		
USDA110	wild-type	USDA, Beltsville MD
BjUW1	USDA110 pMA105	This Work
BjUW2	USDA110 pMA106	This Work
BjUW4	USDA110 pMA108	This Work
BjUW5	USDA110 pMA109	This Work
BjUW8	USDA110 ΔBlr2885	This Work
BjUW9	USDA110 ΔBlr3732	This Work
BjUW10	USDA110 pMA107 #1	This Work

Continued on Next Page...

Table 2.1 – continued from previous page

Strain or Plasmid	Relevant Characteristics	Reference
BjUW11	USDA110 pMA107 #2	This Work
BjUW12	USDA110 pMA108	This Work
BjUW13	USDA110 ΔBll6073	This Work
BjUW14	USDA110 pMA109	This Work
BjUW15	USDA110 ΔBll0225 and ΔBll0226	This Work
BjUW16	USDA110 ΔBlr3725 and ΔBlr3726	This Work
BjUW17	USDA110 ΔBlr3725 and ΔBlr3726 #2	This Work
BjUW18	BjUW9 pMA107 #1	This Work
BjUW19	BjUW9 pMA107 #2	This Work
BjUW20	BjUW16 pMA110#1	This Work
BjUW21	BjUW16 pMA110#2	This Work
BjUW22	BjUW15 pMA111#1	This Work
BjUW23	BjUW15 pMA110#2	This Work
BjUW24	BjUW9 pMA111#1	This Work
BjUW25	BjUW9 pMA111#2	This Work
BjUW26	BjUW9 pMA105#1	This Work
BjUW27	BjUW9 pMA105#2	This Work
BjUW28	BjUW9 ΔBlr2885 #1	This Work
BjUW29	BjUW9 ΔBlr2885 #2	This Work

Continued on Next Page...

Table 2.1 – continued from previous page

Strain or Plasmid	**Relevant Characteristics**	**Reference**
BjUW30	BjUW9 ΔBlr3725 and ΔBlr3726 #1	This Work
BjUW31	BjUW9 ΔBlr3725 and ΔBlr3726 #2	This Work
BjUW32	BjUW15 ΔBlr3725 and ΔBlr3726 #1	This Work
BjUW33	BjUW15 ΔBlr3725 and ΔBlr3726 #2	This Work
BjUW34	USDA110 pMA176 single recombinant	This Work
BjUW36	Spontaneous Sm^R-derivative of USDA110	This Work
BjUW37	USDA110 pMA175 single recombinant	This Work
BjUW40	USDA110 pMA221 single recombinant	This Work
BjUW41	USDA110 pMA221 single recombinant	This Work
BjUW42	USDA110 pMA222 single recombinant	This Work
BjUW43	USDA110 pMA222 single recombinant	This Work
BjUW44	USDA110 pMA223 single recombinant	This Work
BjUW45	USDA110 pMA223 single recombinant	This Work
BjUW46	USDA110 pMA225 single recombinant	This Work
BjUW47	USDA110 pMA225 single recombinant	This Work
BjUW48	USDA110 pMA224 single recombinant	This Work
BjUW49	USDA110 pMA224 single recombinant	This Work
BjUW50	USDA110 pMA227 single recombinant	This Work
BjUW51	USDA110 pMA227 single recombinant	This Work

Continued on Next Page...

Table 2.1 – continued from previous page

Strain or Plasmid	**Relevant Characteristics**	**Reference**
BjUW52	USDA110 pMA232 single recombinant	This Work
BjUW53	USDA110 pMA232 single recombinant	This Work
BjUW54	USDA110 pMA232 single recombinant	This Work
S. meliloti		
Rm5000	SU47 *rif5*	[95]
Rm1021	SU47 str-21, Sm^R	[236]
RmP110	Rm1021*pstC*$^+$	[58]
RCR2011	SU47 wild-type	[373]
Rm2011	SU47 *str-21*, Sm^R	[236]
Rm41	*S. meliloti* wild-type isolate	[281]
102-F34	wild-type strain	[72]
102-F51	wild-type isolate of *S. meliloti*	[260]
AK631	Rm41 *exoB631*	[100]
CC2013	wild-type isolate of *S. meliloti*	[83]
104A14	wild-type isolate of *S. meliloti*	[322]
Sinorhizobium sp. strain BL3	wild-type strain, highly salt-tolerant. Isolated from Thailand. Rf^R, Sm^R	[345]
Sinorhizobium sp. NGR234	Broad-host range *Sinorhizobium* isolate	[354]

Continued on Next Page...

Table 2.1 – continued from previous page

Strain or Plasmid	**Relevant Characteristics**	**Reference**
Rm7055	Rm1021 *exoY*::Tn*5*	[207, 244]
Rm7022	Rm1021 *exoE*::Tn*5*	[207]
Rm7053	Rm1021 *exoD*::Tn*5*	[207]
Rm8002	Rm1021 *phoA*	[214]
Rm8369	Rm8002 *exoF*369::Tn*phoA*	[215]
Rm11105	Rm1021 *phbC*1::Tn*5*	[46]
Rm11107	Rm1021 *bdhA*1::Tn*5*	[46]
Rm11144	Rm1021 *phbC*1::Tn*5*-233	[46]
Rm11347	Rm1021 *phbB*::ΩSmSp	[7]
Rm11377	Rm1021 *ace8*::Tn*5*	Charles Lab, Unpublished
Rm11378	Rm1021 *ace9*::Tn*5*	Charles Lab, Unpublished
Rm11379	Rm1021 *ace11*::Tn*5*	Charles Lab, Unpublished
Rm11405	Rm1021 putative purine metabolism mutant	Charles Lab, Unpublished
Rm11417	Rm5000 *phaZ*::ΩSmSp	This work
Rm11430	Rm1021 *phaZ*::ΩSmSp	This work

Continued on Next Page...

Table 2.1 – continued from previous page

Strain or Plasmid	**Relevant Characteristics**	**Reference**
Rm11478	*glgA2*::ωSpSm	[378]
Rm11479	*glgA1*::ΔPstI *glgA2*::ωSpSm	[378]
Rm11482	*glgA1*::ΔPstI	[378]
SmUW1	Rm1021*pstC*$^+$ *nolR*$^+$	Charles Lab, Unpublished
SmUW3	Rm1021 *expR*$^+$ *nolR*$^+$ *pstC*$^+$	Charles Lab, Unpublished
SmUW6	Rm1021 *expR*$^+$	Charles Lab, Unpublished
SmUW13	ϕ-Rm7055 transduced into SmUW6	Charles Lab, Unpublished
SmUW24	ϕ-Rm7055 transduced into SmUW6	Charles Lab, Unpublished
SmUW33	ϕ-Rm11105 transduced into SmUW3	This Work
SmUW34	ϕ-Rm11107 transduced into SmUW3	This Work
SmUW35	ϕ-Rm11347 transduced into SmUW3	This Work
SmUW36	ϕ-Rm11430 transduced into SmUW3	This Work
SmUW41	Δ*phbA* Mutant	This Work
SmUW81	SB100 *phaZ*::ΩSmSp	This work

Continued on Next Page...

Table 2.1 – continued from previous page

Strain or Plasmid	**Relevant Characteristics**	**Reference**
SmUW83	SB104 *phaZ*::ΩSmSp	This work
SmUW85	SB108 *phaZ*::ΩSmSp	This work
SmUW178	Rm1021 *phbC gfp lacZ* single recombinant of pMA233	This Work
SmUW180	Rm1021 *phbC gusA* single recombinant of pMA234	This Work
SmUW182	Rm1021 *phbAB gfp lacZ* single recombinant of pMA235	This Work
SmUW184	Rm1021 *phbAB gusA* single recombinant of pMA236	This Work
SRmA102	*S. meliloti* isolate	I. Oresnik
SmA818	pRme2011a-cured strain of *S. meliloti* Rm2011	[256]
S. meliloti-042BM	salt-tolerant wild-type strains	[383]
RmF114	Rm1021 Δω5033-5064::Tn*5*-233	[47]
RmF117	Rm1021 Δω5060-5033::Tn*5*-233	[47]
RmF121	Rm1021 *dctD16*::Tn*5*	[97]
RmF153	Rm1021 *dctB12*::Tn*5*-132	[392]
RmF506	Rm1021Δ ω5040::Tn*5*-233 ΔG506	[47]
RmF514	Rm1021 Δω5061-5047::Tn*5*-11	[47]
RmF642	Rm1021 *dctA14*::Tn*5*	[394]
RmF638	Rm1021 Δω5145-5061::Tn*5*-233	[47]
RmF666	Rm1021 Δω5146-5111::Tn*5*-233	[47]
RmF680	Rm1021 Δω5146-5111::Tn*5*-233	[47]

Continued on Next Page...

Table 2.1 – continued from previous page

Strain or Plasmid	**Relevant Characteristics**	**Reference**
RmF693	Rm1021 Δω5085-5142::Tn*5*-233	[47]
RmF726	Rm1021Δ ω5085-5061::Tn*5*-233	[47]
RmF728	Rm1021Δ ω5177-*lac-56*::Tn*5*	[47]
RmF332	Rm1021 *dctA*::Tn*5*	[97]
RmF909	Rm1021 Δω5085-5047::Tn*V*	[47]
RmF930	Rm1021 *nifA239*::Tn*5*	Charles Lab, Unpublished
RmF932	Rm1021 *ntrC*::Tn*r*	Charles Lab, Unpublished
RmG270	Rm1021 ω5033-5007::Tn*5*-233 ω5085-5047::Tn*5*-Tp	[44]
RmG271	Rm1021 Δω5033-5007::Tn*V* 5149-5079::Tn*5*-233	[44]
RmG277	Rm1021 Δω5020-5011::Tn*5*-*oriT* 5149-5079::Tn*5*-233 ω5085-5047::Tn*5*-Tp	[44]
RmG373	Rm1021 Δ ω5177-5079::Tn*5*-*oriT*	[47]
RmG462	Rm1021 Δω5011-5033::Tn*5*-*oriT*	[47]
RmG470	Rm1021 Δω5025-5007	[47]
RmG471	Rm1021 Δω5033-5025	[47]
RmG472	Rm1021 Δω5026-5007	[47]
RmG506	Rm1021 Δω5040::Tn*5*-233 G506	[47]

Continued on Next Page...

Table 2.1 – continued from previous page

Strain or Plasmid	**Relevant Characteristics**	**Reference**
Rm5071	Rm5000 *nifH*::Tn*5*	[96]
Rm5378	Rm1021 Δω5020-5011::Tn*5*-*oriT*	[97]
Rm5408	Rm1021 Δω5033-5007::Tn*5*-233	[47]
Rm5416	Rm1021 Δω5007-5011::Tn*5*-233	[97]
Rm5422	Rm1021 *ntrA75*::Tn*5*	[97]
SB100	Rm1021 *phaP1*::pK19 *mob*	[379]
SB104	Rm1021 *phaP2* precise deletion	[379]
SB108	Rm1021 *phaP1 phaP2*	[379]
SMc00880-fg	RmP110 pTH1703-SMc00880-fg	[161]
SMc03878-fg	RmP110 pTH1703-SMc03878-fg	[161]
SMc00880-fl	RmP110 pTH1703-SMc00880-fl	[161]
SMc00136-fl	RmP110 pTH1703-SMc00136-fl	[161]
SMb21010-fg	RmP110 pTH1703-SMb21010-fg	[161]
SMc01571-fl	RmP110 pTH1703-SMc01571-fl	[161]
SMc02271-fl	RmP110 pTH1703-SMc02271-fl	[161]
SMc02271-fg	RmP110 pTH1703-SMcc02271-fg	[161]
SMc00268-fl	RmP110 pTH1703-SMc00268-fl	[161]
SMc02322-fg	RmP110 pTH1703-SMc02322-fg	[161]
SMc02322-fl	RmP110 pTH1703-SMc02322-fl	[161]

Continued on Next Page...

Table 2.1 – continued from previous page

Strain or Plasmid	Relevant Characteristics	Reference
SMc02522-fg	RmP110 pTH1703-SMc02522-fg	[161]
SMc02522-fl	RmP110 pTH1703-SMc02522-fl	[161]
SMc01500-fl	RmP110 pTH1703-SMc01500-fl	[161]
SMc00264-fl	RmP110 pTH1703-SMc00264-fl	[161]
SMc02339-fl	RmP110 pTH1703-SMc02339-fl	[161]
SMa0329-fg	RmP110 pTH1703-SMa0329-fg	[161]
SMa0329-fl	RmP110 pTH1703-SMa0329-fl	[161]
SMb21159-fl	RmP110 pTH1703-SMb21159-fl	[161]
SMb20493-fl	RmP110 pTH1703-SMb20493-fl	[161]
SMa0187-fl	RmP110 pTH1703-SMa0187-fl	[161]
SMa1367-fl	RmP110 pTH1703-SMa1367-fl	[161]
SMa0335-fg	RmP110 pTH1703-SMa0335-fg	[161]
SMa0335-fl	RmP110 pTH1703-SMa0335-fl	[161]
SMc04391-fl	RmP110 pTH1703-SMc04391-fl	[161]
SMc04391-fg	RmP110 pTH1703-SMc04391-fg	[161]
SMa2019-fg	RmP110 pTH1703-SMa2019-fg	[161]
SMa2019-fl	RmP110 pTH1703-SMa2019-fl	[161]
SMa1757-fg	RmP110 pTH1703-SMa1757-fg	[161]
SMa1757-fl	RmP110 pTH1703-SMa1757-fl	[161]

Continued on Next Page...

Table 2.1 – continued from previous page

Strain or Plasmid	**Relevant Characteristics**	**Reference**
SMc00326-fl	RmP110 pTH1703-SMc00326-fl l	[161]
SMc01698-fg	RmP110 pTH1703-SMc01698-fg	[161]
SMc00553-fg	RmP110 pTH1703-SMc00553-fg	[161]
SMb20871-fg	RmP110 pTH1703-SMb20871-fg	[161]
SMc01157	RmP110 pTH1703-SMc01157-fg	[161]
SMc01955	RmP110 pTH1703-SMc01955-fl	[161]
SMa0326	RmP110 pTH1703-SMa0326-fl	[161]
SMc03878-fg	pTH1703-SMc03878-fg	[161]
Plasmids		
pK19*mobsacB*	Suicide vector Km^R	[310]
pGEMTEasy	Cloning vector for PCR-generated DNA fragments, Amp^R	Promega
pJET	Blunt-end cloning vector for PCR-generated DNA fragments, Amp^R	Promega
pET30a-c	Inducible over-expression vector	EMD Chemicals Inc.
pRK7813	RK2 derivative carrying pUC9 polylinker. Tc^R	[169]
pRK2013	ColE1 replicon with RK2 transfer region. Nm-Km^R	[94]
pRK600	pRK2013 *npt*::Tn*5*, Cm^R; Nm-Km^R	[96]
pBBR1-MCS2	Broad-host-range cloning vector, Km^R	[196]

Continued on Next Page...

Table 2.1 – continued from previous page

Strain or Plasmid	**Relevant Characteristics**	**Reference**
pTH1703	pTH1591 carrying EcoRV-XhoI fragment from pTH1726	[58]
pTH1705	pTH1591 carrying EcoRV-XhoI fragment from pTH1728	[58]
pTH1946	Km^R-Nm^R replacing Gm^R in pTH1703	[58]
pTH1947	Km^R-Nm^R replacing Gm^R in pTH1705	[58]
pMA100	pGEMTEasy Blr2885 AD joined fragment	This Work
pMA101	pGEMTEasy Blr3732 AD joined fragment	This Work
pMA102	pGEMTEasy Bll4360 AD joined fragment	This Work
pMA103	pGEMTEasy Bll4548 AD joined fragment	This Work
pMA104	pGEMTEasy Bll6073 AD joined fragment	This Work
pMA105	pK19*mobsacB* Blr2885 AD from pMA100	This Work
pMA106	pK19*mobsacB* Blr3732 AD from pMA101	This Work
pMA107	pK19*mobsacB* Bll4360 AD from pMA102	This Work
pMA108	pK19*mobsacB* Bll4548 AD from pMA103	This Work
pMA109	pK19*mobsacB* Bll6073 AD from pMA104	This Work
pMA110	pK19*mobsacB* Bll0225/Bll0226 AD	This Work
pMA111	pK19*mobsacB* Blr3725/Blr3726 AD	This Work
pMA156	pRK7813 Blr2885	This Work
pMA118	pRK7813 Blr3732	This Work
pMA119	pRK7813 Bll4360	This Work

Continued on Next Page...

Table 2.1 – continued from previous page

Strain or Plasmid	Relevant Characteristics	Reference
pMA120	pRK7813 Bll4548	This Work
pMA121	pRK7813 Bll6073	This Work
pMA122	USDA110 cosmid clone complementing Rmf121#3	This Work
pMA123	USDA110 cosmid clone complementing Rmf121 #4	This Work
pMA124	USDA110 cosmid clone complementing Rmf121 #5	This Work
pMA125	USDA110 cosmid clone complementing Rmf121 #8	This Work
pMA126	USDA110 cosmid clone complementing Rmf153 #2	This Work
pMA127	USDA110 cosmid clone complementing Rmf726	This Work
pMA128	USDA110 cosmid clone complementing Rmf332 #1	This Work
pMA129	USDA110 cosmid clone complementing Rmf332 #2	This Work
pMA130	USDA110 cosmid clone complementing Rmf642 #1	This Work
pMA131	USDA110 cosmid clone complementing Rmf642 #4	This Work
pMA132	USDA110 cosmid clone complementing Rmf642 #5	This Work
pMA133	USDA110 cosmid clone complementing Rmf651 #2	This Work
pMA134	USDA110 cosmid clone complementing Rmf651 #5	This Work
pMA148	pET30a Blr3732	This Work
pMA150	pET30a Bll4548	This Work
pMA152	pET30a Blr2885	This Work
pMA153	pET30b Bll4360	This Work

Continued on Next Page...

Table 2.1 – continued from previous page

Strain or Plasmid	**Relevant Characteristics**	**Reference**
pMA154	pET30b Blr6073	This Work
pMA157	pRK7813 SMc02770	This work
pMA158	pET30b SMc02770	This work
pMA166	pGemTEasy carrying internal Blr3723 fragment	This Work
pMA170	pGemTEasy carrying complete *B. japonicum dctBD* operon	This Work
pMA172	pMA170 with central SgrAI fragment of *dctBD* deleted	This Work
pMA174	pMA172 with ΩSmSp cassette inserted in central EcoRV site of truncated *dctBD*	This Work
pMA175	pK19*mobsacB* carrying Δ*dctBD*ΩSmSp from pMA174	This Work
pMA176	pK19*mobsacB* carrying internal Blr3723 fragment from pMA166	This Work
pMA187	pBBR1MCS2 carrying *phbA* cross-over PCR product	This Work
pMA188	pGEMTEasy carrying *phbA* deletion cross-over PCR product	This Work
pMA190	pK19*mobsacB* carrying *phbA* deletion cross-over PCR product sub-cloned from pMA188	This Work
pMA197	pMA127 Tn*5* inserted into Blr3723	This Work
pMA198	pBBR1MCS2 Blr6145 plus 50 bp upstream sequence	This Work
pMA199	pJET Bll1718 Complete ORF	This Work
pMA200	pJET Bll1718 Truncated ORF	This Work
pMA201	pJET Blr3723 Complete ORF	This Work

Continued on Next Page...

Table 2.1 – continued from previous page

Strain or Plasmid	**Relevant Characteristics**	**Reference**
pMA202	pJET Blr3840 Complete ORF	This Work
pMA203	pJET Blr3840 Truncated ORF	This Work
pMA204	pJET Blr4298 Truncated ORF	This Work
pMA205	pJET Blr6145 Truncated ORF	This Work
pMA206	pJET Bll7095 Complete ORF	This Work
pMA207	pJET Bll7095 Truncated ORF	This Work
pMA208	pJET Blr4298 Complete ORF	This Work
pMA209	pSW213 Blr3723 from pMA201	This Work
pMA210	pSW213 Blr3840 from pMA202	This Work
pMA211	pSW213 Blr4298 from pMA208	This Work
pMA212	pJET Blr6145 Complete ORF	This Work
pMA214	pSW213 Bll7095 from pMA206	This Work
pMA216	pSW213 Blr6145 from pMA212	This Work
pMA217	pSW213 Bll1718 from pMA199	This Work
pMA219	pJET Blr7187 Truncated ORF	This Work
pMA220	pJET Blr7187 Complete ORF	This Work
pMA221	pK19*mob* Bll1718 Truncated from pMA200	This Work
pMA222	pK19*mob* Bll7095 Truncated from pMA207	This Work
pMA223	pK19*mob* Blr6145 Truncated from pMA205	This Work

Continued on Next Page...

Table 2.1 – continued from previous page

Strain or Plasmid	**Relevant Characteristics**	**Reference**
pMA224	pK19*mob* Blr7187 Truncated from pMA219	This Work
pMA225	pK19*mob* Blr3840 Truncated from pMA203	This Work
pMA226	pSW213 Blr7187 from pMA220	This Work
pMA227	pK19*mob* Blr4298 Truncated from pMA204	This Work
pMA228	pJET *S. meliloti phbC* ORF	This Work
pMA229	pJET *S. meliloti phbA* ORF	This Work
pMA230	pJET *S. meliloti phbB* ORF	This Work
pMA231	pJET *S. meliloti phbAB* operon ORF	This Work
pMA233	pTH1703 *S. meliloti phbC gfp lacZ* subcloned from pMA228	This Work
pMA234	pTH1703 *S. meliloti phbC gusA* subcloned from pMA228	This Work
pMA235	pTH1703 *S. meliloti phbAB gfp lacZ* subcloned from pMA231	This Work
pMA236	pTH1703 *S. meliloti phbAB gusA* subcloned from pMA231	This Work
pAZ101	pGEMTeasy carrying 835 bp fragment of SMc02770	This work
pAZ102	pAZ101 *phaZ*::ΩSmSp	This work
pAZ103	pK19*mobsacB phaZ*::ΩSmSp	This work
pD82	pLAFR1 cosmid clone from Rm1021 library carrying *exoF* and neighbouring genes	[207]
pD82*exoF*::Tn*phoA*	pD82 *exoF*::Tn*phoA*	This work
Phage		

Continued on Next Page...

Table 2.1 – continued from previous page

Strain or Plasmid	**Relevant Characteristics**	**Reference**
ϕM12	*S. meliloti* transducing phage	[95]

2.3 Plant Growth Conditions

Plant nutrient solution recipe is listed in Appendix A.4.

2.3.1 Alfalfa (*Medicago sativa*)

Alfalfa plants (*Medicago sativa* c.v. Iroqouis) were routinely grown for nodulation experiments with *S. meiloti*. Seed were surface-sterilized by rinsing with 95% EtOH for five minutes, followed by rinsing in 1% hypochlorite for five minutes, and ten rinses with sterile dH_2O of five minutes each. Seeds were germinated for 36-48 hours on water agar plates (1.5% agar in dH_2O) in the dark at room temperature. Seedlings showing no signs of contamination were moved to sterile growth boxes, consisting of three Magenta (Sigma GA-7 vessel) plant tissue boxes (Sigma-Aldrich, St. Louis MO) with the top box inverted to act as an aseptic barrier and containing vermiculite that had been soaked in plant nutrient solution. Five seedlings were planted per box and each inoculant *S. meliloti* strain was typically tested in triplicate. After emergence, each growth box was inoculated with 5 ml of a saturated *S. meliloti* culture diluted 1:50 in sterile dH_2O. Plants were grown for approximately 28 days post-inoculation in a growth chamber (Conviron CMP3244, Model # EF7, Controlled Environments Ltd., Winnipeg) with 16 h, 25°C day/8 h, 20°C night and light intensity of 300 μmoles $m^{-2}s^{-1}$. Shoot dry mass was measured by harvesting the shoot portion of each plant and drying it at 60°C until constant mass was achieved.

2.3.1.1 Nodulation Kinetics

Nodulation kinetics were analysed by monitoring the appearance of nodules on alfalfa plants grown on 1% agar slats containing plant nutrient solution. Assays

were conducted in 25 x 150 mm glass tubes with translucent polypropylene caps (Sigma-Aldrich, St. Louis MO). One two-day old seedling was transferred to a single slant and, following a three-day incubation, was inoculated with 1 ml of a saturated *S. meliloti* culture diluted 1:50 in sterile dH_2O. Plants were grown for approximately 28 days post-inoculation in a growth chamber (Conviron CMP3244, Model # EF7, Controlled Environments Ltd., Winnipeg) with 16 h, 25°C day/8 h, 20°C night and light intensity of 300 μmoles $m^{-2}s^{-1}$. For each inoculant *S. meliloti* strain, typically ten plants were inoculated. Nodule appearance was scored daily for 28-days post-inoculation.

2.3.1.2 Competition Assay for Nodule Occupancy

Alfalfa plants for competition assays were prepared and grown in Magenta jars as described above. For the competition assays, inoculations were carried out by mixing 1:50 dilutions of saturated cultures of the two different strains in different proportions (10:1, 1:1, 1:10) prior to inoculation. 28 days post-inoculation the plants were harvested and the nodules collected; approximately 20 nodules were harvested per Magenta jar. The nodules were surface-sterilized with 1% sodium hypochlorite for approximately 15 minutes, washed twice with LB and then squashed in a few drops of TY containing 0.3 M sucrose. The resultant suspension was streaked on TY. Four single colonies from each streak plate were subsequently screened for the antibiotic-resistance marker or growth phenotype associated with each strain. The bacterial population of each nodule was thus scored as consisting of a single strain or a mixture of two strains.

To determine the precise ratio of each strain in the initial inoculum, serial dilutions of each saturated culture were conducted and CFU/ml was calculated following plating of these dilutions on TY.

2.3.2 *Medicago truncatula*

Seed pods were gently cracked with a hammer on a wire mesh, and ground so that seeds fell through the mesh and were collected below. Prior to germination, seeds were scarified by soaking in 5 volumes of concentrated H_2SO_4 for 5 minutes with gentle agitation. The acid was decanted carefully and the seeds were rinsed with sterile dH_2O approximately 5 times. Following scarification, seeds were sterilized in 5 volumes of commercial-grade Javex (5.25% NaOCl) for 3 minutes and then washed 10 times in dH_2O. After the final rinse, seeds were left in dH_2O and placed in the dark at 4°C for 24-48 hours prior to germination for 36-48 hours on water agar plates (1.5% agar in dH_2O) in the dark at room temperature. Seedlings showing no signs of contamination were moved to sterile growth boxes, consisting of three Magenta (Sigma GA-7 vessel; Sigma-Aldrich, St. Louis MO) plant tissue boxes with the top box inverted to act as an aseptic barrier and containing vermiculite that had been soaked in plant nutrient solution. Five seedlings were planted per box and each inoculant *S. meliloti* strain was typically tested in triplicate. After emergence, each growth box was inoculated with 5 ml of a saturated *S. meliloti* culture diluted 1:50 in sterile dH_2O. Plants were grown for approximately 28 days post-inoculation in a growth chamber (Percival Scientific, DiaMed Lab Supplies Inc.) at 22°C in a 18 h day/6 h night cycle. Shoot dry mass was measured by harvesting the shoot portion of each plant and drying it at 60°C until constant mass was achieved.

2.3.3 Soybean (*Glycine max*)

Soybean seeds were surface sterilized by rinsing with 95% EtOH for five minutes, followed by rinsing in 1% hypochlorite for five minutes, and ten rinses with sterile dH_2O of five minutes each. Seeds were germinated for 48 hours on water agar

plates (1.5% agar in dH_2O) in the dark at room temperature. Following germination, seedlings were transferred to sterilized pots that were filled with sterilized vermiculite soaked in plant nutrient solution. Seedlings were incubated at room temperature for 3 days and then, following emergence, inoculated with 5 ml of saturated *B. japonicum* culture diluted 1:50 in sterile dH_2O. Plants were incubated under high-pressure sodium lamps, supplemented with regularly space compact fluorescent bulbs on an 18 h day/6 h night cycle. Plants were watered every second day with approximately 300 ml of sterile dH_2O. After two weeks, sterile plant nutrient solution was used in place of water for two consecutive waterings after which, plants were again watered with sterile dH_2O. Uninoculated controls were spaced at regular intervals throughout the growth facility to monitor sterility and to indicate the possibility of cross-contamination. Plants were grown for five weeks post-inoculation and were then harvested. At this point, uninoculated controls were carefully checked for evidence of nodulation.

2.3.3.1 Competition Assay for Nodule Occupancy

Soybean plants for competition assays were prepared and grown in sterilized pots as described above. For the competition assays, inoculations were carried out by mixing 1:50 dilutions of saturated cultures of the two different strains in different proportions (10:1, 1:1, 1:10) prior to inoculation. 28 days post-inoculation the plants were harvested and the nodules collected; approximately 20 nodules were harvested per pot. The nodules were surface-sterilized with 1% sodium hypochlorite for approximately 15 minutes, washed twice with AG broth and then squashed in a few drops of liquid AG. The resultant suspension was streaked on AG. Four single colonies from each streak plate were subsequently screened for the Sm^R marker associated with the wild-type strain BjUW36. The bacterial population of each nodule was thus scored as consisting of a single strain or a mixture of two strains.

To determine the precise ratio of each strain in the initial inoculum, serial dilutions of each saturated culture were conducted and CFU/ml was calculated following plating of these dilutions on AG.

2.4 Molecular Biology Techniques

2.4.1 Small-Scale Preparation of Plasmid DNA

Plasmid DNA was routinely isolated using the Solution I, II, III alkaline lysis protocol [307]. All alkaline lysis solutions are described in Appendix A.2. 1.5 ml of a 5 ml culture of *E. coli* cells carrying the plasmid of interest were grown to saturation overnight and harvested at 13,000 rpm in a microcentrifuge. For low- and medium-copy-number plasmids, the supernatant was decanted and the process repeated. The supernatant was decanted and the pellet resuspended in 100 μl of cold Solution I. 200 μl of freshly prepared Solution II was added and the solutions were mixed by inversion 4-6 times. Following a short incubation (less than 5 minutes) at room temperature, 150 μl cold Solution III was added and the sample mixed gently by inversion. The cell debris and genomic DNA were pelleted by centrifugation at 13,000 rpm for 5 minutes and the supernatant was transferred to a fresh tube. Soluble proteins were removed from the plasmid-containing supernatant by chloroform extraction (Section 2.4.3.1) before being precipitated by the addition of 0.8 volumes ice cold isopropanol. This sample was vortexed and incubated at -20°C for 3 minutes before centrifugation at 13,000 rpm for 30 minutes. The DNA pellet was washed briefly in 70% EtOH and dried at room temperature before being resuspended in an appropriate volume of sterile dH_2O. Plasmid DNA was typically stored at either room temperature or -20°C.

When high-quality, high-purity DNA was needed for sequencing, plasmid DNA

was isolated using a Sigma (Sigma-Aldrich, St. Louis MO) miniprep kit as per manufacturer's directions.

2.4.2 Small-Scale Preparation of Genomic DNA from *S. meliloti* and *B. japonicum*

All genomic DNA preparation solutions are described in Appendix A.2. Genomic DNA was isolated using standard protocols [236, 255]. Strains were grown to saturation and cultures were pelleted at 13,000 rpm in a microcentrifuge tube. Pellets were resuspended in 2.5 ml cold $T_{10}E_{25}$ pH 8.0 buffer. 250 μl of lysozyme solution was added and the sample was mixed gently before incubation for 1 hour at 37°C. 300 μl SDS-protease solution was added and the sample was mixed gently and incubated for an additional 1-2 hours at 37°C. Proteins were removed from the sample by the addition of 500 μl phenol, gentle mixing and centrifugation at 10,000 rpm for 10 minutes. The aqueous layer, including the interface, was transferred to a fresh tube; 150 μl of 5 M ammonium acetate and 3 ml ice-cold isopropanol were added and the sample was mixed gently. The DNA precipitate was removed by spooling around a sterile glass rod. The spooled DNA was rinsed briefly by immersion in 500 μl of each of ice-cold 70% EtOH and ice-cold 95% EtOH. The spooled DNA was air-dried briefly and then resuspended in 500 μl $T_{10}E_1$ pH 8.0 buffer and stored at 4°C.

Alternatively, genomic DNA was isolated using the small-scale genomic DNA isolation kit from MolBiol (Mo Bio Inc., Carlsbad CA) as per manufacturer's instructions. When isolating DNA from *B. japonicum*, 4 ml of saturated culture was used per extraction rather than the 1.8 ml recommended by the manufacturer.

2.4.3 DNA Clean-Up

2.4.3.1 Phenol and Phenol/Chloroform Extraction

An equal volume of buffer-saturated phenol:chloroform (1:1) was added to the DNA and the solution was mixed by vortexing. Most DNA solutions were vortexed for 10 sec, except for high molecular weight DNA which was gently rocked. The solution was then centrifuged for 3 min and the aqueous layer was carefully removed and transferred to a new tube. Two successive chloroform extractions were then used to remove all traces of phenol. An equal volume of chloroform was added to the aqueous layer, mixed and then centrifuged for 3 minutes. The aqueous layer was transferred to a new tube and the DNA was cleaned by ethanol precipitation.

2.4.3.2 Ethanol Precipitation

25 μl of 10 M NH_4OAc was added to each sample, and the volume brought up to 100 μl with dH_2O. 2 volumes of ice cold 95% EtOH was then added, the sample was vortexed to mix and then the samples were incubated at -20°C for a minimum of 30 minutes. The samples were centrifuged at maximum speed for 30 minutes and the supernatant decanted. The pellet was washed in 70% EtOH, air-dried, and resuspended in an appropriate volume of dH_2O.

2.4.4 DNA Manipulations

2.4.4.1 Restriction Digests and Gel Electrophoresis

All electrophoresis solutions are described in Appendix A.2.3.

Standard protocols were used to maniplate DNA [307]. Restriction digests were typically performed using enzymes purchased from Fermentas (Fermentas Canada

Inc., Burlington ON). Reaction mixes were incubated at 37°C for 30 min (for a diagnostic digest) to overnight (for Southern analysis).

The restriction products were typically analysed by gel electrophoresis using 1% agarose in Tris-Acetate-EDTA (TAE) buffer. Gels contained either EtBr or Gel Red™ (Biotium Inc., Hayward CA) to facilitate subsequent visualization of the DNA. Samples were mixed with an appropriate volume of 6X loading dye (see Appendix A.2) and run at 120-150 V for approximately 1 hour. Samples for Southern blot analysis were typically run for 5-6 hours. Typically a 1 kb molecular weight standard (Fermentas Canada Inc., Burlington ON) was included on each gel.

When specific restriction fragments were needed for subsequent experiments, the band of interest was cut from the gel and the DNA fragment isolated using either the Roche DNA Extraction Kit (Roche Diagnostics Canada, Mississauga ON) or Fermentas DNA Extraction Kit (Fermentas Canada Inc., Burlington ON) as per manufacturer's instructions.

2.4.4.2 Ligation

Restriction digests were typically cleaned by EtOH precipitation prior to ligation. The volume in which the pellet was resuspended was calculated based on the needs of each specific reaction.

Routine sticky-end ligations were performed by overnight incubation at room temperature in a 10μl volume. T4 DNA ligase from Fermentas (Fermentas Canada Inc., Burlington ON) was used as per manufacturer's instructions.

Blunt-end ligations into pJET (Fermentas Canada Inc., Burlington ON) were carried out using the CloneJet kit as per manufacturer's instructions.

2.4.4.3 Transformation of Plasmid DNA into *E. coli*

Plasmid DNA was typically transformed into chemically competent *E. coli* cells (Section 2.4.4.4).

50 μl competent cells were mixed with the appropriate volume of DNA and inclubated on ice for at least 30 minutes before being heat shocked for 90 seconds at 42°C. Cells were returned to ice for 2 minutes and were allowed to recover for at least 1 hour at 37°C in 1 ml LB before being plated onto selective media.

2.4.4.4 Preparation of Chemically Competent *E. coli*

Competent *E. coli* cells were prepared from LB-grown cultures harvested at OD_{600} between 0.4 and 0.6. Cells were harvested by centrifugation at 3,000 rpm for 10 min at 4°C (Sorvall GSA rotor) and washed in 20 ml 0.1 M $MgCl_2$. The cells were harvested for a second time by centrifugation at 3,000 rpm for 10 min at 4°C (Sorvall GSA rotor), resuspended in 20 ml 0.1 M $CaCl_2$ and incubated at 4°C for 4 hours. Cells were collected by centrifugation at 3,000 rpm for 10 min, resuspended in 10 ml of ice-cold 100 mM $CaCl_2$ containing 15% glycerol, and aliquoted into pre-chilled microcentrifuge tubes before storage at -70°C.

2.4.4.5 Transfer of plasmid DNA by Conjugation into *S. meliloti* and *B. japonicum*

Conjugation was typically performed by triparental mating between an *E. coli* donor, an *E. coli* helper carrying pRK600, and a recipient.

Matings into *S. meliloti* were performed by combining 1 ml saturated broth culture of the *S. meliloti* recipient with 500 μl each of the *E. coli* donor and helper strains. All strains were washed, prior to mixing, in 0.85% NaCl to remove antibiotics. Mating mixtures were pelleted and resuspended in 50 μl for spotting onto

a non-selective LB or TY plate. Matings were incubated overnight at 30°C before the spot was resuspended in 1 ml 0.85% NaCl. Serial dilutions of the resuspended mating spot were made in 0.85% NaCl and 100 μl of the appropriate dilutions were plated onto selective media.

Matings into *B. japonicum* used essentially the same strategy described for *S. meliloti* except that between 5 and 10 ml of the recipient *B. japonicum* strain were used in each mating, and mating spots were incubated for a minimum of 72 hours.

2.4.4.6 *in vitro* Mini Tn*5* Mutagenesis of Plasmid DNA

in vitro mini Tn*5* mutagenesis of plasmid DNA was performed using the EpiCentre® EZ-Tn*5*™ Insertion Kit (EpiCentre Biotechnologies, Madison WI, USA), as per manufacturer's instructions.

2.4.4.7 Homologous Recombination

Mutagenesis by allelic replacement was typically accomplished by conjugal transfer of the desired fragment on the vector pK19*mobsacB* [310]. pK19*mobsacB* carries the broad-host-range transfer machinery of plasmid RP4 and a modified *sacB* gene from *Bacillus subtilis* with a narrow-host-range replication origin and the MCS of pUC19.

2.4.4.8 Generalized Transduction into *S. meliloti*

Transductions were employed to facilitate the transfer of markers between different *S. meliloti* strains using the ΦM13 generalized transducing phage [95]. This phage infects the host and produces progeny phage within the host cell. Some of the progeny phage mis-package host genomic DNA in place of phage DNA and this results in the production of transducing particles. When these transducing particles

are used to infect a new host they will infect the host cell but the infection will not result in the production of new phage. Instead, the packaged DNA can be maintained in the host cell by a double recombination event. Transductants can then be isolated by selection for the desired marker (or by screening for loss of a marker).

As mentioned above, transductions into *S. meliloti* were performed using ΦM13 generalized transducing phage [95]. A phage lysate was prepared by addition of 50 μl undiluted ΦM13 phage stock (of titre 10^{10} PFU/ml) to a mid-log culture of *S. meliloti* at OD_{600} 0.3 - 0.5 grown in LBMC. This was incubated for 6-8 hours (or overnight), at which point cell lysis was evident. Unlysed cells were subsequently killed by the addition of 2 drops of chloroform and cell debris was centrifuged out at 2000 x *g* for 5 minutes. This lysate was stored at 4°C until needed.

Transductions were performed by addition of 0.5 ml lysate to 0.5 ml late-log culture grown in LBMC. Cells were then incubated at room temperature for 30 minutes to allow phage adsorption to the recipient cells. Phage were then removed by three rounds of pelleting and resuspension in 1.5 ml dH_2O. Following the final wash, the pellet was resuspended in 250 μl dH_2O and plated on the appropriate selective media.

2.4.4.9 DNA Sequencing

Sequencing reactions were carried out using ABI BigDye terminator chemistry at either the University of Waterloo sequencing facility, using a Applied Biosystems 3130xl Genetic Analyzer, or at the Mobix Lab at McMaster University using a 3730 DNA Analyzer (Applied Biosystems, Foster City, CA, USA).

2.4.4.10 PCR

PCR cloning reactions were performed using an Eppendorf Mastercycler® gradient thermocycler (Eppendorf, Toronto, ON) and KOD Polymerase reagents from Novagen (EMD Biosciences, San Diego, CA). A typical cloning PCR reaction is described in Appendix A.7.1.

PCR products for cloning were run on a 1% agarose gel and the band corresponding to the appropriate PCR product was excised and purified by gel extraction. If restriction sites were included in the primers of the PCR product, the purified DNA was digested and ligated directly into the destination vector using T4 DNA Ligase (Fermentas Canada Inc., Burlington ON). In the event that direct cloning was not practical, the PCR product was ligated into the cloning vector, pGem-TEasy (Promega, Madison WI) as per manufacturer's instructions.

2.4.4.11 Cross-Over PCR

Cross-over PCR [154] was used to construct fragments for in-frame mutageneses and allelic replacements. Cross-over PCR reactions were performed using an Eppendorf Mastercycler® gradient thermocycler (Eppendorf, Toronto, ON) and KOD Polymerase reagents from Novagen (EMD Biosciences, San Diego, CA). A typical crossover PCR reaction is described in Appendix A.7.2.

2.4.4.12 Colony PCR

PCR reactions for screening purposes were performed using a modified version of standard protocols [403] in an Eppendorf Mastercycler® gradient thermocycler (Eppendorf, Toronto, ON) and NEB Taq reagents (New England Biolabs® Inc., Ipswich, MA). Cells were resuspended in 100 μl dH_2O, boiled at 94°C for 10 minutes, cooled to 4°C and centrifuged to pellet out the cell debris; the supernatant was

then used as the template in the subsequent PCR reaction. A typical colony PCR reaction is described in Appendix A.7.3.

2.4.4.13 Primer Design

A complete list of primers used in this study is shown in Table 2.2. Tm was calculated across hybridizing nucleotides as 4(G + C) + 2(A + T).

Primer design and analysis was performed using Amplify 3X for MacOSX (Bill Engels, University of Wisconsin WI). Primers were purchased from Sigma Genosys (Sigma-Aldrich, St. Louis MO).

Table 2.2: Primers used in this study

Primer Name	**Tm (°C)**	**Use**	**Sequence**
Blr2885A	62°C	Upstream primer for cross-over PCR of Blr2885	GCAACGGTGTGGTATGGCA
Blr2885B	81°C	Upstream cross-over primer with sticky end for deletion of Blr2885	CAGGATCAGGAACAGCAGGTGGATGGAAGCGAAATCAAG
Blr2885C	70°C	Downstream cross-over primer with sticky end for deletion of Blr2885	CACCTGCTGTTCCTGATCCTGGACCTGATGTGGGACAAC
Blr2885D	55°C	Downstream primer for cross-over PCR of Blr2885	ACTTTTGGCTCGCTGATGT
Blr3732A	54°C	Upstream primer for cross-over PCR of Blr3732	CAGCAAGGCGGTCAATAAAT
Blr3732B	68°C	Upstream cross-over primer with sticky end for deletion of Blr3732	ATCCGAGATCAGGGACAGTTCCGAGTTCAGCAAATAGCA
Blr3732C	69°C	Downstream cross-over primer with sticky end for deletion of Blr3732	GAACTGTCCCTGATCTCGGATCTCGGCAGCAACCTCTAT

Continued on Next Page...

Table 2.2 – continued from previous page

Primer Name	**Tm (°C)**	**Use**	**Sequence**
Blr3732D	52°C	Downstream primer for cross-over PCR of Blr3732	CGCTTCTTCGGATTCTCA
Bll4360A	56°C	Upstream primer for cross-over PCR of Bll4360	GTCCCTCAACGCCAACAC
Bll4360B	72°C	Upstream cross-over primer with sticky end for deletion of Bll4360	GAACTGGAGCACGATCTGCTCGGTGTCCGACAGCCAGTA
Bll4360C	71°C	Downstream cross-over primer with sticky end for deletion of Bll4360	GAGCAGATCGTGCTCCAGTTCAAGGTGCCCGTCTACAAC
Bll4360D	53°C	Downstream primer for cross-over PCR of Bll4360	CAGGATGCCAGTGAAAATCA
Bll4548A	58°C	Upstream primer for cross-over PCR of Bll4548	AAGCAGCCGTTCCAGACC
Bll4548B	70°C	Upstream cross-over primer with sticky end for deletion of Bll4548	CACCTGGTCGAACAGGATCTGCCAGTCGGTGAGATAGAC

Continued on Next Page...

Table 2.2 – continued from previous page

Primer Name	**Tm (°C)**	**Use**	**Sequence**
Bll4548C	71°C	Downstream cross-over primer with sticky end for deletion of Bll4548	CAGATCCTGTTCGACCAGGTGGAGCCGAGCAATCACCTC
Bll4548D	54°C	Downstream primer for cross-over PCR of Bll4548	GTAGATGCGATGACCAAAGC
Bll6073A	59°C	Upstream primer for cross-over PCR of Bll6073	CCGTCGGGGTGTGGTTTG
Bll6073B	71°C	Upstream cross-over primer with sticky end for deletion of Bll6073	CTGGATGAGCACCTGGAACAGAAGATGCGTGCTCCAGTC
Bll6073C	71°C	Downstream cross-over primer with sticky end for deletion of Bll6073	CTGTTCCAGGTGCTCATCCAGGACGAGTGGCTGAAGTTG
Bll6073D	56°C	Downstream primer for cross-over PCR of Bll6073	GCAGAAGTCCATCCTCAAGC
Bll0225A	68°C	Upstream primer with PstI site for cross-over PCR of Bll0225 and Bll0226	CCTCTGCAGGGGAAGAGTACGCAACGCAAC

Continued on Next Page...

Table 2.2 – continued from previous page

Primer Name	**Tm (°C)**	**Use**	**Sequence**
Bll0225B	72°C	Upstream cross-over primer with sticky end for deletion of Bll0225 and Bll0226	CACCACGACCTGATCCTCGCACAGAATCTGGCCCATGATGA
Bll0225C	73°C	Downstream cross-over primer with sticky end for deletion of Bll0225 and Bll0226	TGCGAGGATCAGGTCGTGGTGGACGTGCTGGAAAAGTCC
Bll0225D	66°C	Downstream primer with BamHI for cross-over PCR of Bll0225 and Bll0226	CGAGGATCCAGCGGCCAGAGATAGTTGAG
Blr3724A	66°C	Upstream primer with PstI site for cross-over PCR of Blr3724 and Blr3725	CCTCTGCAGCTCGGCATCGACAAGTTC
Blr3724B	72°C	Upstream cross-over primer with sticky end for deletion of Blr3724 and Blr3725	GTGCTCTTCGTCCTCATGGAGCGTTTCTCCTGCGGAATGC

Continued on Next Page...

Table 2.2 – continued from previous page

Primer Name	**Tm (°C)**	**Use**	**Sequence**
Blr3724C	71°C	Downstream cross-over primer with sticky end for deletion of Blr3724 and Blr3725	CTCCATGAGGACGAAGAGCACAATGGTCAGAAGGGCCAG ATG
Blr3724D	66°C	Downstream primer with BamHI for cross-over PCR of Blr3724 and Blr3725	CGAGGATCCCAGGCGATGATATTCGAGTGC
Blr2885F	70°C	Forward primer for cloning of Blr2885, carries BamHI site	CCTGGATCCTGAACGCGCCGACGGGAC
Blr2885R	59°C	Reverse primer for cloning of Blr2885, carries EcoRI site	CGAGAATTCTCATGTCGATCTCTTCCC
Blr3732F	62°C	Forward primer for cloning of Blr3732, carries BamHI site	CCAGGATCCATGAATCGGCCATTCAAC
Blr3732R	63°C	Reverse primer for cloning of Blr3732, carries EcoRI site	CGAGAATTCTCAGTTCGCCTTCGCTTTC

Continued on Next Page...

Table 2.2 – continued from previous page

Primer Name	**Tm (°C)**	**Use**	**Sequence**
Bll4360F	65°C	Forward primer for cloning of Bll4360, carries HindIII site	CCTAAGCTTATGGCCACGACCGACACG
Bll4360R	67°C	Reverse primer for cloning of Bll4360, carries BamHI site	CGAGGATCCCTATGCGCGAACCCTGAC
Bll4548F	69°C	Forward primer for cloning of Bll4548, carries BamHI site	CCTGGATCCATGGCGGCGAAGACAGGC
Bll4548R	69°C	Reverse primer for cloning of Bll4548, carries EcoRI site	CGAGAATTCTCAGGCGCTGCGGGCCAG
Bll6073F	61°C	Forward primer for cloning of Bll6073, carries HindIII site	CCTAAGCTTATGAGCGTCGTGAAGGTATTTC
Bll6073R	60°C	Reverse primer for cloning of Bll6073, carries EcoRI site	CGAGAATTCTTAGCTGTGGACGTAGTC

Continued on Next Page...

Table 2.2 – continued from previous page

Primer Name	**Tm (°C)**	**Use**	**Sequence**
Bll0322F	66°C	Forward primer for cloning of Bll0322, carries BamHI site	CCTGGATCCATGAACAGGAGGGGACGAC
Bll0322R	66°C	Reverse primer for cloning of Bll0322, carries EcoRI site	CGAGAATTCTCACCTCGGATCGAGCAGGC
Bll1718F	64°C	Forward primer for cloning and mutagenesis of Bll1718, carries KpnI site	CCTGGTACCATGACCACCATGGCAAC
Bll1718R	60°C	Reverse primer for cloning of Bll1718, carries BamHI site	CCTGGATTCTCATGTGCTTGTAGTGTC
Bll1718RT	60°C	Reverse primer for mutagenesis of Bll1718, carries Mph1103I site	CATATGCATCAGGAGAACCTGCAGAAC
Bll3840F	64°C	Forward primer for cloning and mutagenesis of Bll3840, carries KpnI site	CCTGGTACCATGACGTCATTCGCGATC

Continued on Next Page...

Table 2.2 – continued from previous page

Primer Name	**Tm (°C)**	**Use**	**Sequence**
Bll3840R	68°C	Reverse primer for cloning of Bll3840, carries EcoRI site	CCTGAATTCTCAGGCCGTGATGGCCGCTTG
Bll3840RT	59°C	Reverse primer for mutagenesis of Bll3840, carries Mph1103I site	CATATGCATAACGGAGATGAACAGCAC
Blr4298F	62°C	Forward primer for cloning and mutagenesis of Blr4298, carries KpnI site	CCTGGTACCATGACAACGACAACGATG
Blr4298R	64°C	Reverse primer for cloning of Blr4298, carries EcoRI site	CCTGAATTCTCAGTCCGTCGTGATCGC
Blr4298RT	63°C	Reverse primer for mutagenesis of Blr4298, carries Mph1103I site	CATATGCATACCTGGAGGATCTCGCCTTG
Blr6145F	68°C	Forward primer for cloning and mutagenesis of Blr6145, carries KpnI site	CCTGGTACCATGTCGACCATTGCCGCG

Continued on Next Page...

Table 2.2 – continued from previous page

Primer Name	**Tm (°C)**	**Use**	**Sequence**
Blr6145R	67°C	Reverse primer for cloning of Blr6145, carries EcoRI site	CCTGAATTCCTAGCCCGCCGTCACGTC
Blr6145RT	62°C	Reverse primer for mutagenesis of Blr6145, carries Mph1103I site	CATATGCATAGAACAGCACCTGGAGCAC
Bll7095F	65°C	Forward primer for cloning and mutagenesis of Bll7095, carries KpnI site	CCTGGTACCATGTGTCCGTCAATACGCTG
Bll7095R	66°C	Reverse primer for cloning of Bll7095, carries EcoRI site	CCTGAATTCTCAAGCGGCCGATTGCGTC
Bll7095RT	60°C	Reverse primer for mutagenesis of Bll7095, carries Mph1103I site	CATATGCATGAAGTAGCGGATCGTCTT
Bll7187F	63°C	Forward primer for cloning and mutagenesis of Bll7187, carries KpnI site	CCTGGTACCATGACACAGATCGCGATC

Continued on Next Page...

Table 2.2 – continued from previous page

Primer Name	**Tm (°C)**	**Use**	**Sequence**
Bll7187R	71°C	Reverse primer for cloning of Bll7187, carries EcoRI site	CCTGAATTCTTACGCGCCGCCGCCCGG
Bll7187RT	62°C	Reverse primer for mutagenesis of Bll7187, carries Mph1103I site	CATATGCATTCAGGAGCACTTGCAGGAG
Blr3730F	61°C	Forward primer for mutagenesis of Blr3730 and Blr373, carries BglII site	CCTAGATCTTGCTGGTTCAGGAGATGAC
Blr3730R	72°C	Reverse primer for mutagenesis of Blr3730 and Blr3731, carries NotI site	CGAGCGGCCGCTCACGGAGAGGCGTTT GATC
Bll1718F	64°C	Forward primer for cloning and mutagenesis of Bll1718, carries KpnI site	CCTGGTACCATGACCACCATGGCAAC
Bll1718RT	60°C	Reverse primer for mutagenesis of Bll1718, carries Mph1103I site	CATATGCATCAGGAGAACCTGCAGAAC

Continued on Next Page...

Table 2.2 – continued from previous page

Primer Name	**Tm (°C)**	**Use**	**Sequence**
Bll1718R	60°C	Reverse primer for cloning of Bll1718, carries BamI site	CCTGGATTCTCATGTGCTTGTAGTGTC
Blr3723F	65°C	Forward primer for cloning of Blr3723, carries KpnI site	CCTGGTACCGTGTCCGCAACAATCACTG
Bll3723F	65°C	Forward primer for cloning of Blr3723, carries KpnI site	CCTGGTACCGTGTCCGCAACAATCACTG
Blr3723R	64°C	Reverse primer for cloning of Blr3723, carries EcoRI site	CCTGAATTCTTAGCCCGTCGTTACGGC
Blr3723FT	68°C	Forward primer for mutagenesis of Blr3723, carries BglII site	CCTAGATCTGGTCGTCTCCGGCATTGCGC
Blr3723RT	74°C	Reverse primer for mutagenesis of Blr3723, carries NotI site	CGAGCGGCCGCGATGAAAAGCGTCGCCAGC
Blr3840F	64°C	Forward primer for cloning and mutagenesis of Blr3840, carries KpnI site	CCTGGTACCATGACGTCATTCGCGATC

Continued on Next Page...

Table 2.2 – continued from previous page

Primer Name	**Tm (°C)**	**Use**	**Sequence**
Blr3840RT	59°C	Reverse primer for mutagenesis of Blr3840, carries Mph1103I site	CATATGCATAACGGAGATGAACAGCAC
Blr3840R	68°C	Reverse primer for cloning of Blr3840, carries Mph1103I site	CCTGAATTCTCAGGCCGTGATGGCCGCTTG
Blr4298F	62°C	Forward primer for cloning and mutagenesis of Blr4298, carries KpnI site	CCTGGTACCATGACAACGACAACGATG
Blr4298RT	63°C	Reverse primer for mutagenesis of Blr4298, carries Mph1103I site	CATATGCATACCTGGAGGATCTCGCCTTG
Blr4298R	64°C	Reverse primer for cloning of Blr4298, carries EcoRI site	CCTGAATTCTCAGTCCGTCGTGATCGC
Blr6145F	68°C	Forward primer for cloning and mutagenesis of Blr6145, carries KpnI site	CCTGGTACCATGTCGACCATTGCCGCG

Continued on Next Page...

Table 2.2 – continued from previous page

Primer Name	**Tm (°C)**	**Use**	**Sequence**
Blr6145RT	62°C	Reverse primer for mutagenesis of Blr6145, carries Mph1103I site	CATATGCATAGAACAGCACCTGGAGCAC
Blr6145R	67°C	Reverse primer for cloning of Blr6145, carries EcoRI site	CCTGAATTCCTAGCCCGCCGTCACGTC
Bll7095F	65°C	Forward primer for cloning and mutagenesis of Bll7095, carries KpnI site	CCTGGTACCATGTGTCCGTCAATACGCTG
Bll7095RT	60°C	Reverse primer for mutagenesis of Bll7095, carries Mph1103I site	CATATGCATGAAGTAGCGGATCGTCTT
Bll7095R	66°C	Reverse primer for cloning of Bll7095, carries EcoRI site	CCTGAATTCTCAAGCGGCCGATTGCGTC
Bll7187FT	60°C	Forward primer for mutagenesis of Bll7187	TCGTGCTCGGAGTGCTCATC
Bll7187RT2	54°C	Reverse primer for mutagenesis of Bll7187	AACATCTTTGCGGCCTTG

Continued on Next Page...

Table 2.2 – continued from previous page

Primer Name	**Tm (°C)**	**Use**	**Sequence**
Bll7187RDS	55°C	Reverse primer for cloning of Bll7187	TCGATCCGTGTCGCTTTAC
Bll7187F502	50°C	Forward primer for cloning of Bll7187	TGCAAAATCAATGCGTTC
SMc03879A	63°C	Forward primer for cross-over PCR of SMc08379, carries EcoRI site	CGCGAATTCATCAACTGGCGGAGAAAG
SMc03879B	71°C	Upstream cross-over primer with sticky end for deletion of SMc08379	TGCGAGGATCAGGTCGTGGTGGGGACGTTCCTCATATTTG
SMc03879C	72°C	Downstream cross-over primer with sticky end for deletion of SMc03879	CACCACGACCTGATCCTCGCAGAGTGGGAGGCGAGTATG
Smc03879D	68°C	Downstream primer for cross-over PCR of SMc03879D, carries XbaI site	GCTCTAGAGCCGGAAAGCCGAGGGCAC

Continued on Next Page...

Table 2.2 – continued from previous page

Primer Name	**Tm (°C)**	**Use**	**Sequence**
Smc03879F	64°C	Forward primer for cloning of SMc03879, carries HindIII site	CGCAAGCTTCATGAGCAATCCCTCGATC
Smc03879R	64°C	Reverse primer for cloning of SMc03879, carries XbaI site	GCTCTAGATTACAGGCGTTCCACGCAC
pJETF	61°C	pJET1.2 forward sequencing primer	CGACTCACTATAGGGAGAGCGGC
pJETR	57°C	pJET1.2 reverse sequencing primer	AAGAACATCGATTTTCCATGGCAG
T7 Sequencing primer	48°C	pGEMTEasy T7 sequencing primer	TAATACGACTCACTATAGGG
Sp6 Sequencing primer	42°C	pGEMTEasy Sp6 sequencing primer	TAATACGACTCACTATAGGG

2.4.5 Cosmid Library Construction

2.4.5.1 Preparation of Inserts

Partial digestion of genomic DNA was optimized by gradient digest. Approximately 15 ng/μl of genomic DNA was used per enzyme tested. In a tube, 15 μl genomic DNA was mixed with 100 μl 10X digest buffer and the volume was brought up to 500 μl with dH_2O. This mixture was incubated on ice 30 mins. The reaction mix was then aliquoted into 15 tubes (60 μl was added to the first tube; 30 μl was added to the remaining 14) and 5 units of the appropriate restriction enzyme (tyically Sau3AI) was added to the first tube. A concentration gradient was established by transferring 30 μl from the first tube into the second, mixing, then transferring 30 μl from tube 2 into tube 3 and so on. 30 μl was removed from the final tube and discarded. The reactions were incubated at 37°C for 30 minutes and the reactions were stopped by the addition of 1 μl 0.5 M EDTA mixed with 6X loading dye. The digests were run on an agarose gel and the enzyme concentration that gives fragments of approx. 25-50kb was selected for subsequent use.

Once an appropriate enzyme concentration had been determined, the genomic DNA was partially digested by combining 33 μl 10X restriction buffer, 10 μg genomic DNA, restriction enzyme and the volume was brought up to 330 μl with dH_2O. The reaction mix was incubated at 37°C for 30 minutes and the reactions were stopped by heat inactivation at 65°C for 15 minutes. The reaction was cleaned up by a single phenol/chloroform extraction followed by two chloroform extractions and an ethanol precipitation (Section 2.4.3). The digested DNA was then resuspended in 6 μl dH_2O.

2.4.5.2 Preparation of Cosmid DNA

Cosmid DNA was prepared using a standard miniprep protocol as described in Section 2.4.1. The cosmid DNA digested by combining 20 μg cosmid DNA with 6 μl BamHI, 10 μl 10X restriction buffer and dH_2O to 100 μl. The digest was incubated at 37°C and allowed to go to completion. The reaction was cleaned up by a single phenol/chloroform extraction followed by two chloroform extractions and an ethanol precipitation (Section 2.4.3). The digested DNA was then resuspended in 180 μl $T_1E_{0.1}$, to give a final concentration of approximately 300 ng/μl DNA.

2.4.5.3 Ligation of Library Inserts into Cosmid DNA

8 μl digested cosmid DNA was mixed with 6 μl partially digested genomic DNA, incubated at 42°C for 10 minutes and then cooled to room temperature. 2 μl 10X ligation buffer and 2 μl T4 ligase were then added, mixed and the reaction allowed to proceed overnight at room temperature. The ligase was then inactivated by incubation at 65°C for 15 minutes prior to use, and the ligation reaction checked by running 1 μl on a 0.8% agarose gel.

2.4.5.4 Library Construction, Packaging and Transfection

Packaging was performed using the EpiCentre® MaxPlax™ Lambda Packaging Extract (EpiCentre Biotechnologies, Madison WI, USA), as per manufacturer's instructions.

Cells were grown in an appropriate medium with no antibiotic (antibiotic inhibits the ability of phage to infect) and supplemented with 10 mM $MgSO_4$ and 0.2% (w/v) maltose to OD_{600} of 1.0. Cells were harvested by centrifugation and diluted to OD_{600} of 0.5 in 10 mM $MgSO_4$. 1:10 and 1:50 dilution of the packaging reaction were prepared by dilution in phage dilution buffer (Appendix A.2.6); 25

μl each dilution was mixed with 25 μl bacterial cells and incubated at room temperature for 30 minutes. The reaction mix was then combined with 200 μl LB and incubated at 37°C for 1 hour with agitation every 15 minutes. Transfectants were selected by plating the cells on LB with an appropriate antibiotic and incubated overnight at 37°C. The resulting colonies were pooled by suspending them in LB broth and then the library was expanded for storage by growth to late-log phase at 37°C.

2.4.6 Southern Blot Analysis

All Southern Blot solutions are described in Appendix A.2.5.

2.4.6.1 Probe Labelling

Oligonucleotide DNA probes for use in Southern Blot hybridization were labelled using the DIG terminal transferase DIG labelling kit from Roche (Roche Diagnostics Canada, Mississauga ON) as per manufacture's instructions. The oligonucleotides that were used in this reaction were typically designed for PCR purposes and had no additional modifications. Following labelling, the probe was diluted in 14 ml of hybridization buffer. Typically 1 μl of probe was saved to check labelling efficiency.

2.4.6.2 Sample Preparation

Southern blot analyses for *B. japonicum* necessitated high-quality genomic DNA, which was typically prepared using the MolBio genomic DNA extraction kit as described in Section 2.4.2.

Genomic DNA was digested to completion in a total volume of 50 μl. The complete digestion reaction was then run on a 0.8% agarose gel an 50 V for approximately 4-5 hours to ensure complete separation of DNA fragments. Gels were

stained with EtBr and visualized using a Fluorochem® 8000 UV transilluminator (Alpha Innotech Corp., San Leandro, CA). Gels were depurinated by treatment with 0.25 M HCl for 10 minutes followed by two, 15 minute washes in transfer buffer to neutralize pH. DNA was transferred to a nitrocellulose membrane (Boehringer Mannheim Canada; Laval QC) overnight in transfer buffer using standard techniques [307]. Following transfer, the membrane was neutralized with 5X SSC for 10 minutes and the DNA was cross-linked to the membrane using a UV crosslinker (Bio-Rad, Hercules, CA). The membrane was then incubated for one hour at the hybrdization temperature in hybridization buffer before the addition of DIG-labelled probe. Hybridization was carried out overnight in a hybridization oven at a temperature of 55°C.

2.4.6.3 Southern Blot Visualization

Following hybridization, probes were decanted and stored at -20°C to be reused. Blots were typically washed twice for 15 minutes at room temperature in 50 ml stringency buffer A, followed by two 15 minute washes in 50 ml stringency buffer B at the hybridization temperature. Blocking and detection steps were carried out using a Tris-NaCl buffer base.

Hybridization was detected by chemiluminescence following treatment with anti-DIG-conjugated alkaline phosphatase and CDP-Star. Membranes were stripped for reuse by two 15 minute washes in stripping buffer.

2.5 Bacterial Growth Assays

2.5.1 Bacterial Growth Curves

2.5.1.1 Bioscreen-C Growth Curve Machine

Cells were grown to saturation in an appropriate complex medium, and standardized to OD_{600} by dilution. Cells (1 ml) were then washed by pelleting and washing in 0.85% NaCl, followed by resuspension in 10 ml minimal medium with no carbon source. A 1:1000 dilution of this culture was used to inoculate an appropriate volume of minimal medium containing the carbon source of interest. Each well of the 100-well plate was inoculated with 400 μl of inoculum; typically triplicate samples were set up for each test. Samples were incubated at 30°C, with readings taken every 10 minutes, preceded by 30 seconds of shaking.

2.5.1.2 Traditional Test Tube Method

Cells were grown to saturation in an appropriate complex medium, and washed twice in 0.85% saline. A 0.15 ml aliquot of washed cells was subcultured into 5 ml of minimal medium supplemented with the appropriate carbon source in a 16 mm x 150 mm culture tube. Tubes were placed vertically in a rack in a shaking incubator set at 180 rpm, 30°C. Growth was followed by measuring absorbance at 600 nm. Upon completion of the growth test, culture purity was checked by streaking on TY or AG agar.

2.5.2 Starvation Assay

Saturated TY cultures were washed twice to remove traces of nutrients, and were subcultured 1:50 into carbon-free M9 medium. These cultures were incubated at

30°C, with shaking at 180 rpm. Viable cell counts were monitored at weekly intervals by plating serial dilutions on TY agar. Samples at t=0 were each given a relative value of 1, and all subsequent samples are compared to this starting value. Samples were typically set up as triplicate cultures.

2.6 Protein Analysis

All protein solutions are described in Appendix A.3.

2.6.1 Protein Sample Preparation

2.6.1.1 Routine Confirmation of Over-Expression

Typically, protein samples were analysed following overnight incubation of *E. coli* BL21(λDE3) pLysS cultures at 37°C in autoinduction medium. For routine confirmation of over-expression, 200 μl of cells were pelleted and resuspended in 100 μl SDS-PAGE loading buffer. Samples were boiled at 100°C in a dry heat block for 10 minutes and then cooled to room temperature before use. Typically 20 μl of sample was run on an SDS-PAGE gel for analysis.

2.6.1.2 Verification of Samples by SDS-PAGE

Protein samples were analysed on a single dimension SDS-PAGE protein gel using the Bio-Rad Mini Protean 2 system (Bio-Rad, Hercules, CA). Approximately 4 ml 12% SDS-PAGE gel preparation was added to the unit, overlaid with dH_2O and allowed to solidify for 30-45 minutes. The dH_2O was then removed and replaced with 4% stacking gel preparation; a comb was added and the gel was allowed to solidify for 30-45 minutes. The gels were transferred to the running apparatus in 1X

Tris-Glycine running buffer. 20 μl samples were loaded into the wells; a control lane of protein ladder (Fermentas Canada Inc., Burlington ON) was always included. Gels were run at 80 V for 20 minutes and then 120 V for 2 hours before staining in Coomassie Brilliant Blue straining solution for approximately 30 minutes to 1 hour. Gels were destained overnight in destain solution and then visualized on a whitelight transilluminator.

2.6.1.3 Coomassie Brilliant Blue Staining

The gel was incubated in a volume of coomassie brilliant blue stain solution sufficient to submerge it completely, for approximately 1 hr on a slowly rocking platform. The gel was then typically destained from 6 hr to overnight at room temperature on a slowly rocking platform. The destained gel would be scanned and the image saved as a .tif file.

2.6.2 Western Blot Analysis

All solutions pertaining to Western Blot experiments are described in Appendix A.3.2.

2.6.2.1 Western Blot Preparation

Proteins were transferred from the SDS-PAGE gel to a Millipore Immobilon-P polyvinylidene difluoride (PVDF) membrane (Millipore, Billerica, Mass, USA) using an BioRad Mini-Protean-II system (Bio-Rad, Hercules, CA) as per manufacturer's instructions. Protein transfer typically took 2-5 hr at 25mA, depending upon gel size and total surface area of gels to be transferred. Transfer efficiency was monitored by analysing the transfer of protein standards, and occasionally by

subsequent staining of the PVDF membrane using a coomassie brilliant blue membrane stain. Following transfer, the membrane was blocked from 30 min to overnight in 5% dried milk blocking buffer prior to a brief wash in TEN and subsequent incubation with the appropriate dilution of primary antibody. The membranes were typically probed with a 1:50,000 dilution of mouse monoclonal anti-HIS primary antibody (Sigma-Aldrich, St. Louis MO) for 2 hr, although this was extended up to overnight if increased sensitivity was required. This was followed by a thorough wash in approximately 2 l TEN on a slowly rocking platform. A 1:20,000 dilution of alkaline phosphatase-conjugated GAM secondary antibody (Sigma-Aldrich, St. Louis MO) was used to probe for the presence of the primary antibody. The membranes were exposed to the secondary antibody solution for approximately 1 hr before being thoroughly washed in TEN.

2.6.2.2 Western Blot Visualization

Hybridization was visualized by chemiluminescent detection using alkaline-phosphatase conjugated secondary antibody. Samples were detected using the Typhoon system (GE Canada, Mississauga ON).

2.6.3 Protein Purification Under Native Conditions

All solutions pertaining to protein purification under native conditions are described in Appendix A.3.3.

BL21(λDE3) pLysS [64, 334] was used in all over-expression and purification analyses. This strain expresses T7 RNA polymerase from a *lac* promoter. This gene is present on the lambda lysogen called DE3. The pLysS plasmid limits leaky expression and confers chloramphenicol resistance. Expression was induced overnight using autoinduction media (Appendix A.1.1.10).

50 ml of overnight culture was harvested by centrifugation. Cells were lysed by the addition of 1 ml of Bugbuster reagent (EMD Chemicals Inc., Darmstadt, Germany) and10 μl of Benzonase (EMD Chemicals Inc., Darmstadt, Germany. The lysate was incubated on a rocking platform for 15 min at room temperature and then centrifuged for 20 min at 4°C at 16,000 rpm. The crude extract fraction (supernatant) was transferred to a new tube. 50 μl of Ni-NTA resin (EMD Chemicals Inc., Darmstadt, Germany) was added to the crude extract and the mix was incubated on the rocking platform at 4°C for 10 min before centrifugation at 700 rpm for 1 minute. The pellet was washed three times in 1 ml wash buffer (Appendix A.3.3). The bound protein was sequentially eluted with 50 μl of: 200 mM imidazole, 400 mM imidazole and 1 M imidazole elution butter. The resultant fractions were analysed on an SDS PAGE gel and quantitated by Bradford assay.

2.6.4 Bradford Assay

Protein sample concentration was determined by Bradford assay using the BioRad protein assay reagent (Bio-Rad, Hercules, CA). 100 μl of a 1 mg/ml BSA stock solution was diluted in 900 μl dH_2O. This 1:10 stock was then further diluted in dH_2O to produce 2, 4, 6, 8, 10 and 12 μg/ml protein standards in a final volume of 800 μl. Appropriate dilutions of the protein samples were then made to produce a final volume of 800 μl in dH_2O. 200 μl of Biorad reagent was added to each standard and each sample. All samples were incubated at room temperature for 5 minutes. Absorbance was assayed in a spectrophotometer using 800 μl dH_2O plus 200 μl reagent as a blank. A standard curve was constructed by plotting absorbance versus concentration for the BSA standards and the formula of that line was used to extrapolate concentration of the unknown samples.

2.7 Biochemical Assays

2.7.1 Preparation of Crude Cell Extract

Cell cultures were grown in an appropriate medium and under appropriate conditions. Cells were harvested by centrifugation, the pellets washed twice in 20 mM Tris-HCl pH 7.8, 1 mM $MgCl_2$ buffer, and stored at -20°C. Prior to sonication, pellets were suspended in 4 ml of sonication buffer (20 mM Tris-HCl pH 7.8, 1 mM $MgCl_2$, 10% glycerol, 10 mM β-mercaptoethanol) per gram of wet weight of pellet, and then maintained on ice. Cells were disrupted by sonication at 4°C for 4 min at 30 s intervals. Cell debris was removed by centrifugation and the resultant cell-free extracts were stored at 70°C until needed. Protein concentration was determined using standard techniques [307] (see Section 2.6.4).

2.7.2 PHB Analysis

2.7.2.1 PHB Isolation from Free-Living Cells

Cultures for PHB assays were grown in 250 ml Erlenmeyer flasks containing 50 ml of high-carbon medium. For *S. meliloti* this was typically YMB; for *B. japonicum* MAG was used. Cultures were grown at 30°C and 180 rpm for 48 hours (*S. meliloti*) or 72 hours (*B. japonicum*). *S. meliloti* cells were typically harvested, washed once in 0.85% NaCl and resuspended in 50 ml 0.85% NaCl. Owing to the extremely mucoid nature of *B. japonicum* cells grown under PHB-inducing conditions, *B. japonicum* cells were not subjected to these saline washes. PHB was extracted from 2 ml of cells, the remaining 48 ml were pelleted, dried at 60°C until constant mass was achieved and used to determine cell dry mass.

PHB content was determined using a modified version of the colourimetric assay developed by Law and Slepecky [200]. This assay is based in the hydrolysis of PHB

and subsequent conversion of the monomer to crotonic acid by concentrated H_2SO_4. Crotonic acid has an absorption maximum at 235 nm. The amount of crotonic acid can be used to determine PHB content of the initial sample. PHB content is expressed as a percentage of total cellular dry mass.

Following the initial harvest, no plasticware was used in the PHB extraction protocol; all glassware was washed thoroughly in boiling chloroform and rinsed in EtOH prior to use to remove any traces of plasticizers. Cells were pelleted in screw-capped pyrex centrifuge tubes (Corning Inc., Lowell, MA) at 6,000 rpm for 10 minutes. The cell pellet was washed in dH_2O and pelleted again before being resuspended in 2.0 ml of 5.25% NaOCl (Javex) and incubated at 37°C for 1 hour to allow for complete cell lysis to occur. The samples were then pelleted at 6,000 rpm for 15 minutes and washed in 5 ml dH_2O. This was followed by a wash in 5 ml EtOH and a final wash in 5 ml acetone. The pellet, which was white in colour, was allowed to dry before the PHB was extracted by the addition of 10 ml of cold chloroform. The tubes were capped, vortexed and transferred to a boiling water bath. The tubes were removed from the water bath and vortexed every 1-2 minutes for 10 minutes before cooling to room temperature. If necessary, pressure was released by loosening the caps periodically. Once cool, the tubes were vortexed again and 1 ml was removed and transferred to a glass test tube. The chloroform was allowed to evaporate at room temperature for 24-48 hours before addition of 10 ml concentrated H_2SO_4. The tubes were then capped with marbles and transferred to a boiling water bath for 10 minutes, after which time they were removed and allowed to cool to room temperature. After mixing well by vortex, OD from 220-280 nm was measured (Spectra Max 190, Molecular Devices).

A standard curve was obtained by assaying known quantities of PHB. Standard solutions were prepared from a 1 mg/ml PHB stock, made by adding 10 mg PHB (Sigma-Aldrich, St. Louis MO) to 10 ml cold chloroform and heating in a boiling

water bath to dissolve. From this, a 100 μg/ml stock was prepared. Aliquots of 0-100 μg PHB were transferred to test tubes and the chloroform was allowed to evaporate before addition of 10 ml H_2SO_4 and processing as described above.

2.7.2.2 PHB Isolation from Soybean Bacteroids

Soybean bacteroids was isolated in a crude preparation using a modified version of protocols described by Wong and Evans [391], and Vassileva and Ignatove [371]. Nodules were removed, by hand, from mature plants approximately 5 weeks post-inoculation. 2-4 g of nodules were crushed with a mortar and pestle in 2 volumes of 50 mM Tris-HCl (pH 8.4). The homogenate was filtered through 4 layers of cheesecloth and centrifuged at 300 x g for 10 minutes to remove large debris. The supernatant was then transferred to a deplasticized screw-capped pyrex centrifuge tubes (Corning Inc., Lowell, MA) and centrifuged for 15 minutes at 8,000 x g and 4°C to pellet the bacteroids. The pellet was washed twice in dH_2O and dried at 60°C. The pellet was weighed and then hydrolyzed overnight in 0.2 ml 5.25% NaOCl (Javex) per mg bacteroid pellet.

Following incubation, the lysate was pelleted at 8,000 x g for 20 minutes then washed once with dH_2O and once with acetone. The pellet was then dried and processed as described above.

2.7.2.3 Isolation of Native PHB Granules

Native PHB granules were isolated using a protocol modified from those described previously by Merrick and Doudoroff, Gebauer and Jendrossek, Preusting *et al* and Wang *et al* [108, 240, 277, 379]. The *S. meliloti* PHB depolymerase mutant Rm11430 was grown to saturation in 500 ml YMB. Cells were harvested and washed in 0.05 M potassium phosphate buffer (pH 7.0). The cell pellet was resuspended

in 30 ml 0.05 M potassium phosphate buffer (pH 7.0) and cells were lysed by three passages through an French Press.

Six Ultra-Clear^{TM} Beckman Ultracentrifuge tubes (Beckman-Coulter, Mississauga ON) were prepared with a discontinuous sucrose gradient as follows:

- 8 ml 2 M sucrose in 10 mM Tris-HCl (pH 8.0)
- 8 ml 1.66 M sucrose in 10 mM Tris-HCl (pH 8.0)
- 8 ml 1.33 M sucrose in 10 mM Tris-HCl (pH 8.0)
- 8 ml 1 M sucrose in 10 mM Tris-HCl (pH 8.0)

5 ml crude cell lysate was layered on top of the gradient and the tubes were centrifuged at 26,000 rpm for 15 hours in a Beckman SW28 Ultracentrifuge rotor (Beckman-Coulter, Mississauga ON). The PHB granule layer is clearly visible as a discrete band at the interface of the 1.66 M and 1.33 M sucrose layers. The granules were removed from the gradient and washed twice in 10 mM Tris-HCl (pH 8.0). Granules were stored at 4°C until use.

2.7.3 Alkaline Phosphatase Assay

Alkaline phosphatase activity of *exoF*::Tn*phoA* fusions in *S. meliloti* strains was measured according to the method of Brinkmann and Beckwith [31]. Cells were grown to an OD_{600} of 0.7. 1 ml of culture was washed twice in 1 M Tris-HCl (pH 8.0), and resuspended in 1 ml 1 M Tris-HCl (pH 8.0). The OD_{600} of this cell suspension was then measured. Following a 10 min equilibration period at 37°C, 50 μl of 4 mg/ml *p*-nitrophenyl phosphate (NPP) was added to start the reaction. The reaction was allowed to continue for 11 min at 37°C before being stopped by the addition of 50 μl of 1M K_2HPO_4. The cells were pelleted and 50

μl of the supernatant was diluted in 450 μl of 1 M Tris-HCl (pH 8.0) and OD_{420} was measured. Units (U) of alkaline phosphatase activity were calculated using the formula:

$$U=\frac{1000 \text{ x } OD600}{\text{Time(min) x } OD600}$$

Assuming a molar coefficient of 16,000 for *p*-nitrophenyl phosphate, 1 U is equal to 0.062 nmol of NPP hydrolyzed per min at a cell $OD_{600}$of 1. Therefore:

$$\text{nmol NPP hydrolyzed per min} = \text{ U} \times 0.062$$

2.7.4 *phbA* Assay

2.7.4.1 Preparation of Crude Cell Extract

Cells were grown in 50 ml complex medium to late-log phase and then harvested by centrifugation. The pellet was washed once in 50 ml 0.1 M Tris-HCl (pH 7.5) and resuspended in 5 ml 0.1 M Tris-HCl (pH 7.5). Cells were disrupted on ice by sonication in 4 cycles of 15 seconds on, 15 seconds off at 90% max setting.

2.7.4.2 Assay of β-Ketothiolase Activity

PhbA activity of *S. meiloti* was measured using a modified version of standard protocols [184, 249]. The assay measures the decrease of E_{303} of the Mg^{2+}-Enol complex of acetoacetyl-CoA as it is converted to acetyl-CoA. 10 μl 7 mM acetoacetyl-CoA, 100 μl 0.4 M $MgCl_2$, and 750 μl 0.1 M Tris-HCl (pH 8.1) were mixed together and incubated at 30°C for 2 minutes. 10 μl crude cell extract was added to this solution and the reaction was started by the addition of 30 μl 3.4 M CoA. The decrease in absorbance at OD_{300} was measured and activity was calculated using a molar extinction coefficient of 12.9 $cm^2.\mu mol^{-1}$ [159]. One U of activity is defined as the

amount needed to catalyze the formation or cleavage of 1 μmol acetoacetyl-CoA in 1 minute. The formula used to calculate activity is as follows:

$$\frac{\text{Units}}{\text{min}} = \frac{\frac{\Delta \text{A}}{\text{min}} \times 1.5}{(1.726 \times 10^4) \times 1}$$

2.7.5 Exopolysaccharide Quantitation

Solutions used in the isolation and quantitation of EPS are detailed in Appendix A.6.

2.7.5.1 Isopropanol Precipitation of Exopolysaccharide

Cells were grown to saturation in 50 ml high-carbon medium (YMB for *S. meliloti*; MAG for *B. japonicum* in a 250 ml Erlenmeyer flask. 25 ml cells were pelleted at 6,000 rpm for 20 mins and the supernatant was transferred to a fresh tube. The cell pellet was washed in 25 ml 1 M NaCl 10 mM EDTA and, following pelleting, the supernatant was combined with the supernatant from the initial harvest. The combined supernatants were centrifuged at 6,000 rpm for 20 mins to remove all traces of cell debris and were then transferred to clean 250 ml glass beakers. EPS was precipitated by the addition of 2 volumes (100 ml) ice cold isopropanol. The beakers were covered with aluminium foil and incubated overnight at 4°C to facilitate the precipitation.

Following overnight incubation, the EPS precipitate wass removed by successive rounds of centrifugation at 8,000 rpm for 20 mins in pre-weighed 50 ml centrifuge tubes. The pellet was then dried at 60°C overnight.

2.7.5.2 Exopolysaccharide Quantitation by Mass

25 ml cells from the original culture were pelleted at 6,000 rpm for 20 mins in pre-weighed tubes. The pellet was then dried at 60°C until constant mass was achieved in order to allow quantitation of CDM.

The dried EPS pellet and tube were weighed and the EPS mass determined by subtracting the combined weight from the weight of the pre-weighed tube.

EPS was expressed as EPS as a percent of CDM

2.7.5.3 Exopolysaccharide Quantitation by Anthrone Assay

The anthrone assay used is a modified version of the protocols described by Morris *et al* [247] and Trevelyan & Harrison [353].

25 ml cells from the original culture were pelleted at 6,000 rpm for 20 mins in pre-weighed tubes. The pellet was then dried at 60°C until constant mass was achieved in order to allow quantitation of CDM.

Anthrone reagent must be prepared fresh daily. The recipe for preparation is described in Appendix A.6. The dried EPS pellet was dissolved in 5 ml dH_2O. When necessary, 1:10 dilutions of the dissolved EPS were prepared. EPS for each sample was typically measured in duplicate from 2 independent cultures. 5 ml anthrone reagent was added to each test tube and the tubes were incubated on ice. 1 ml EPS sample was layered on top of the anthrone reagent and the tubes were capped with marbles. The tube contents were mixed by thorough vortexing. The tubes were transferred to a vigorously boiling water bath and heated for precisely 10 minutes (note, the time and intensity of heating are extremely important). The tubes were then removed from the boiling water bath and plunged into an ice-cold water bath for at least 2 mins. The intensity of the green colour was measured at 620 nm (Spectra Max 190, Molecular Devices) against an H_2SO_4 blank.

A standard curve of glucose blanks from 0-25 μg glucose was also generated, and the formula used to determine EPS content of each of the unknown samples. This EPS content was then expressed as μg of glucose equivalents as a percentage of CDM.

2.8 Desiccation Assay Techniques

2.8.1 On-Seed Survival Assays

On-seed survival was typically assayed by inoculating 400 g soybean seeds with 1.1 ml of saturated culture amended with 20% proprietary extender solution. The soybean-culture mix was vigorously shaken for 30 seconds before 5 seeds were removed, in triplicate, to 10 ml PBS in a sterile glass test tube. The tubes were vortexed vigorously for 60 seconds and then serially diluted. 100 μl of the three highest dilutions were plated in duplicate to determine CFU/seed at t=0. Samples were then assayed in this manner at appropriate intervals. Between sampling, inoculated seeds were maintained at 16°C, with approximately 70% humidity.

2.8.2 Filter Desiccation Assays

Desiccation tolerance was initially screened in using the filter desiccation protocol kindly provided by Dr Mike Kahn's lab at Washington State University (J. Humann, personal communication).

200 μl of saturated cultures were transferred to 36 wells of a 96-well plate (in order for the mutants to all fit onto the Whatman #1 filter only 36 can be picked per plate).

Each assay was performed using both YMA and TY. A sterile Whatman #1

filter (Whatman Canada Ltd., Toronto ON) was placed over the centre of each plate, and allowed to become completely moist. Colonies were replicated from the 96-well plate onto each plate using a 48-prong replicator. The plates were then incubated at 30°C until growth was uniform.

After sufficient growth had formed on the replicated plates, the filter was removed asceptically with forceps and placed cell-side-up on a sterile petri dish. The filter was left to dry in the 30°C incubator inside a plastic tub for 1 week. The filters were rehydrated by inverting them onto fresh YMA plates and incubated in the 30°C incubator until growth was evident, checking every 12-24 hours and recording any differences between patches.

2.8.3 96-Well Plate Desiccation Assays

Desiccation tolerance was assayed in a 96-well plate using the agar plug method kindly provided by Dr Mike Kahn's lab at Washington State University (J. Humann, personal communication). Assays were carried out in sterile 96-well plates (VWR International, Mississauga ON).

50 μl YMA were added to each of the wells of the 96-well plate. Plates were allowed to solidify and then wrapped in parafilm until needed. Liquid cultures were grown to saturation in the appropriate media and normalized to the same staring OD_{600} by dilution. Each column (12 columns in total) was inoculated with 4 μl in triplicate, for a total of 24 wells per sample. An airpore tape sheet (Qiagen Inc., Mississauga ON) was placed over the entire plate, leaving the paper strip still attached at the ends to facilitate easy removal. The 96-well plate lid was then replaced (over the airpore strip) and the plate was incubated at 30°C for 48 hours. After 48 hours, the airpore sheet was pulled back to reveal the first row of wells, to which 100 μl PBS was added. The PBS was removed, along with the agar plug,

and transferred to a test tube containing 4.9 ml PBS. This solution was vortexed vigorously and serial dilutions out to 10^{-6} were performed. 100 μl of these dilutions were plated, in duplicate, on an appropriate medium in order to determine CFU/ml at t=0. 96-well plates were then incubated at 30°C and samples were removed in this fashion at regular time points (typically 1, 2, 4, 8 and 16 weeks).

2.9 Microscopy Techniques

All microscopy solutions are described in Section A.8.

2.9.0.1 Preparation of Samples for Scanning Electron Microscopy (SEM)

Samples were fixed in sufficient 2.5% glutaraldehyde to be completely submerged and were then incubated for 1 hour at 4°C. Samples were washed three times in phosphate buffer (PB) for 20 minutes each. At this point samples could be left for up to 1 week if necessary. Samples were then dehydrated in a series of acetone as follows: 20% for 10 minutes; 50% for 10 minutes; 70% for 2 x 10 minutes; 95% for 10 minutes; 100% for 2 x 10 minutes. Samples were subjected to critical point drying using liquid CO_2 as the transitional fluid, before being mounted on aluminium stubs and coated with a thin layer of gold using a sputter-coater. Samples were examined at an accelerating voltage of 15 kV on a Hitachi S-570 scanning electron microscope (Hitachi, Tokyo, Japan).

2.9.0.2 Preparation of Samples for Transmission Electron Microscopy (TEM)

Plants were harvested 28-30 days post-inoculation. Roots were washed to remove traces of vermiculite, and the nodules were transferred into primary fixative (4%

formaldehyde, 1% glutaraldehyde in 80 mM HEPES pH 7.0) and cut into small pieces. The samples were subjected to 4 cycles of vacuum infiltration (2 mins per cycle) and were left overnight at 4°C. Following infiltration, the nodules were washed thoroughly in sterile water, and stained for 4 hours in 1% OsO_4. The nodules were washed again in water and dehydrated through a gradient of acetone. The nodules were embedded in epon araldite resin and transferred to BEEM capsules for 48 hours at 60°C. Ultrathin sections were cut using a Reichert Ultracut E microtome, and were stained with uranyl acetate and lead citrate using standard techniques [372]. Samples were analysed in a Philips CM10 transmission electron microscope at an accelerating voltage of 60 kV.

Chapter 3

Poly-3-Hydroxybutyrate Synthesis in *Bradyrhizobium japonicum*

3.1 Poly-3-Hydoxybutyrate Metabolism in *Bradyrhizobium japonicum*

PHB metabolism appears to play a diverse role in the metabolism of a range of different prokaryotes. In *R. leguminosarum*, PHB synthesis has been shown to help regulate the carbon and redox balance of the tricarboxylic acid (TCA) cycle [377] and in *S. meliloti, phbC* mutants are impaired in their ability to grow on PHB cycle intermediates [40]. In addition, *phbC* mutants of *Rhizobium etli* demonstrate higher levels of N_2-fixation during symbiosis [43] presumably because they are channelling all of the available carbon into N_2-fixation rather than into carbon storage; *S. meliloti phbC* mutants show slightly decreased levels of N_2-fixation [7], and are also defective in competition for nodulation relative to the wild-type parental strain, Rm1021 [390]. It has been suggested that accumulation of PHB during saprophytic growth may be advantageous during nodule initiation or invasion [390] although the

mechanisms through which this provision is made remain elusive.

Like many strains of rhizobia, *Bradyrhizobium japonicum* is capable of synthesizing high levels of polyhydroxyalkanoates (PHA) under sub-optimal growth conditions (reviewed in [351]) in which growth is inhibited by the lack of a key nutrient but carbon supplies are abundant. These intracellular carbon stores can later be mobilized to support metabolism under conditions of carbon starvation, such as those experienced during long-term inoculant storage. In agreement with this hypothesis, a *phbC* mutant in *Azospirillum brasilense* demonstrated a reduced survival capacity in the absence of an exogenous carbon supply [172]. Furthermore, PHA/PHB has been shown to protect the cell from a wide range of stresses, including heat shock, UV irradiation, exposure to an oxidizing agent, and osmotic shock [174], suggesting that the effects of PHA/PHB at the cellular level are diverse. The PHB cycle in *S. meliloti* has been characterized, and is outlined in Figure 1.8. Each gene in this cycle, except for *phaZ*, has been identified and analyses of mutant phenotypes have shown that the ability to synthesize and utilize PHB is important in competitive growth and long-term survival [390].

Unlike *S. meliloti*, *B. japonicum* elicits the formation of determinate nodules on the roots of its host symbiont, soybean. Bacteroids of *B. japonicum*, and other determinate-nodule-forming rhizobia, are capable of accumulating large amounts of PHB during symbiosis. Indeed, some reports cite that *B. japonicum* bacteroids may contain 30-70% PHB by mass [18, 122, 391], an amount that does not appear to fluctuate relative to nitrogenase activity, but which does decline during periods of carbon stress such as periods of darkness or during seed production by the host plant [18, 17, 391]. While it is conceivable that PHB synthesis during symbiosis might compete with nitrogenase for photosynthate, the ability of bacteroids from determinate nodules to undergo a process of reverse differentiation following nodule senescence [132, 231, 235, 337, 357] makes it likely that the accumulated PHB

gives the cells a competitive advantage when released into the soil. Assisting the bacteroids in PHB accumulation potentially benefits the host plant by "seeding" the soil with a population of viable rhizobia that would be available to nodulate the next generation of plants after seed formation and plant death.

Analysis of the recently completed genome sequence of *B. japonicum* [178, 179] suggested the presence of five PHA/PHB synthase homologues (Blr2885, Blr3732, Bll4360, Bll4548, and Bll6073) – one of which (Bll4360) was shown to be able to functionally complement a *S. meliloti phbC* mutation – and two *phbAB* operons (Bll0225/Bll0226 and Blr3724/Blr3725) predicted to encode acetyl-CoA acetyltransferase and acetoacetyl-CoA reductase [7]. These genes are distributed throughout the entire genome, as depicted in Figure 1.9. The presence of so many copies of *phbC* suggests a significant role for PHA synthase in *B. japonicum* metabolism, although it is not known if each of these genes encodes a functional PHA synthase and, at the time this study was initiated, no studies had been conducted to investigate this further.

Over 59 PHA synthase genes have now been cloned and characterized (reviewed in [351]) and multiple sequence alignments show that these genes share an overall identity of 8-96% with only eight strictly conserved, catalytically important amino acids [285]. The five predicted *phbC* genes in *B. japonicum* range in size from 300 to 600 amino acids (discussed in Section 1.3.1), which is within the range of known PHA synthases [7]. All five of the *B. japonicum* genes also contain the modified lipase box motif, GX[S/C]XG, and at least seven of the eight highly conserved residues found among *phbC* genes (see Figure 3.1 and Table 3.1) [7, 285].

The five *phbC* genes were cloned separately by PCR into pRK7813 [169] and the ability of each to complement the pleiotropic phenotype of the *S. meliloti phbC* mutant was examined. Of the five *phbC* homologues, only Blr3732 and Bll4360 were able to complement the PHB synthesis phenotype of *S. meliloti phbC* mutant.

Furthermore, Blr3732, Bll4360 and Bll6073 all demonstrated a partial capacity to complement the acetoacetate growth phenotype of the *S. meliloti phbC* mutant, but none was able to fully restore growth on acetoacetate. Interestingly, recent data has shown that Bll6073, an apparently non-complementing homologue, is up-regulated in bacteroids [308, 309].

In order to determine whether different PHB synthases are used in symbiosis relative to free-living growth, mutants of the *phbC* genes as well as of both phbAB operons were constructed by allelic replacement. Single mutants of three of the *phbC* loci (Blr2885, Blr3732 and Bll6073) and both *phbAB* operons (Bll0225/Bll0226 and Blr3724/Blr3725) we constructed by cross-over PCR and allelic replacement. In addition, double mutants of both *phbAB* operons as well as different combinations of *phbAB* and *phbC* genes, have been constructed. The effects of these mutations on free-living and symbiotic phenotypes was assessed.

This study highlights the complex metabolic networks that are characteristic of the *Rhizobiaceae* and demonstrates that the PHB cycle plays an integral role in central carbon metabolism in these bacteria under free-living and symbiotic conditions. While previous studies have elucidated the mechanisms by which PHB is synthesized and degraded, very little work has addressed the regulation and co-ordination of PHB metabolism in each growth phase. This study represents the next step in understanding the integral role that carbon metabolism has to play in the life cycle of rhizobia.

Figure 3.1: Boxshade alignment of *B. japonicum* PhbC amino acid sequences. Black boxes indicate residues conserved in all PHA synthases; Red boxes indicate the modified lipase box motif

Table 3.1: Conserved catalytic residues in *S. meliloti phbC* and their corresponding residues in each of the *B. japonicum phbC* ORFs

Rm1021	Blr2885	Blr3732	Bll4360	Bll4548	Bll6073
S290	S92	S247	S277	S100	S348
C349	C151	C306	C336	C154	C348
G352	G154	G309	G339	G157	G351
D381	D180	D338	D368	D182	D380
W450	W251	W406	W253	W437	W449
D504	D306	D462	D491	D307	D503
G531	G333	G489	G518	E334	G530
H532	H334	H490	H519	P335	H531

3.2 Results and Discussion

3.2.1 Cloning of *B. japonicum phbC* Open Reading Frames

All strains and plasmids described in this chapter are listed in Table 2.1. For ease of reading, a summary of the relevant strains and plasmids are listed in Tables 3.2 and 3.3. Primers were designed against the 5' and 3' regions of each *phbC* open reading frame, and are listed in Table 2.2. Each ORF was amplified by PCR using KOD polymerase (EMD Biosciences, San Diego, CA) and following standard protocols [307]. As described in Table 2.2, primers were designed to include restriction sites in the 5' and 3' regions, to facilitate easy cloning from the purified PCR product directly into pRK7813 [169]. The resultant plasmids, described in Table 2.1 were transferred into the *phbC* mutant strain of *S. meliloti*, Rm11105, by triparental mating (Section 2.4.4.5) and transconjugants were isolated by plating on TY Sm_{200} Tc_{10}. Following three rounds of streak purification, transconjugants were assayed for the ability of the plasmid construct to complement several characteristic *phbC* phenotypes of *S. meliloti*.

3.2.2 Complementation of *S. meliloti phbC* Mutant by *B. japonicum phbC* ORFs

As described previously, the *phbC* mutant of *S. meliloti* demonstrates a pleiotropic phenotype (reviewed in [351]). The cloned *B. japonicum phbC* genes were each tested for their ability to complement the *S. meliloti* Rm11105 PHB synthesis, EPS synthesis and acetoacetate utilization phenotypes.

Table 3.2: Summary of strains constructed in the analysis of *B. japonicum* PHB metabolism

Strain	Relevant Characteristics
USDA110	wt
BjUW1	USDA110 pMA105
BjUW2	USDA110 pMA106
BjUW4	USDA110 pMA108
BjUW5	USDA110 pMA109
BjUW8	USDA110 ΔBlr2885
BjUW9	USDA110 ΔBlr3732
BjUW10	USDA110 pMA107 #1
BjUW11	USDA110 pMA107 #2
BjUW12	USDA110 pMA108
BjUW13	USDA110 ΔBll6073
BjUW14	USDA110 pMA109
BjUW15	USDA110 ΔBll0225 and ΔBll0226
BjUW16	USDA110 ΔBlr3725 and ΔBlr3726
BjUW17	USDA110 ΔBlr3725 and ΔBlr3726 #2
BjUW18	BjUW9 pMA107 #1
BjUW19	BjUW9 pMA107 #2
BjUW20	BjUW16 pMA110#1
BjUW21	BjUW16 pMA110#2
BjUW22	BjUW15 pMA111#1
BjUW23	BjUW15 pMA110#2
BjUW24	BjUW9 pMA111#1
BjUW25	BjUW9 pMA111#2
BjUW26	BjUW9 pMA105#1
BjUW27	BjUW9 pMA105#2
BjUW28	BjUW9 ΔBlr2885 #1
BjUW29	BjUW9 ΔBlr2885 #2
BjUW30	BjUW9 ΔBlr3725 and ΔBlr3726 #1
BjUW31	BjUW9 ΔBlr3725 and ΔBlr3726 #2
BjUW32	BjUW15 ΔBlr3725 and ΔBlr3726 #1
BjUW33	BjUW15 ΔBlr3725 and ΔBlr3726 #2

Table 3.3: Summary of plasmids constructed or used in the analysis of *B. japonicum* PHB metabolism

Plasmid	Relevant Characteristics
pK19*mobsacB*	Suicide vector Km^R
pGEMTEasy	Cloning vector for PCR-generated DNA fragments, Amp^R
pRK7813	RK2 derivative carrying pUC9 polylinker. Tc^R
pMA100	pGEMTEasy Blr2885 AD joined fragment
pMA101	pGEMTEasy Blr3732 AD joined fragment
pMA102	pGEMTEasy Bll4360 AD joined fragment
pMA103	pGEMTEasy Bll4548 AD joined fragment
pMA104	pGEMTEasy Bll6073 AD joined fragment
pMA105	pK19*mobsacB* Blr2885 AD from pMA100
pMA106	pK19*mobsacB* Blr3732 AD from pMA101
pMA107	pK19*mobsacB* Bll4360 AD from pMA102
pMA108	pK19*mobsacB* Bll4548 AD from pMA103
pMA109	pK19*mobsacB* Bll6073 AD from pMA104
pMA110	pK19*mobsacB* Bll0225/Bll0226 AD
pMA111	pK19*mobsacB* Blr3725/Blr3726 AD
pMA156	pRK7813 Blr2885
pMA118	pRK7813 Blr3732
pMA119	pRK7813 Bll4360
pMA120	pRK7813 Bll4548
pMA121	pRK7813 Bll6073

3.2.2.1 Restoration of EPS Synthesis

Exopolysaccharide synthesis was analysed by observing mucoidy of the colonies when grown on high-carbon media. Wild-type *S. meliloti* demonstrates a characteristic mucoid phenotype when grown under PGB-inducing conditions; this mucoidy is absent in the *phbC* strain Rm11105. As shown in Figure 3.2 when grown on Yeast Mannitol agar (YMA), only Blr3732 and Bll4360 were able to restore EPS production in Rm11105.

3.2.2.2 Restoration of PHB Accumulation

The ability to complement the PHB synthesis phenotype of Rm11105 was determined in two ways. Initially, each complemented clone was screened on YMA containing Nile Red. Nile Red is a dye that binds to PHB granules in the cytoplasm of the cell, and fluoresces under UV light. As shown in Figure 3.3, only Blr3732 and Bll4360 appeared to be able to complement the PHB synthesis phenotype of this mutant.

In order to more quantitatively characterize PHB synthesis by these complemented clones, PHB content was also determined by organic extraction [200], following growth to saturation in yeast mannitol broth. The data presented in Table 3.4 confirm the results of the screening on YMA-Nile Red, showing that only Blr3732 and Bll4360 are capable of complementing the PHB synthesis phenotype of Rm11105.

3.2.2.3 Complementation of Carbon Source Utilization Phenotype of the *S. meliloti phbC* Mutant

Rm11105 lacks the ability to grow on either acetate or acetoacetate as a sole carbon source. All Rm11105 *B. japonicum phbC* transconjugants were tested for their

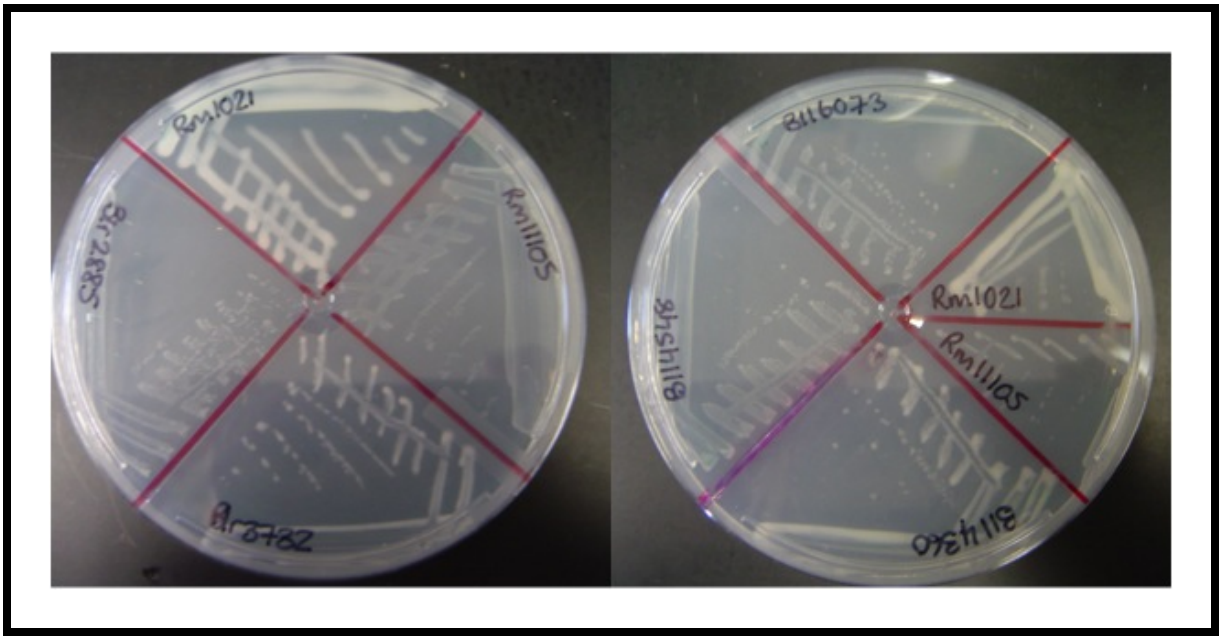

Figure 3.2: Complementation of EPS phenotype of *S. meliloti phbC* mutant with *B. japonicum phbC* genes

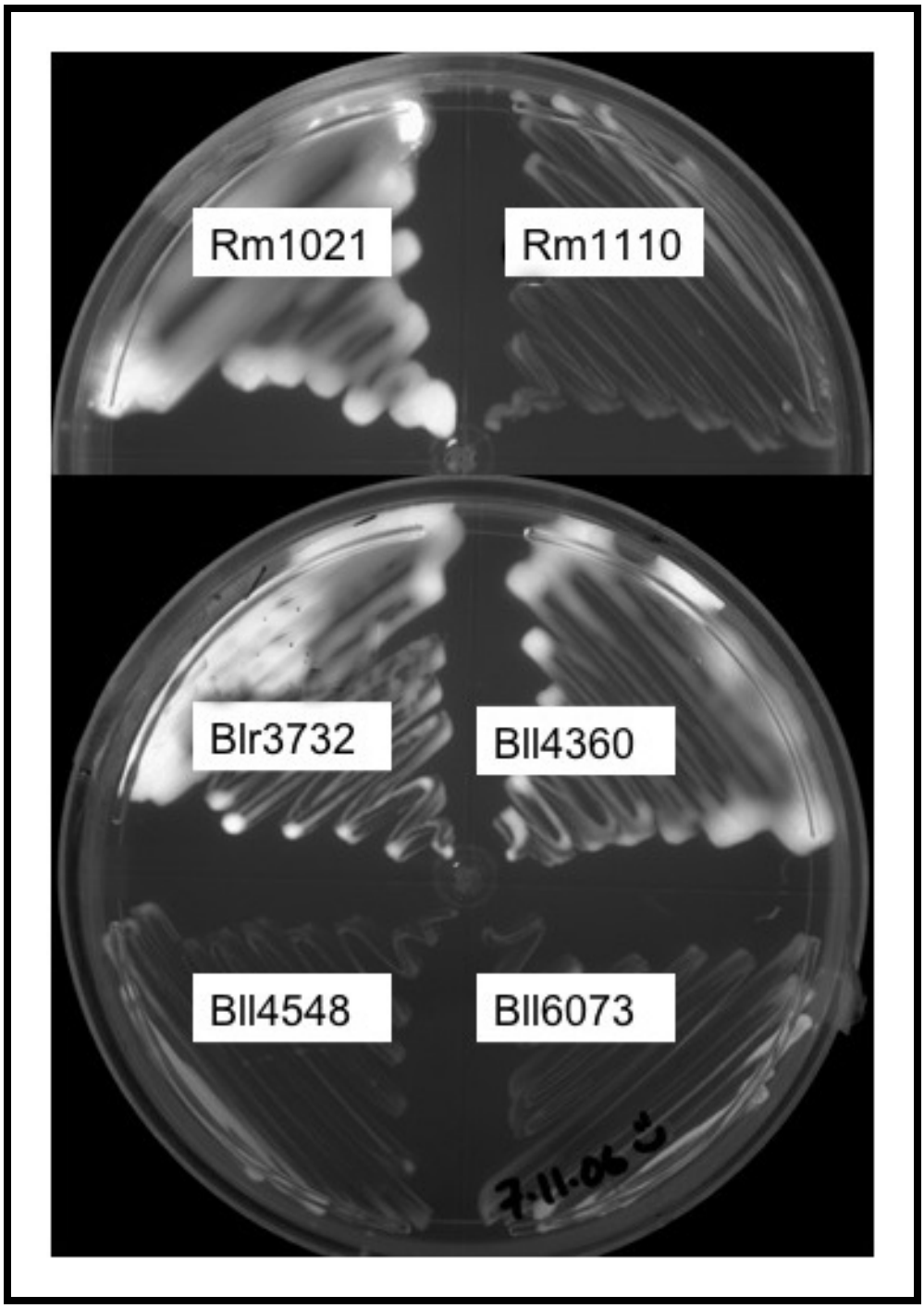

Figure 3.3: Complementation of the PHB phenotype of *S. meliloti phbC* mutant with *B. japonicum phbC* genes on YMA containing Nile Red

Table 3.4: PHB accumulation by *S. meliloti* Rm11105 complemented with *B. japonicum phbC* genes

Strain	% PHB (w/w)
Rm1021	18.9
Rm11105	0.2
Rm11105 Blr2885	0.3
Rm11105 Blr3732	14.9
Rm11105 Bll4360	17.3
Rm11105 Bll4548	2.2
Rm11105 Bll6073	0.9

ability to complement the carbon utilization phenotypes of Rm11105. The results of these growth curves are shown in Figures 3.4, 3.5 and 3.6.

As shown in Figure 3.6 only Blr3732, Bll4360 and Bll6073 all demonstrated a partial capacity to complement the acetoacetate growth phenotype of the *S. meliloti* *phbC* mutant, but none was able to fully restore growth on acetoacetate. Interestingly, recent data has shown that Bll6073, an apparently non-complementing homologue, is up-regulated in bacteroids [308, 309].

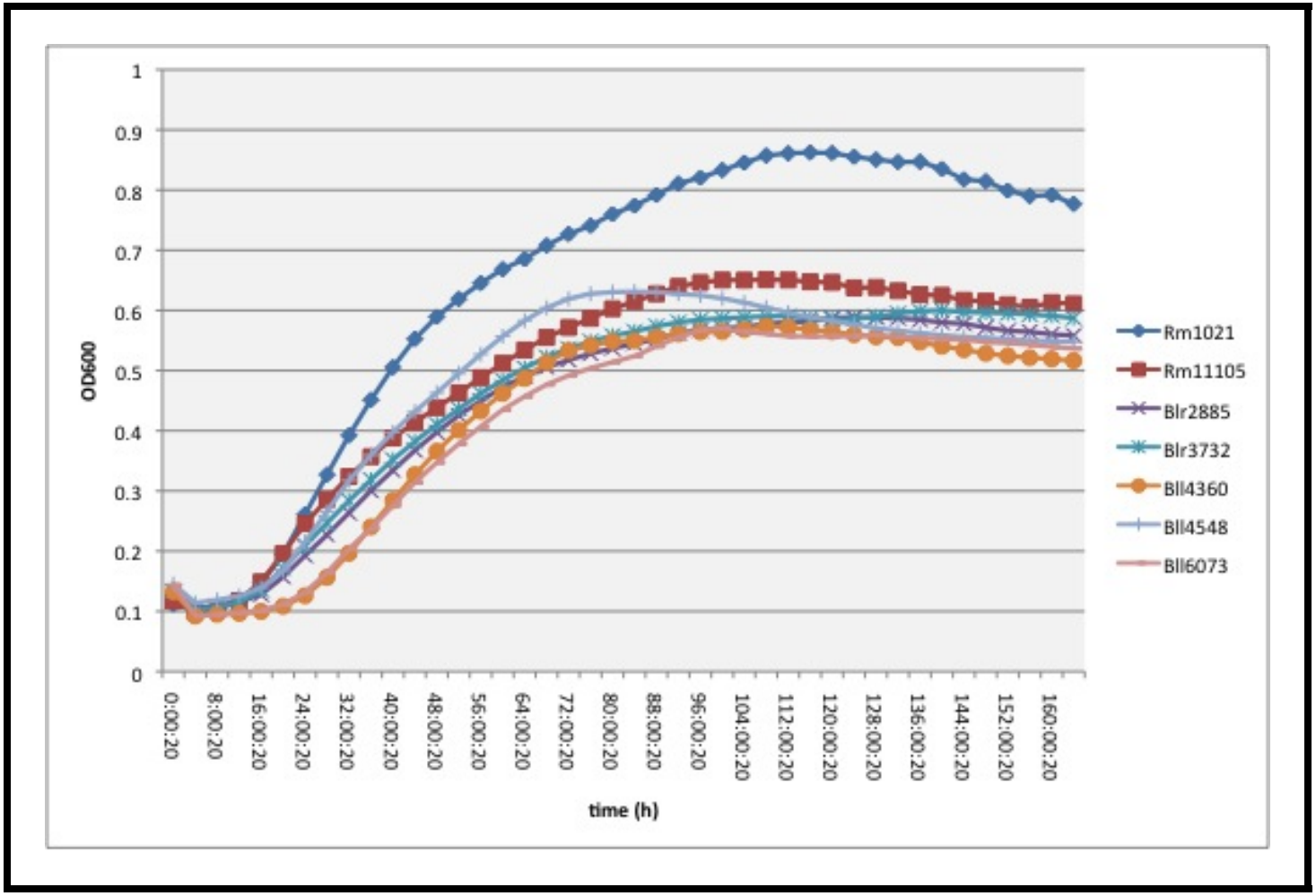

Figure 3.4: Growth curve of *S. meliloti phbC* mutant strain Rm11105 in VMM Glucose medium. VMM Glucose served as the positive control for all *S. meliloti* Rm11105 growth curves

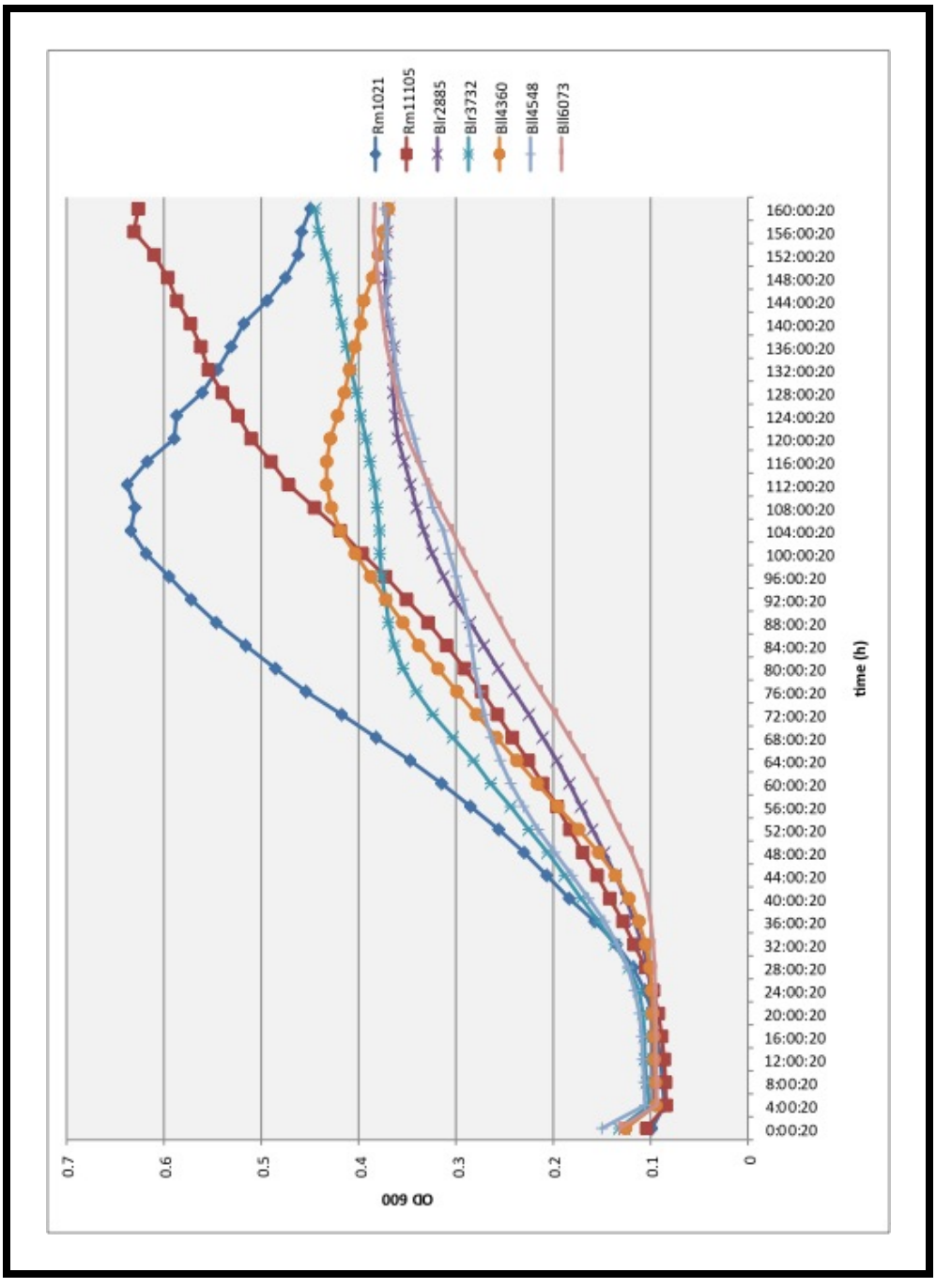

Figure 3.5: Growth curve of *S. meliloti phbC* mutant strain Rm11105 in VMM acetate medium

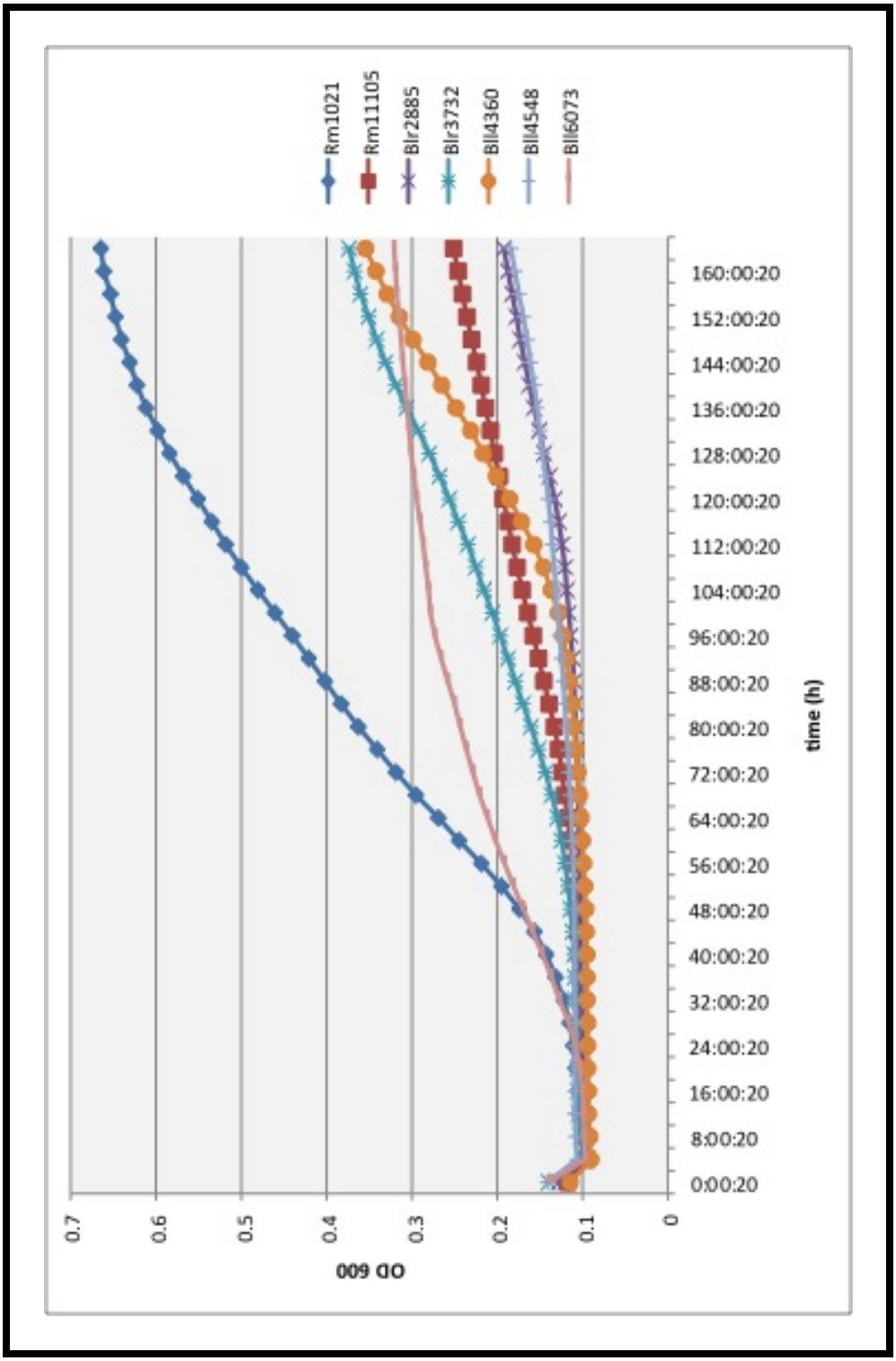

Figure 3.6: Growth curve of *S. meliloti phbC* mutant strain Rm11105 in VMM Acetoacetate medium

3.2.3 PHB Metabolism in *B. japonicum*

3.2.3.1 Characterization of *B. japonicum* Antibiotic Resistance Profile

A problem that quickly became apparent was the inherent tolerance that *B. japonicum* demonstrates towards many commonly used laboratory antibiotics [56]. For this reason it was important to establish precisely which antibiotics could be used as selective agents by determining how sensitive *B. japonicum* USDA110 is to various antimicrobial agents. By spot-plating serial dilutions of *B. japonicum* USDA110 onto AG plates containing various concentrations of antibiotics, an elementary resistance profile was compiled (Table 3.5). These data suggest that kanamycin resistance would be the most useful selectable marker, and that the inherent resistance of *B. japonicum* to tetracycline would make it a useful antibiotic for counter-selection against *E. coli* donor strains. The data are summarized in Table 3.5 and form the basis for the antibiotic concentrations documented in Appendix A.1.2.3.

3.2.3.2 Construction of *B. japonicum* PHB Synthesis Mutants

Single deletion mutants of three of the five *phbC* genes and both *phbAB* operons of *B. japonicum* were generated by crossover PCR [336] (Figure 3.7). Primer sets were designed such that the crossover PCR would generate a construct that would produce an in-frame deletion as a result of allelic replacement in the host genome. Primers used in constructing deletion mutants were designed in sets of four and were designated A, B, C, and D based on the location of their target sequence relative to those highlighted in Figure 3.7. A complete list of primers may be found in Table 2.2. The initial round of PCR produced an upstream product (A/B) and a downstream product (C/D), that were confirmed by gel electrophoresis. These products were purified by gel extraction and used as the template for the second round of PCR using primers A and D to generate a joined fragment that was then cloned into

Table 3.5: Antibiotic resistance profile of *B. japonicum* USDA110 grown on AG medium supplemented with different concentrations of antibiotics

Antibiotic	Final Concentration (μg/ml)				
Streptomycin	50	100	150	200	400
	R	S	S	S	nd
Neomycin	50	100	150	200	400
	R	R	R	nd	nd
Tetracycline	10	25	50	200	600
	R	R	R	S	S
Chloramphenicol	25	50	100	200	400
	R	R	R	nd	nd
Rifampicin	25	50	100	200	400
	R	R	R	nd	nd
Gentamycin	20	40	100	150	200
	R	R	R	R	R
Kanamycin	25	50	100	200	400
	R	S	S	S	S

Note, growth is scored as either R (resistant, growth was evident above background) or S (sensitive, no discernible growth).
nd: not determined

the general cloning vector pGEM-TEasy®. This product was confirmed by PCR and subsequently cloned into the suicide vector pK19*mobsacB* [310]. All of these plasmid constructs are documented in Table 2.1. This construct was transferred into *B. japonicum* by triparental mating, as described in Section 2.4.4.5, and single recombinants were selected by plating on AG $Km_{50}Tc_{10}$. Following three successive rounds of streak purification on AG $Km_{50}Tc_{10}$, double recombinants were isolated by growing the strains to saturation in AG with no selection and plating serial dilutions of up to 10^{-4} on AG containing 5% sucrose. Sucrose-Resistant colonies were then patched onto both AG sucrose and AG Km_{50} to distinguish between true double-recombinants and single recombinants with *sacB* inactivation. True double recombinants were then screened for the deletion by colony PCR (Section 2.4.4.12) and confirmed by gel electrophoresis. A representative gel is shown in Figure 3.8. Two *phbC* double mutants have also been constructed, as has a double mutant of both *phbAB* operons. For reasons that remain unclear, two of the *phbC* open reading frames proved recalcitrant to mutation.

3.2.3.3 Symbiotic Phenotype of *B. japonicum phbC* and *phbAB* Mutants

The presence of so many putative *phbC* and *phbAB* open reading frames suggests that PHB production may be important under different physiological conditions. It is tempting to speculate that PHB production may be differentially regulated under free-living and symbiotic conditions. Furthermore, since PHB production during symbiosis would appear to divert carbon away from nitrogen fixation, it is important to determine whether elimination of PHB production during symbiosis has an effect on plant dry mass. In order to determine the symbiotic phenotype of the *B. japonicum* PHB synthesis mutants, a soybean growth facility was constructed by suspending high-pressure sodium lamps from a traditional greenhouse bench and

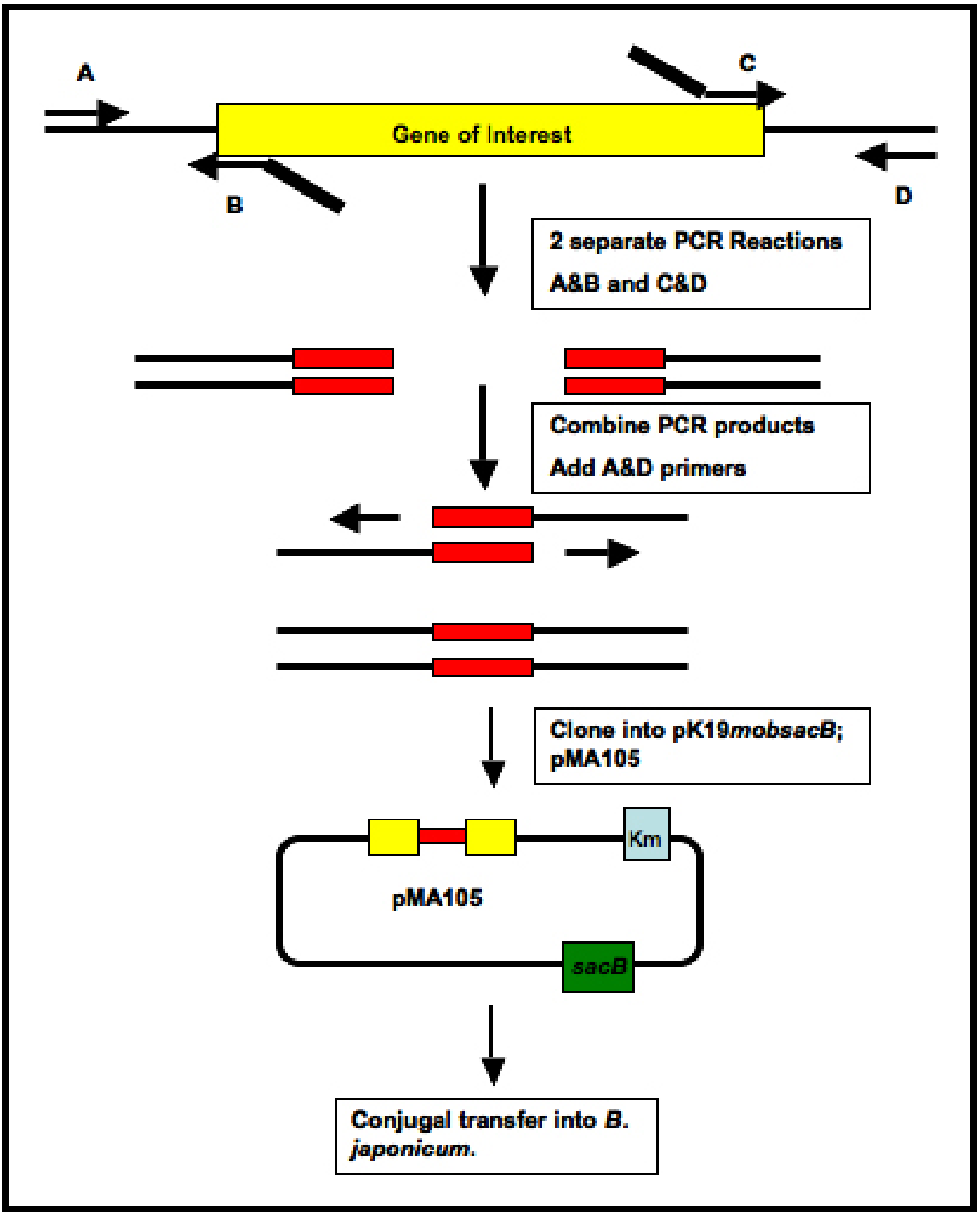

Figure 3.7: Crossover PCR strategy used to construct *phbC* and *phbAB* mutations in *B. japonicum*

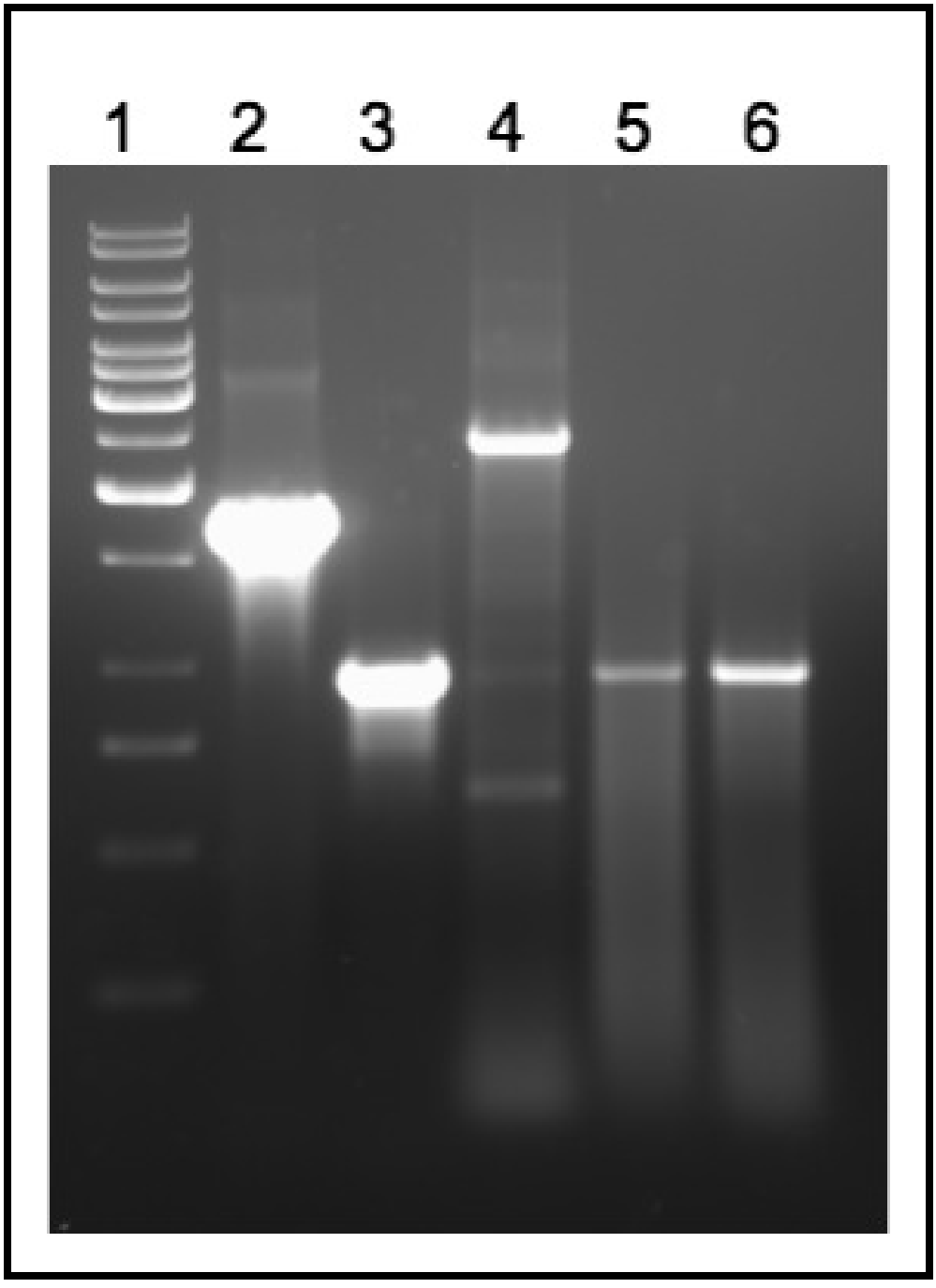

Figure 3.8: Colony PCR of Blr2885 and Blr3724/3725 constructions. 1: 1 kb ladder; 2: WT Blr2885; 3: Mutant Blr2885; 4: WT Blr3724/3725; 5 and 6: Mutant Blr3724/3725

supplementing the light production with compact fluorescent bulbs (Figure 3.9). This facilitated the growth of up to 30 pots of soybean simultaneously, with no detectable innoculum cross-contamination.

The data in Table 3.6 (from triplicate experiments) show that plants inoculated with PHB synthesis mutants do appear to show reduced plant mass relative to those inoculated by the wild-type strain. This reduction in plant mass is reproducible but, when analysed using a Student's t-test, the data are not statistically significant except in the case of plants inoculated with BjUW9.

3.2.3.4 PHB accumulation of *B. japonicum phbC* and *phbAB* Mutants

Each mutant strain was tested for the ability to accumulate PHB under both free-living and symbiotic conditions. For analysis of free-living PHB accumulation, the standard PHB assay, using an organic extraction [200], was modified for use with *B. japonicum* and was used to quantitate PHB accumulation in cells grown under high-carbon conditions. *B. japonicum* USDA110 cannot utilize mannitol as a sole carbon source, so it was necessary to modify the standard high-carbon growth conditions in order to induce PHB accumulation. A high-carbon medium containing an excess of arabinose and gluconate, which gave optimal growth relative to other PHB-inducing media, was developed for this purpose (Appendix A.1).

To measure PHB accumulation in symbiosis, PHB had to be extracted directly from the bacteroids. Soybean plants were grown as describe in Section 2.7.2.2 and nodules were removed from the resultant root structures. The process of bacteroid isolation is modified from Wong and Evans [391], and Vassileva and Ignatove [371] and depicted in Figure 3.10.

As shown in Table 3.7, knocking out Bll0225/6 (*phbAB*, mutant BjUW15) was sufficient to eliminate PHB production by *B. japonicum* USDA110 under free-living

Figure 3.9: Soybean growth facility constructed within the Charles lab at the University of Waterloo. This set-up employed two high-pressure sodium bulbs, augmented by compact fluorescent bulbs and was capable of holding up to 30 pots simultaneously without cross-contamination

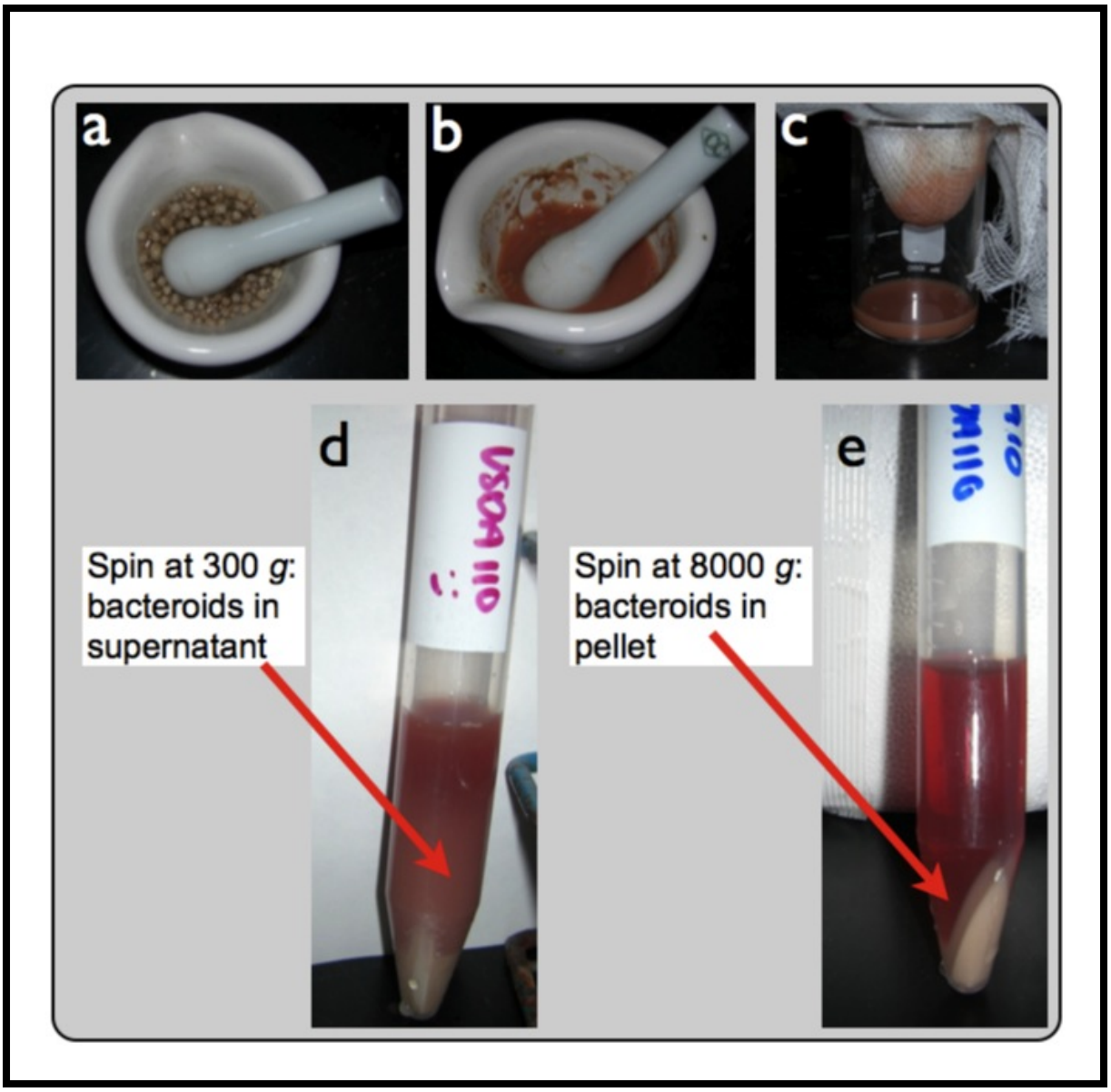

Figure 3.10: The process of bacteroid isolation from soybean nodules. Nodules were weighed and then crushed using a pestle and mortar (a, b), and the resultant crushate was filtered through three layers of cheesecloth (c). The filtered crushate was centrifuged at 300 x *g* (d) and the supernatant transferred to a fresh tube for a second centrifugation step at 8,000 x *g* (e). The supernatant was decanted and the resultant bacteroid-containing pellet was dried and subject to organic PHB extraction following standard techniques [200]

Table 3.6: Shoot dry masses of soybean plants Inoculated with different *B. japonicum* PHB synthesis mutants

Strain	Relevant Characteristics	Average Mass per Plant (g)
Uninoculated	negative control	0.61[a]
USDA110	wild-type	1.60[a]
BjUW8	*phbC* Blr2885	1.09
BjUW9	*phbC* Blr3732	0.90[a]
BjUW13	*phbC* Bll6073	1.31
BjUW15	*phbAB* Bll0225 and Bll0226	1.22
BjUW16	*phbAB* Blr3724 and Blr3725	1.04
BjUW28	BjUW8 Blr3732	1.66
BjUW31	BjUW9 Blr3732	1.66
BjUW32	BjUW15 Blr3724 and Blr3725	1.13

[a] These differences are statistically significant

conditions; Blr3724/5 *phbAB*, mutant BjUW16) is required for PHB production during symbiosis. This is the first example of *B. japonicum* mutants that are unable to synthesize PHB.

3.2.3.5 Rhizosphere Competitiveness of *B. japonicum* PHB Synthesis Mutants

The PHB synthesis mutants of *S. meliloti* demonstrate a distinct loss of rhizosphere competitiveness relative to the wild-type strain [9]. To determine whether a similar correlation between PHB synthesis capacity and nodulation competitiveness exists in *B. japonicum*, the three *phbAB* mutants BjUW15, BjUW16 and BjUW32 were all tested for their ability to compete for nodulation with BjUW36, a spontaneous Sm^R-derivative of the wild type strain USDA110. BjUW36 was isolated by plating cells from 1 ml of a saturated culture of *B. japonicum* USDA110 on AG Sm_{200}. The resultant colony was streak purified three times on AG Sm_{200} before use.

The data in Table 3.8 show the results of these competition assays. In each trial, approximately 15 nodules were crushed and the bacteroids screened for Sm^R or Sm^S. These data show that, similarly to *S. meliloti*, PHB synthesis mutants of *B. japonicum* also demonstrate reduced rhizosphere competitiveness.

3.2.3.6 Growth Phenotypes of *B. japonicum phbC* and *phbAB* Mutants

PHB synthesis mutants of *S. meliloti* demonstrate an inability to grow on the PHB cycle intermediates acetoacetate and 3-hydroxybutyrate. Each of the *B. japonicum* PHB mutants was analysed for growth on these carbon sources to determine if this phenotype was consistent between the two species. Growth curves were generated using the Bioscreen-C growth curve machine (see Section 2.5.1.1) and were

Table 3.7: PHB accumulation by *B. japonicum* PHB synthesis mutants under both free-living and symbiotic conditions, expressed as mg PHB as percent cell dry mass

	mg PHB as % CDM	
Strain	Free-Living	Bacteroid
USDA110	11.6	17.2
BjUW8	13.1	nd
BjUW9	9.3	15.6
BjUW13	11.4	nd
BjUW15	3	17.6
BjUW16	12.3	6.7
BjUW32	1.3	1.2

Table 3.8: Nodulation competitiveness of the *B. japonicum phbAB* mutants co-inoculated in the described ratios with the wild-type strain USDA110 on Soybean (*Glycine Max*) plants

Strain (%) in innoculum	No. nodules tested	Nodule occupancy (%)		
		Strain 1	Strain 2	Both
USDA110 (10) + BjUW36 (90)	17	13	2	2
USDA110 (50) + BjUW36 (50)	15	6	6	3
USDA110 (90) + BjUW36 (10)	18	1	16	1
BjUW36 (10) + BjUW15 (90)	16	5	10	1
BjUW36 (50) + BjUW15 (50)	17	10	4	3
BjUW36 (90) + BjUW15 (10)	18	16	2	0
BjUW36 (10) + BjUW16 (90)	17	0	14	3
BjUW36 (50) + BjUW16 (50)	18	6	8	4
BjUW36 (90) + BjUW16 (10)	nd	nd	nd	nd
BjUW36 (10) + BjUW32 (90)	12	1	10	1
BjUW36 (50) + BjUW32 (50)	13	8	2	3
BjUW36 (90) + BjUW32 (10)	8	8	0	0

nd: not determined

followed for 10 days in Vincent's Minimal Medium (Appendix A.1), supplemented with the appropriate carbon source. A representative samples of these growth curves is shown in Figures 3.11, 3.12 and 3.13. As can be seen in these graphs, no discernible difference was observed between wild-type *B. japonicum* USDA110 and any of the PHB synthesis mutants, suggesting that the regulatory pathways for carbon metabolism differ between *S. meliloti* and *B. japonicum*.

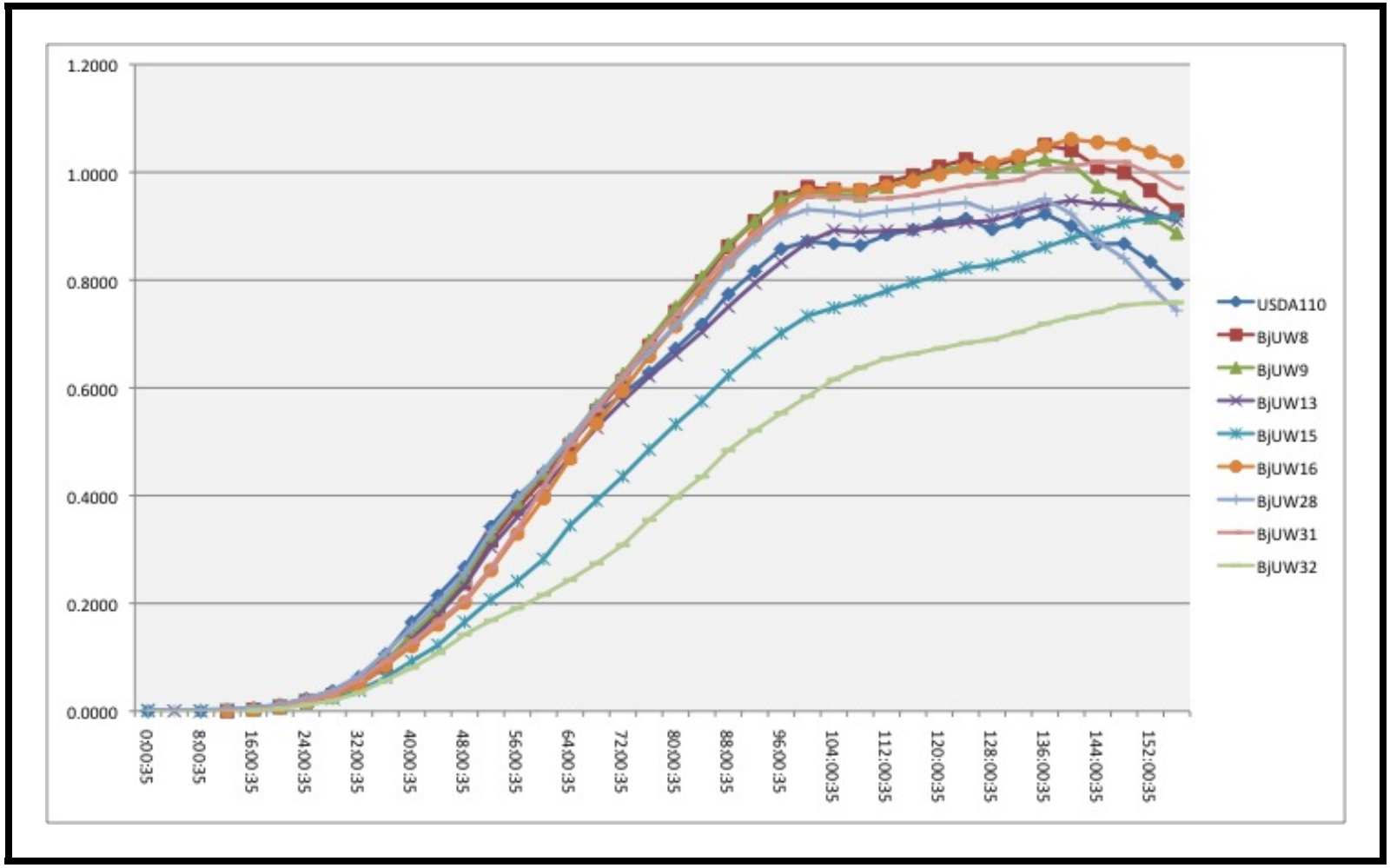

Figure 3.11: Growth curve of *B. japonicum* PHB mutants on Arabinose Gluconate (AG) medium. AG served as the positive control for all *B. japonicum* growth curves

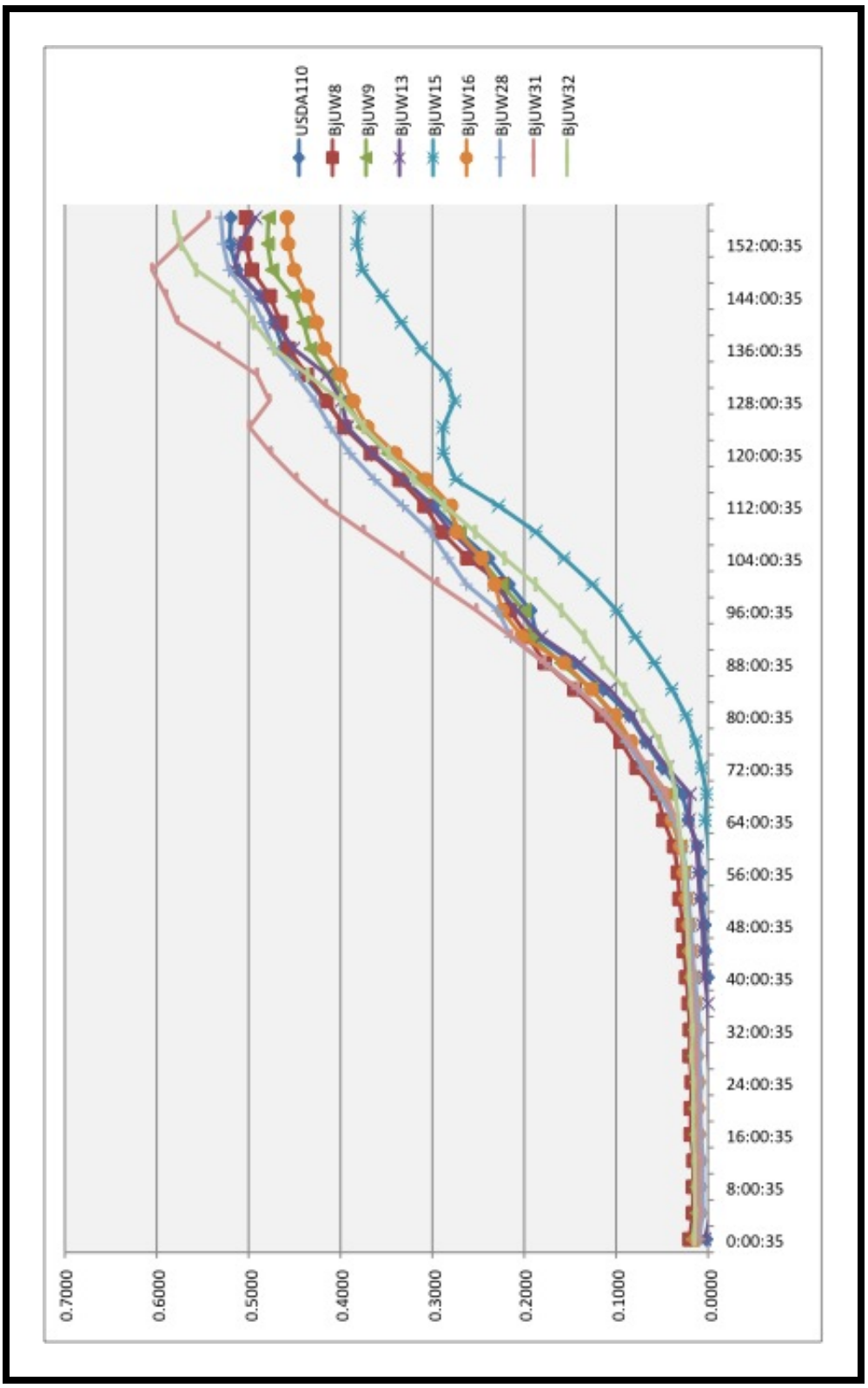

Figure 3.12: Growth curve of *B. japonicum* PHB mutants on VMM containing acetoacetate as the sole carbon source

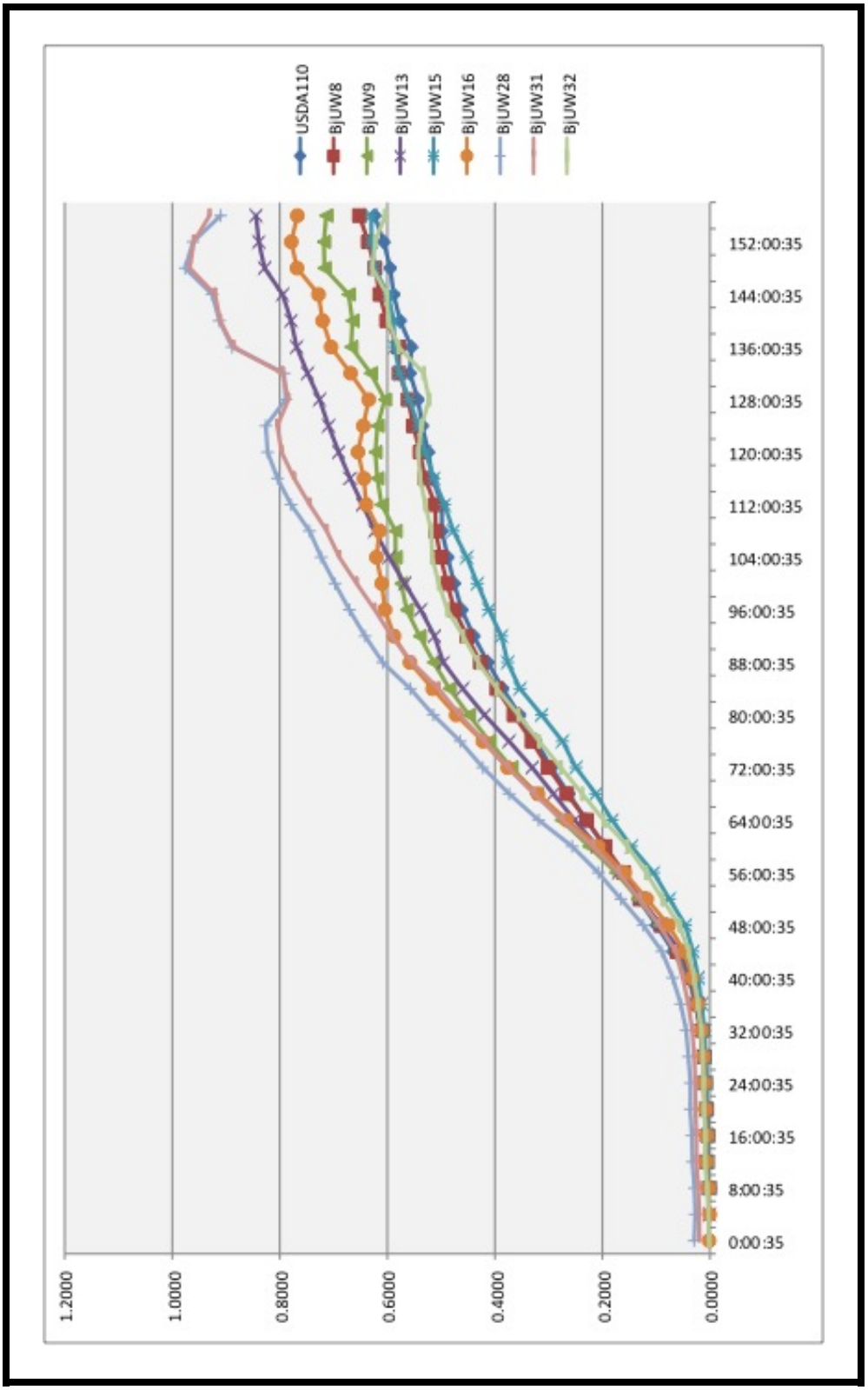

Figure 3.13: Growth curve of *B. japonicum* PHB mutants on VMM containing DL-Hydroxybutyrate as the sole carbon source

3.2.3.7 Exopolysaccharide Accumulation by *B. japonicum phbC* and *phbAB* Mutants

PHB synthesis mutants of *S. meliloti* also demonstrate a distinctly non-mucoid phenotype when grown under PHB-inducing conditions. This is in contrast to the parental strain Rm1021, which appears mucoid when grown on high-carbon media (although notably less mucoid than the $expR^+$ strains). Isolation of exopolysaccharide (EPS) from *S. meliloti* Rm1021 and PHB cycle intermediates demonstrates a significant reduction in EPS production in these strains. As evidenced by the ease with which PHB synthesis mutants form a compact pellet upon centrifugation (Figure 3.14), it would appear that these strains demonstrate a similar reduction in EPS biosynthetic capacity.

A quantitative analysis of *B. japonicum* EPS biosynthesis was conducted using a standard isopropanol EPS precipitation protocol (modified from [221] as described in Section 2.7.5). This protocol is described in detail in Section 2.7.5. The data shown in Table 3.9, confirm the visual observation depicted in Figure 3.14. These data show that *B. japonicum* PHB synthesis mutants demonstrate a similar reduction in EPS production to that exhibited by the non-PHB producing mutants of *S. meliloti*.

3.3 Conclusions

While only two isomers, Blr3732 and Bll4360, could complement PHB synthesis and EPS production phenotypes of Rm11105, three isomers (Blr3732, Bll4360 and Bll6073) demonstrated a partial ability to confer growth on acetoacetate (Figure 3.6). It is noteworthy however, that none of the *phbC* isomers was able to fully restore growth of Rm11105 on acetoacetate. Since all of these genes were expressed

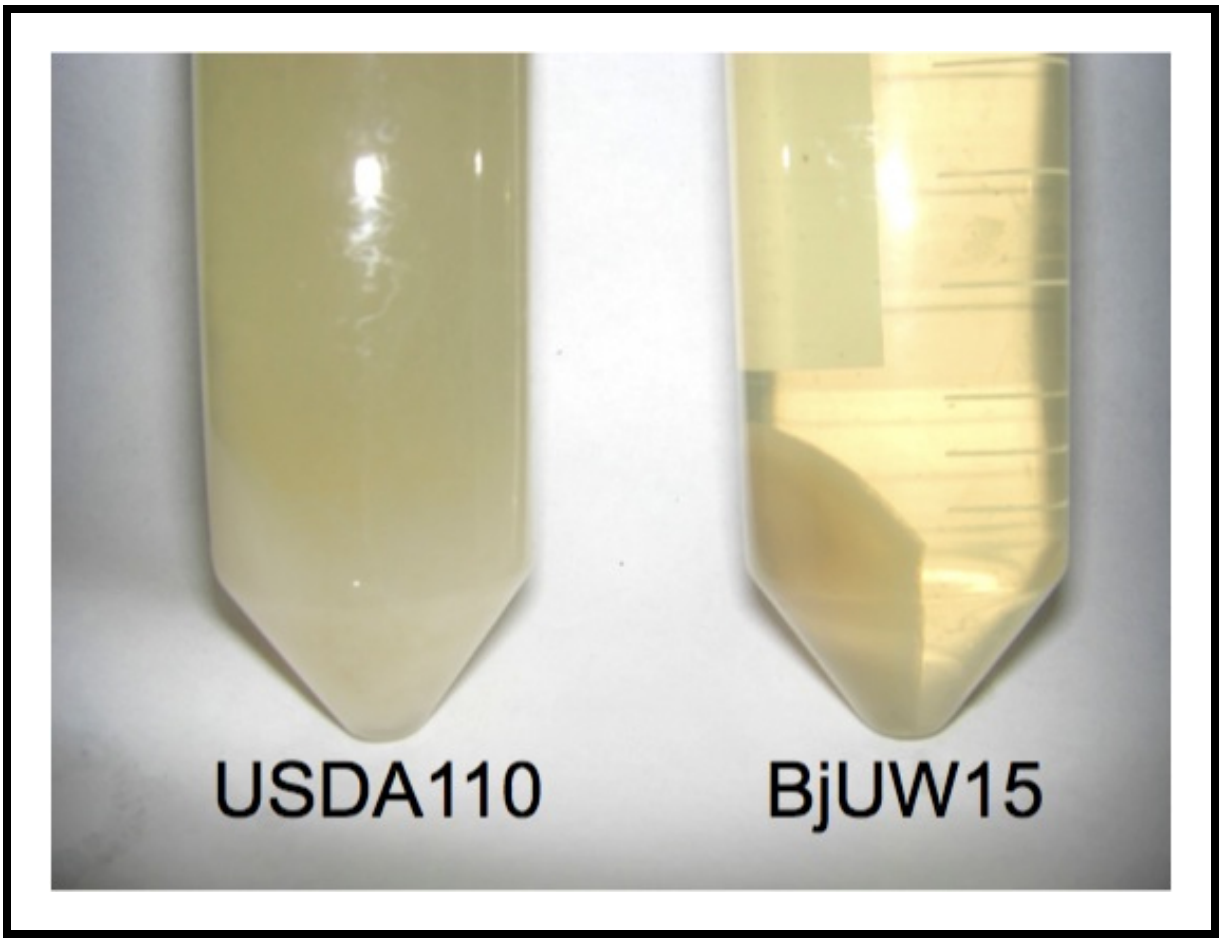

Figure 3.14: The EPS phenotype of the *B. japonicum* PHB synthesis mutants is evident following centrifugation of a saturated culture. PHB synthesis mutant BjUW15 forms a compact pellet following centrifugation for 30 minutes at 8,000 rpm; the wild-type strain USDA110 remains recalcitrant to pelleting at this level of centrifugation

Table 3.9: EPS accumulation by *B. japonicum* PHB synthesis mutants expressed as mg EPS as percent cell dry mass

Strain	mg EPS as % CDM
USDA110	8.29
BjUW9	8.28
BjUW13	6.77
BjUW15	5.09
BjUW16	10.32
BjUW32	5.08

from the *lacZ* promoter on pRK7813, it is unlikely that any lack of complementation could be attributed to lack of expression.

The results presented here clearly demonstrate that PHB synthesis by *B. japonicum* is regulated differently under symbiotic and free-living conditions through the actions of PhbA and PhbB. It is apparent that *phbAB* Bll0225 and Bll0226 are up-regulated only during symbiosis, while Blr3724 and Blr3725 are primarily active under free-living conditions. Suzuki *et al.* demonstrated that bacteroids of *B. japonicum* possessed two classes of 3-ketothiolases [338]. These two classes could be distinguished from each other by their specificity for either acetoacetyl-CoA or 3-ketodecanoyl-CoA. Since some PHB synthesis does occur in strains BjUW15, it is conceivable that in the wild-type strain these two specificities represent activity from Blr3724 and Bll0225. Further work is needed to establish the regulatory mechanisms by which these genes are controlled, although earlier work has demonstrated that NADH is a potent inhibitor of the acetoacetyl-CoA-specific enzyme [338]. This introduces a potential role for NADH in promoting inhibition during early nodule senescence when NADH concentrations in the bacteroid may be expected to rise due to reduced nitrogen fixation [338].

It is interesting to note that the symbiotic phenotype of *B. japonicum* PHB synthesis mutants is quite different to that observed for PHB synthesis mutants of *Rhizobium etli* [43]. Plants inoculated with *R. etli phaC* mutants had higher shoot dry masses relative to those inoculated with wild type cells [43]. Furthermore, these plants possessed higher nitrogen contents and the bacteroids demonstrated higher levels of nitrogenase activity [43]. These data might suggest that, in *R. etli*, PHB synthesis in symbiosis occurs at the expense of nitrogen fixation. In contrast, a comparison of the data presented in Tables 3.6 and 3.7 suggest that in *B. japonicum*, PHB accumulation during symbiosis does not occur at the expense of plant biomass formation. Indeed, the only statistically significant difference in plant dry

mass was a decrease in mass observed in plants inoculated with BjUW9, which carries a deletion in Blr3732. This mutation did not affect PHB accumulation under free-living conditions; symbiotic PHB accumulation was not determined. The reason for this difference remains unclear, although it is conceivable that the increased reductive power observed in the *R. etli* mutant may be channelled into nitrogen fixation. A similar analysis of NAD^+/NADH ratios in the *B. japonicum* PHB synthesis mutants would be necessary to determine if this reductive capacity is mirrored in *B. japonicum*. It is tempting to speculate however, that a similar capacity might not exist in *B. japonicum*, accounting for the discrepancy in symbiotic efficiency observed between the two species.

While the reason for so many copies of the enzymes responsible for PHB synthesis remain unclear, it is conceivable that the products of the 2 different *phbAB* operons and the five *phbC* genes are structurally distinct. Since PHB synthase is believed to be substrate-specific [66], it is tempting to speculate that the existence of multiple isomers of all three biosynthesis genes may contribute to the production of a more diverse repertoire of PHA end products. Indeed, in *phbB* in *W. eutrophus*, the substrate specificities of the two isomers of *phbA* are believed to account for the production of PHB containing either 3-hydroxybutyrate or 3-hydroxyvalerate since the PHB synthase of this organism is specific for D-(-)-hydroxybutyrate, the product of the NADPH-linked *phbB* variant [142]. It is also conceivable that the *phbC* variants of *B. japonicum* may represent soluble and granule-associated forms. In *W. eutrophus*, soluble PHB synthase is found when the cells are grown under carbon-limited conditions; upon transition to nitrogen limitation, PHB accumulation is upregulated and granule-associated PhbC can be detected, coupled with a disappearance of soluble enzyme [143]. Further work needs to be done to determine under what conditions the different isoforms are upregulated. It should be possible to construct relatively simple *lacZ* transcriptional fusions by single recom-

bination into the *B. japonicum* genome. These fusions would facilitate the analysis of each gene's transcriptional activation under different conditions. These fusions have been constructed for *S. meliloti* (see Table 2.1) and are described in more detail in Section 9.1.

The correlation between PHB synthesis and EPS synthesis under free-living conditions is interesting. Since it is comparable to the link seen in *S. meliloti* Rm11105, it is conceivable that the regulation of PHB synthesis and EPS under free-living conditions is similar in both species. Given the well documented requirement for EPS in the establishment of nitrogen-fixing symbioses between *S. meliloti* and *M. sativa* [120], it was interesting to observe a similar phenomenon in *B. japonicum* (Table 3.8). Strain BjUW16 demonstrates wild-type EPS and PHB synthesis under free-living conditions (Tables 3.9 and 3.7) but is unable to synthesize PHB in symbiosis and appears to be unimpaired in rhizosphere competitiveness. This lends further credence to the discussion in Section 6.3 that, while the production of small amounts of EPS is sufficient to establish a successful symbiosis [120], it is insufficient to permit competition with wild-type strains producing higher levels of the EPS, if one assumes that the EPS itself is playing a role in signalling during early nodulation. This is further corroborated by earlier work by Bhagwat *et al.*, who reported a link between EPS synthesis in *B. japonicum* and rhizosphere competitiveness [22].

Despite the link between EPS production, PHB synthesis and rhizosphere competitiveness that is consistent between *S. meliloti* and *B. japonicum*, it is interesting to note that PHB synthesis mutants of *B. japonicum* do not exhibit comparable carbon utilization phenotypes to *S. meliloti*. As shown in Figures 3.11, 3.12 and 3.13, *B. japonicum* PHB synthesis mutants exhibit growth that is comparable to wild type USDA110 on acetoacetate and DL-hydroxybutyrate. The slight reduction in growth that is observed in BjUW32 and BjUW15 is most likely attributed to

reduced optical activity due to the reduction in EPS exhibited by this strain. This is corroborated by the control assay on AG (Figure 3.11), in which this reduction in optical density is apparent.

The reason for the recalcitrance of Bll4360 and Bll4548 to mutagenesis remains unclear. The construction of single recombinants of both Bll4360 and Bll4548 was successful; however, upon screening of subsequent double recombinants, 100% of all recombinants were identified as wild-type. It is conceivable, although without precedent, that either of these genes may play a necessary role in maintaining viability of *B. japonicum* under free-living conditions. Analysis of the surrounding genomic regions did not result in the identification of any potentially essential genes whose function may have been disrupted by mutagenesis, lending credence to the theory that the PHB synthases themselves may be the important genes. Given the pleiotropic nature of the *phbC* mutation in *S. meliloti*, it is tempting to speculate that either of these genes may confer additional properties upon *B. japonicum* that are essential for viability. Further analysis of these genes and their resultant products would be necessary to speculate further on this issue.

Chapter 4

The Analysis of On-Seed Survival, Desiccation Tolerance and Ion Sensitivity in Rhizobia

4.1 Introduction

The application of live rhizobial cells to legume seeds is the basis for the North American agricultural inoculant industry. The bacteria in these inoculants are able to establish nitrogen-fixing symbioses, via the formation of root nodules, with leguminous plants. The result of this association is a reduction in the need for exogenous nitrogen fertilizer, which has both environmental and economic benefits to the grower. The live bacterial inoculants are delivered in various different formulations (liquid, peat or granular) to be used as a seed coating or direct addition to the soil surrounding the seed (in furrow). About 95% of the formulations are applied on-seed. One of the most important factors determining the performance of these inoculants is their ability to survive for long periods of time once applied to the seeds. This property is known as on-seed survival (OSS). Superior OSS translates

into greater planting time flexibility and more efficient delivery of bacterial cells to the field.

S. meliloti, the symbiont of alfalfa, has the longest OSS of any major commercial rhizobial inoculant species. Indeed, the OSS of *S. meliloti* is sufficiently long as to allow pre-coated seeds to be taken directly to the market. This allows for immediate planting by the grower and negates the need for specialized equipment to apply the inoculant. Furthermore, it has the added convenience of allowing planting to be delayed, e.g. for bad weather, without having to re-inoculate the seeds. The current industry standards for planting time windows are shown in Table 1.2. Although reports indicate that there has been considerable improvement in bacterial survival under storage conditions, these improvements have not led to a significant improvement in OSS [42]. Previous studies have reported a 95% decrease in viability in rhizobia applied on-seed after 4 hours with 83% of those surviving died after another 22 h in the soil [296]. Additives, including glucose, maltose, sorbitol, sucrose, glutamate, trehalose, polyvinylpyrrolidone, montmorillonite clay, and gum arabic have been tested for their ability to increase OSS with varying degrees of success [38, 54, 303, 332, 374]. In practice however, most of these additives either did not provide a sufficiently significant improvement in OSS, or were not economically viable.

Bacterial death on-seed is believed to be the result of desiccation-induced stress, due to irreparable membrane damage [37]. Studies investigating cell-surface changes in response to desiccation noted a thickening of the cell wall following transfer from broth cultures into peat carrier; this cell surface modification was also correlated with increased OSS [93]. Previous studies in *S. meliloti* have shown a close correlation between poly-3-hydroxybutyrate (PHB) and succinoglycan exopolysaccharide synthesis [7]. PHB is typically accumulated under conditions where carbon is abundant but growth is limited by the availability of another key nutrient (reviewed in

[351]). The accumulated carbon stores can then be degraded to support cellular metabolism under carbon starvation conditions such as those experienced during long-term inoculant storage. Consistent with such a role, a PHB synthesis mutant of *Azospirillum brasilense* also exhibited a reduction in survival ability [173].

In this study we investigate the desiccation tolerance, ion sensitivity and OSS properties of a number of wild-type and mutant *S. meliloti* and *B. japonicum* strains. The effects of PHB synthesis are analysed by assessing desiccation tolerance of PHB mutants under both PHB-inducing and non-inducing conditions. We report the results of a large-scale screen of ion-sensitivity across a spectrum of wild-type and mutant *S. meliloti* strains, as well as show evidence of biofilm formation by inoculant bacteria on the surface of the seed.

4.2 Results and Discussion

All strains used in this study are described in Table 2.1. For ease of reading, a summary of relevant strains is also included in Table 4.1

Table 4.1: Summary of strains used in the analysis of desiccation tolerance, ion sensitivity and OSS

Strain	Relevant Characteristics	Reference
B. japonicum		
USDA110	wt	USDA, Beltsville MD
BjUW8	USDA110 ΔBlr2885	This Work
BjUW9	USDA110 ΔBlr3732	This Work
BjUW13	USDA110 ΔBll6073	This Work
BjUW15	USDA110 ΔBll0225 and ΔBll0226	This Work
BjUW16	USDA110 ΔBlr3725 and ΔBlr3726	This Work
BjUW28	BjUW9 ΔBlr2885 #1	This Work
BjUW31	BjUW9 ΔBlr3725 and ΔBlr3726 #2	This Work
BjUW32	BjUW15 ΔBlr3725 and ΔBlr3726 #1	This Work
S. meliloti		
Rm5000	SU47 *rif5*	[95]
Rm1021	SU47 str-21, Sm^R	[236]
RmP110	Rm1021$pstC^+$	[58]
RCR2011	SU47 wild-type	[373]
Rm2011	SU47 *str-21*, Sm^R	[236]
102-F34	wild-type strain	[72]
102-F51	wild-type isolate of *S. meliloti*	[260]

Continued on Next Page...

Table 4.1 – continued from previous page

Strain	Relevant Characteristics	Reference
AK631	Rm41 *exoB631*	[100]
CC2013	wild-type isolate of *S. meliloti*	[83]
Rm7055	Rm1021 *exoY*::Tn*5*	[207, 244]
Rm7022	Rm1021 *exoE*::Tn*5*	[207]
Rm7053	Rm1021 *exoD*::Tn*5*	[207]
Rm8002	Rm1021 *phoA*	[214]
Rm8369	Rm8002 *exoF*369::Tn*phoA*	[215]
Rm11105	Rm1021 *phbC*1::Tn*5*	[46]
Rm11107	Rm1021 *bdhA*1::Tn*5*	[46]
Rm11144	Rm1021 *phbC*1::Tn*5*-233	[46]
Rm11347	Rm1021 *phbB*::ΩSmSp	[7]
Rm11377	Rm1021 *ace8*::Tn*5*	Charles Lab, Unpublished
Rm11378	Rm1021 *ace9*::Tn*5*	Charles Lab, Unpublished
Rm11379	Rm1021 *ace11*::Tn*5*	Charles Lab, Unpublished
Rm11405	Rm1021 putative purine metabolism mutant	Charles Lab, Unpublished

Continued on Next Page...

Table 4.1 – continued from previous page

Strain	Relevant Characteristics	Reference
Rm11417	Rm5000 *phaZ*::ΩSmSp	This work
Rm11430	Rm1021 *phaZ*::ΩSmSp	This work
Rm11478	*glgA2*::ωSpSm	[378]
Rm11479	*glgA1*::ΔPstI *glgA2*::ωSpSm	[378]
Rm11482	*glgA1*::ΔPstI	[378]
SmUW1	Rm1021*pstC*$^+$ *nolR*$^+$	Charles Lab, Unpublished
SmUW3	Rm1021 *expR*$^+$ *nolR*$^+$ *pstC*$^+$	Charles Lab, Unpublished
SmUW6	Rm1021 *expR*$^+$	Charles Lab, Unpublished
SmUW13	ϕ-Rm7055 transduced into SmUW6	Charles Lab, Unpublished
SmUW41	Δ*phbA* Mutant	This Work
SmA818	pRme2011a-cured strain of *S. meliloti* Rm2011	[256]
S. meliloti-042BM	salt-tolerant wild-type strains	[383]
RmF114	Rm1021 Δω5033-5064::Tn*5*-233	[47]
RmF117	Rm1021 Δω5060-5033::Tn*5*-233	[47]
RmF121	Rm1021 *dctD16*::Tn*5*	[97]

Continued on Next Page...

Table 4.1 – continued from previous page

Strain	Relevant Characteristics	Reference
RmF153	Rm1021 *dctB12*::Tn*5*-132	[392]
RmF506	Rm1021Δ ω5040::Tn*5*-233 ΔG506	[47]
RmF514	Rm1021 Δω5061-5047::Tn*5*-11	[47]
RmF642	Rm1021 *dctA14*::Tn*5*	[394]
RmF638	Rm1021 Δω5145-5061::Tn*5*-233	[47]
RmF666	Rm1021 Δω5146-5111::Tn*5*-233	[47]
RmF680	Rm1021 Δω5146-5111::Tn*5*-233	[47]
RmF693	Rm1021 Δω5085-5142::Tn*5*-233	[47]
RmF726	Rm1021Δ ω5085-5061::Tn*5*-233	[47]
RmF728	Rm1021Δ ω5177-*lac-56*::Tn*5*	[47]
RmF332	Rm1021 *dctA*::Tn*5*	[97]
RmF909	Rm1021 Δω5085-5047::Tn*V*	[47]
RmF930	Rm1021 *nifA239*::Tn*5*	Charles Lab, Unpublished
RmF932	Rm1021 *ntrC*::Tn*r*	Charles Lab, Unpublished
RmG270	Rm1021 ω5033-5007::Tn*5*-233 ω5085-5047::Tn*5*-Tp	[44]
RmG271	Rm1021 Δω5033-5007::Tn*V* 5149-5079::Tn*5*-233	[44]

Continued on Next Page...

Table 4.1 – continued from previous page

Strain	Relevant Characteristics	Reference
RmG277	Rm1021 Δω5020-5011::Tn*5-oriT* 5149-5079::Tn*5*-233 ω5085-5047::Tn*5*-Tp	[44]
RmG373	Rm1021 Δ ω5177-5079::Tn*5-oriT*	[47]
RmG462	Rm1021 Δω5011-5033::Tn*5-oriT*	[47]
RmG470	Rm1021 Δω5025-5007	[47]
RmG471	Rm1021 Δω5033-5025	[47]
RmG472	Rm1021 Δω5026-5007	[47]
RmG506	Rm1021 Δω5040::Tn*5*-233 G506	[47]
Rm5071	Rm5000 *nifH*::Tn*5*	[96]
Rm5378	Rm1021 Δω5020-5011::Tn*5-oriT*	[97]
Rm5408	Rm1021 Δω5033-5007::Tn*5*-233	[47]
Rm5416	Rm1021 Δω5007-5011::Tn*5*-233	[97]
Rm5422	Rm1021 *ntrA75*::Tn*5*	[97]
Sinorhizobium sp. strain BL3	wild-type strain, highly salt-tolerant. Isolated from Thailand. Rf^R, Sm^R	[345]
Sinorhizobium sp. NGR234	Broad-host range *Sinorhizobium* isolate	[354]
SMc00880-fg	RmP110 pTH1703-SMc00880-fg	[161]
SMc03878-fg	RmP110 pTH1703-SMc03878-fg	[161]

Continued on Next Page...

Table 4.1 – continued from previous page

Strain	Relevant Characteristics	Reference
SMc00880-fl	RmP110 pTH1703-SMc00880-fl	[161]
SMc00136-fl	RmP110 pTH1703-SMc00136-fl	[161]
SMb21010-fg	RmP110 pTH1703-SMb21010-fg	[161]
SMc01571-fl	RmP110 pTH1703-SMc01571-fl	[161]
SMc02271-fl	RmP110 pTH1703-SMc02271-fl	[161]
SMc02271-fg	RmP110 pTH1703-SMcc02271-fg	[161]
SMc00268-fl	RmP110 pTH1703-SMc00268-fl	[161]
SMc02322-fg	RmP110 pTH1703-SMc02322-fg	[161]
SMc02322-fl	RmP110 pTH1703-SMc02322-fl	[161]
SMc02522-fg	RmP110 pTH1703-SMc02522-fg	[161]
SMc02522-fl	RmP110 pTH1703-SMc02522-fl	[161]
SMc01500-fl	RmP110 pTH1703-SMc01500-fl	[161]
SMc00264-fl	RmP110 pTH1703-SMc00264-fl	[161]
SMc02339-fl	RmP110 pTH1703-SMc02339-fl	[161]
SMa0329-fg	RmP110 pTH1703-SMa0329-fg	[161]
SMa0329-fl	RmP110 pTH1703-SMa0329-fl	[161]
SMb21159-fl	RmP110 pTH1703-SMb21159-fl	[161]
SMb20493-fl	RmP110 pTH1703-SMb20493-fl	[161]
SMa0187-fl	RmP110 pTH1703-SMa0187-fl	[161]

Continued on Next Page...

Table 4.1 – continued from previous page

Strain	Relevant Characteristics	Reference
SMa1367-fl	RmP110 pTH1703-SMa1367-fl	[161]
SMa0335-fg	RmP110 pTH1703-SMa0335-fg	[161]
SMa0335-fl	RmP110 pTH1703-SMa0335-fl	[161]
SMc04391-fl	RmP110 pTH1703-SMc04391-fl	[161]
SMc04391-fg	RmP110 pTH1703-SMc04391-fg	[161]
SMa2019-fg	RmP110 pTH1703-SMa2019-fg	[161]
SMa2019-fl	RmP110 pTH1703-SMa2019-fl	[161]
SMa1757-fg	RmP110 pTH1703-SMa1757-fg	[161]
SMa1757-fl	RmP110 pTH1703-SMa1757-fl	[161]
SMc00326-fl	RmP110 pTH1703-SMc00326-fl l	[161]
SMc01698-fg	RmP110 pTH1703-SMc01698-fg	[161]
SMc00553-fg	RmP110 pTH1703-SMc00553-fg	[161]
SMb20871-fg	RmP110 pTH1703-SMb20871-fg	[161]
SMc01157	RmP110 pTH1703-SMc01157-fg	[161]
SMc01955	RmP110 pTH1703-SMc01955-fl	[161]
SMa0326	RmP110 pTH1703-SMa0326-fl	[161]
SMc03878-fg	pTH1703-SMc03878-fg	[161]

4.2.1 Characterization of the Desiccation Tolerance of Selected Strains of Bacteria

4.2.1.1 Characterization of the On-Seed Survival Phenotype of Selected Strains of Rhizobium

An initial screen, using an industry-standard on-seed survival (OSS) assay was performed using a standard assay for OSS (described in Section 2.8) in order to define the baseline levels of OSS for strains used in this study.

The standard OSS assay described in Section 2.8 involves inoculation of seeds with between 6 x 10^9 and 7 x 10^9 CFU/ml to achieve a minimum seed titre in soybean of 1.25 x 10^6 CFU/seed at the point of inoculation. The inoculated seeds were kept covered during the experimental period, and maintained at approximately 18°C and 70% humidity. At defined time points, groups of five soybean seeds were removed in triplicate and transferred to 10 ml of phosphate-buffered saline (PBS). The seeds were washed by vigorous vortexing, and the resultant cell-suspension was titrated to extinction (10^{-6}) in PBS, at which point the average CFU/ml in the PBS wash solution was expected to be less than 250 CFU/ml. 100 μl of each of the appropriate dilutions were spread-plated onto yeast-mannitol agar (YMA) and the CFU/seed of each sample group was calculated from countable plates containing 30-300 colonies.

Several wild-type and mutant strains of *Sinorhizobium meliloti* were assessed using a modified version of the *Bradyrhizobium japonicum* on-seed survival assay protocol. The results of these assays are shown in Figures 4.1, 4.2, and 4.3. These data suggest that there is a large degree of variability in the OSS profiles of *S. meliloti*. Figure 4.1 shows that strain SmA818 appears to be particularly compromised with respect to OSS, and this strain was subsequently studied in more detail. Additional experiments using this industry-standard protocol were conducted and

the results are shown in Figure 4.4 and 4.5. The data in Figure 4.5 are equivalent to that in Figure 4.4, but in Figure 4.5, the data have all been normalized to the starting CFU/ml of the culture with the lowest starting titre; the implications for which are discussed in more detail in Section 4.2.2. These data suggest that SmA818 is impaired in OSS capacity, although additional experiments discussed in the following sections make these data inconclusive.

4.2.1.2 OSS Under PHB-Inducing and Non-Inducing Conditions

The OSS capacity of *S. meliloti* and *B. japonicum* PHB synthesis mutants was assessed under PHB-inducing conditions. In the case of *S. meliloti*, OSS was also assessed under non-inducing conditions (TY) to facilitate a direct comparison. These data are shown in Figures 4.6, 4.7, and 4.8. These data suggest that PHB synthesis has little effect on the OSS capacity of *B. japonicum*, but that in *S. meliloti* the *phbC* mutant strain Rm11105 appears to demonstrate reduced OSS under PHB-inducing conditions, implying a potential role for PHB in the long-term survival of cells under adverse storage conditions.

4.2.1.3 Media Additives and Conditioning

Trehalose has long been known to improve the desiccation tolerance of bacteria and its ability to enhance desiccation tolerance in *B. japonicum* has been documented in the literature [332]. The ability of trehalose to enhance OSS in *S. meliloti* was tested by growing the cells in media supplemented with 10 mM trehalose prior to inoculation. In addition, the effect of conditioning the cells prior to inoculation, by growth in a medium of high osmotic potential, was also measured; osmotic shock might induce the synthesis of cytoplasmic osmoprotectants. Cells were grown in media supplemented with 0.5% or 1% final concetration of NaCl prior to inocula-

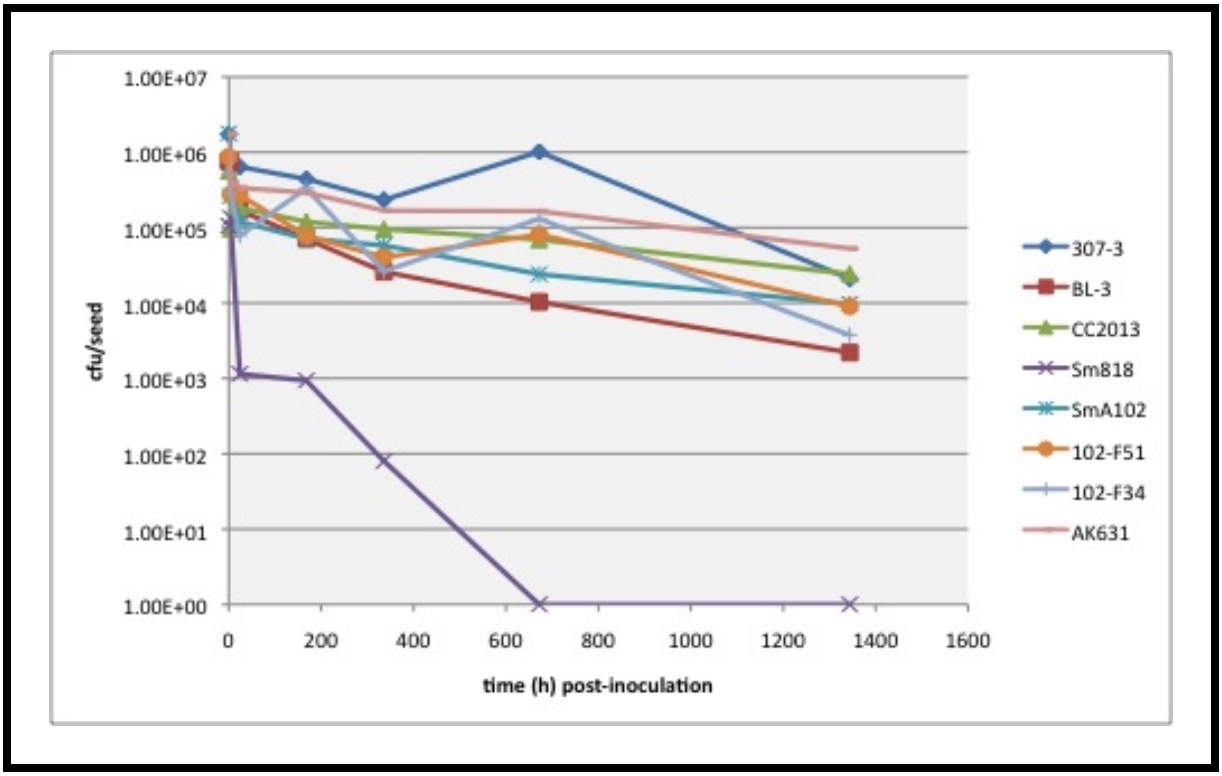

Figure 4.1: On-seed survival profiles of selected *S. meliloti* strains

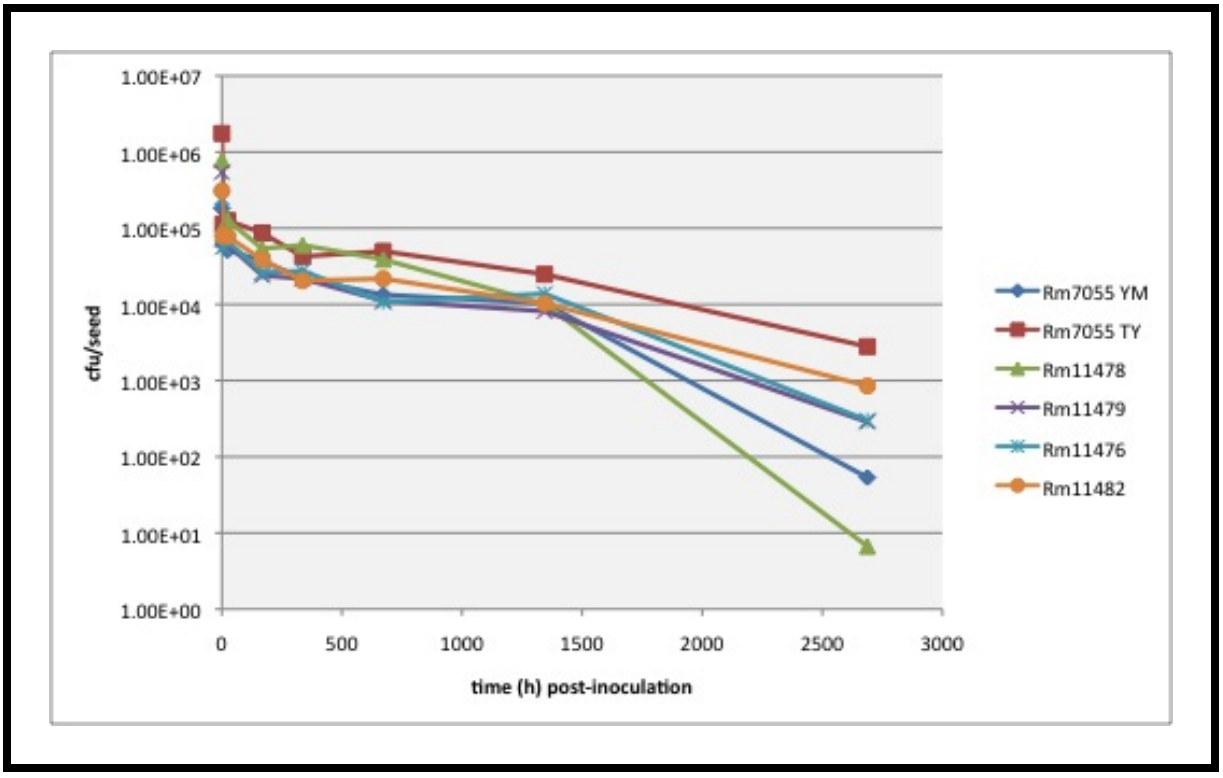

Figure 4.2: On-seed survival profiles of additional selected *S. meliloti* strains

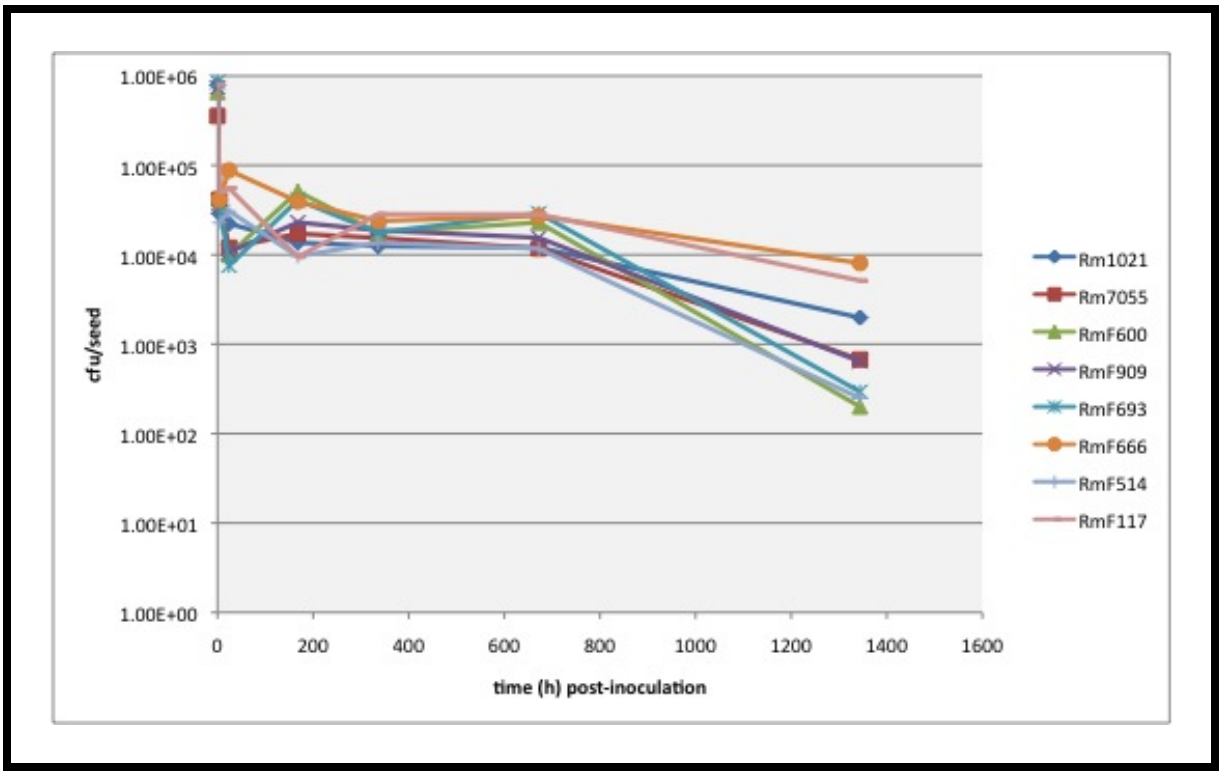

Figure 4.3: On-seed survival profiles of selected *S. meliloti* pSymB mutant strains

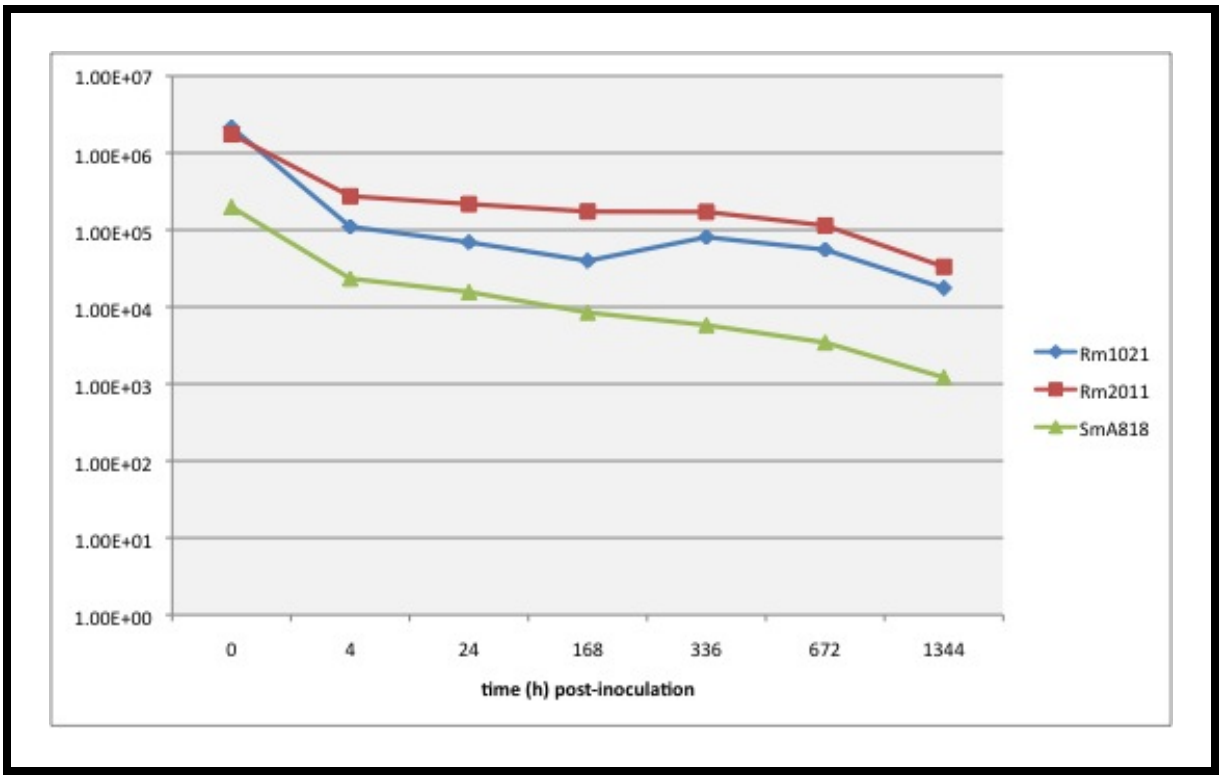

Figure 4.4: On-seed survival profiles of *S. meliloti* pSymA mutant strain

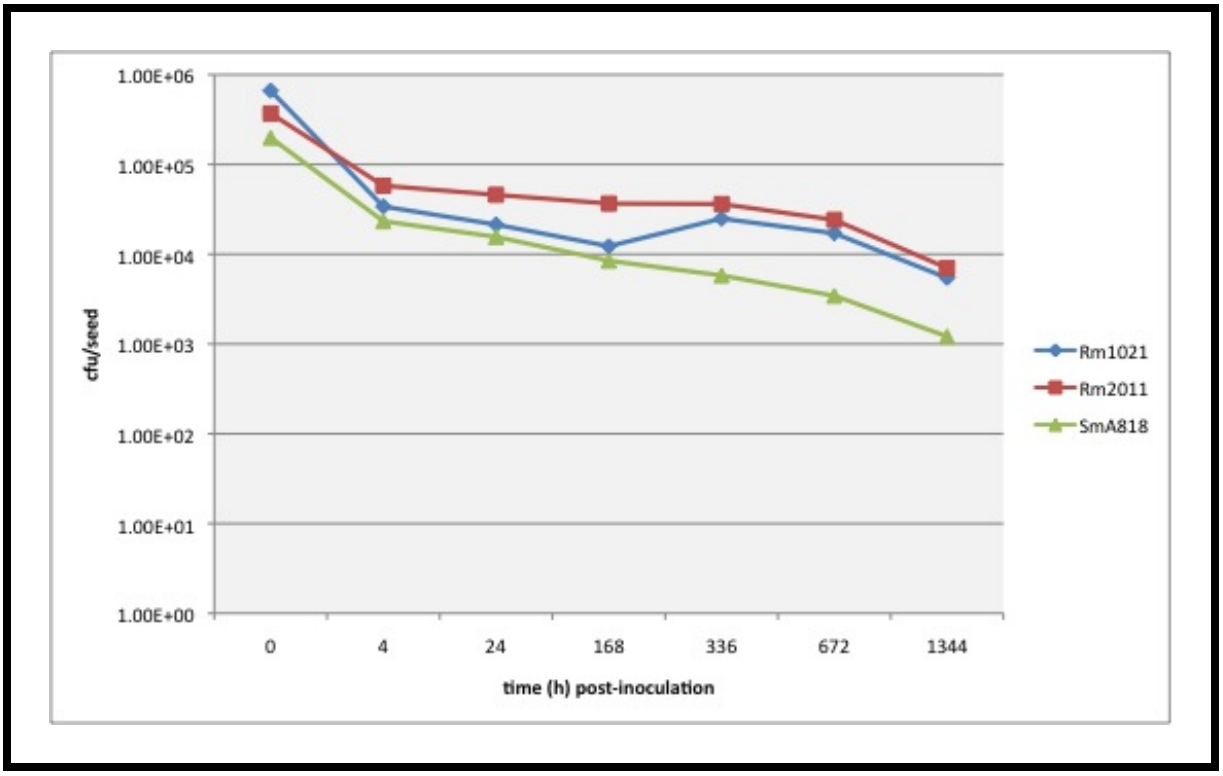

Figure 4.5: On-seed survival profiles of *S. meliloti* pSymA mutant strain, normalized using industry-standard protocols. All data points have been normalized to the starting CFU/ml of the culture with the lowest starting titre

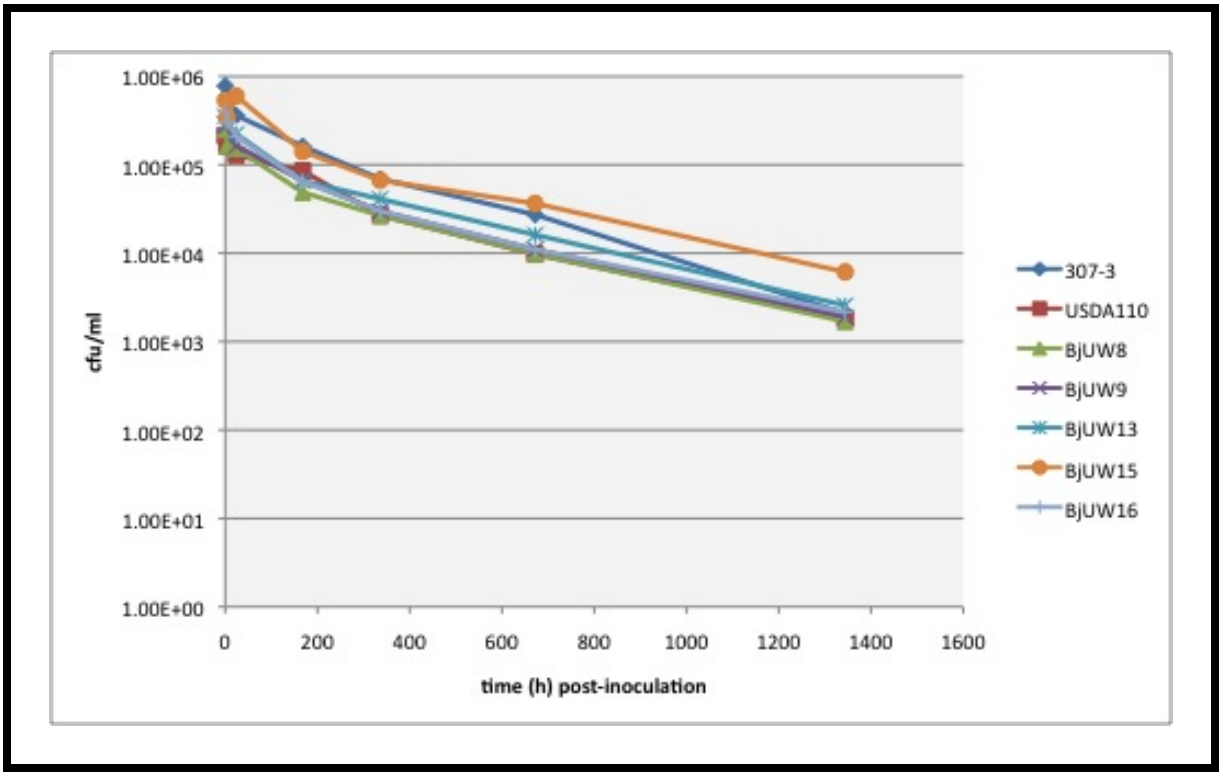

Figure 4.6: On-seed survival profiles of *B. japonicum* PHB-mutant strains grown under PHB-inducing conditions

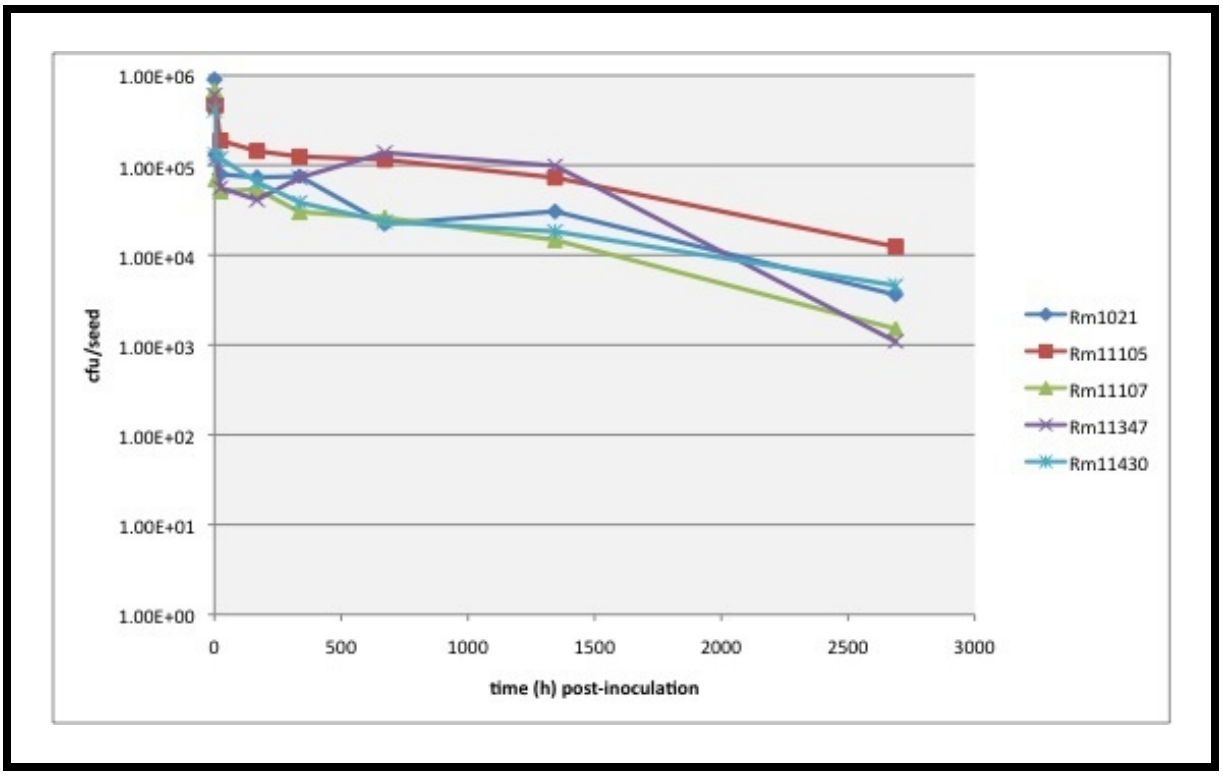

Figure 4.7: On-seed survival profiles of *S. meliloti* PHB-mutant strains grown under non-PHB-inducing conditions in TY medium

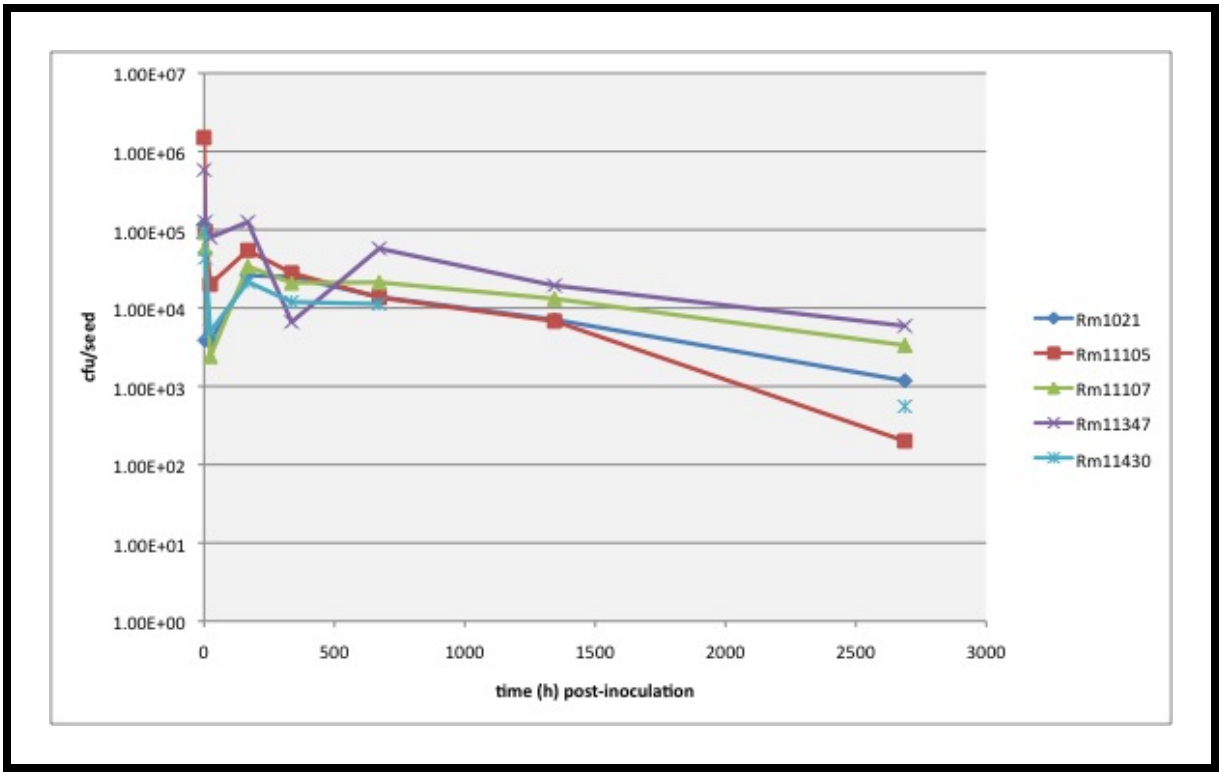

Figure 4.8: On-seed survival profiles of *S. meliloti* PHB-mutant strains grown under PHB-inducing conditions in Yeast Mannitol medium

tion. The results of these trials are depicted graphically in Figure 4.9. These data suggest that addition of trehalose may provide an advantage to cells during the first few weeks post-inoculation but that over the longer-term, improvements in survival appear to be negligible. These data also suggest that pre-conditioning with NaCl did not positively affect OSS.

4.2.1.4 Scanning Electron Microscopy of Inoculated Soybean Seeds

There is considerable evidence to suggest that under desiccation conditions, the bacterial cell surface experiences structural damage [62]. It is also conceivable that, on the seed surface, the bacteria form biofilm-like structures in response to a high inoculum density and the onset of physiological stress. In order to assess whether any visible structural changes occur on-seed, or if biofilm development is induced, scanning electron microscopy (SEM) of the surface of *S. meliloti*-inoculated alfalfa seed was used. These pictures are shown in Figures 4.10, 4.11, 4.12, and 4.13. The data in Figure 4.10 shows evidence for the existence of biofilms on the surface of the seed. When examined at higher magnification, as shown in Figures 4.11 and 4.12, the existence of an extracellular matrix, characteristic of a biofilm, is evident around individual bacterial cells. This is in contrast to the surface of uninoculated seeds, which shown no evidence of biofilm activity (Figure 4.13).

4.2.2 Characterization of the Desiccation Tolerance of Selected Strains of Rhizobium

The data in Figures 4.1, 4.2, 4.3, 4.6, and 4.9 demonstrate a high degree of variability, resulting in data that is less than conclusive. In addition, the industry-standard techniques for data analysis was inconsistent with other standard techniques reported in the scientific literature. Many of these strains were reanalysed using a

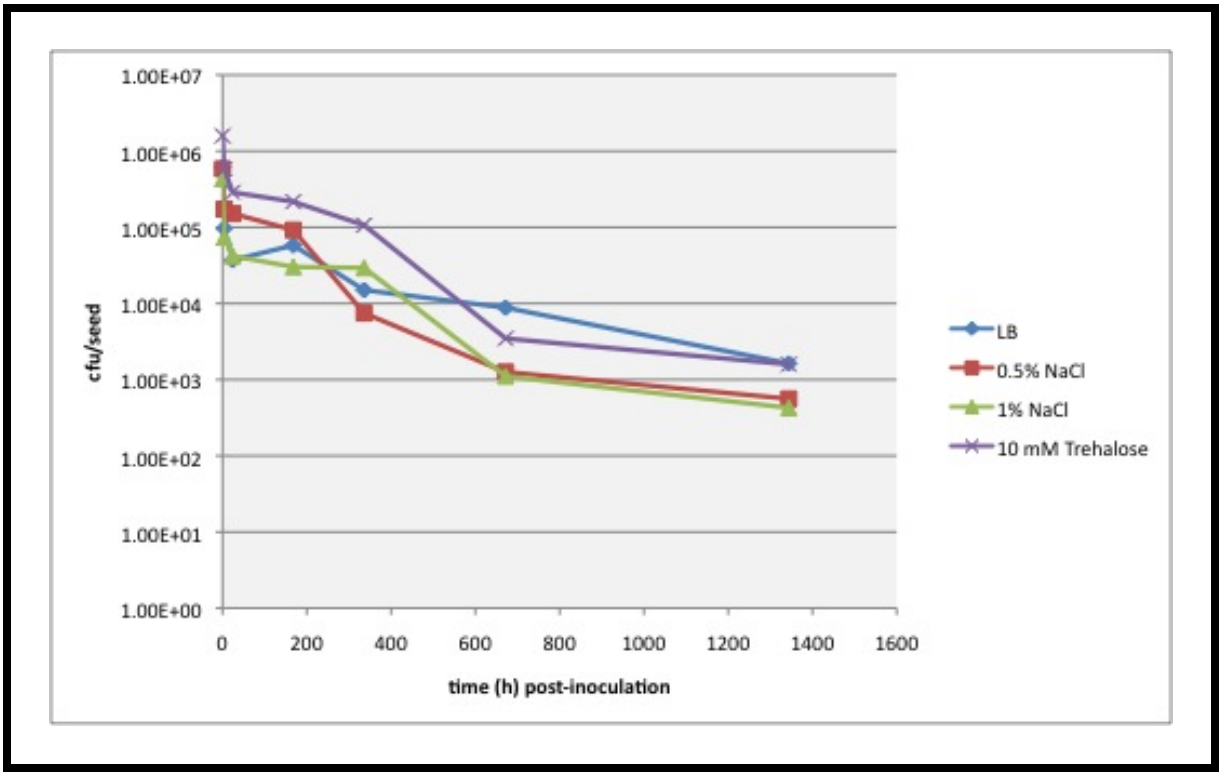

Figure 4.9: On-seed survival profiles of *S. meliloti* Rm1021 grown in LB media supplemented with trehalose of NaCl prior to inoculation

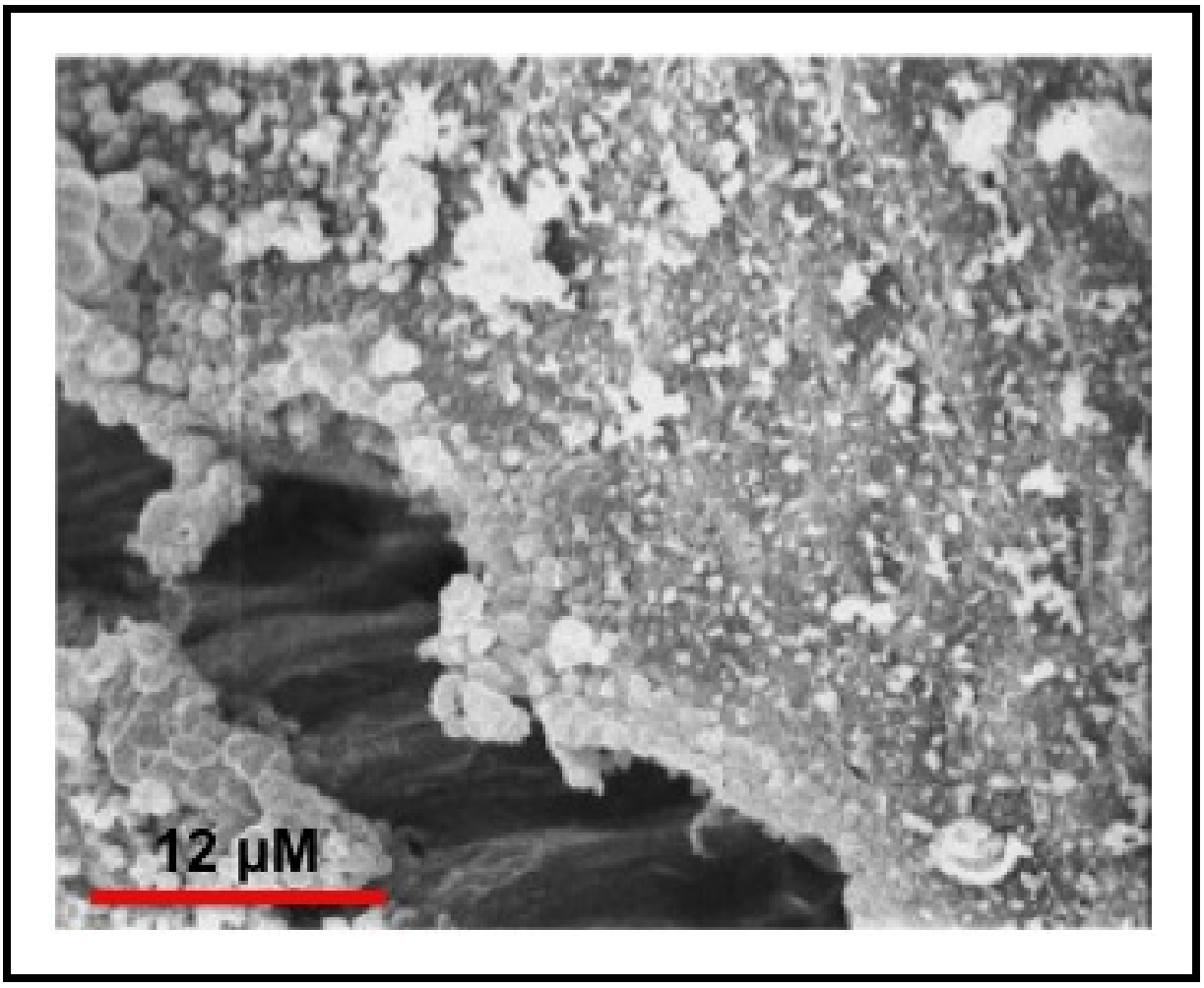

Figure 4.10: Scanning electron micrograph of an alfalfa seed inoculated with *S. meliloti* Rm1021. The surface texture appears to show evidence of biofilm activity at this resolution

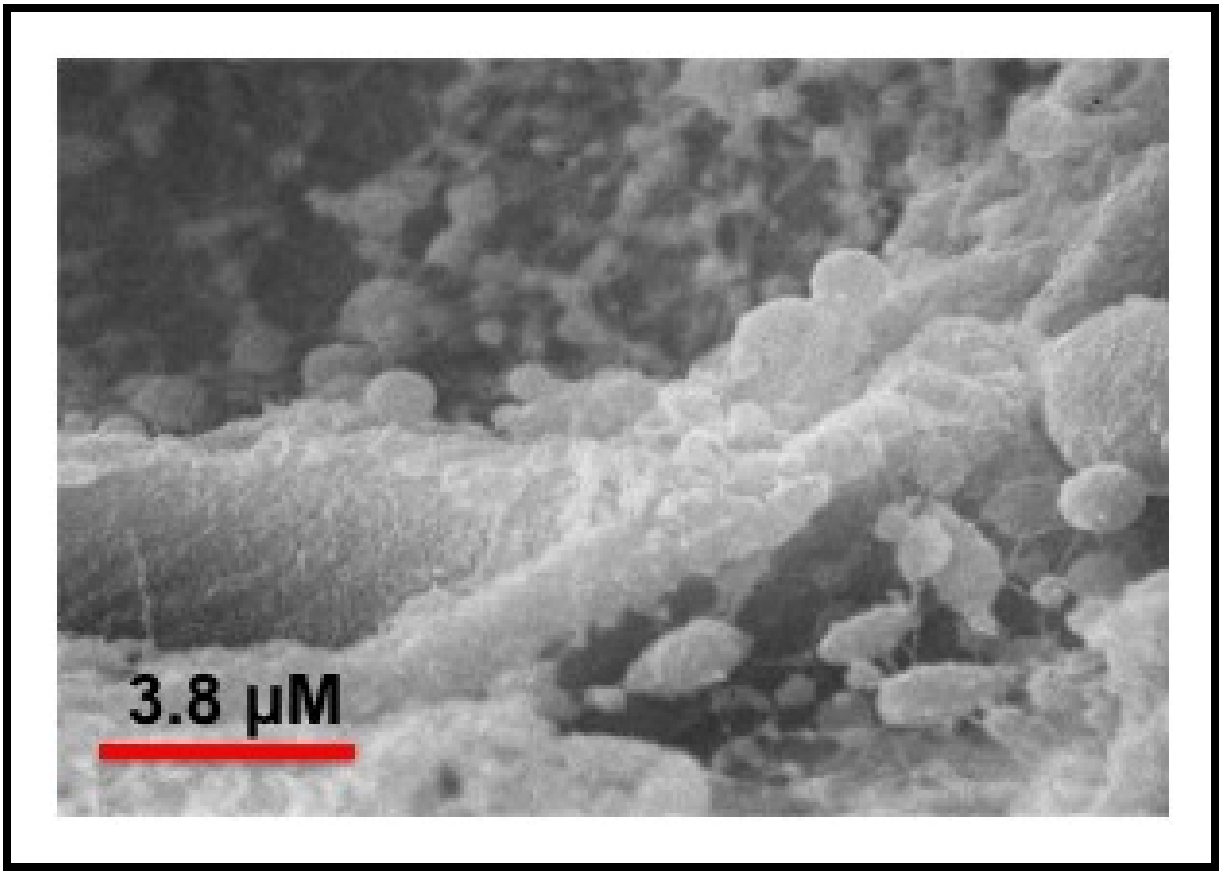

Figure 4.11: Scanning electron micrograph of an alfalfa seed inoculated with *S. meliloti* Rm1021. Bacterial cells are visible and the appearance of an extracellular matrix, consistent with biofilm formation, is evident at this resolution

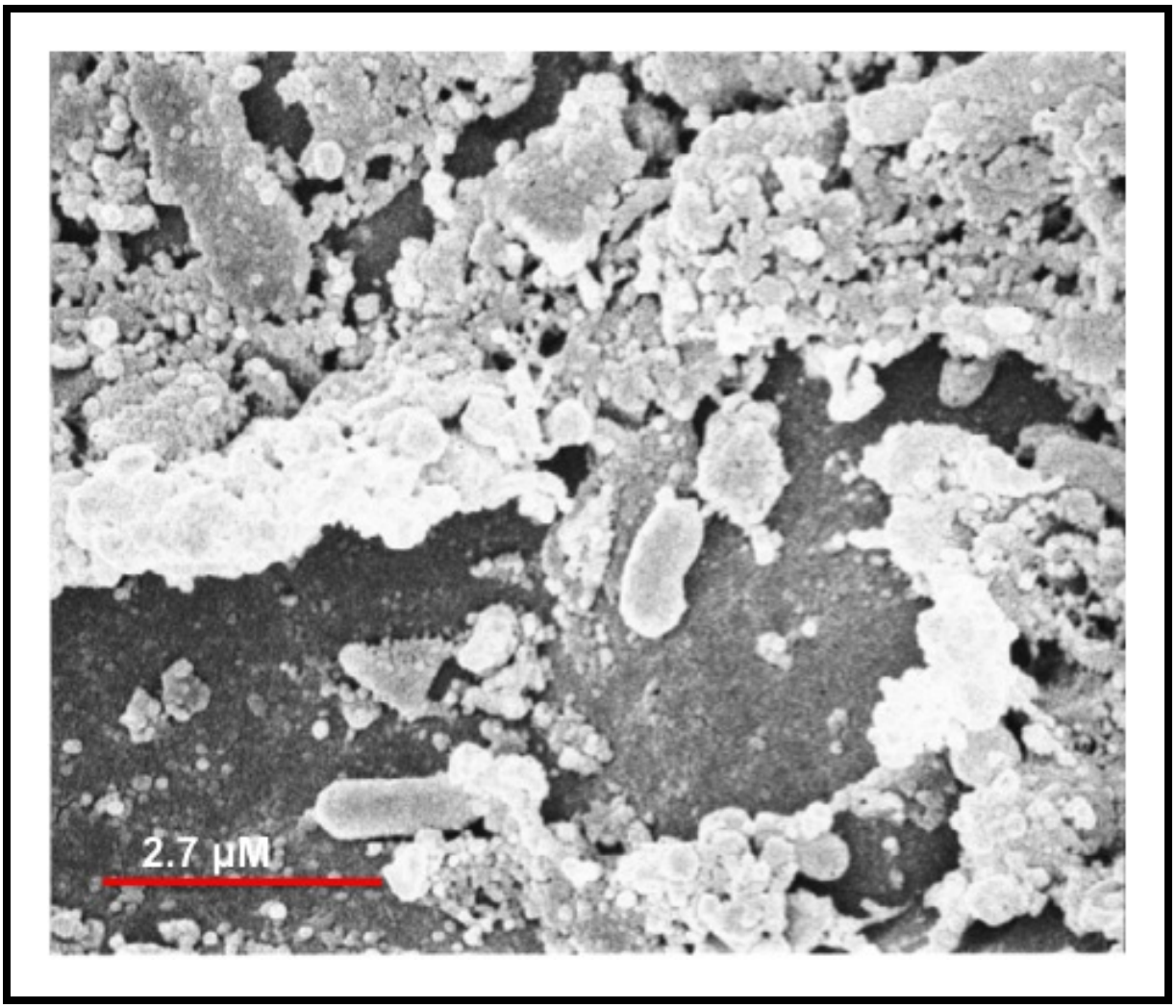

Figure 4.12: Scanning electron micrograph of an alfalfa seed inoculated with *S. meliloti* Rm1021. Bacterial cells are visible and the appearance of an extracellular matrix, consistent with biofilm formation, is evident at this resolution

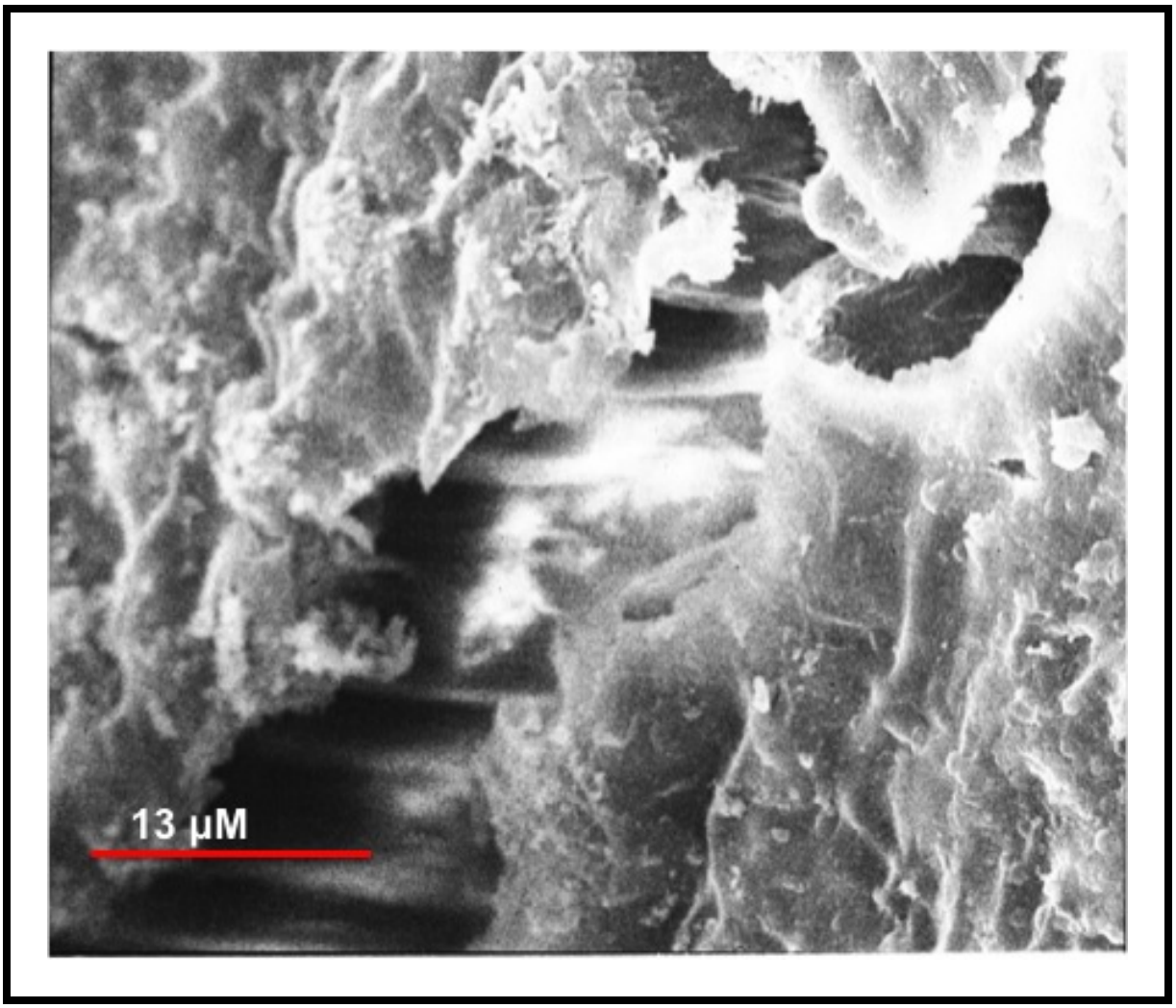

Figure 4.13: Scanning electron micrograph of an uninoculated alfalfa seed. Although the surface texture of the seed is clearly evident, there is a notable absence of bacterial cells on uninoculated seeds

newly developed assay for desiccation tolerance, discussed below.

The industry-standard method of OSS data analysis requires that all samples analysed within a single experiment be normalized to the starting culture with the lowest CFU/ml. A correction factor, by which all subsequent CFU/seed measurements are multiplied, is calculated by dividing the CFU/ml of the culture with the lowest titre by the titre of each individual culture. Data analysed in this fashion often gave very different results than data reported as a percentage survival of the original on-seed titre, as is common in the scientific literature. This is apparent in the analysis of the pSymA-cured strain of *S. meliloti* SmA818. Using the industry-standard method of analysis, this strain had a very low OSS (Figure 4.5); however, as shown in Tables 4.2 and 4.3, when the data were analysed to show percent survival of the original on-seed titre, SmA818 OSS was not discernibly different to that of the wild-type strain Rm1021. It is interesting to note that the parent strain of SmA818, Rm2011, appears to have increased OSS when the data is analysed by either method.

Table 4.2: On-seed survival of *S. meliloti* Rm1021, Rm2011 and SmA818 expressed as percentage of each initial starting culture

Inoculant	0 hours	4 hours	24 hours	168 hours	336 hours	672 hours	1344 hours
Rm1021	100	5.12	3.22	1.85	3.75	2.58	0.82
Rm2011	100	15.69	12.40	9.92	9.81	6.53	1.90
SmA818	100	11.74	7.85	4.26	2.92	1.73	0.61

Table 4.3: On-seed survival of *S. meliloti* Rm1021, Rm2011 and SmA818 analysed by the industry-standard method

Inoculant	0 hours	4 hours	24 hours	168 hours	336 hours	672 hours	1344 hours
Rm1021	6.64×10^5	3.40×10^4	2.14×10^4	1.23×10^4	2.49×10^4	1.71×10^4	5.45×10^3
Rm2011	3.70×10^5	5.80×10^4	4.59×10^4	3.67×10^4	3.63×10^4	2.41×10^4	7.03×10^3
SmA818	1.99×10^5	2.33×10^4	1.56×10^4	8.47×10^3	5.80×10^3	3.45×10^3	1.21×10^3

This variability made data analysis extremely difficult in the scientific context. As a result an alternative method was developed, by which we could test the associated phenotype of desiccation tolerance . Following discussion with Dr. Michael Kahn from Washington State University, we decided to adapt the method that his lab developed for studying desiccation tolerance in rhizobia. This method, described in Section 2.8, involves the inoculation of small agar plugs in the wells of a 96-well plate. Using a porous membrane to allow for consistent desiccation across the entire plate, the samples were at 30°C. Individual plugs were removed at regular intervals and serial dilutions were performed in order to calculate CFU/ml. The titres were used to calculate percent survival based on the starting titre of the inoculated plugs. This method was less time-consuming and less labour-intensive, and the resultant data were easier to analyse.

All *S. meliloti* PHB cycle mutants were retested using this method. These data are shown in Tables 4.4 and 4.5. Surprisingly, during the first 2 weeks of desiccation, strains that cannot synthesize PHB appeared to have higher desiccation tolerance than those that can. This result is counter-intuitive, and would necessitate further investigation in any future study.

Table 4.4: Desiccation profiles of *S. meliloti* PHB cycle mutants grown under non-PHB-inducing conditions. Data presented are expressed as percent survival of the starting sample, and represent the average of three replicates

Inoculant	0 weeks	1 week	2 weeks	3 weeks	4 weeks	6 weeks	8 weeks
Rm1021	100	10.18	3.66	1.17	1.05	0.56	0.24
Rm11105	100	41.28	17.53	25.99	7.58	2.29	5.29
Rm11107	100	25.34	5.07	8.56	0.70	0.34	0.22
Rm11347	100	40.16	27.29	19.75	2.87	10.40	7.39
Rm11430	100	63.88	31.56	14.84	19.03	4.93	3.38
SmUW36	100	26.46	10.91	10.51	3.19	2.04	0.96

Table 4.5: Desiccation profiles of *S. meliloti* PHB cycle mutants grown under PHB-inducing conditions. Data presented are expressed as percent survival of the starting sample, and represent the average of three replicates

Inoculant	0 weeks	1 week	2 weeks	3 weeks	4 weeks	6 weeks	8 weeks
Rm1021	100	13.62	2.32	0.29	0.40	0.01	0.01
Rm11105	100	33.16	5.79	1.25	4.56	0.30	0.50
Rm11107	100	11.99	0.81	0.24	0.04	0.04	0.01
Rm11347	100	33.71	3.05	2.41	0.52	0.60	1.08
Rm11430	100	22.79	2.04	3.07	0.74	0.16	0.41
SmUW36	100	85.65	7.70	2.06	1.65	0.46	0.52

Several additional strains of *S. meliloti*, including those carrying defined deletions in the pSymB megaplasmid, have also been tested using the desiccation tolerance assay. As shown in Table 4.6 RmF728, which carries a defined deletion in pSymB, has extremely poor desiccation tolerance relative to all other strains tested, including RmF726 which carries an overlapping deletion.

Furthermore, Table 4.6 shows the desiccation-resistance profile of the *expR*$^+$ derivatives of Rm1021, SmUW3 and SmUW6. Rm1021 carries an insertion sequence in the *expR* open reading frame. This makes it much less mucoid than many field isolates of *S. meliloti* and thus, much easier to work with in the laboratory. We were interested in seeing if the increased mucoidy exhibited by SmUW3 and SmUW6 translated into enhanced desiccation tolerance. The data in Table 4.6 suggest that these strains do indeed exhibit considerably higher desiccation tolerance than Rm1021. This is consistent with results reported from other organisms [254].

Table 4.6: Desiccation profiles of *S. meliloti* wild-type and mutant strains. Data presented are expressed as percent survival of the starting sample, and represent the average of three replicates

Inoculant	0 weeks	1 week	2 weeks	3 weeks	4 weeks	6 weeks	8 weeks
Rm1021	100	69.43	15.75	13.61	8.81	4.96	2.78
Rm2011	100	30.28	7.86	15.58	8.61	12.30	3.64
SmA818	100	25.49	6.26	11.14	1.75	3.94	1.33
RmF726	100	25.78	7.89	3.47	3.24	4.36	4.16
RmF728	100	6.97	0.95	1.24	0.03	0.07	0.03
RmG271	100	19.44	3.25	1.21	3.00	0.52	2.89
RmG373	100.00	68.62	99.85	15.11	17.44	18.20	27.77
RmG462	100.00	13.78	5.88	9.10	1.27	0.35	1.13
RmG506	100.00	50.75	6.95	4.37	0.82	0.24	0.28
Rm5071	100.00	52.12	8.74	4.21	4.07	1.01	1.55
SmUW3	100.00	160.51	19.98	48.58	15.48	1.02	8.81
SmUW6	100.00	92.28	17.12	32.75	10.87	1.06	8.57

4.2.3 Analysis of Ion Tolerance in *S. meliloti*

Osmotic stress is a consequence of the early stages of desiccation. It is conceivable therefore, that an ability to tolerate osmotic stress may translate into enhanced desiccation tolerance. *S. meliloti* is noted for being particularly halotolerant among rhizobia [28, 30]. Over 200 mutant and wild-type strains of *S. meliloti* were screened for ion sensitivity by replica plating onto modified LB supplemented with either Na^+, K^+, Mg^{2+}, Li^+, or Ca^{2+} in place of the standard 86 mM NaCl. The modified LB are listed below, and the final ion concentration is indicated in each case:

- 350 mM NaCl
- 350 mM KCl
- 50 mM $MgCl_2$
- 50 mM LiCl
- 50 mM $CaCl_2$

The strains selected included a number of wild-type *S. meliloti* isolates from the lab collection, pSymB deletion mutants, PHB mutants, and Short-Chain Dehydrogenase/Reductase (SDR) mutants. Cells were grown to saturation in LB and 300 μl of each culture was transferred to a well of a 96-well plate. These cultures were then transferred to the appropriate test media by replica plating using an EtOH-sterilized 48-prong replica plater designed to transfer culture from a 96-well plate onto a standard petri plate. A photograph of the resultant growth is shown in Figure 4.14. In addition to testing the media listed above, growth was tested on standard LB (0.86 mM NaCl), VMM succinate and VMM mannitol as controls.

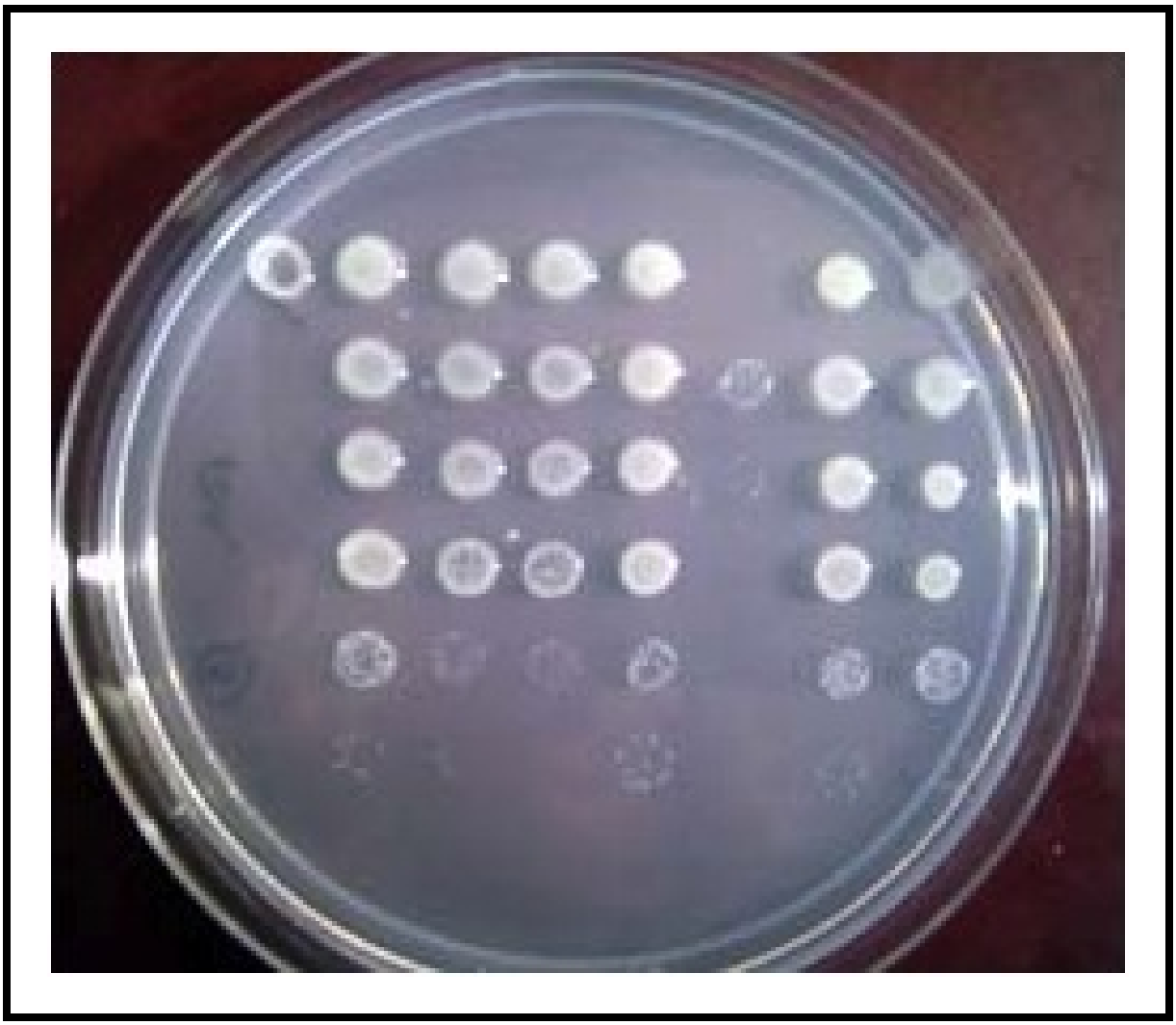

Figure 4.14: Photograph of growth resulting from inoculation using the 48-prong replica plater used to assay ion tolerance

The data shown in Table 4.7 show the results of the preliminary ion sensitivity screens. Growth was scored out of 3, and the data presented represent the average of three replicates.

Table 4.7: Ion Tolerance profiles of *S. meliloti* wild-type and mutant strains. Data presented are expressed as growth scored out of 3, and represent the average of three replicates. 3: Growth equivalet to *S. meliloi* Rm1021 on unmodified LB or VMM Succinate; 2: Growth is 75% of that formed by strains designated as 3; 1: Growth is Visible but poor; 0: No growth

Strain	LB	Succinate	Mannitol	Na^+	Li^+	Mg^{2+}	K^+	Ca^{2+}
Rm1021	3	3	1	2	3	3	2.5	3
Rm2011	2.3	2	1.5	3	3	3	2	3
SmUW3	3	3	1	3	3	3	2	3
SmUW6	3	3	1.5	3	3	3	2.5	3
Rm11105	2.7	3	1	1.5	3	3	2	3
Rm11107	3	3	2.5	3	3	3	3	3
Rm11347	2.7	3	2.5	3	3	3	2	3
Rm11430	3	3	3	3	3	3	2.5	3
SmA818	3	2.7	3	3	3	3	3	3
Sm BL-3	3	3	0	0	3	3	1	3
Rm41	2.7	3	0	0	3	3	0.5	3
Rm104A14	3	3	1	0	0	3	0.5	3
Rm11377	3	3	2	3	3	3	2.5	3
Rm11378	3.3	3.0	2.5	3	3	3	3	3
Rm11379	3	0.7	2.5	3	3	3	2	3
RmF930	3	2.3	2	3	2	3	3	3

Continued on Next Page...

Table 4.7 – continued from previous page

Strain	**LB**	**Succinate**	**Mannitol**	**Na^+**	**Li^+**	**Mg^{2+}**	**K^+**	**Ca^{2+}**
Rm5422	3	1	2	3	3	3	3	3
RmF932	3	2.3	3	3	3	3	3	3
RmF121	3	1.7	2	3	3	3	3	3
SmA102	3	2.7	3	3	3	3	3	3
Rm7055	2	2.7	2	2.5	3	3	2.5	3
Rm7022	2	3	2	2.5	3	3	2	3
Rm7053	3	3	2	3	3	3	2	3
Rm11405	3	2.7	3	2	3	3	3	2.5
Rm8002	2.7	3	0.5	1.5	3	3	2	2.5
Rm5000	3	3	0.5	2.5	3	3	2	3
Rm11478	3	3	3	3	3	3	3	3
Rm11479	3	3	3	3	3	3	3	3
Rm11482	3	3	3	3	3	3	3	3
RmP110	3	2.7	0	2	3.0	NT	1	3.0
SmUW13	3	3	1	3	3	3	3	3
Sm042	3	3	0	1	2.5	3	1	3
102-F34	3	3	1.5	3	3	3	3	2.5
102-F51	3	2.7	1	2	2.5	2	2	1
AK631	1	1	0	0.5	3	3	0	2.5
NGR234	3	3	0	0	0	3	0	3

Continued on Next Page...

Table 4.7 – continued from previous page

Strain	**LB**	**Succinate**	**Mannitol**	**Na^+**	**Li^+**	**Mg^{2+}**	**K^+**	**Ca^{2+}**
RCR2011	2.7	2	0	2.5	3	3	2	3
RCR2012	2.7	2	1.5	2.5	3	3	2	3
CC2013	2	2	1.5	3	2.5	3	0	2.5
Rm1021 pMA165	2.7	3	1	2	3	2.5	2	3
RmG270	2	1.7	1	1	0	3	1	3
RmG271	2	0	0.5	1	0	2	1	3
RmG277	3	1	2	1	0	3	1	3
RmG373	3	0.5	3	3	0	3	2.5	3
RmG462	3	1	1	2	1.5	3	2	3
RmG506	3	3	3	1.5	1	3	2	3
RmF117	3	3	2	3	3	3	3	3
RmF909	2.7	2.7	NT	2	3	3	2	3
RmF638	3	2.3	1	3	3	3	2.5	3
RmF666	3	2.3	0.5	2.5	3	3	2.5	3
RmF680	2	2	0.5	1.5	3	3	2	3
RmF693	2.3	2	1.5	3	3	3	3	3
RmF514	3	2	3	0	0	3	2	3
RmG470	3	2.3	1.5	3	3	3	3	2.5
RmG471	2.5	1	1	2	2	2	2	2

Continued on Next Page...

Table 4.7 – continued from previous page

Strain	**LB**	**Succinate**	**Mannitol**	**Na^+**	**Li^+**	**Mg^{2+}**	**K^+**	**Ca^{2+}**
RmG472	2.5	1	1	2	2	2	2	3
RmF114	2	2	1	2	2	2	2	3
Rm5408	3	2.7	1	3	3	3	3	3
Rm5416	3	2.3	1	3	3	3	3	3
Rm5378	2.7	2.3	1	3	3	3	3	3
RmF726	3	1	1.5	3	2.5	3	3	3
RmF728	3	1	1	0	0	2	0	3
SMc00880-fg	3	3	3	3	3	3	2	3
SMc00880-fl	3	3	3	2	3	3	2	3
SMc00136-fl	3	3	3	3	3	3	2	3
SMb21010-fg	3	3	3	3	3	3	2	3
SMc01571-fl	3	3	3	3	3	3	2	3
SMc02271-fl	3	3	3	3	3	3	2	3
SMc02271-fg	3	3	3	3	3	3	2	3
SMc00268-fl	3	3	3	2	3	3	2	3
SMc02322-fg	3	3	3	3	3	3	2	3
SMc02322-fl	3	3	3	3	3	3	2	3
SMc02522-fg	3	3	3	3	3	3	2	3
SMc02522-fl	3	3	3	3	3	3	2	3
SMc01500-fl	3	3	0	3	3	3	2	3

Continued on Next Page...

Table 4.7 – continued from previous page

Strain	**LB**	**Succinate**	**Mannitol**	**Na^+**	**Li^+**	**Mg^{2+}**	**K^+**	**Ca^{2+}**
SMc00264-fl	3	3	3	3	3	3	1	3
SMc02339-fl	3	3	3	3	3	3	1	3
SMa0329-fg	3	3	3	3	3	3	1	3
SMa0329-fl	3	3	3	3	3	3	1	3
SMb21159-fl	3	3	3	3	3	3	2	3
SMb20493-fl	3	3	3	3	3	3	2	3
SMa0187-fl	3	3	3	3	3	3	1	3
SMa1367-fl	3	3	3	3	3	3	2	3
SMa0335-fg	3	3	3	3	3	3	1	3
SMa0335-fl	3	3	3	3	3	3	2	3
SMc04391-fl	3	3	3	3	3	3	1	3
SMc04391-fg	3	3	3	3	3	3	2	3
SMa2019-fg	3	3	2	3	3	3	2	3
SMa2019-fl	3	3	3	3	3	3	2	3
SMa1757-fg	3	3	3	3	3	3	2	3
SMa1757-fl	3	3	3	3	3	3	1	3
SMc00326-fl	3	3	3	3	3	3	2	3
SMc01698-fg	2	3	3	1	2	3	1	3
SMc00553-fg	3	3	3	1	2	3	1	3
SMb20871-fg	3	3	3	2	2	1	2	3

Continued on Next Page...

Table 4.7 – continued from previous page

Strain	**LB**	**Succinate**	**Mannitol**	**Na^+**	**Li^+**	**Mg^{2+}**	**K^+**	**Ca^{2+}**
SMc01157	3	3	3	3	2	3	2	3
SMc01955	3	3	3	3	3	3	2	3
SMa0326	3	3	3	1	2	3	1	3
SMc03878-fl	3	3	3	3	1	3	2	3

NT: Not Tested

Strains with the most severe ion sensitivities are summarized in Table 4.8.

The pSymB mutant strains with the most severe ion sensitivities carry multiple deletions of pSymB. The regions of pSymB affected in these strains are highlighted in Figure 4.15.

Table 4.8: Summary of key ion-sensitive *S. meliloti* strains. Data presented are expressed as percent survival of the starting sample, and represent the average of three replicates

Strain	LB	Succinate	Mannitol	Na^+	Li^+	Mg^{2+}	K^+	Ca^{2+}
Rm1021	3	3	1	2	3	3	2.5	3
RmP110	3	2.7	0	2	3.0	NT	1	3.0
Rm104A14	3	3	1	0	0	3	0.5	3
RmG270	2	1.7	1	1	0	3	1	3
RmG271	2	0	0.5	1	0	2	1	3
RmG277	3	1	2	1	0	3	1	3
RmG373	3	0.5	3	3	0	3	2.5	3
RmG462	3	1	1	2	1.5	3	2	3
RmG471	2.5	1	1	2	2	2	2	2
RmG472	2.5	1	1	2	2	2	2	3
RmG506	3	3	3	1.5	1	3	2	3
RmF114	2	2	1	2	2	2	2	3
RmF514	3	2	3	0	0	3	2	3
RmF726	3	1	1.5	3	2.5	3	3	3
RmF728	3	1	1	0	0	2	0	3
SMc01698-fg	2	3	3	1	2	3	1	3
SMb20871-fg	3	3	3	2	2	1	2	3
SMc00553-fg	3	3	3	1	2	3	1	3
SMa0326	3	3	3	1	2	3	1	3

4.3 Conclusions

This study highlights some of the key short-comings of the current system of assessing OSS and desiccation tolerance in bacterial systems. Data from these assays are characteristically variable and the assays themselves are extremely sensitive to the slightest changes in the external environment, especially ambient humidity and seasonal temperature variations. Furthermore, this study highlights how easy it is to manipulate the data based on so-called standardization parameters. In analysing any OSS data, it is important to bear in mind these considerations and assess the data with an open mind and an eye to detail. Furthermore, the SEM data presented here suggest that when on-seed, bacteria initiate the formation of biofilm structures (Figures 4.10, 4.11, 4.12, and 4.13). These data are consistent with observations made in *B. japonicum*, which documented significant induction of EPS synthesis genes during the late stages of desiccation [63]. It is conceivable that the capacity of a particular strain to form a biofilm may negatively impact its apparent OSS. Although the OSS assay involves an extended period of vigorous vortexing prior to titration, cells that are part of a biofilm are unlikely to be removed in this manner since biofilms are characteristically able to withstand extended periods of mechanical stress. The preliminary evidence of biofilm formation shown in these SEM micrographs suggests that biofilm formation may have been a factor in influencing the variability of the data generated. It would be prudent in any future studies of OSS to take this into consideration.

The capacity of rhizobia to initiate biofilm formation on-seed may represent an exploitable parameter in inoculant development since it might reasonably be expected to increase the survival of the rhizobia during storage. Initial conditions for biofilm formation are known to be optimal under relatively high humidity and ambient temperature [86]. Manipulating the early inoculation and storage conditions

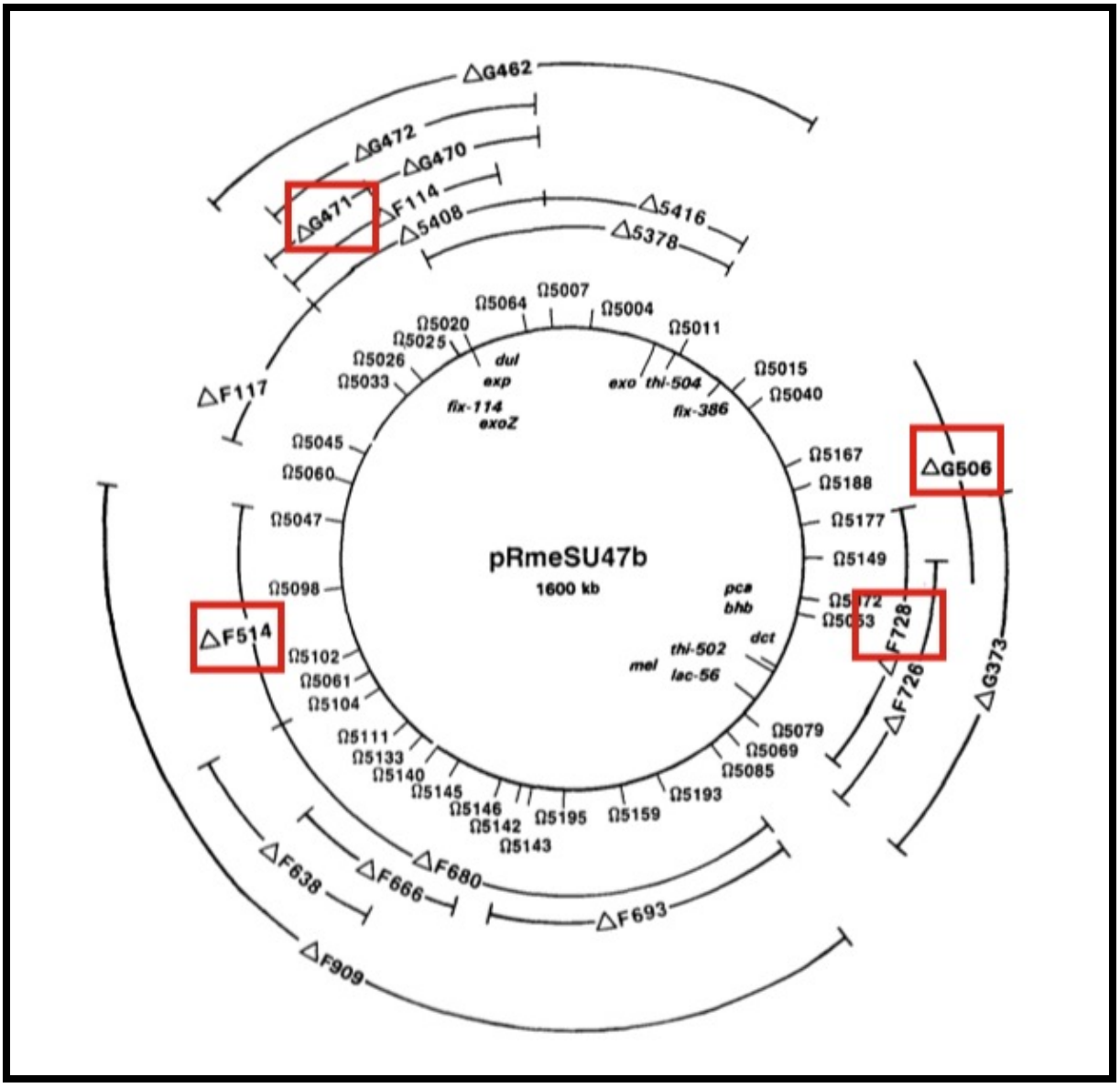

Figure 4.15: Map of pSymB of *S. meliloti* with the regions implicated in ion sensitivity highlighted. Modified from [47]

to maximize biofilm formation and stabilization may enhance longer-term survival of the rhizobial inoculant.

As discussed in Section 1.5, the synthesis of EPS may impact desiccation tolerance in *S. meliloti*. Indeed, previous studies have produced data that indicate that the production of HMW EPS may be expected to increase survival under desiccation conditions [376]. Since the results of our desiccation assay (Table 4.6) suggest that strains with enhanced EPSII synthesis (SmUW3 and SmUW6) have a higher tolerance of desiccation, and because studies have shown that the surface polysaccharides of *S. meliloti* are affected by the osmolarity of the growth conditions [30, 209, 210], it would be interesting to further analyse the particular EPS composition of these strains. Furthermore, a more detailed assessment of the potential links between EPS, desiccation tolerance and ion sensitivity might be achieved by analysing the limits of osmotic stress that SmUW3 and SmUW6 can withstand relative to Rm1021.

Some studies have shown that rhizobia grown in media with low water activity show increased survival during desiccation [50, 225]. The data presented in Figure 4.9 suggest that this is not the case over an extended period of time, for the *S. meliloti* strain Rm1021. Indeed, other studies have presented data that suggest the particular combinations of salts in the growth medium may induce specific physiological responses and that no one combination of osmolytes is necessary or sufficient to induce a protective effect [375]. The data presented here suggest that a link between salt-sensitivity and poor desiccation tolerance in *S. meliloti* might exist, especially in certain strains including RmF728. While the two phenotypes are known to not be completely overlapping, considerable overlap has been identified in some species [167, 246]. The screen conducted in this study has identified several *S. meliloti* pSymB and SDR mutants that demonstrate extremely poor growth on elevated levels of Na^+ and K^+. One of these mutants carries a deletion of a region of

pSymB for which no definable phenotype has previously been attributed. Mutant RmF514, which carries a 181 Kb deletion in pSymB, had been previously identified as having elevated salt-sensitivity relative to the wild-type strain [75, 244], adding validity to the screen that was developed in this study. Furthermore, an *exoFI* mutant has previously been shown to have a marked Mg^{2+} sensitivity [244]; *exoFI* is located within the region that is deleted in strain RmF514.

SMa0326 is annotated as an orthologue of *fab1*, encoding enoyl-ACP reductase (EC 1.3.1.9), and previous work has reported a mutant of it to have a Fix^- phenotype [161]. Previous studies have shown that ion sensitivity can result in reduced rhizosphere competitiveness [244]; further analysis of the competition phenotypes of these ion-sensitive strains might be prudent. Interestingly, this report is the first study to identify a phenotype that can be attributed to the particular SDR mutations in the other three SDR mutants listed in Table 4.8. Further analysis is necessary to confirm the phenotype and determine the precise mechanism of action.

Chapter 5

Mutational Analysis of Dicarboxylate Transport in *Bradyrhizobium japonicum*

5.1 Dicarboxylic Acid Transport and Metabolism in *Bradyrhizobium japonicum*

The capacity of a bacteroid to perform biological nitrogen fixation appears to be limited by the amount of photosynthate delivered to the nodule [138, 141, 299] and is also intimately linked to the ability of bacteroids to transport dicarboxylic acids. While sucrose, other sugars, and sugar alcohols are the most abundant forms of photosynthate in the root nodule [331], previous studies have shown that bacteroids preferentially import organic acids [16]. The bacteroids take atmospheric nitrogen and reduce it to ammonia, which is supplied to the plant in exchange for a source of carbon. The plant supplies the carbon in the form of C_4-dicarboxylic acids which enter the bacteroids through the membrane transport protein DctA. This

relationship is outlined in Figure 5.1. In other rhizobia, DctA mutants are unable to import DCAs and, as a result, form ineffective, nonfixing nodules in symbiosis and are also unable to grow on DCAs as a sole carbon source during free-living growth [11, 27, 99, 114, 293].

Although dicarboxylate transport has been reasonably well studied in other rhizobial systems, relatively little work has been conducted in this area in *B. japonicum*. Previous studies have established that succinate transport in *B. japonicum* cells occurs via an active transport mechanism that is dependent on an energized membrane but that does not directly utilize ATP [229]. Early work has suggested that *B. japonicum* preferentially transports succinate but is also capable of malate import [229, 360]. Studies have also suggested that *B. japonicum* possesses at least two succinate transport systems [157] but no further attempts to characterize them have since been reported. Expression of *S. meliloti dctABD* in *B. japonicum* resulted in enhanced growth rates on dicaroxylates, an increase in succinate uptake, and higher levels of nitrogen-fixation activity [24].

Most rhizobia typically possess only a single copy of the *dctA* gene, along with one copy of the *dctBD* two-component regulatory system. Analysis of the *B. japonicum* USDA110 genome sequence [178, 179] revealed the presence of 7 putative *dctA* homologues and no annotated homologue of *dctBD*. Here we report the identification, cloning and mutagenesis of the 7 *dctA* homologues of *B. japonicum* as well as the identification and cloning of a putative *dctBD* locus.

5.2 Results and Discussion

All plasmids and strains constructed in this study are described in Table 2.1 and have also been summarized in Tables 5.1 and 5.2 for convenience and ease of reading.

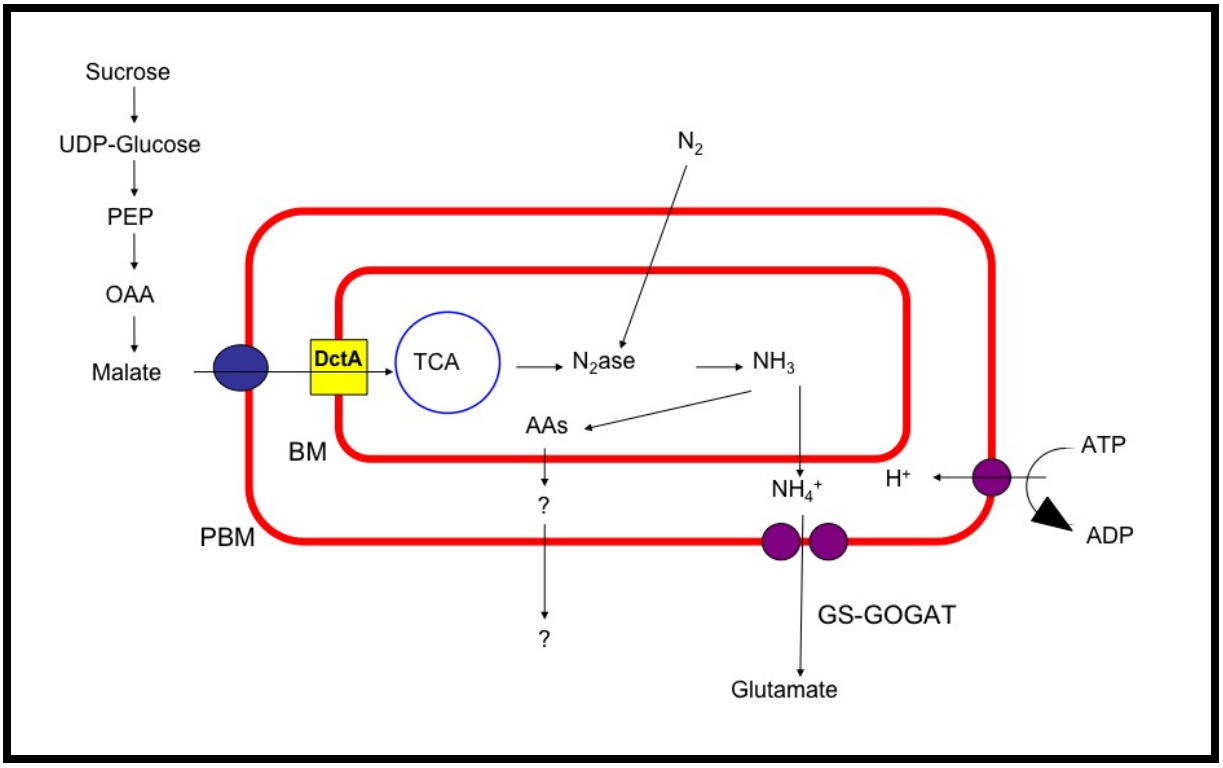

Figure 5.1: Schematic of bacteroid metabolism. The plant provides DCAs to the bacteroid. DCAs pass through a plant-derived transporter in the peribacteroid membrane (PBM) and enter the bacteroid via DctA in the bacteroid membrane

Table 5.1: Summary of plasmids constructed in the analysis of *B. japonicum dct*

Plasmid	Relevant Characteristics
pMA127	USDA110 cosmid clone complementing RmF726 for growth on succinate
pMA166	pGemTEasy carrying internal Blr3723 fragment
pMA170	pGemTEasy carrying complete *B. japonicum dctBD* operon
pMA172	pMA170 with central SgrAI fragment of *dctBD* deleted
pMA174	pMA172 with ΩSmSp cassette inserted in central EcoRV site of truncated *dctBD*
pMA175	pK19*mobsacB* carrying Δ*dctBD*ΩSmSp from pMA174
pMA176	pK19*mobsacB* carrying internal Blr3723 fragment from pMA166
pMA197	pMA127 Tn*5* inserted into Blr3723
pMA198	pBBR1MCS2 Blr6145 plus 50 bp upstream sequence
pMA199	pJET Bll1718 Complete ORF
pMA200	pJET Bll1718 Truncated ORF
pMA201	pJET Blr3723 Complete ORF
pMA202	pJET Blr3840 Complete ORF
pMA203	pJET Blr3840 Truncated ORF
pMA204	pJET Blr4298 Truncated ORF
pMA205	pJET Blr6145 Truncated ORF
pMA206	pJET Bll7095 Complete ORF
pMA207	pJET Bll7095 Truncated ORF
pMA208	pJET Blr4298 Complete ORF
pMA209	pSW213 Blr3723 from pMA201
pMA210	pSW213 Blr3840 from pMA202
pMA211	pSW213 Blr4298 from pMA208
pMA212	pJET Blr6145 Complete ORF
pMA214	pSW213 Bll7095 from pMA206
pMA216	pSW213 Blr6145 from pMA212
pMA217	pSW213 Bll1718 from pMA199
pMA219	pJET Blr7187 Truncated ORF
pMA220	pJET Blr7187 Complete ORF
pMA221	pK19*mob* Bll1718 Truncated from pMA200
pMA222	pK19*mob* Bll7095 Truncated from pMA207
pMA223	pK19*mob* Blr6145 Truncated from pMA205
pMA224	pK19*mob* Blr7187 Truncated from pMA219
pMA225	pK19*mob* Blr3840 Truncated from pMA203
pMA226	pSW213 Blr7187 from pMA220
pMA227	pK19*mob* Blr4298 Truncated from pMA204

Table 5.2: Summary of strains constructed in the analysis of *B. japonicum dct*

Strain	Relevant Characteristics
BjUW34	USDA110 pMA176 single recombinant
BjUW37	USDA110 pMA175 single recombinant
BjUW40	USDA110 pMA221 single recombinant
BjUW42	USDA110 pMA222 single recombinant
BjUW44	USDA110 pMA223 single recombinant
BjUW46	USDA110 pMA225 single recombinant
BjUW48	USDA110 pMA224 single recombinant
BjUW50	USDA110 pMA227 single recombinant
BjUW52	USDA110 pMA232 single recombinant

5.2.1 Determination of the Wild-Type Growth Characteristics of *B. japonicum* USDA110 on Dicarboxylates as Sole Carbon Sources

The ability of wild-type *B. japonicum* USDA110 to grow on the dicarboxylates malate, succinate, and fumarate as sole carbon sources was measured by growth curve analysis using the Bioscreen-C Growth Curve Machine. The data shown in Figure 5.2 suggest that, while *B. japonicum* USDA110 can utilize succinate as a sole carbon source under free-living conditions, it is unable to grow on either malate or fumarate.

5.2.2 Identification of Putative *dctA* and *dctBD* Open Reading Frames

A BLASTP analysis of the *B. japonicum* genome, using the *S. meliloti* DctA and DctBD amino acid sequences, identified seven putative *dctA* loci as well as a putative *dctBD* homologue. These homologues are listed in Table 5.3. Figure 5.3 depicts a Boxshade diagram, constructed from a ClustalW alignment [343] , highlighting the level of sequence conservation between the seven DctA homologues of *B. japonicum* and DctA of *S. meliloti*. Figure 5.4 shows a rooted phylogenetic tree, constructed using ClustalW [343] and Phylip [92], that depicts the relationship between the seven *B. japonicum* DctA sequences and other Rhizobial DctAs.

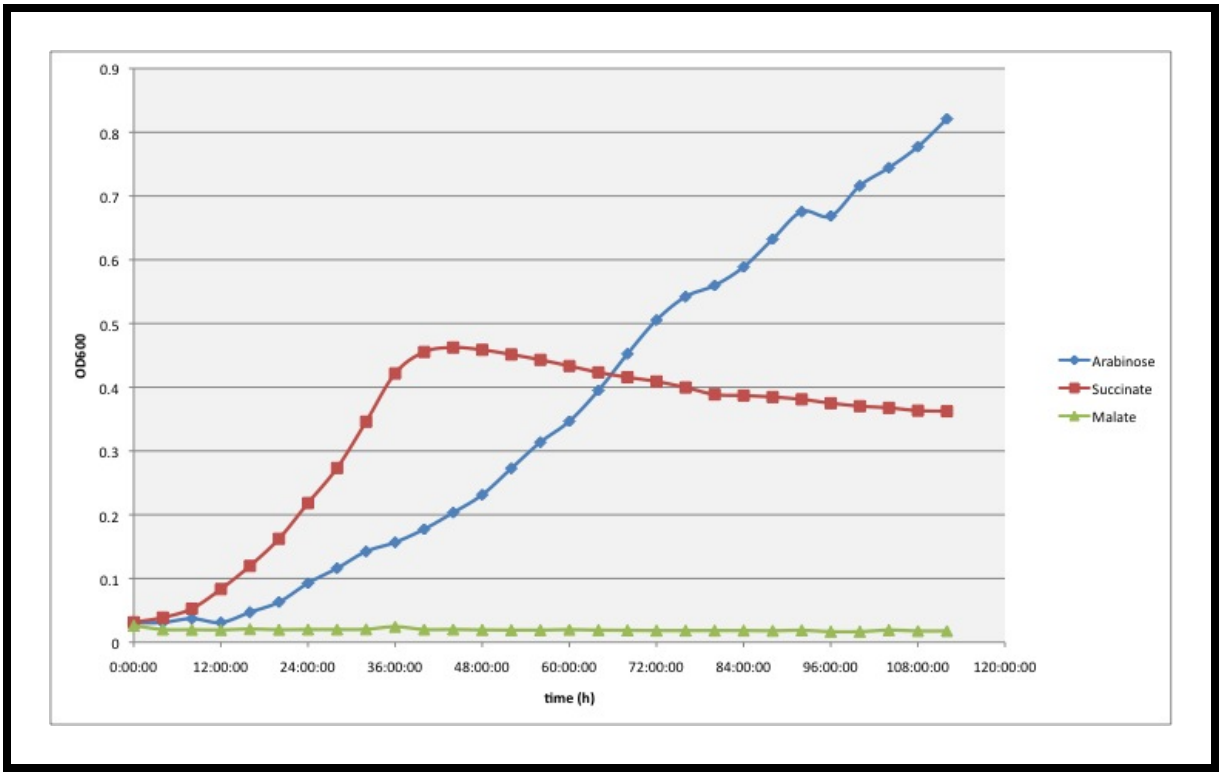

Figure 5.2: Growth of wild-type *B, japonicum* on VMM supplemented with arabinose, succinate or malate as a sole carbon source

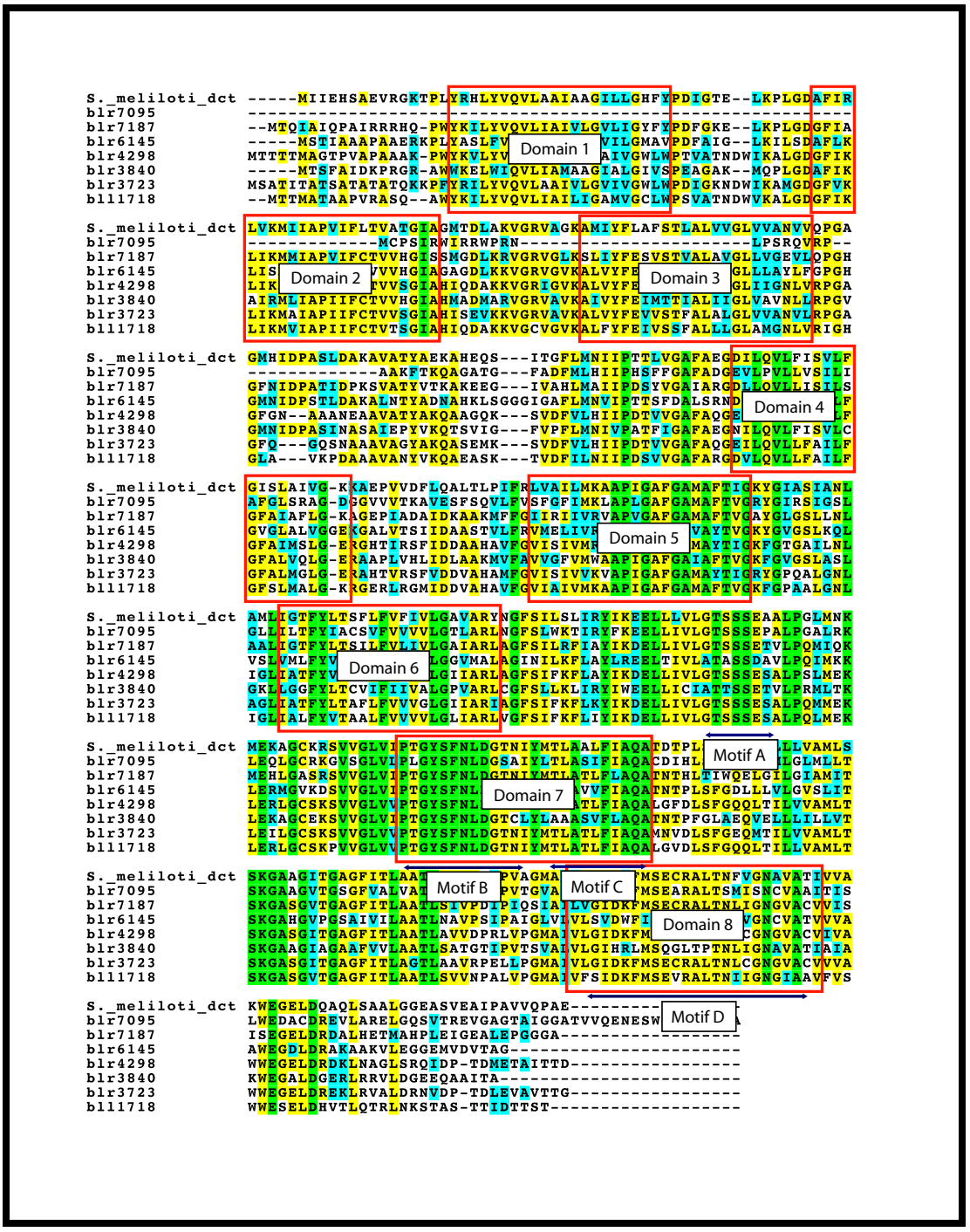

Figure 5.3: Alignment of the seven putative DctA amino acid sequences of *B. japonicum* and DctA of *S. meliloti*. Analysis of the genome sequence of *B. japonicum* USDA110 identified seven putative homologues of *dctA* located throughout the genome. No putative *dctBD* 2-component regulatory system was identified in the annotation. These *dctA* genes encode DctA homologues that share considerable identity with other known DctA proteins, including that of *S. meliloti*. The eight domains and three motifs that show high levels of sequence conservation between all members of the glutamate transporter family of proteins have been indicated.

Table 5.3: Putative dicarboxylate transport genes identified by *in silico* analysis of the *B. japonicum* genome sequence

Gene ID	Annotated Function	% Identity to *S. meliloti* homologue
Blr7187	C_4-dicarboxylate transport protein	61%
Blr3723	C_4-dicarboxylate transport protein	58%
Blr4298	C_4-dicarboxylate transport protein	58%
Blr3840	C_4-dicarboxylate transport protein	54%
Bll1718	C_4-dicarboxylate transport protein	55%
Blr6145	C_4-dicarboxylate transport protein	51%
Bll7095	C_4-dicarboxylate transport protein	49%
Blr3730	two-component hybrid sensor and regulator	29%
Blr3731	two-component response regulator	50%

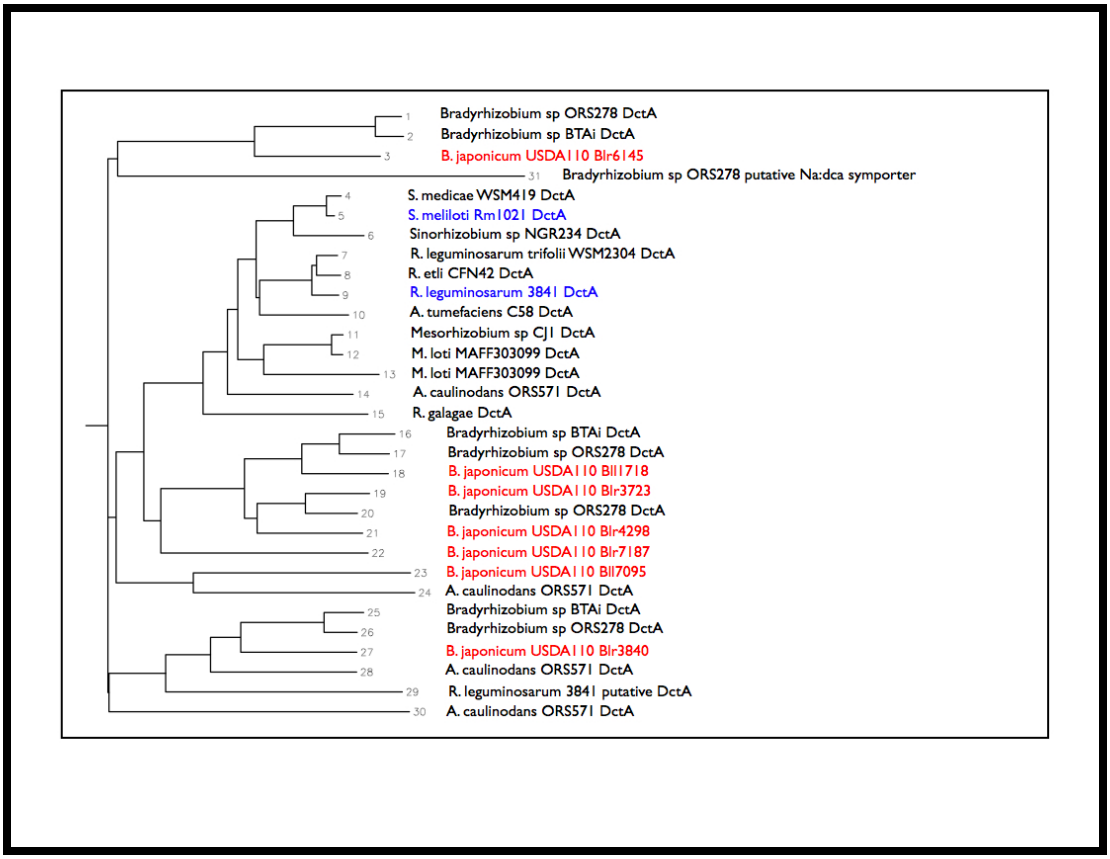

Figure 5.4: Phylogenetic tree of the seven putative DctA amino acid sequences of *B. japonicum* and DctAs of related members of the *Rhizobiales*.

5.2.3 Heterologous Complementation of *S. meliloti dctA* Mutant with *B. japonicum* USDA110 Cosmid Library

The pLAFR1 cosmid library of *B. japonicum* USDA110 [129] was conjugally transferred into *S. meliloti* strains carrying mutations in *dctA* (RmF642), *dctB* (RmF153), *dctD* (RmF121) or *dctABD* (RmF726) [47, 97]. The ability to restore growth on succinate as a sole carbon source was used as selection. Complementing clones were selected and the cosmids mated back into *E. coli* for further analysis. These cosmids were isolated and analysed for unique restriction patterns with BamHI and EcoRI. Figure 5.5 shows a representative BamHI digest. All of the cosmids chosen shared common bands, suggesting that they represent overlapping clones of the same region of the genome. The sample in lane 4 was chosen for further study and the plasmid was named pMA127.

5.2.3.1 Identification of the Complementing *dctA* ORF in pMA127

In silico analysis of different regions of the *B. japonicum* genome was used to match the digestion pattern seen in Figure 5.5 to a specific genomic region. The complementing clones all mapped to a region in the genome that is particularly rich in genes responsible for energy production; Figure 5.6 shows a map of this region. Gene identity was confirmed by EZ-Tn*5* *in vitro* mutagenesis using the EpiCentre® EZ-Tn*5*™ Insertion Kit (EpiCentre Biotechnologies, Madison WI, USA). Kan^R transposon mutants of pMA127 were selected in *E. coli*, and mutants were conjugally transferred into *S. meliloti* RmF728 and screened for loss of the ability to complement the succinate phenotype of RmF728. Subsequent sequencing identified the *dctA* ORF as Blr3723 and the mutated plasmid was named pMA197.

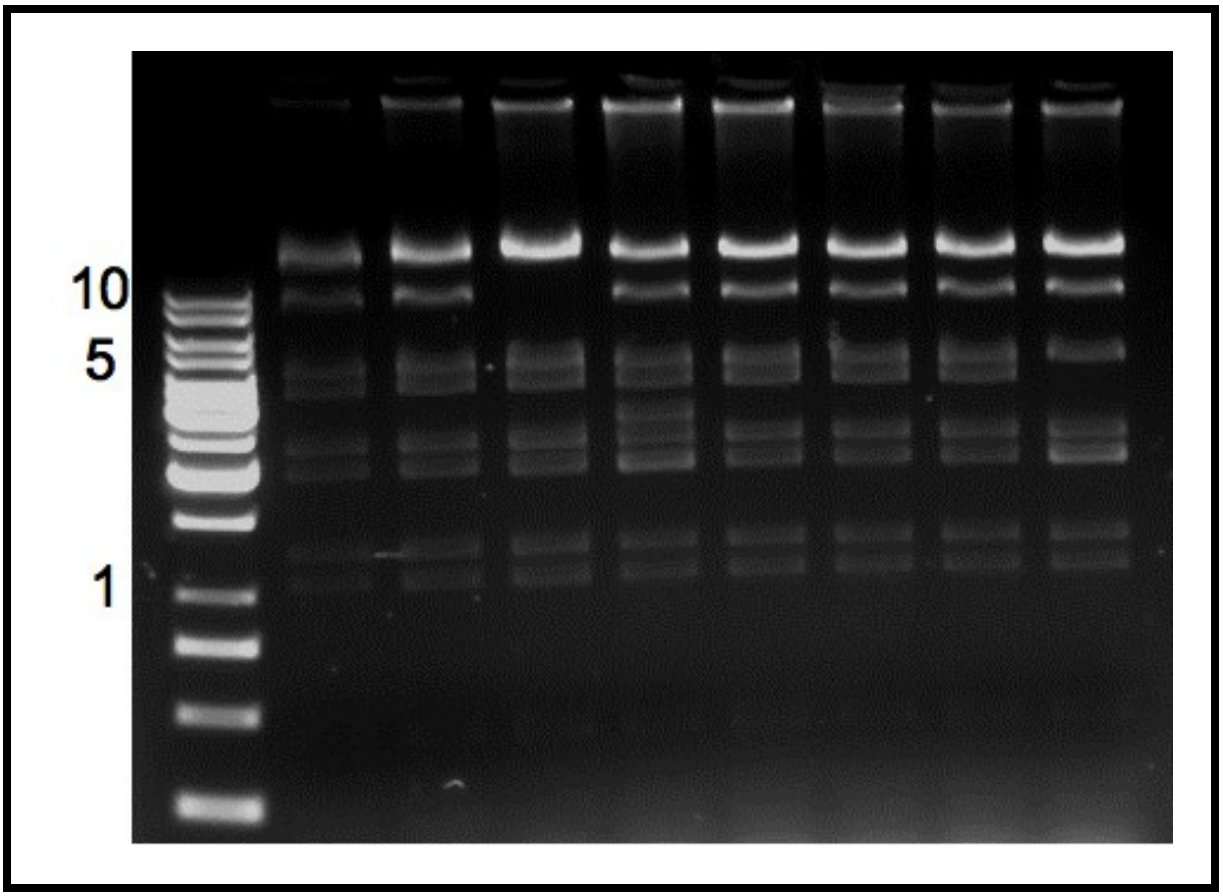

Figure 5.5: Restriction digest of eight cosmids isolated from the *B. japonicum* cosmid library for their ability to complement the succinate utilization phenotype of *S. meliloti dctA*, *dctB*, *dctD* and *dctABD* mutants

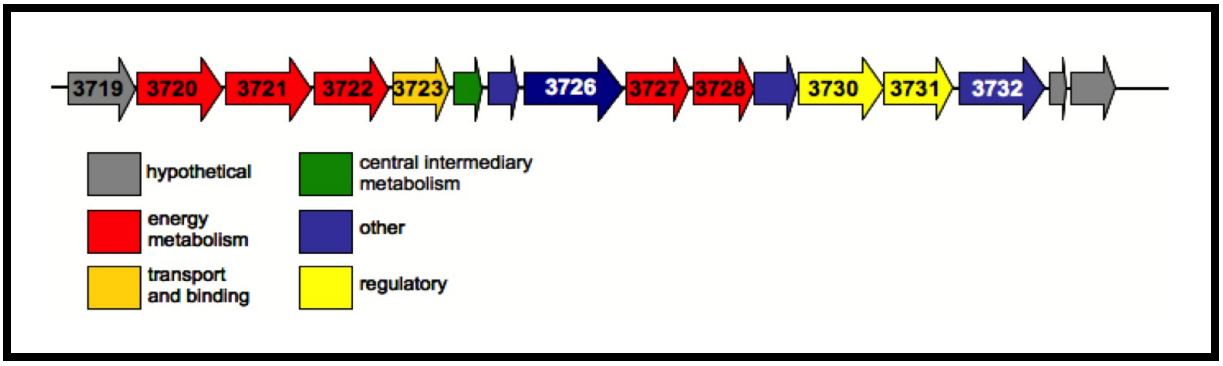

Figure 5.6: Map of the region of the genome found in pMA127 and pMA131. Blr3723 is a putative *dctA* and Blr3730/3731 is a putative dctAB two-component regulatory system

5.2.3.2 Testing the Ability of pMA127 and pMA197 to Complement the Free-living Phenotype of *S. meliloti* Dct Mutants

The ability of pMA127 and pMA197 to complement the free-living phenotype of RmF121 (*dctD*), RmF153 (*dctB*) and RmF642 (*dctA*) was tested. The cosmids were transferred into each strain by triparental mating and transconjugants were selected on TY Sm_{200} Nm_{200} Tc_{10}. The transconjugants were then screened for growth on LB, VMM Glucose, VMM Succinate, VMM Arabinose 1 μg/ml FOA, and VMM Arabinose 5 μg/ml FOA. The results are shown in Table 5.4. These data are quite interesting. It appears that pMA127 is able to complement all three *dct* mutations in *S. meliloti*. Interestingly, pMA197 does not appear to complement the *dctB* and *dctD* mutants, which is unexpected since both of these mutants have functional *dctA*s and the cosmid should still carry a functional *dctBD*. This suggests that the *B. japonicum dctBD* located on the cosmid is unable to recognize the *S. meliloti dctA* promoter. It also provides an explanation for why, although *B. japonicum* has seven homologues of *dctA*, the heterologous complementation screen only identified one region as capable of complementing the *S. meliloti dct* mutants.

Table 5.4: Complementation analysis of pMA127 and pMA197 under free-living conditions

Strain	LB	VMM Glu	VMM Ara	VMM Succ	VMM Ara 1 μg/ml FOA	VMM Ara 5 μg/ml FOA
Rm1021	++++	+++	+++	++++	+	-
RmF121	++++	+++	++	+	++	+++
RmF121 pMA127	++++	+++	++	++++	+	++
RmF121 pMA197	++++	+++	+++	+	++	+++
RmF153	++++	+++	++	+	+	+++
RmF153 pMA127	+++	+++	++	++++	+	+
RmF153 pMA197	++++	+++	++	+	++	+++
RmF642	++++	+++	++	+	++	+++
RmF642 pMA127	++++	+++	++	++++	+	+
RmF642 pMA197	++++	+++	++	+	++	+++

5.2.3.3 Testing the Ability of pMA127 and pMA197 to Complement the Symbiotic Phenotype of *S. meliloti* Dct Mutants

Previous studies have shown that, unlike in other species of rhizoba, *S. meliloti dctA* expression is independent of *dctBD* during symbiosis [90, 381, 394]. Although this alternative symbiotic activation (ASA) phenomenon is well documented, its mechanism of action remains unclear. A *dctA::lacZ* fusion is expressed in nodules of a *dctD* mutant [25, 380] but the pattern of expression differs to that of a wild-type strain (reviewed in [396]). DctB/DctD-dependent *dctA* expression is seen in the infection and fixation zones of the nodule; DctB/DctD-independent *dctA* expression is not seen until the transition from early to late symbiotic bacteroid development [25]. In order for DctB/DctD-independent activation of *dctA* to occur, the *cis*-acting regulatory elements found in the 5' one-third of the *dctA* coding region must be present; this region is not needed for DctB/DctD-dependent activation [25].

The ability of pMA127 and pMA197 to complement the symbiotic phenotype of RmF642, the *dctA* mutant of *S. meliloti* was tested by inoculating *Medicago sativa* plants with each strain and measuring the shoot dry mass (SDM) of the plants at 4-weeks post-inoculation. Nodules from the plants inoculated with RmF642 pMA127 and RmF642 pMA197 were surface-sterilized, crushed and the contents screened for Tc^R and Nm^R to confirm retention of the cosmids. The data shown in Figure 5.7 show that neither pMA127 nor pMA197 can complement the *S. meliloti dctA* mutant in symbiosis. Figure 5.8 shows a representative photograph of alfalfa plants from this experiment; the Fix^- phenotype of the RmF642 and RmF642 pMA127 inocula is clearly apparent. When considered in the light of the data presented in the previous sections, it is likely that the *dctA* promoter from *B. japonicum* cannot be recognized by either DctB/DctD or the DctB/DctD-independent regulatory elements in *S. meliloti*.

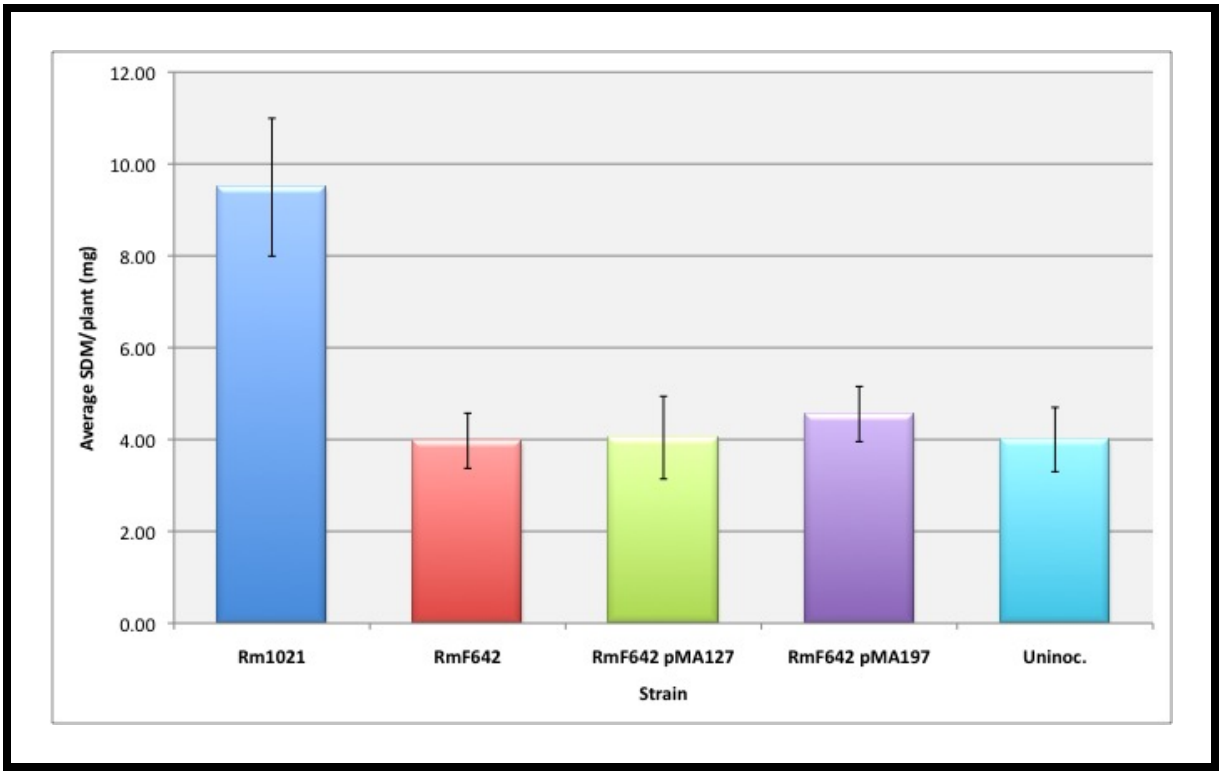

Figure 5.7: Shoot dry masses of *M. sativa* plants inoculated with *S. meliloti dctA* mutant RmF642, and complemented clones

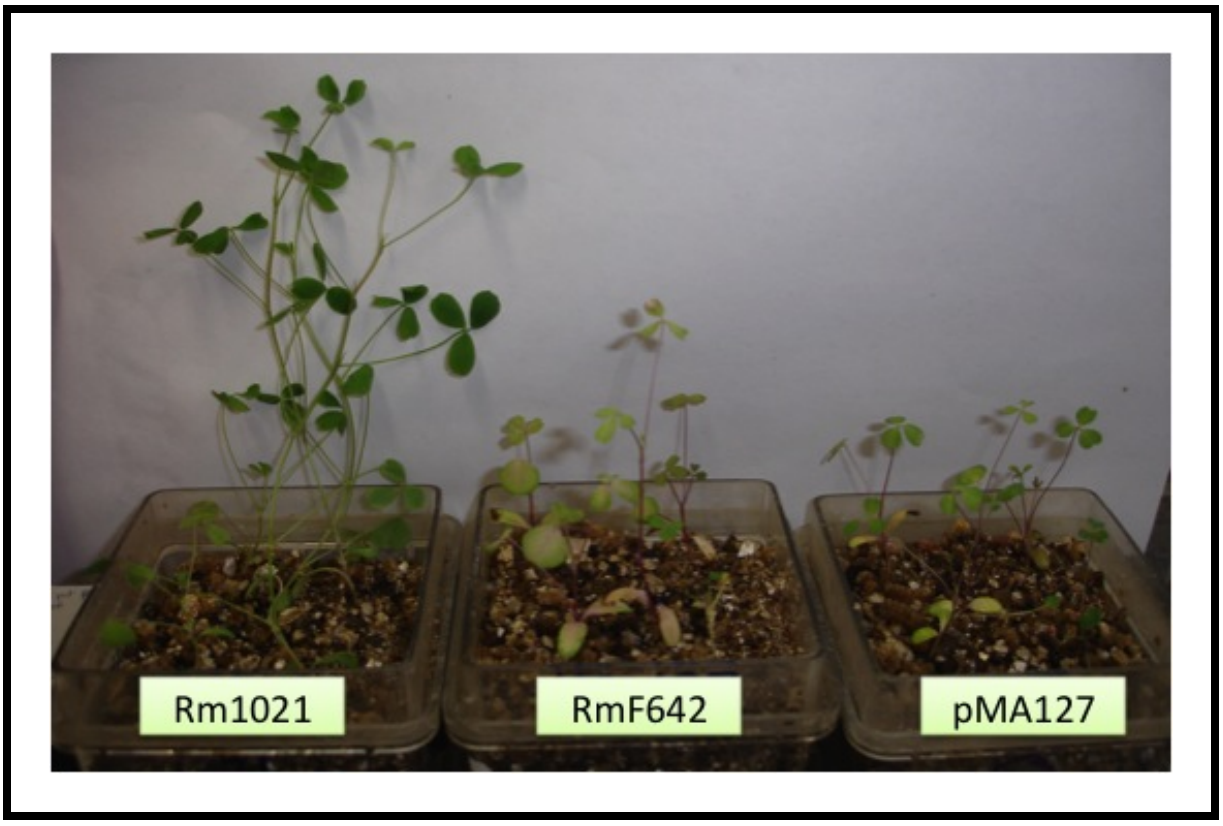

Figure 5.8: Representative photograph of *M. sativa* plants inoculated with wild-type *S. meliloti* Rm1021, *S. meliloti dctA* mutant RmF642, and RmF642 pMA127

5.2.4 Cloning of *B. japonicum dctA* Open Reading Frames

In order to determine which of the seven *dctA* ORFs of *B. japonicum* were capable of complementing the *dctA* phenotype of *S. meliloti* RmF642, all seven *dctA* ORFs were cloned into the broad host-range vector pSW213 [48]. All primers used in the cloning reactions are described in Table 2.2. Each ORF was cloned as a PCR product into the PCR capture vector pJET (Fermentas Canada Inc., Burlington ON) and the insert was verified by restriction digest and sequencing. The ORFs were then subcloned into pSW213 and the insert and orientation verified by PCR before transferring into RmF642 by triparental conjugation.

5.2.4.1 Complementation of *S. meliloti* RmF642 Free-Living Phenotypes

The ability of each of the cloned *dctA* genes to complement the free-living phenotype of RmF642 was tested by analysing their respective growth curves, generated using the BioscreenC Growth Curve machine. Growth was tested on VMM Succinate, VMM Succinate IPTG, and VMM Glucose IPTG 1 μg/ml. The results of these growth curves are shown in Figures 5.9, 5.10, 5.11, 5.12, and 5.13.

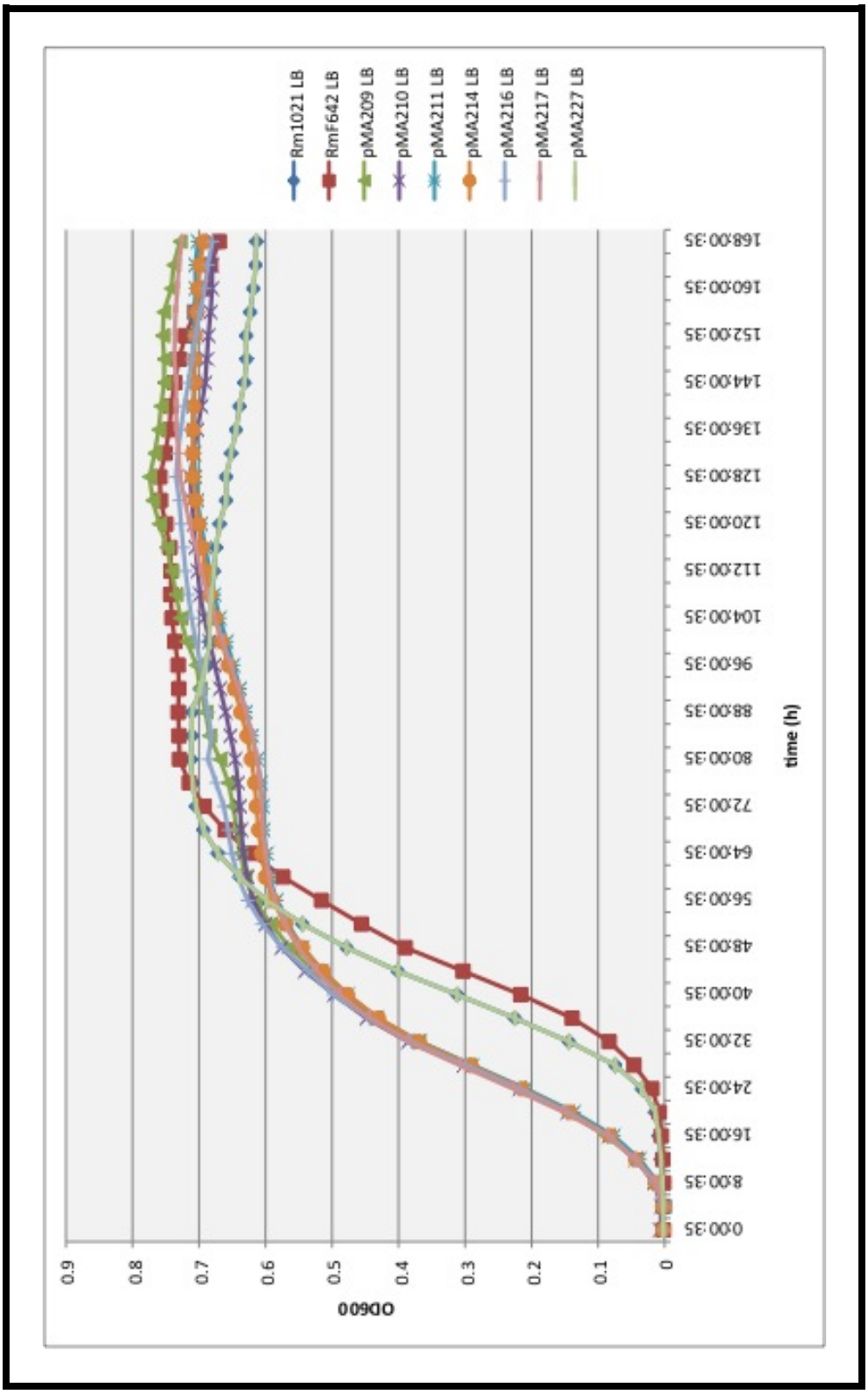

Figure 5.9: Growth curves of *S. meliloti* Rm1021, RmF642 and RmF642 complemented clones on LB

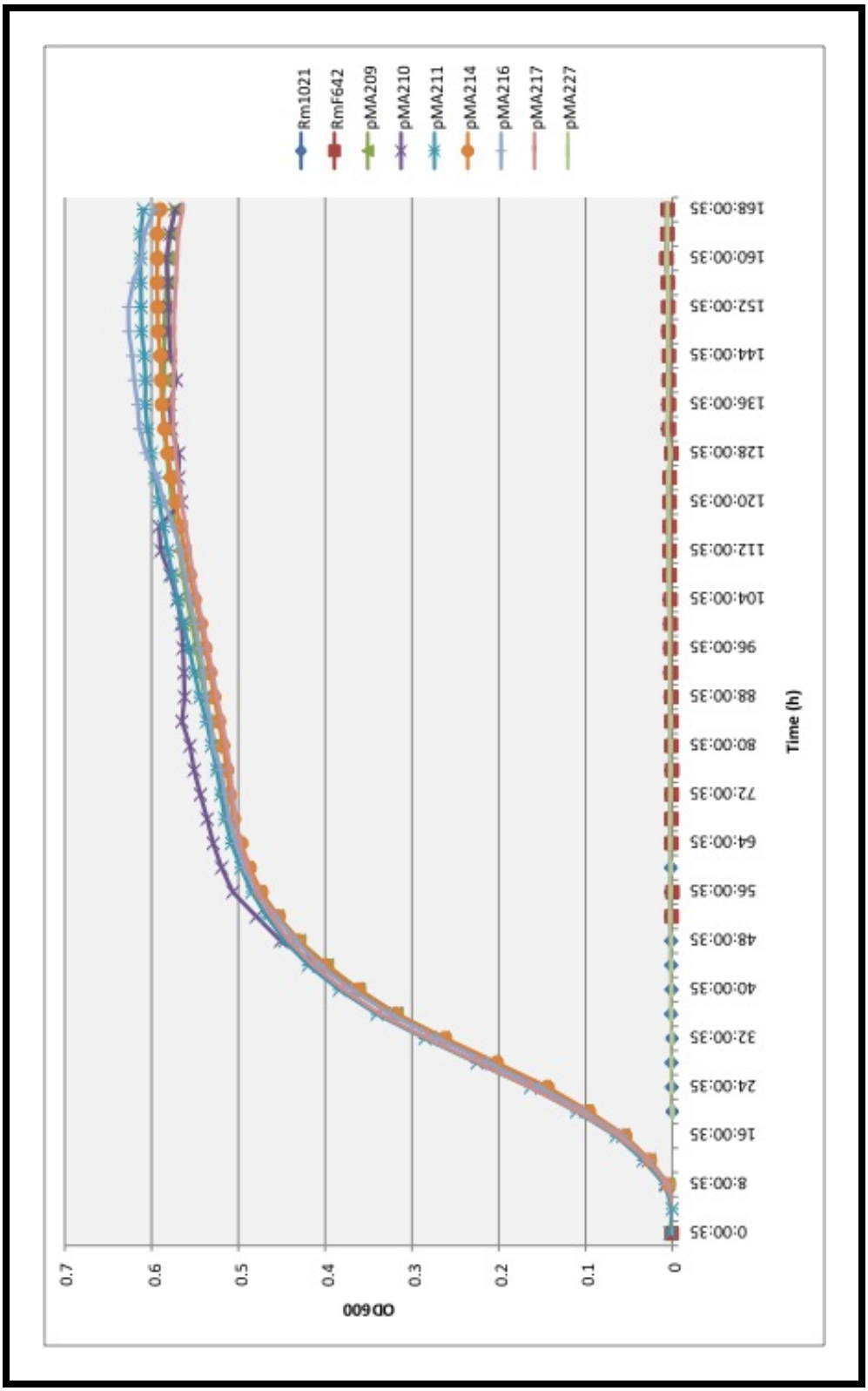

Figure 5.10: Growth curves of *S. meliloti* Rm1021, RmF642 and RmF642 complemented clones on LB Tc_{10}

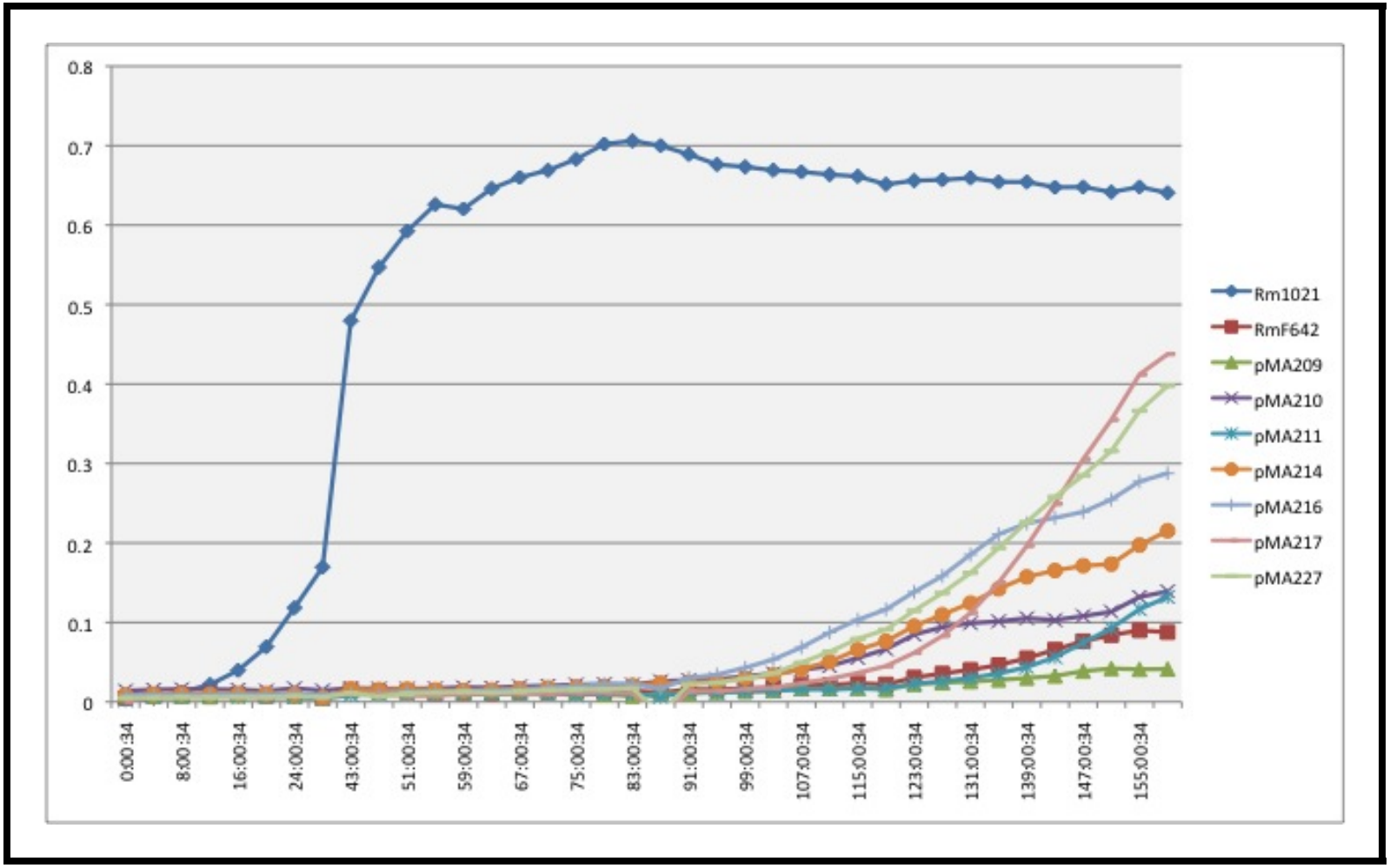

Figure 5.11: Growth curves of *S. meliloti* Rm1021, RmF642 and RmF642 complemented clones on VMM Succinate

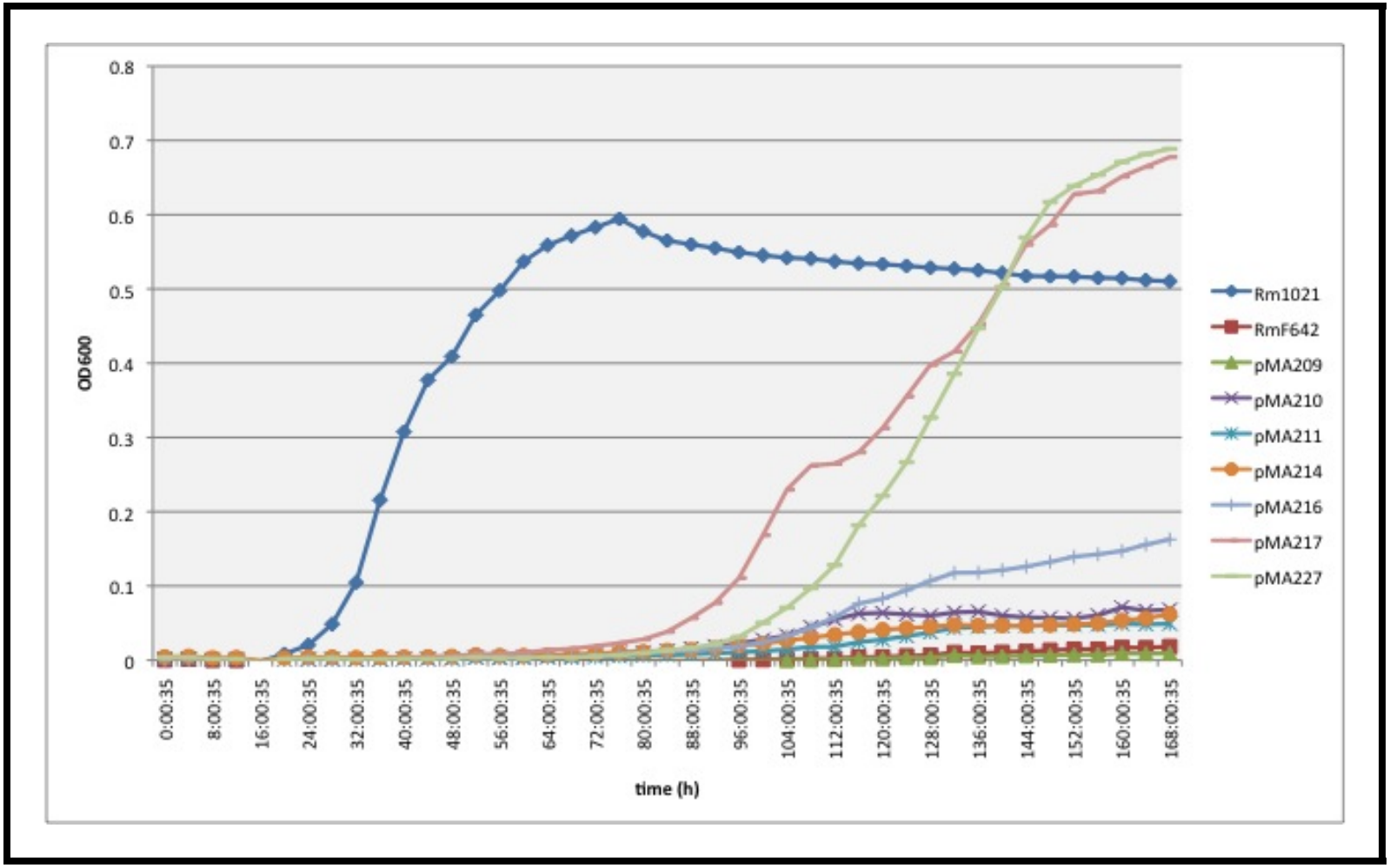

Figure 5.12: Growth curves of *S. meliloti* Rm1021, RmF642 and RmF642 complemented clones on VMM Succinate with 1 mM IPTG

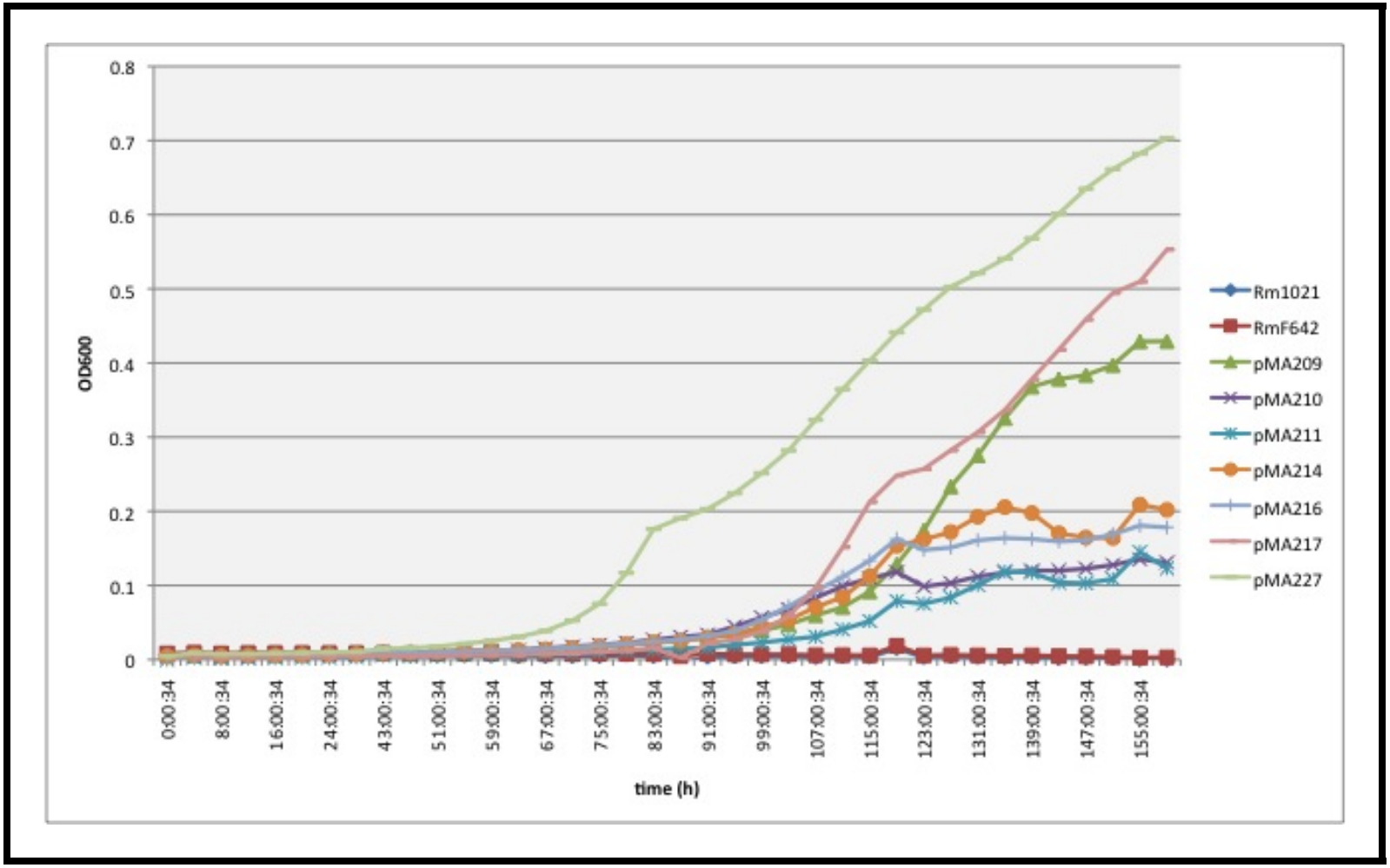

Figure 5.13: Growth curves of *S. meliloti* Rm1021, RmF642 and RmF642 complemented clones on VMM Succinate with 1 mM IPTG and Tc_{10}

Figures 5.9 and 5.10 act as controls to show that all strains grew well on a complex medium (LB), and that the Tetracycline was sufficient to inhibit growth of both Rm1021 and RmF642 over the complete duration of the experiment. Figure 5.11 shows that, in the absence of the inducer IPTG, very little growth on succinate is observed in any of the complemented strains before approximately 100 hours of incubation; at which point Rm1021 has already reached stationary phase. Figure 5.13 show that, even in the presence of inducer, induction does not occur until at least 60-80 hours of incubation, suggesting that perhaps the $lacI^q$ inducible promoter system in pSW213 does not work well in*S. meliloti*. These figures do show, however, that complementation is apparent from pMA227 (Blr4298), pMA217 (Bll1718) and pMA209 (Blr3723) and that some degree of partial complementation is achieved from the other four ORFs. It is interesting to compare Figures 5.12 and 5.13; it appears that the presence of Tc enhances the complementation capacity of the clones *dctA* ORFs. It is conceivable that the presence of the Tc provides the selective pressure for plasmid maintenance prior to induction of the *dctA* genes since induction is not realized until much later into the experiment. Conversely, it is also possible that the Tc is being used as a carbon source by the complemented clones; however, the data in Figure 5.10 suggest that this is not the case. These data show that growth of both Rm1021 and RmF642 is completely inhibited through the complete duration of the growth curve, suggesting that these strains do not have the capacity to utilize the Tc as a carbon source, or that the efficacy of the Tc is reduced following prolonged exposure to light.

5.2.5 Mutagenesis of *B. japonicum dctA*

An internal 500 bp fragment of Blr3723 was amplified and captured in pGEMTEasy (Promega, Fischer Scientific Ltd., Nepean ON). The insert was confirmed by sequencing and subcloned into pK19*mobsacB*. The resultant construct was transferred

into *B. japonicum* USDA110 by triparental conjugation; recombinants were selected on AG Km_{50} Tc_{10} and streak purified three times. The mutagenesis was confirmed by Southern Blot. A representative Southern Blot is shown in Figure 5.14.

Following successful mutagenesis of Blr3723, mutants of the remaining six *dctA* ORFs were constructed in a similar fashion. PCR amplification was used to clone the first 500 bp of each of the *dctA* ORFs. These fragments were captured in pJET (Fermentas, Burlington ON), confirmed by sequencing and then subcloned into pK19*mob* [310]; subclones were screened by restriction digest for plasmids containing inserts in the reverse orientation. Mutants of *B. japonicum* were constructed by conjugal transfer of the pK19*mob* clones from *E. coli*. Recombinants were selected on AG Km_{50} Tc_{10} and streak purified three times. The resultant mutant strains are described in Table 2.1 and summarized in 5.2.

5.2.5.1 Analysis of Free-Living Phenotypes of *B. japonicum dctA* Mutants

The free-living phenotype of each *B. japonicum dctA* mutant was analysed by assessing growth on AG, AG Km_{25}, VMM Arabinose, VMM Succinate and VMM Maleate/Arabinose FOA 2 μg/ml. Growth curves were set up in the BioScreen-C Growth Curve machine and were allowed to run for 10 days. The results of these growth curves are shown in Figures 5.15, 5.16, 5.17, and 5.18. The data in Figures 5.15 and 5.16 show that all of the mutants grow well on the complex medium AG and AG supplemented with Km_{25} while the wild-type USDA110 is unable to grow on AG Km_{25}. Figure 5.17 shows that, as expected, all of the strains are able to grow in VMM using arabinose as a sole carbon source. Interestingly, as shown in Figure 5.18, all of the *dctA* mutants were capable of growth on succinate as a sole carbon source. This suggests that all of the mutants still possess a functional dicarboxylate system, an assumption that is supported by the observation that

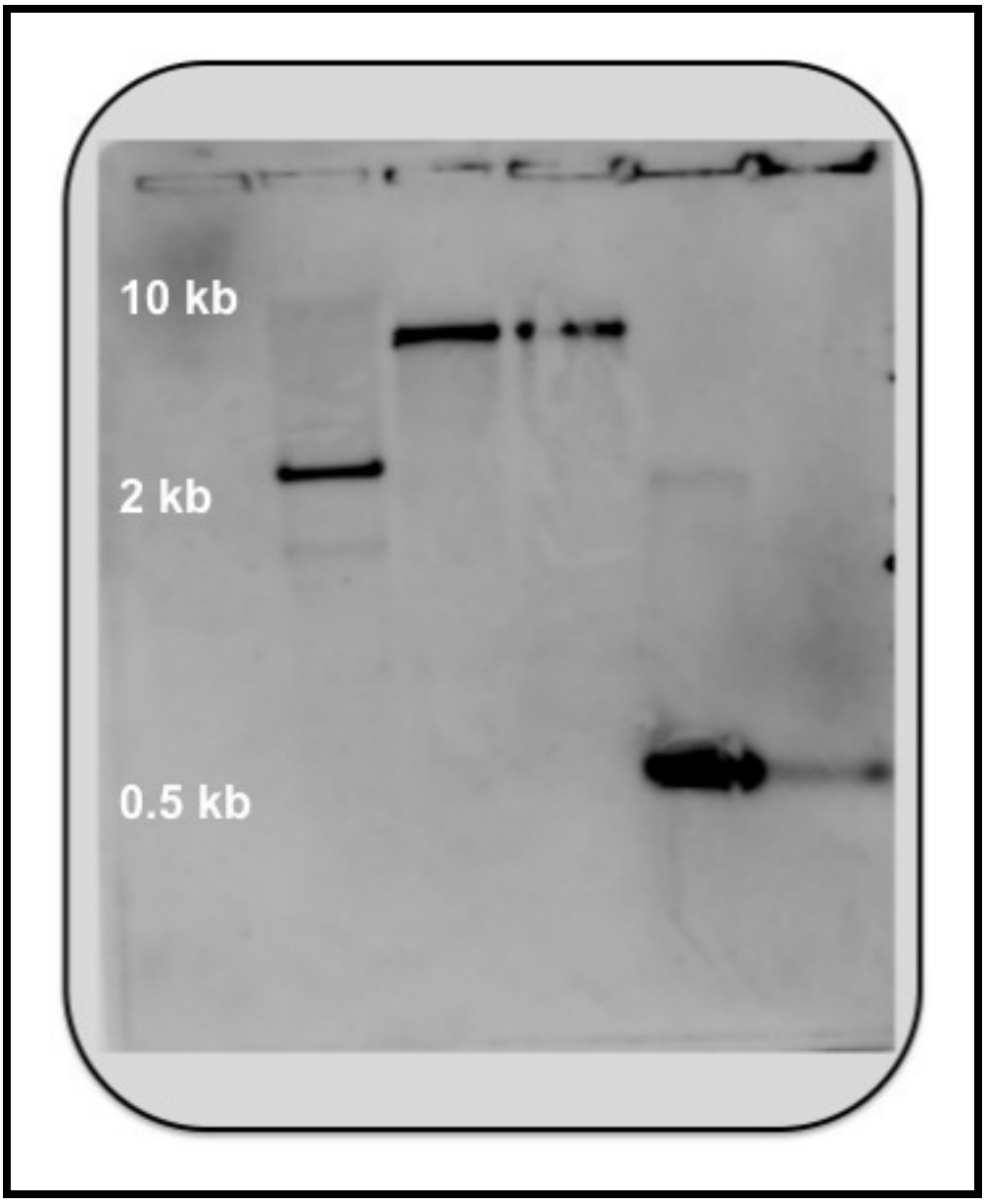

Figure 5.14: Southern blot of *B. japonicum* Blr3723 Mutagenesis. Lane 1: Empty; Lane 2: Wild-type USDA110; Lanes 3 and 4: BjUW34; Lane 5: pMA176 (1:10 dilution); Lane 6: pMA176 (1:100 dilution)

no growth occurred in VMM Maleate/Arabinose FOA 2 μg/ml (data not shown), which shows that none of the mutants are capable of growth in the presence of FOA (note, maleate was included in this medium as a potent inducer of *dctA* expression in *S. meliloti*) [398].

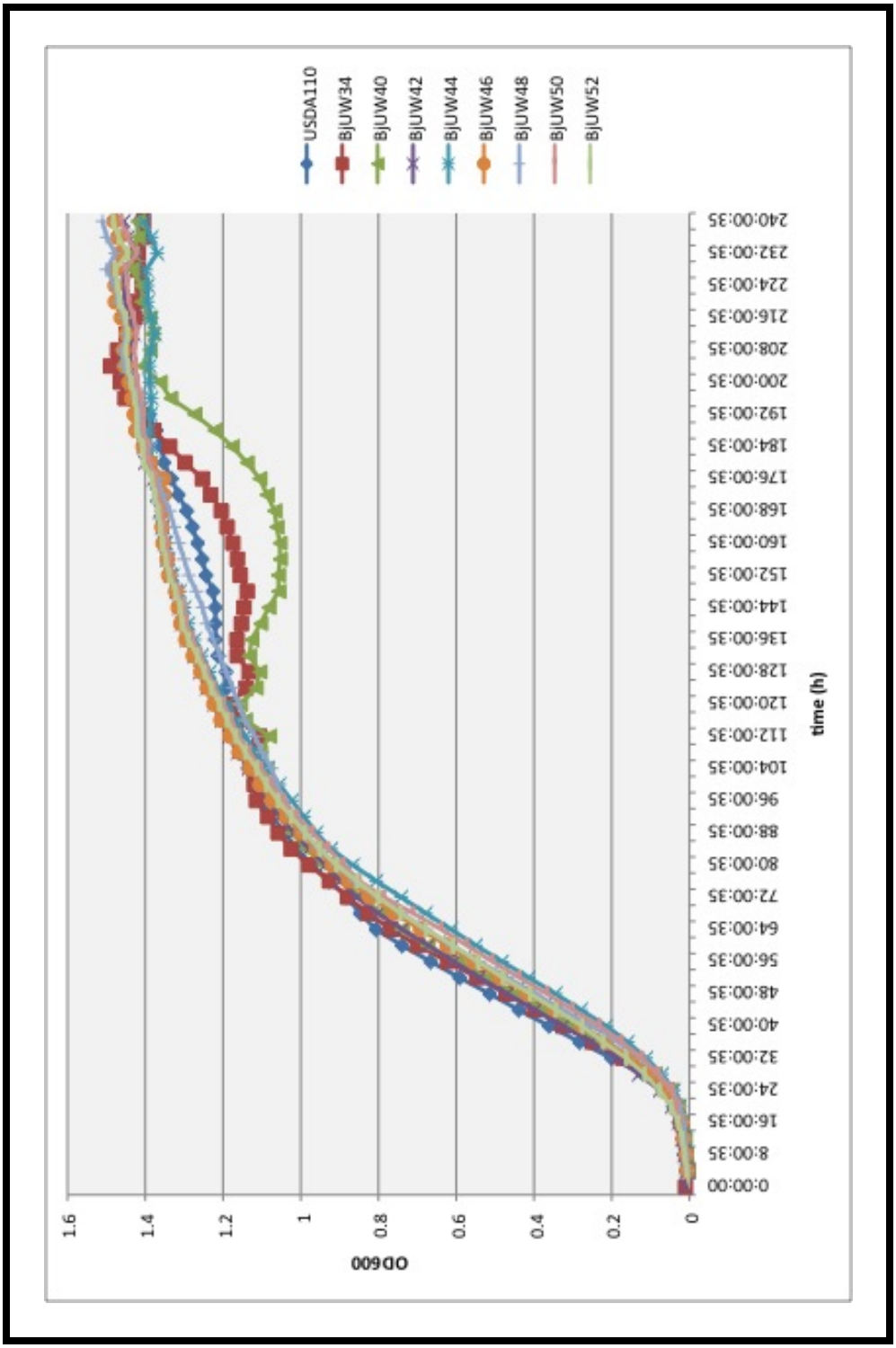

Figure 5.15: Growth curves of *B. japonicum dctA* mutants in AG medium

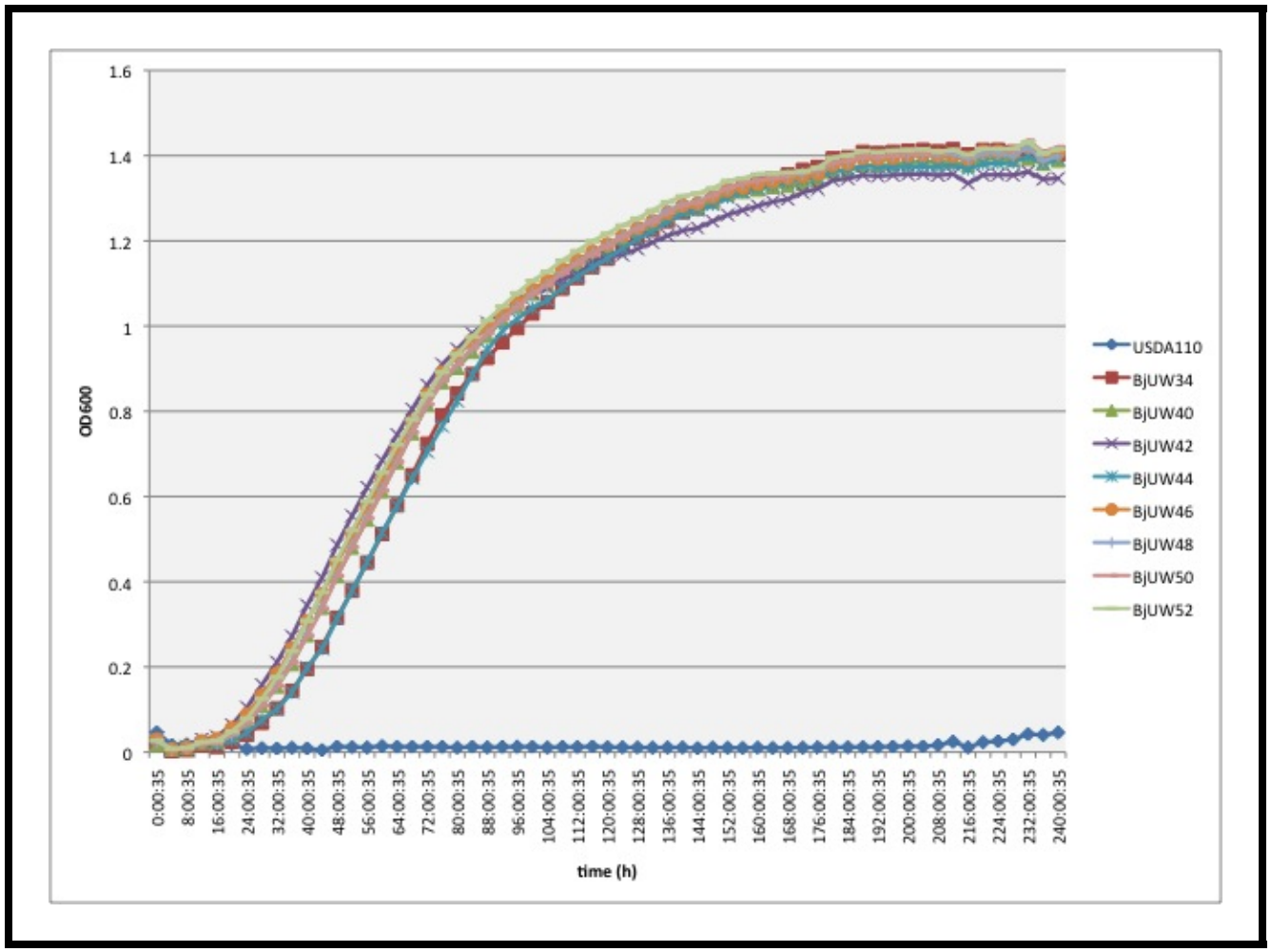

Figure 5.16: Growth curves of *B. japonicum dctA* mutants in AG medium supplemented with 25 μg/ml kanamycin

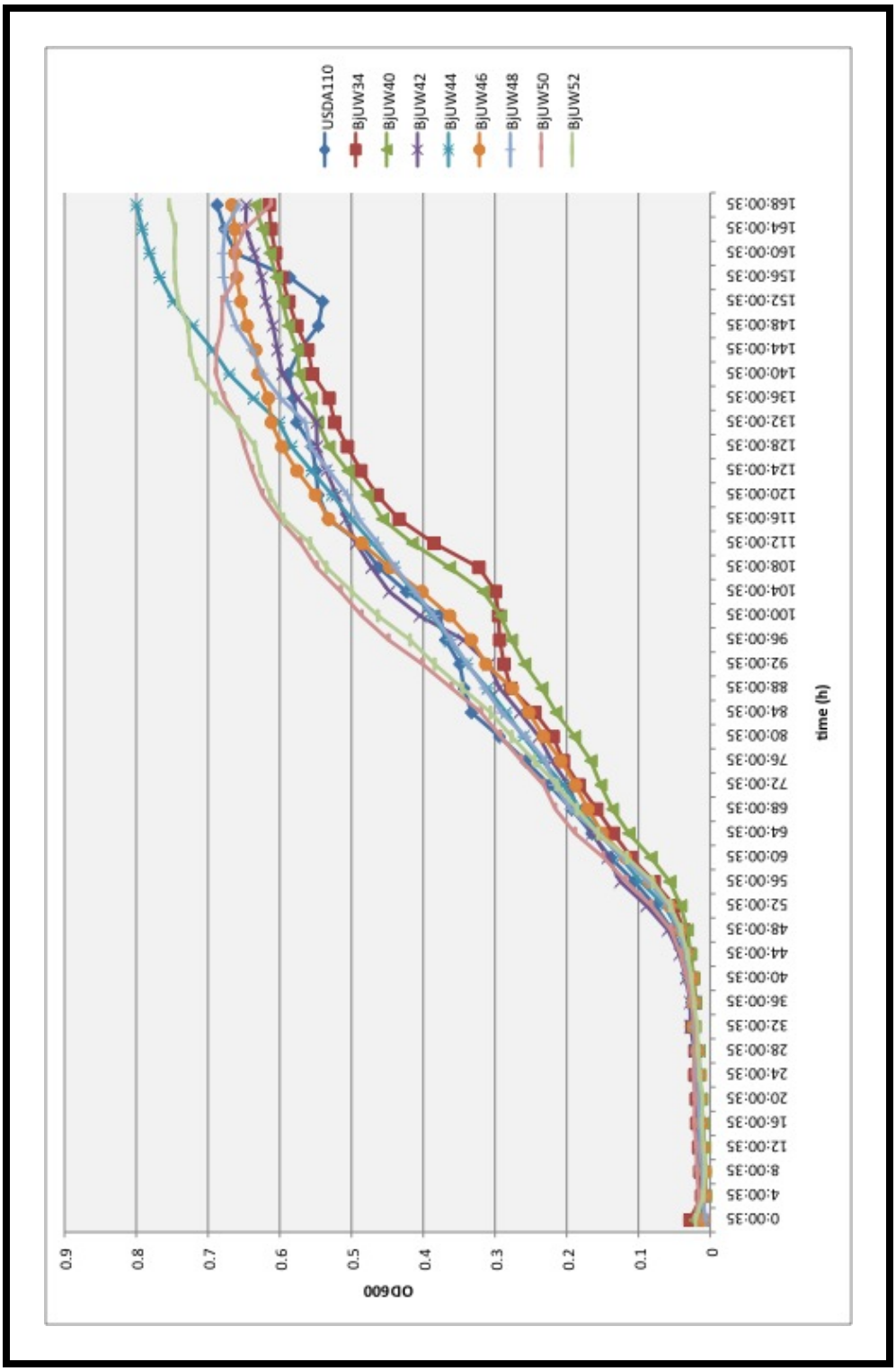

Figure 5.17: Growth curves of *B. japonicum dctA* mutants in VMM Arabinose medium

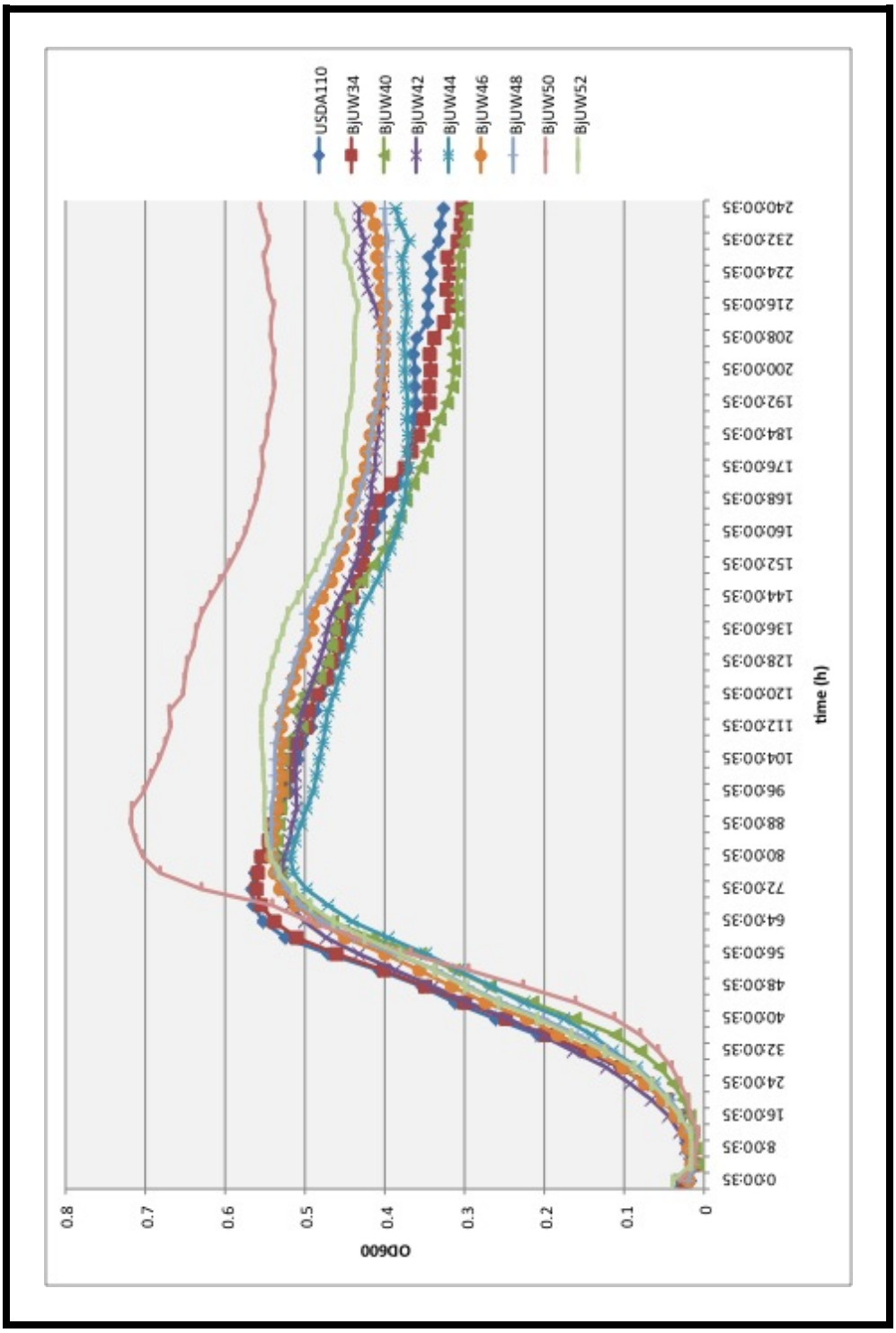

Figure 5.18: Growth curves of *B. japonicum dctA* mutants in VMM Succinate medium

5.2.5.2 Analysis of the Symbiotic Phenotype of *dctA* Mutant BjUW34

The symbiotic phenotype of BjUW34 was tested, as described in Section 2.3 by inoculating soybean plants with a culture of BjUW34 and comparing the shoot dry mass (SDM) of the resultant plants with those inoculated with wild type *B. japonicum* USDA110. The data are shown in Figure 5.19. These data show that there is no significant difference in the shoot dry masses of plants inoculated with wild-type *B. japonicum* relative to those inoculated with the mutant strain.

5.2.6 Construction of *dctBD* Mutants of *B. japonicum*

In order to construct a deletion mutant of Blr3730 and Blr3731, the complete operon was amplified by PCR and cloned into pGEMTEasy (Promega, Fischer Scientific Ltd., Nepean ON). The resultant plasmid was named pMA170 and the insert was confirmed by sequencing. The central portion of the *dctBD* operon was excised from the insert in pMA170 by digestion with SgrAI; the two external portions were religated together and the loss of the internal region was confirmed by restriction analysis. The resultant plasmid was named pMA172. In order to generate a mutant with a selectable marker, an ΩSmSp cassette was subcloned out of pTC265 as a SmaI fragment and ligated into the EcoRV site within the truncated *dctBD* construct. The resultant construct was confirmed by sequencing and was named pMA174. The insert from pMA174 was then subcloned into pK19*mobsacB* to generate pTH175.

pTH175 was transferred into *B. japonicum* USDA110 by triparental conjugation and single recombinants were selected on AG Am_{50} Tc_{10}. Recombinants were streak purified three times on AG Am_{50} Tc_{10} and the resultant strain was screened for sucrose sensitivity. The resultant clone was named BjUW37.

In order to generate a *dctBD* mutant, it would be necessary to grow up BjUW37

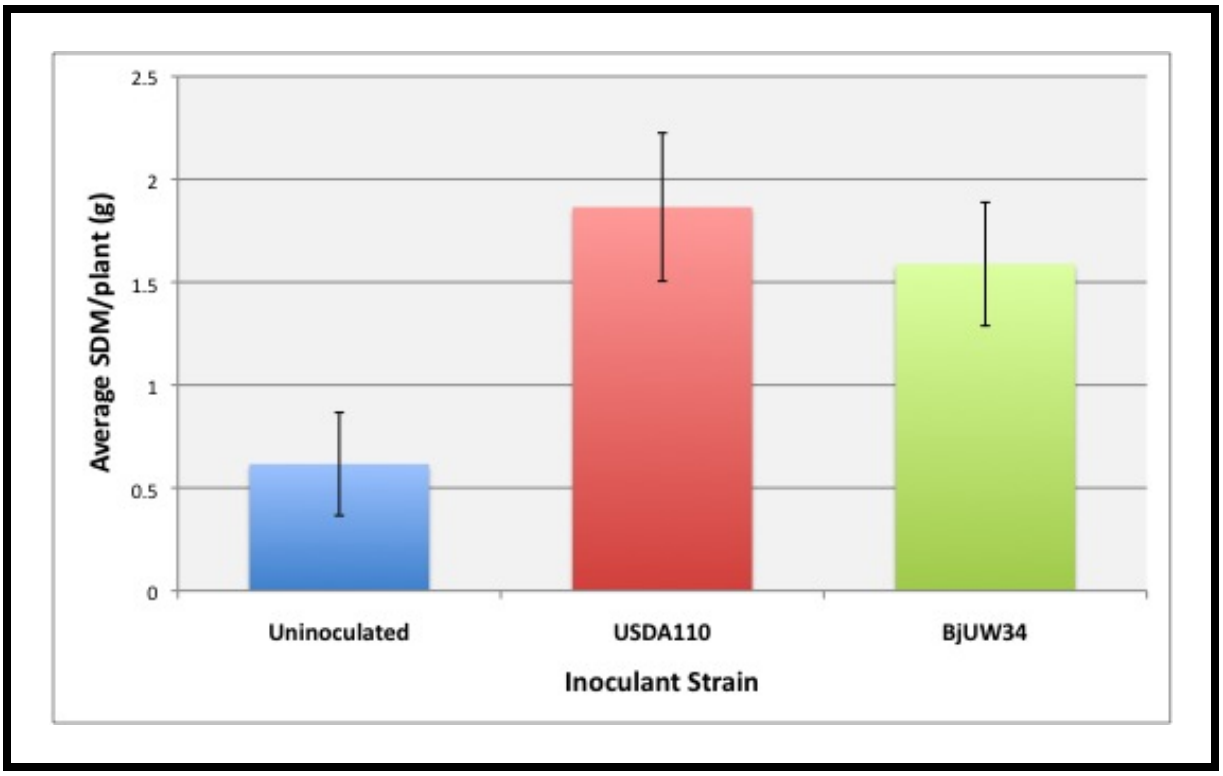

Figure 5.19: Average shoot dry masses of soybean plants inoculated with wild-type *B, japonicum* and the *dctA* mutant BjUW34

in the absence of selection, and then plate on AG sucrose Sm_{100} to select for double recombinants that have retained the mutant version of the *dctBD* operon. Despite several attempts to do this however, we have been unsuccessful in isolating double recombinants. It is unclear at this point why this region is recalcitrant to mutagenesis although, as shown in Figure 5.6, this region of the genome is extremely dense in metabolically relevant genes; it is conceivable that double recombinants are not viable due to polar effects on downstream genes, which include a putative tRNA-dihydrouridine synthase ORF.

5.3 Conclusions

The high degree of conservation among the *dctA* homologues of *B. japonicum* is intriguing and suggests that they may also be functional, perhaps under different physiological conditions. Interestingly, *B. japonicum* also possesses 2 copies of *rpoN* [197] which, in other rhizobia, is required for *dctA* expression under free-living conditions. It is conceivable that different homologues of *dctA* may be controlled by different homologues of RpoN. Furthermore, in *S. meliloti* expression of *dctA* becomes independent of *dctBD* during symbiosis. It is tempting to speculate that in *B. japonicum* other homologues of *dctA* may be activated under these conditions.

The data presented here support the hypothesis that *B. japonicum dctA* genes permit a level of redundancy that allows loss of gene function without impairing free-living growth. It would be interesting to measure the symbiotic capacity of the other six *B. japonicum dctA* mutants, given the observation that BjUW34 does not appear to be impaired in symbiotic capacity.

The data suggest that, in order to complement *S. meliloti, dctA* activation from the native *B. japonicum* promoter requires the presence of an active *B. japonicum* DctB/DctD. Interestingly however, when expressed from an *S. meliloti*-inducible

promoter, all seven ORFs have some capacity to transport sufficient succinate to support growth, and Blr4298, Blr3723 and Bll1718 are all capable of supporting near wild-type levels of growth.

The widely known, and potentially physiologically relevant, substrates for the rhizobial Dct system include succinate, malate, fumarate, aspartate and oxaloacetate (reviewed in [396]). Interestingly, our data suggest that *B. japonicum* USDA110 cannot grow on malate or fumarate as a sole carbon source (Figure 5.2). Interestingly, previous studies have shown that bacteroids of *B. japonicum* appear to possess a transporter system that is capable of transporting both succinate and malate [360]. Based on the data presented here, it appears likely that the malate-specific dicarboxylate transporters are only expressed under symbiotic conditions. It would therefore be interesting to determine whether any of the *B. japonicum dctA* ORFs are capable of supporting growth of *S. meliloti* on malate or fumarate. Whether this phenomenon is due to an inability to trasport the substrate by the DctA protein itself, or an inability to induce DctB/DctD is unclear, but testing the ability of the individual *dctA* homologues to complement growth on malate and fumarate in *S. meliloti* will help to answer this question.

Further work is needed to determine why *dctBD* has, thus far, been recalcitrant to mutagenesis. It is conceivable that allelic replacement of *dctBD* causes polar effects on downstream genes. It is also possible that DctB/DctD may be involved in the regulation of other genes that are essential to growth under free-living conditions.

Chapter 6

Identification and characterization of the intracellular poly-3-hydroxybutyrate depolymerase enzyme PhaZ of *Sinorhizobium meliloti*

6.1 PhaZ in *Sinorhizobium meliloti*

S. meliloti forms indeterminate nodules on the roots of its host plant alfalfa (*Medicago sativa*). These nodules are characterized by the existence of a persistent apical meristem and an elongated morphology. Within the nodule, the bacteroids persist and progress through defined zones of bacteroid differentiation [149]. Indeed, loss of PHB granules from the cytoplasm of the bacteria invading indeterminate nodules is a well-documented phenomenon that occurs at a specific point within bac-

teroid development [148]. Bacteroids of indeterminate nodules undergo such large physiological and metabolic changes relative to those of determinate nodules [239] that, until recently, it was unclear whether mature bacteroids within indeterminate nodules retained the capacity to synthesize and store PHB. A recent study [213] clearly demonstrated that bacteroids of *R. leguminosarum* bv. *viciae*, which forms indeterminate nodules on pea plants, retain the capacity to synthesize and store large quantities of PHB but only when carbon supply is in excess and bacteroid metabolism is limited by the availability of a key nutrient (reviewed in [351]).

During saprophytic growth, PHB accumulation occurs during periods of nutrient deprivation when carbon is in excess. This strategy is employed by many species of bacteria. The first step in PHB degradation is catalyzed by a substrate-specific depolymerase. PHB undergoes a transition from an amorphous granule in the intracellular state to a denatured semi-crystalline form upon release into the environment. As a result, different PHB depolymerases are employed depending on the nature of the substrate. While extracellular depolymerases have been identified and characterized in a wide variety of bacteria, very little is yet known about their intracellular counterparts. To date, only a handful of intracellular PHB depolymerases have been reported in the literature, most of which appear to lack the typical lipase box motif (Gly-X-Ser-X-Gly) associated with extracellular PHB depolymerases [1, 106, 174, 189, 301, 356]. While the enzymes responsible for the synthesis and storage of PHB have been characterized in a wide variety of bacteria, including the rhizobia (reviewed in [351]), only a few studies have investigated the role of intracellular PHB depolymerases and, to date, no studies have reported the characterization of a rhizobial PHB depolymerase.

PhaZ was identified as the putative intracellular PHB depolymerase in *S. meliloti* based on *in silico* analyses of the genome sequence and comparisons to other intracellular PHA depolymerase sequences. Here we report the cloning and characteriza-

tion of PhaZ from *S. meliloti*. This work is the first report of a PHB depolymerase mutant in *S. meliloti* and, indeed, in the *Rhizobiaceae*. This work also represents the final step in genetic characterization of the complete PHB cycle in these bacteria, since all other enzymes of both the synthetic and degradative pathways have been studied previously in *S. meliloti* [7, 9, 8, 40, 46, 52, 275, 349, 378, 379, 390]. To the best of our knowledge, this work also documents the first confirmed example of the presence of intracellular PHB granules in N_2-fixing bacteroids of *S. meliloti*.

6.2 Results and Discussion

6.2.1 Identification of the *S. meliloti phaZ* Open Reading Frame and Construction of an *S. meliloti phaZ* mutant

All plasmids and strains constructed in this study are described in Table 2.1. The *phaZ* gene was identified as a 1272 bp open reading frame SMc02770 in the *S. meliloti* genome sequence [104] by comparison to *phaZ* of *W. eutropha* [302]. The amino acid sequences of these two proteins share 51% identity. Interestingly, like *phaZ* of *W. eutropha*, the PhaZ protein of *S. meliloti* does not possess a Gly-X-Ser-X-Gly lipase box motif [162] that is characteristic of many extracellular PHB depolymerases. The absence of this motif implies that these intracellular PhaZ homologues may use a different active site structure than extracellular PHB depolymerases. Primers were designed to internal regions of *phaZ* to amplify a fragment (from S35 to F292) by PCR, and the resultant 835 bp fragment was cloned into pGEM®-T Easy (Promega) to generate pAZ101. An internal disruption of the cloned *phaZ* fragment was generated by introducing a ΩSmSp cassette as a Cfr91 fragment into the unique KpnI site at 299 bp to yield pAZ102. The *phaZ*::ΩSmSp

was subsequently excised as an EcoRI fragment and subcloned into pK19*mobsacB* to give pAZ103. pAZ103 was introduced into *S. meliloti* Rm5000 by triparental mating using *E. coli* MT616 as a helper strain. Single recombinants were identified by selecting for Rf^R, Sm^R, Sp^R transconjugants. Putative double recombinants were identified by plating onto TY Sm Sp Sucrose (5%). Subsequent screening for loss of vector-encoded Nm^R confirmed the loss of pK19*mobsacB*. The resultant Rf^R, Sm^R, Sp^R, Nm^S *phaZ* mutant was designated Rm11417. The mutagenesis was confirmed by Southern blot using the *phaZ* PCR product as a probe. The probe hybridized to a 1.55 kb EcoRI fragment of genomic DNA in the wild-type strain Rm5000, and to a 3.55 kb fragment in Rm11417, confirming the presence of the 2 kb ΩSmSp cassette (data not shown). This mutation was transduced into Rm1021 using the ϕM12 phage by standard techniques [95] and the resultant mutant was designated Rm11430.

6.2.2 Cloning of *phaZ* Gene for Complementation Assays

Primers Smc02770F and Smc02770R (Table 2.2) were designed to the 5' and 3' regions of SMc02770, incorporating HindIII sites into the 5' and 3' ends as well as a 3' terminal His tag. The PCR product was cloned as a HindIII fragment into pRK7813 and the resultant construct was named pMA157. This construct was introduced into Rm11430 by triparental conjugation using *E. coli* MT616 as the mobilizer strain.

6.2.3 Analysis of the Carbon-Utilization Phenotype of the *S. meliloti phaZ* Mutant

The growth of Rm11430 was compared to that of Rm1021, Rm11105 [46], Rm11107 [46] and Rm11347 [7] on TY, YMA, and minimal media containing 15 mM acetate

(A), acetoacetate (AA) or D-3-hydroxybutyrate (HB) as sole carbon sources. As seen in Table 6.1, no difference in growth phenotype was observed between Rm11430 and Rm1021.

6.2.4 Analysis of the Carbon-Starvation *S. meliloti phaZ* Mutant to Tolerate Long-Term Carbon Starvation

The ability of the *phaZ* mutant strain to withstand long-term carbon starvation was tested, relative to both Rm1021 and Rm11105, by incubation for 4 weeks in M9 liquid medium with no added carbon source. Cells were grown to late-log in YMB and washed twice in M9. A 1:50 dilution was used to inoculate 75 ml of M9 salts. Starting cfu/ml was determined immediately following inoculation by serial dilution of a 1 ml aliquot. Starting cultures typically contained approximately 2 x 10^5 cfu/ml. These starting values were each given a relative value of 1. 1 ml samples were removed at 7 day intervals and serial dilutions were used to determine cfu/ml. Values presented are the averages of 3 independent cultures. The data in Figure 6.1 show that the ability to synthesize and/or break down PHB has a significant impact on long-term survival in the absence of an exogenous carbon source. The wild-type strain Rm1021 is capable of increasing cell density during the early stages of starvation, presumably by degrading readily mobilizable intracellular carbon stores, a pattern which is not seen in either the *phaZ* or *phbC* mutants.

6.2.5 PHB Synthesis in *phaZ* mutants of *S. meliloti*

To assess the effect of the *phaZ* lesion on PHB content in Rm11430, total PHB accumulation by stationary-phase cells was measured and compared to the wild-type strain Rm1021. Cells were grown to stationary phase in either TY or YMB and the accumulated PHB was measured as a total cellular dry weight (% w/w

Table 6.1: Growth phenotypes of *S. meliloti* PHB cycle mutants

2*Strain	Relevant Characteristics	YMA Phenotype	Carbon Source Utilization			
			Glucose	D-3-HB	Acetate	AA
Rm1021	wild-type	Mucoid	+	+	+	+
Rm11105	*phbC*::Tn*5*	Dry	+	-	+	-
Rm11107	*bdhA*::Tn*5*	Mucoid	+	-	+	+
Rm11347	*phbB*Ω	Dry	+	-	+	-
Rm11430	*phaZ*ΩSmSp	Mucoid	+	+	+	+

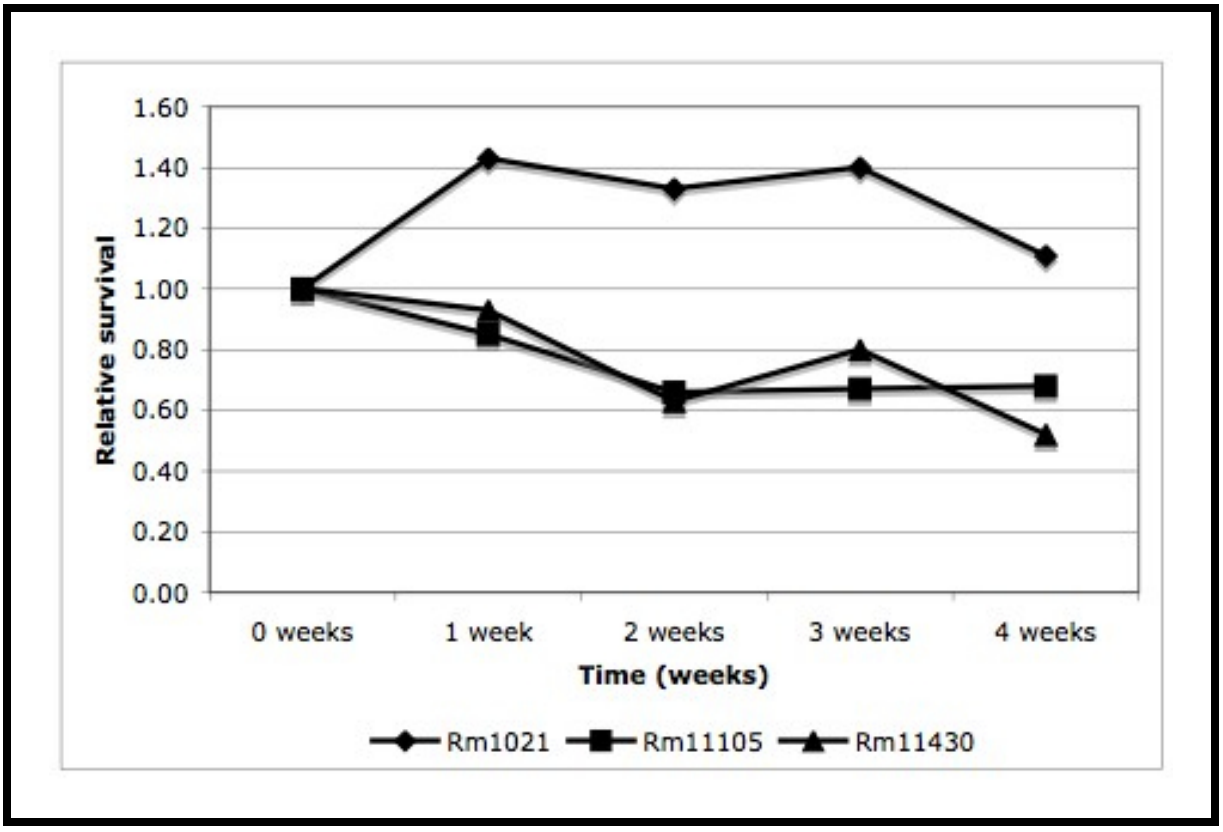

Figure 6.1: Viable cell counts of *S. meliloti* PHB mutants following incubation in minimal media with no exogenous carbon source added

±SD). These data are shown in Table 6.2. Under both conditions tested, Rm11430 demonstrates significantly increased PHB accumulation relative to Rm1021 suggesting that, while synthesis of PHB is not impaired, the lesion in *phaZ* inhibits degradation of PHB. The PHB accumulation phenotype of Rm11430 is complemented by pMA157, demonstrating a clear relationship between the presence of PhaZ and PHB accumulation.

6.2.6 Regulation of Succinoglycan Biosynthesis

The product of the *exoF* gene is involved in the transfer of the first sugar, galactose, to the lipid carrier, upon which the subunits of succinoglycan are assembled [290]. pD82*exoF*::Tn*phoA* was constructed by homologous recombination between *exoF* carried on pD82 [207] and the chromosomal *exoF*::Tn*phoA* fusion of strain Rm8369 [214]. The resultant plasmid was used to measure the transcriptional activity of *exoF* in different *S. meliloti* PHB mutant backgrounds when grown under different culture conditions. A Student's t-test was used to analyse the data and determine statistical significance of the observed differences. The results presented in Table 6.3 represent the mean of three independent samples and show that Rm11430 demonstrates a statistically significant increase in *exoF* transcription when grown in YM media, while synthetic mutants Rm11105 and Rm11347 exhibit a reduction in *exoF* expression. This is consistent with the observation that colonies formed by Rm11430 appear larger and more mucoid on YM agar than Rm1021.

6.2.7 PHB Accumulation During Symbiosis

Unlike bacteroids of determinate nodules, bacteroids of *S. meliloti* do not accumulate PHB during symbiosis (reviewed in [351]). Interestingly, a mutant of *R. leguminosarum*, unable to cycle amino acids between the bacteroid and plants,

Table 6.2: PHB accumulation during free-living growth

Strain	Relevant Characteristics	PHB Accumulation % cell dry mass
Rm1021	wild-type	18.94
Rm11105	*phbC*::Tn*5*	0.24
Rm11430	*phaZ*ΩSmSp	28.55
Rm11430 pMA157	*phaZ*ΩSmSp pRK7813 *phaZ*	7.39

Table 6.3: *exoF::phoA* Alkaline phosphatase assay

Strain	Relevant Characteristics	Activity (U)	Std Error
Rm1021	wild-type	14.115	0.331
Rm11105	*phbC*::Tn*5*	9.681[a]	0.264
Rm11347	*phbB*Ω	6.226[a]	0.223
Rm11107	*bdhA*::Tn*5*	16.134	0.714
Rm11430	*phaZ*ΩSmSp	15.663[a]	0.296

[a] These differences are statistically significant from the value recorded for Rm1021, when analysed using a two-tailed Student's t-test

showed apparent accumulation of PHB in the bacteroid [213]. This suggests that the pathway for PHB metabolism can function within bacteroids of indeterminate nodules, however accumulation of PHB only occurs under extreme circumstances for example, when carbon is in excess and bacteroid metabolism is limited by the availability of a key nutrient. To confirm that *S. meliloti* bacteroids are capable of PHB synthesis and accumulation, alfalfa nodules induced by Rm11430 were prepared, sectioned and analysed by TEM. Figure 6.2B clearly shows that bacteroids of Rm11430 accumulate PHB during symbiosis, with numerous, electron-transparent, PHB granules visible within the cytoplasm of the bacteroids when viewed by TEM. This is in contrast to bacteroids of Rm1021, shown in Figure 6.2A, which demonstrate a notable absence of PHB.

Figure 6.3 shows that, in symbiosis with the host plant alfalfa, there is no significant difference in shoot dry mass of plants inoculated with the *phaZ* mutant Rm11430 and the wild-type strain Rm1021. Plants inoculated with Rm11430 had an average shoot dry mass (SDM) of 10.51 mg compared to 11.06 mg for plants inoculated with Rm1021, both of which were significantly different to the uninoculated controls, which had an average SDM of 4.13 mg. This is interesting since it suggests that PHB accumulation, as confirmed in Figure 6.2 does not occur at the expense of the *S. meliloti-M.sativa* symbiosis.

6.2.8 Analysis of Nodulation Competitiveness

The ability of *S. meliloti* Rm11430 to compete for nodule occupancy was assayed by co-inoculating alfalfa plants with different strain combinations. Table 6.4 shows that, when co-inoculated in approximately equal ratios with the wild-type strain, Rm11430 demonstrated no discernable difference in competitiveness relative to Rm1021. The percentage of Rm11430 in the original inoculum was similar to

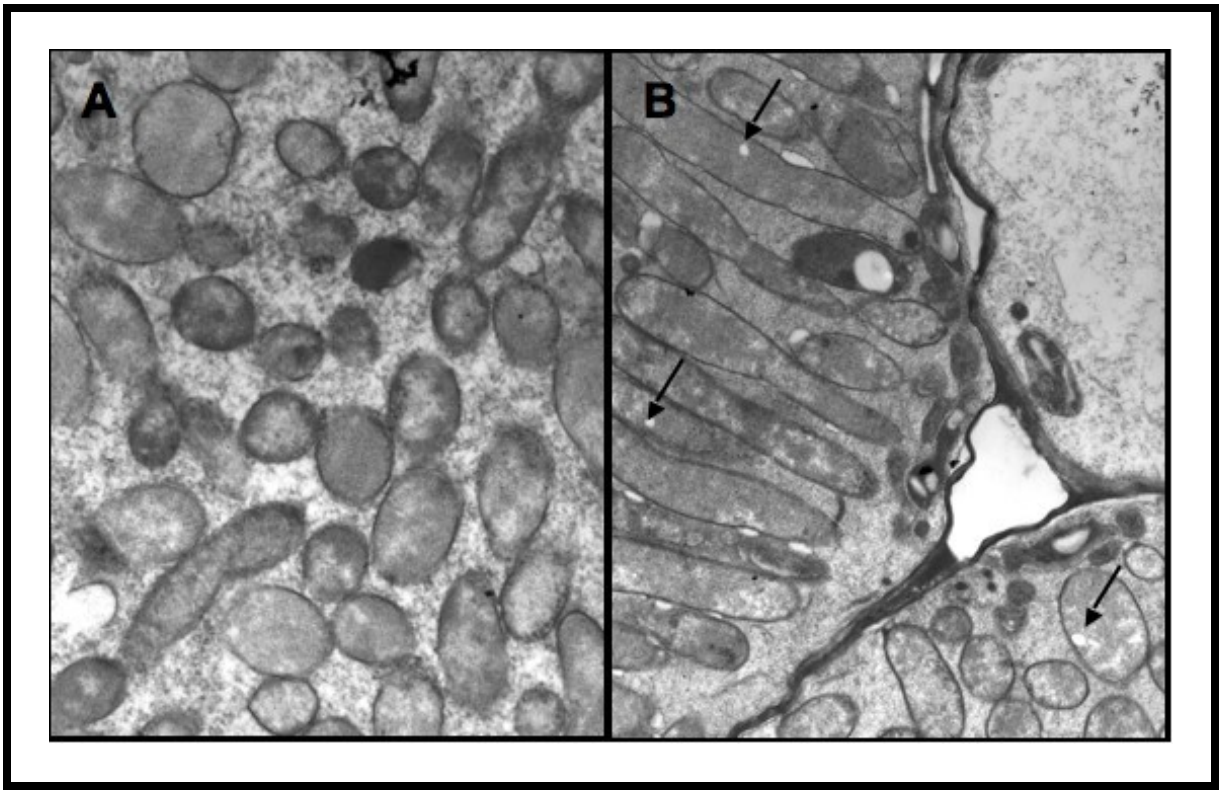

Figure 6.2: Bacteroids of Rm1021 (A) and Rm11430 (B). Electron-transparent PHB granules are clearly visible in bacteroids of Rm11430

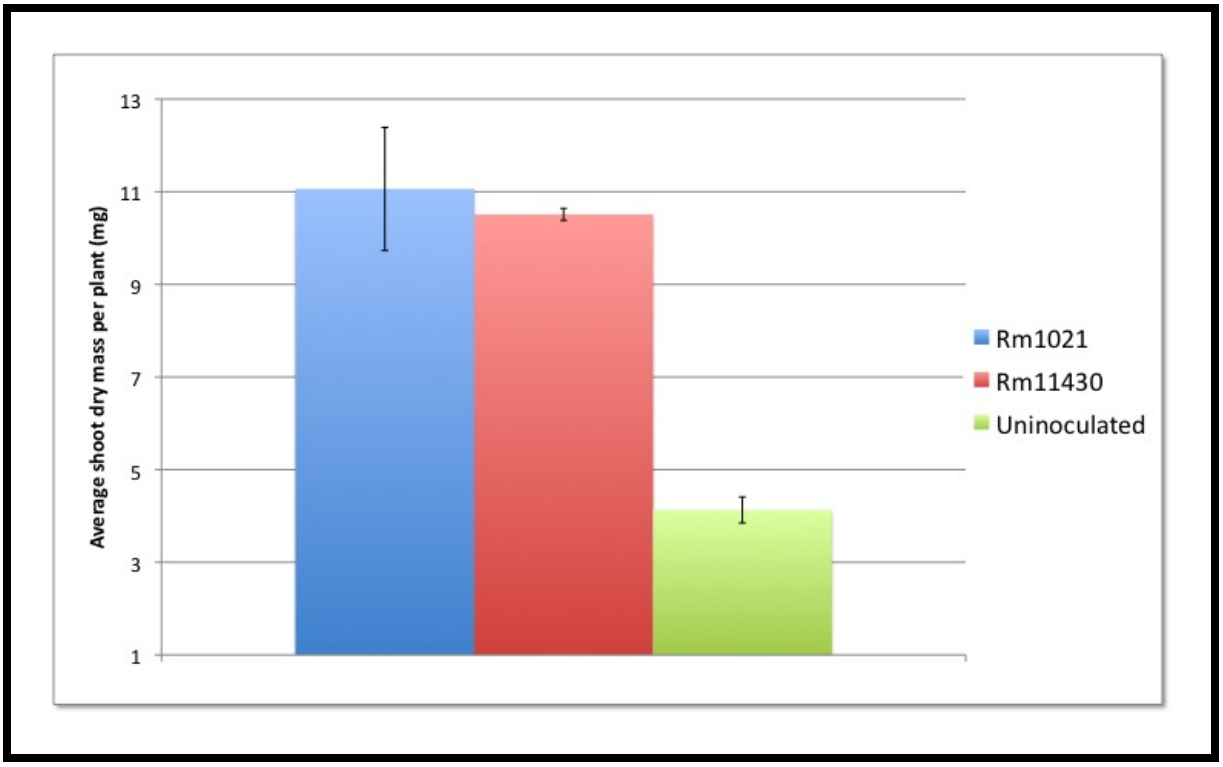

Figure 6.3: Shoot Dry Masses of Alfalfa Plants Inoculated with either Rm1021 or Rm11430

the percentage of nodules that it occupied. In agreement with previous studies [9], both Rm11105 (*phbC*) and Rm11107 (*bdhA*) demonstrated significantly reduced competitiveness relative to wild-type. Table 6.4 also shows that both Rm11105 and Rm11107 also demonstrate reduced competitiveness relative to Rm11430, with the *phbC* phenotype being more pronounced than the *bdhA* phenotype.

6.2.9 Analysis of PhaZ Activity *in vitro*

6.2.9.1 Purification of PhaZ Under Native Conditions

In order to fully characterize the activity of the *S. meliloti* PhaZ enzyme, the *phaZ* ORF was cloned into pET30b (EMD Biosciences, San Diego, CA) to generate pMA158 (Table 2.1). pMA158 was transformed into $CaCl_2$-competent *E. coli* BL21 (λDE3) pLysS [64, 334]; transformants were selected on LB Cm_{25} Km_{25}. Over-expression of *phaZ* was achieved by growth of the transformants in autoinduction (AI) medium (Section A.1) supplemented with Km_{100} and Cm_{25}, as described in Section A.1.2. Over expression was confirmed by SDS-PAGE analysis and a representative gel is shown in Figure 6.4. An uninduced sample was prepared by growth of the cells in AI medium lacking lactose.

PhaZ was purified under native conditions using an Ni-NTA resin (EMD Biosciences, San Diego, CA) as described in Section 2.6.3. Samples were eluted in 250 mM, 400 mM and 1 M imidazole elution buffer and the best concentration was determined to be 400 mM following analysis of the eluate on a 12.5% SDS-PAGE gel. A representative gel is shown in Figure 6.5.

6.2.9.2 Purification of Native PHB Granules

In order to assay PhaZ activity, it will be necessary to isolate native PHB granules using conditions that would maintain their intracellular form. Samples were

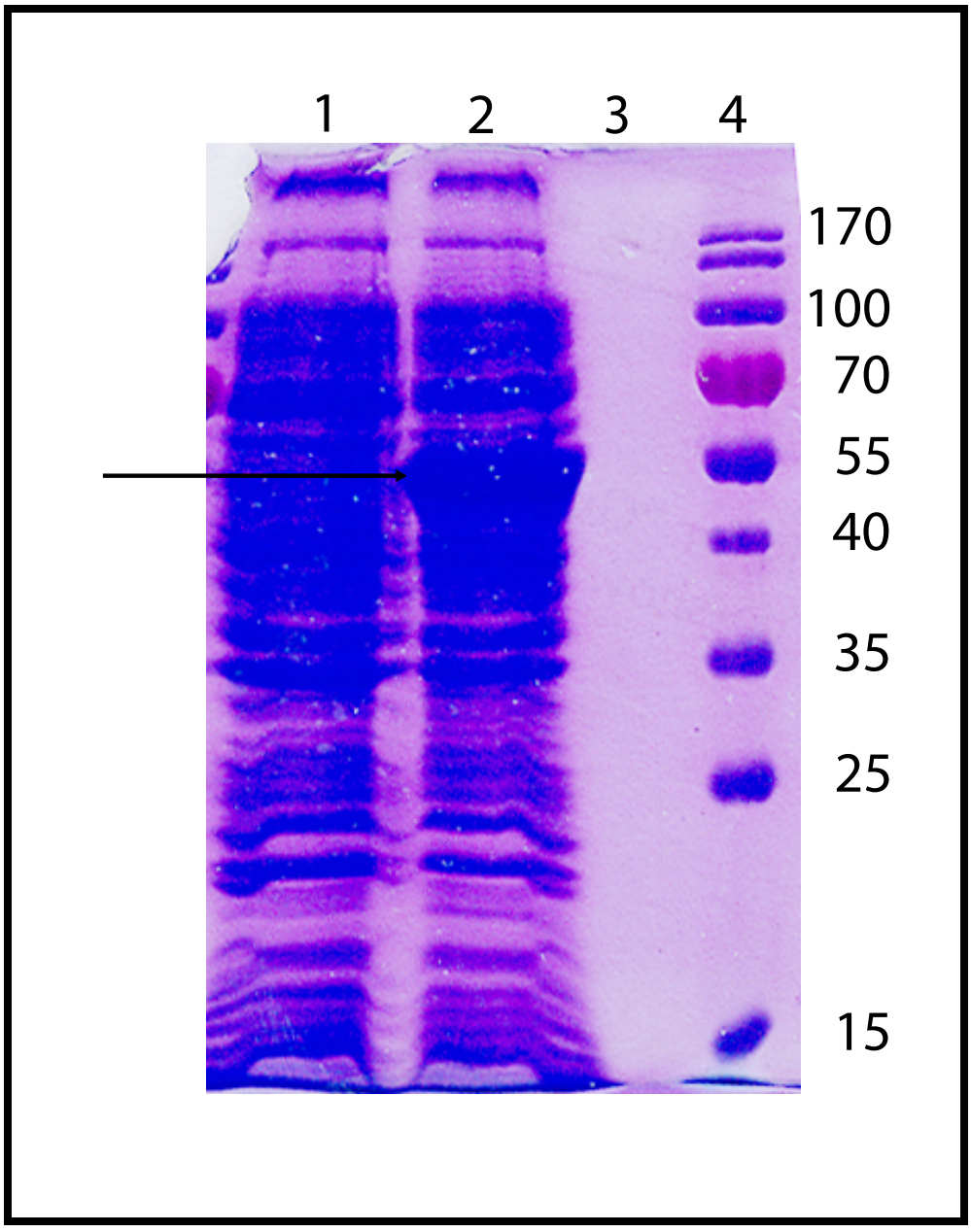

Figure 6.4: Overexpression of *S. meliloti phaZ* from pMA158 in *E. coli* BL21 (λDE3) pLysS. Lane 1: uninduced sample; Lane 2: induced sample; Lane 3: empty; Lane 4: MW standard. The sizes of the molecular weight markers, in kDa, are indicated

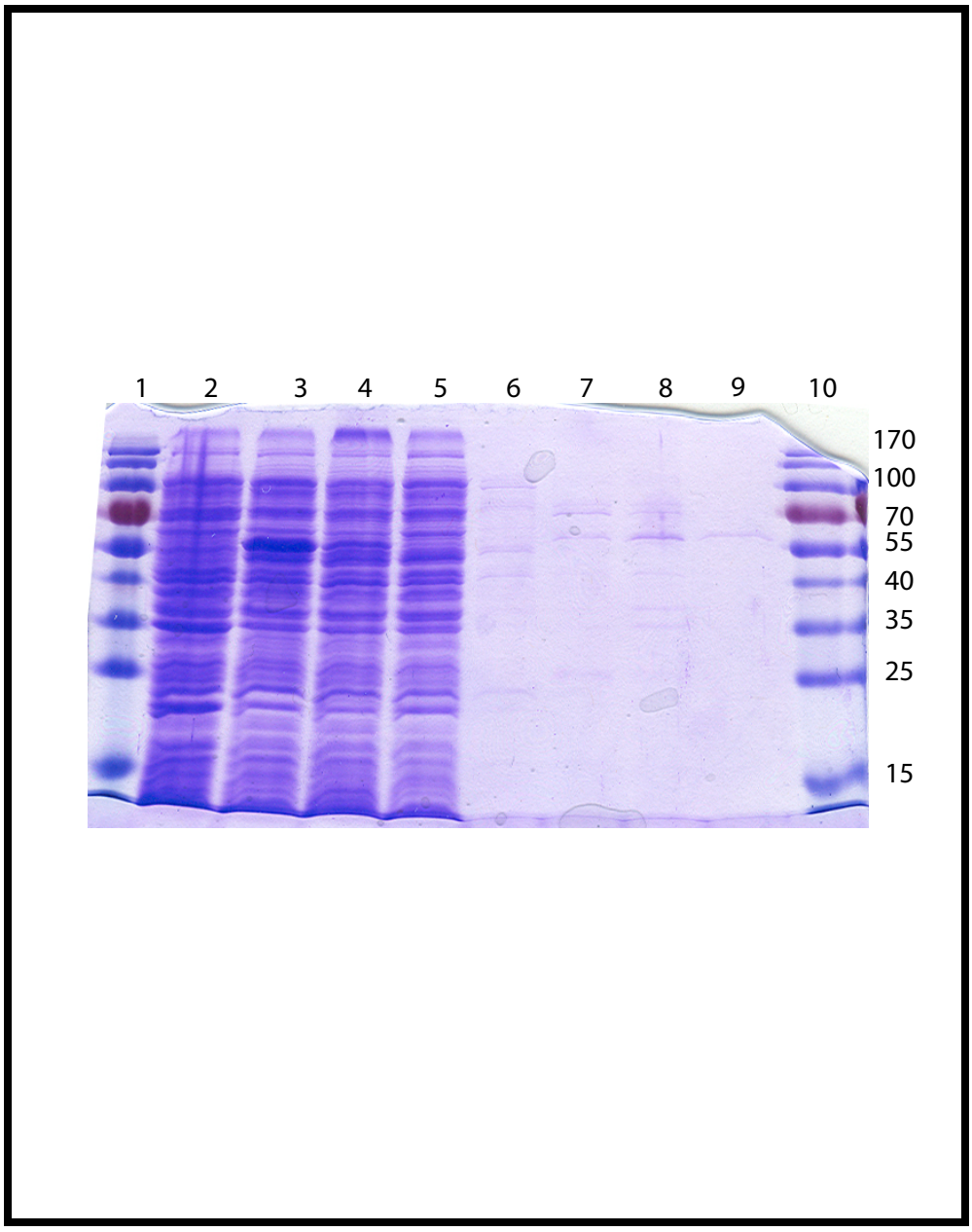

Figure 6.5: SDS-PAGE gel of *S. meliloti phaZ* fractions during purification under non-denaturing conditions. Lane 1: MW marker; Lane 2: uninduced sample; Lane 3: induced sample; Lane 4: crude cell extract; Lane 5: flow-through; Lane 6: wash eluate; Lane 7: eluate 250 mM imidazole; Lane 7: eluate 400 mM imidazole; Lane 7: eluate 1 M imidazole. The sizes of the molecular weight markers, in kDa, are indicated

prepared as described in Section 2.7.2.3 and PHB was separated out using a discontinuous sucrose gradient. The resultant fractionation can be seen in Figure 6.6. The PHB granules can be removed from the gradient and stored at 4°C until needed.

6.3 Conclusions

Previous studies have demonstrated that the ability of certain bacteria to synthesize, accumulate and metabolize intracellular PHB stores is important in enhancing their capacity to survive unfavourable growth conditions [173, 216, 298, 339]. Rhizobia in the soil environment must contend with varying nutrient conditions, from the carbon-deficient bulk soil, to the carbon-rich rhizosphere [365]. The ability to accumulate and utilize carbon stores would be highly advantageous, allowing rhizobia to cope with fluctuating carbon conditions, and thus, make them more competitive against other bacterial populations [65]. Previous studies have shown that mutant strains of *S. meliloti*, unable to synthesize (*phbC*) or degrade (*bdhA*) PHB, show a significant reduction in competitiveness for nodule occupancy [9, 390], with mutants that are unable to synthesize PHB exhibiting a much greater loss in competitiveness than those unable to degrade PHB [9].

This is the first study in which the competitiveness of an *S. meliloti phaZ* mutant has been investigated. It was expected, based upon the phenotype of the *bdhA* mutant [9], that the *phaZ* mutant would exhibit reduced nodulation competitiveness. Interestingly, the *phaZ* mutant was as competitive as wild-type in co-inoculation experiments, and consistently out-compteted both *phbC* and *bdhA* mutants (Table 6.4). Studies in *Azotobacter vinelandii* have demonstrated a role for PHB in protection of the cell against environmental stresses including PHB, oxidative stress and UV damage [252]. It is conceivable that the ability of the *phaZ* mutant to out-compete the *phbC* and *bdhA* mutants is due to an enhanced ability

Figure 6.6: Fractionation of crude cell extract over a discontinuous sucrose gradient for isolation of PHB granules. Granules were isolated from *S. meliloti* Rm11430 cells grown to saturation in Yeast Mannitol broth

to tolerate the conditions encountered in the soil and rhizosphere as a result of the increased cytoplasmic PHB concentration.

Interestingly, the *phaZ* mutant exhibits a similar reduction in long-term survival during starvation to the *phbC* mutant (Figure 6.1). This suggests that the inability to degrade PHB is just as detrimental to the cells as the inability to accumulate it. This also confirms that PHB degradation does play a significant role in fueling cellular metabolism under adverse conditions, and that glycogen synthesis and degradation is not able to replace the function of PHB metabolism under these conditions.

Previous studies have shown that *S. meliloti* mutants defective in PHB synthesis also exhibit a significant reduction in succinoglycan production under conditions favouring both succinoglycan and PHB production [275], suggesting that these pathways share common regulatory circuitry. *S. meliloti phbB* and *phbC* mutants exhibit non-mucoid colony morphology on carbon-rich media, while *bdhA* mutants show a mucoid colony morphology. This study further augments these observations by showing that a *phaZ* mutant is not only mucoid, but has up-regulated exopolysaccharide production relative to the wild-type strain.

The role of EPS in the establishment of nitrogen-fixing symbioses between *S. meliloti* and *M. sativa* has long been acknowledged [120], but the precise mechanism of interaction remains elusive. Mutants unable to synthesize EPS are characteristically Fix$^-$. The observation that *phbC* and *phbB* mutants of *S. meliloti* are still able to establish successful symbioses [7] suggests that synthesis of succinoglycan in these mutants, albeit at a reduced level, is still sufficient to facilitate nodulation. This is consistent with previous reports which suggest that the production of small amounts of low-molecular-weight (LMW) EPS is sufficient to establish a successful symbiosis [120]. Indeed, it is conceivable that the competition defect observed in *phbC* mutants of *S. meliloti* may be due to extremely low levels of succinoglycan

production. Rm11105 may produce sufficient succinoglycan to establish an effective symbiosis but, assuming that the succinoglycan itself is playing a role in signalling during early nodulation, not enough to allow it to compete with strains producing higher levels of the EPS. Interestingly, the *phaZ* mutant demonstrates wild-type competitiveness and is able to out-compete both the *phbC* and *bdhA* mutants for nodulation. This indicates that EPS production is not the sole determinant in the competition phenotype of other PHB cycle mutants. It is conceivable that another metabolic pathway that is dependent on D-3-HB metabolism may play a role in nodulation competitiveness. It is noteworthy that, although it has higher succinoglycan production than Rm1021, the *phaZ* mutant was not more competitive than the wild-type strain. This implies that there is a critical level of succinoglycan, above which, further gains in competitiveness are not seen.

It is conceivable that, when PHB synthesis is inhibited, intermediates required for succinoglycan are not synthesized efficiently. It is also possible that, in the absence of a functional PHB synthesis pathway, enzymes required for succinoglycan may be inhibited or down-regulated. Furthermore, it has been suggested that acetyl phosphate may provide a regulatory link between PHB and succinoglycan synthesis [245]. Studies in the thermophyllic *Synechococcus* sp. strain MA19, have shown that acetyl phosphate is involved in the post-translational regulation of PHB synthase *in vitro*, and that this regulation is concentration-dependent [245]. As well, this study revealed that the enzyme phosphotransacetylase, which converts acetyl-CoA to acetyl phosphate, is only active under PHB-accumulating conditions. In *E. coli*, acetyl phosphate is known to function as a global signal that acts through two-component regulatory signals [230], perhaps via direct phosphorylation of the response regulator [187] itself. Furthermore, the ChvI protein, of the *S. meliloti* ExoS-ChvI two-component regulatory system, is able to autophosphorylate in the presence of acetyl phosphate *in vitro* [365]. Since PHB synthesis mutants may

excrete excess acetyl-CoA, levels of acetyl phosphate will likely be low under these conditions. Therefore, intracellular levels of acetyl phosphate may be an important factor in the ExoS-ChvI-dependent regulation of succinoglycan synthesis.

Bacteroids of determinate nodules, in contrast to those found in indeterminate nodules, can accumulate up to 50% of their cellular dry mass as PHB (reviewed in [351]). The synthesis of PHB during symbiosis however, presumably occurs at the expense of symbiotic nitrogen fixation; a theory that is corroborated by the observation that a *phaC* mutant of *R. etli* demonstrates higher levels of nitrogenase activity relative to wild-type [43]. Bacteroids of indeterminate nodules do not accumulate PHB during symbiosis. It has been suggested [43] that this may be the reason why the *S. meliloti*-alfalfa symbiosis is more effective than that of *B. japonicum*-soybean or *R. etli*-bean [137]. Interestingly the data presented in this study suggest that forced accumulation of PHB by *S. meliloti* during symbiosis does not appear to have a negative effect on plant yield, suggesting that PHB synthesis during symbiosis is not the only determinant of symbiotic performance.

Table 6.4: Nodulation competitiveness of the *S. meliloti* wild-type strain and *bdhA*, *phbC* and *phaZ* mutants co-inoculated in the described ratios on *M. sativa* plants

Strain (%) in inoculum	No. nodules tested	Nodule occupancy (%)		
		Strain 1	Strain 2	Both
Rm11430 (60) + Rm1021 (40)	18	61.1	22.2	16.7
Rm11430 (91) + Rm1021 (9)	15	93.3	6.7	0
Rm11430 (54) + Rm11105 (46)	16	100	0	0
Rm11105 (59) + Rm1021 (41)	15	6.7	93.3	0
Rm11105 (88) + Rm1021 (12)	20	5	75	20
Rm11430 (51) + Rm11107 (49)	20	65	35	0
Rm11107 (49) + Rm1021 (51)	14	21.4	78.6	0
Rm11107 (77) + Rm1021 (23)	15	86.7	0	13.3
Rm11107 (44) + Rm11144 (56)	19	94.7	0	5.3

Chapter 7

Mutational Analysis of the Role of β-Ketothiolase (PhbA) in *Sinorhizobium meliloti*

7.1 Introduction

In many species of bacteria, the glyoxylate shunt (Figure 1.7) represents an essential pathway for the assimilation of tricarboxylic acid (TCA) cycle intermediates during growth on C_2-compounds (reviewed in Section 1.3). Interestingly, in *S. meliloti*, only *aceA* (isocitrate lyase) is required for growth on acetate [282]; mutants of *glcB* (malate synthase) retain the capacity to grow on acetate [282], perhaps indicating an as-yet uncharacterized metabolic pathway for the assimilation of acetate in these organisms.

A recent proposal has suggested that there is present in certain bacteria, an alternate pathway for assimilation of acetate that would bypass the need for the glyoxylate cycle in organisms that do not possess the enzyme, isocitrate lyase (Figure

7.1) [91]. In these organisms, acetate is assimilated through the ethylmalonyl-CoA pathway, which has significant overlap with the anabolic half of the PHB cycle, including reliance on the PHB intermediate 3-hydroxybutyryl-CoA. A class of mutants in *Sinorhizobium meliloti*, designated *bhbA-D*, are able to grow on acetate, but not on hydroxybutyrate or acetoacetate [45]. These phenotypes, along with the previously unexplained hydroxybutyrate phenotypes of *phbB* and *phbC* mutants, suggest that an ethylmalonyl-CoA-like pathway may be present in *S. meliloti*, and that this pathway may overlap with the PHB cycle. A model for the proposed pathway interaction is depicted in Figure 7.2.

In an attempt to further quantify the roles of PhbA, PhbB and PhbC in exporting carbon from the PHB cycle, including the requirements for granule association on the activities of PhbA and PhbB, an in-frame mutant of *S. meliloti phbA* was constructed and its phenotype analysed.

7.2 Results and Discussion

7.2.1 Construction of In-Frame *phbA* Mutant

Because the α-ketothiolase PhbA represents an input/output point of the PHB cycle, but is not required for the PHB cycle itself, and because *phbA* is in an operon upstream of *phbB*, prior PHB cycle studies have not included generation of a *phbA* mutant. In order to study the effects of a *phbA* mutant without polar effects on *pbhB*, an in-frame deletion of *phbA* was generated.

In *S. meliloti, phbAB* are predicted to form a single operon [3]. In order to construct a mutant of *phbA* without disrupting the activity or regulation of *phbB*, cross-over PCR was used [154, 336]. The primers used are listed in Table 2.2. The primers were designed such that the resultant cross-over PCR product yielded a

fragment that contained the *phbB* ORF, with an intact native ribosome binding site (RBS), under the control of the native operon promoter. This construct was cloned into pGEMTEasy and subcloned into both pBBR1MCS2 [196], to yield pMA187, and pK19*mobsacB* [310], to yield pMA190. pMA187 should be capable of complementing a *phbB* mutant of *S. meliloti*, and was constructed as a means of testing the in-frame nature of the *phbA* deletion.

In order to generate a *phbA* mutant of *S. meliloti*, pMA190 was conjugally transferred into *S. meliloti* Rm1021 and single recombinants were isolated by selection on TY Sm_{200} Nm_{200}. Following three successive rounds of streak purification, the resultant recombinants were grown up without selection and plated on TY containing 5% sucrose in order to select for strains that had undergone a second recombination event. Double recombinants were screened for Nm^S in order to confirm loss of pMA190. Confirmed double recombinants were then screened by colony PCR in order to differentiate between wild-type revertants and *phbA* deletion mutants. The resultant strain was confirmed by PCR and named SmUW41.

7.2.2 PHB Synthesis by the *phbA* Mutant of *S. meliloti*

SmUW41 was screened for PHB synthesis using the Nile Red PHB screen [323] described in Section 2.2. Single colonies were smeared onto YMA supplemented with Nile Red and allowed to grow for approximately 72 hours. The resultant growth was analysed for fluorescence under UV light. The photograph shown in Figure 7.3 show that SmUW41 synthesizes no detectable PHB.

7.2.3 EPS Synthesis by the *phbA* Mutant of *S. meliloti*

Exopolysaccharide biosynthesis was quantitated by isopropanol precipitation of the soluble EPS secreted into the growth medium, as described in Section 2.7.5. Al-

though the SmUW41 strain is visibly more mucoid than Rm1021 when grown on YMA, no detectable EPS production by SmUW41 was detected in this assay (data not shown). This might suggest that an increase in mucoidy does not translate into significantly higher secretions of EPS, and that accumulation of capsular polysaccharide and biosynthesis of exopolysaccharide are not as closely correlated as first thought.

7.2.4 Carbon Utilization Phenotype of the *S. meliloti phbA* Mutant

Growth curves were set up using the BioScreenC growth curve machine. Growth was assessed in VMM supplemented with 15 mM of either glucose, acetate, acetoacetate, or DL-Hydroxybutyrate. The results of these growth curves are shown in Figures 7.4, 7.5, 7.6, and 7.7. These data show that the *phbA* strain SmUW41 cannot grow on acetoacetate (Figure 7.6), even after extended periods of incubation; this is in contrast to Rm11105 and Rm11347, both of which demonstrate compromised, but delayed, growth on acetoacetate.

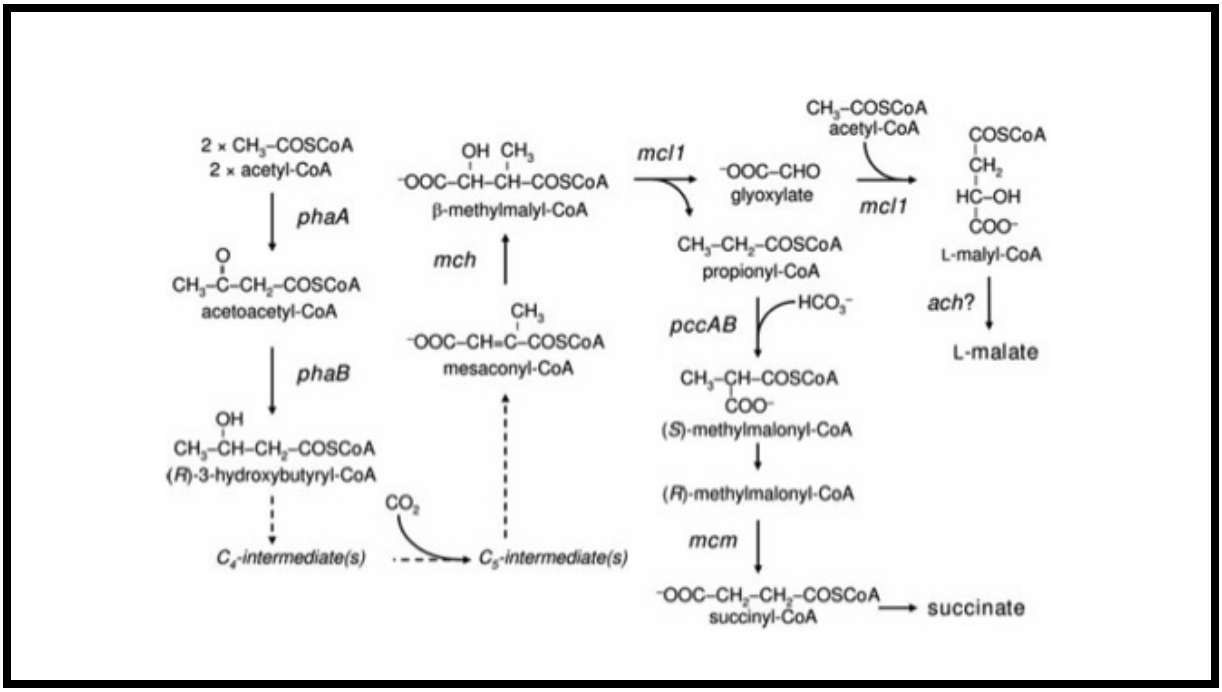

Figure 7.1: Proposed alternative pathway for acetyl-CoA assimilation [91].

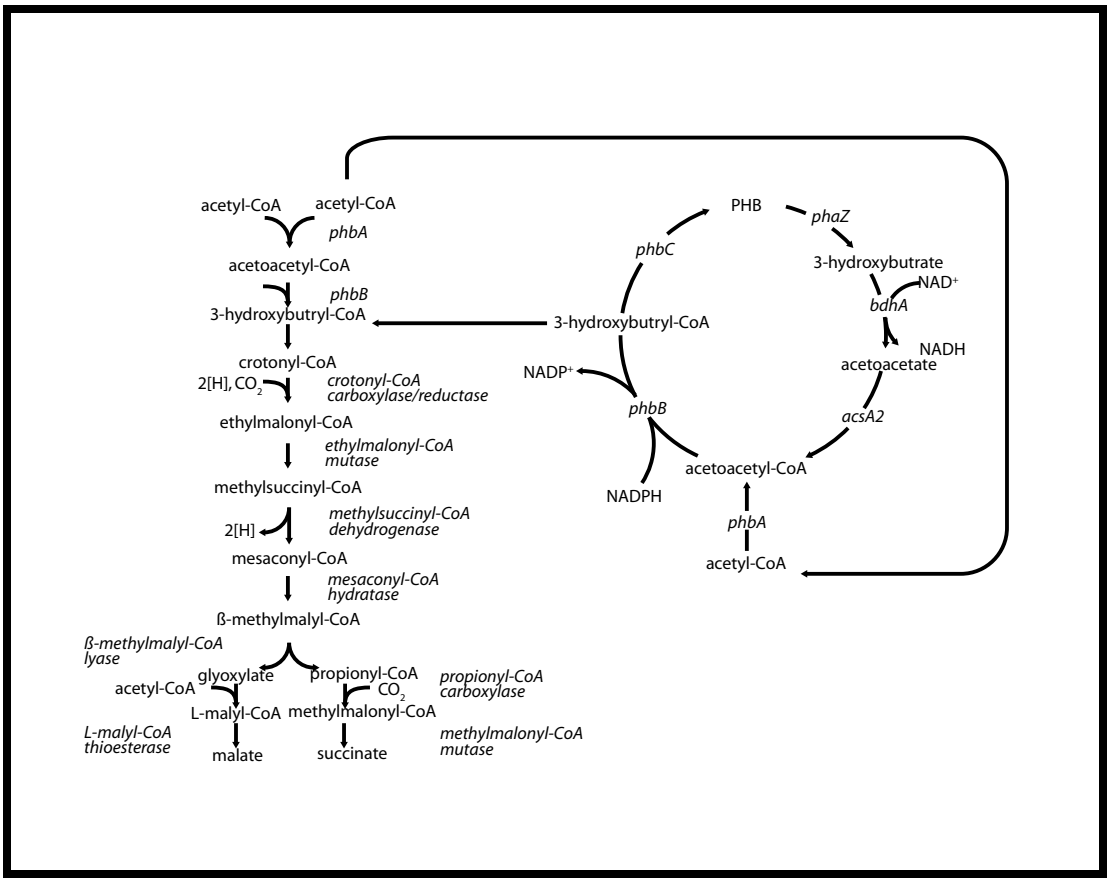

Figure 7.2: A model for the proposed interaction of the PHB Cycle of *S. meliloti* with a potential ethylmalonyl-CoA pathway

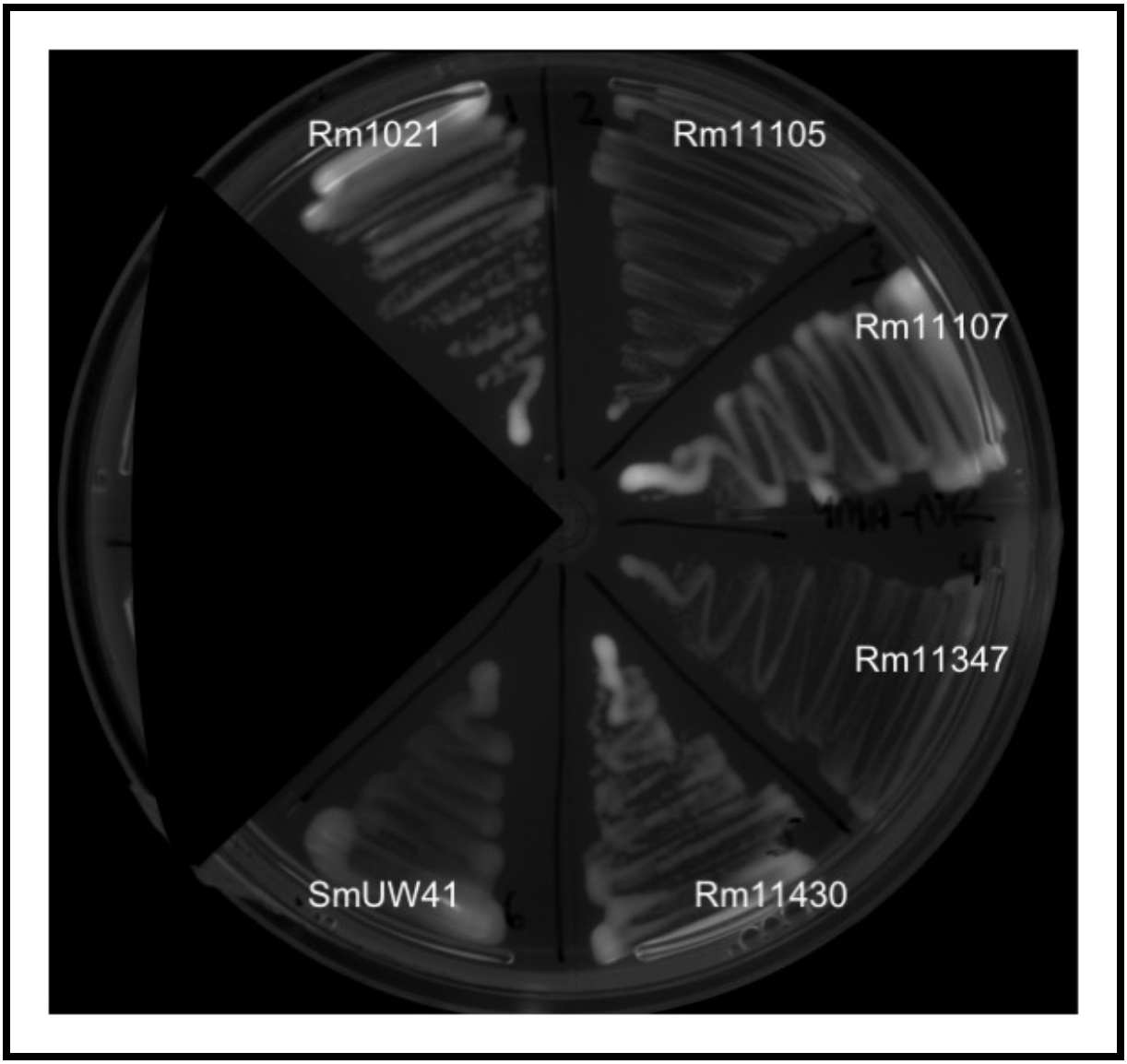

Figure 7.3: Growth of the *S. meliloti phbA* mutant SmUW41, and other PHB Cycle mutants, on YMA supplemented with Nile Red. The lack of fluorescence from strains Rm11105, Rm11347 and SmUW41 indicate that no PHB accumulation is present in these cells. That is in contrast to Rm1021, Rm11107 and Rm11430 which all accumulate large quantities of cytoplasmic PHB under these conditions, as evidenced by the fluorescence

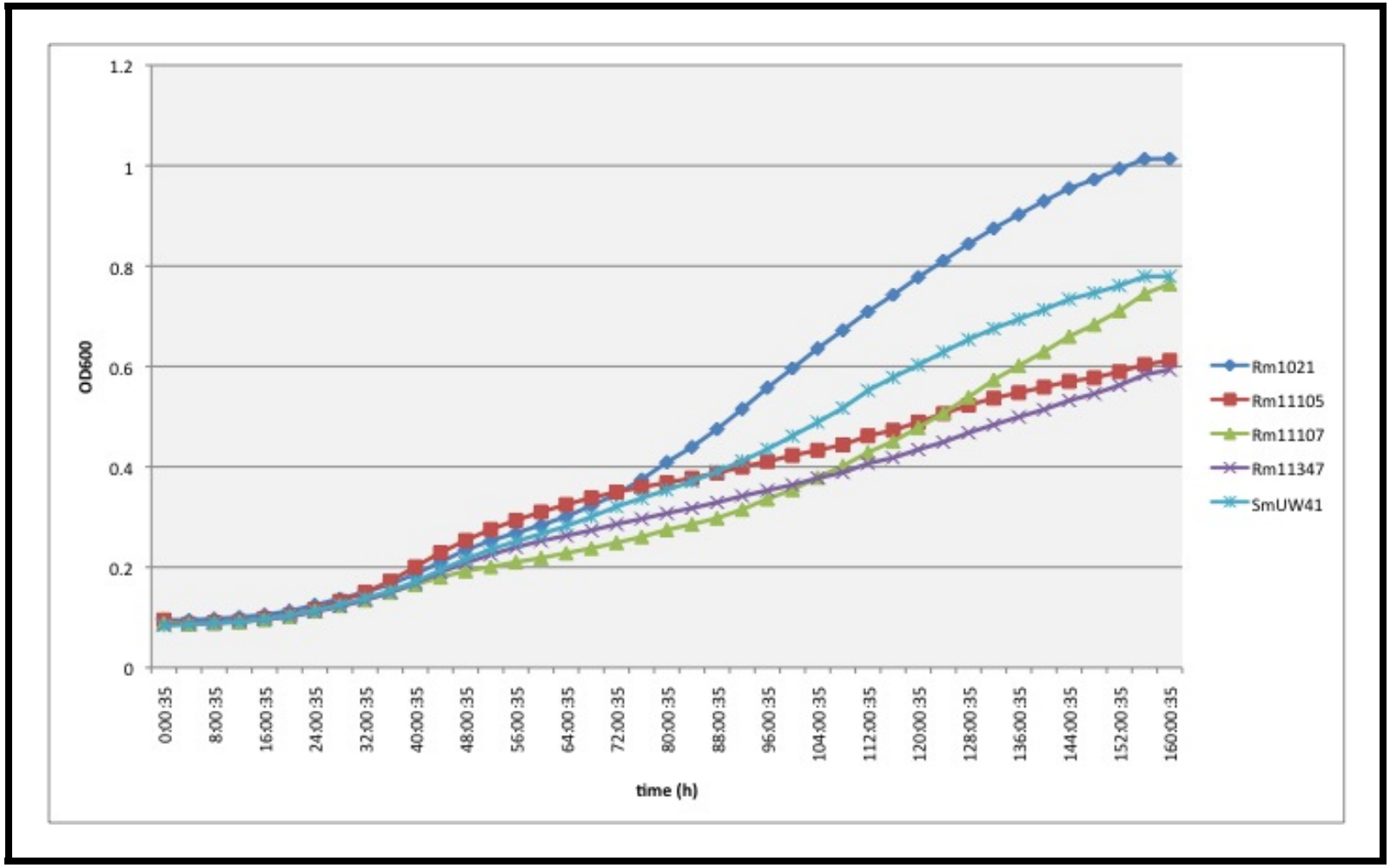

Figure 7.4: Growth curves of the *S. meliloti phbA* mutant SmUW41, and other PHB Cycle mutants, in VMM Glucose medium

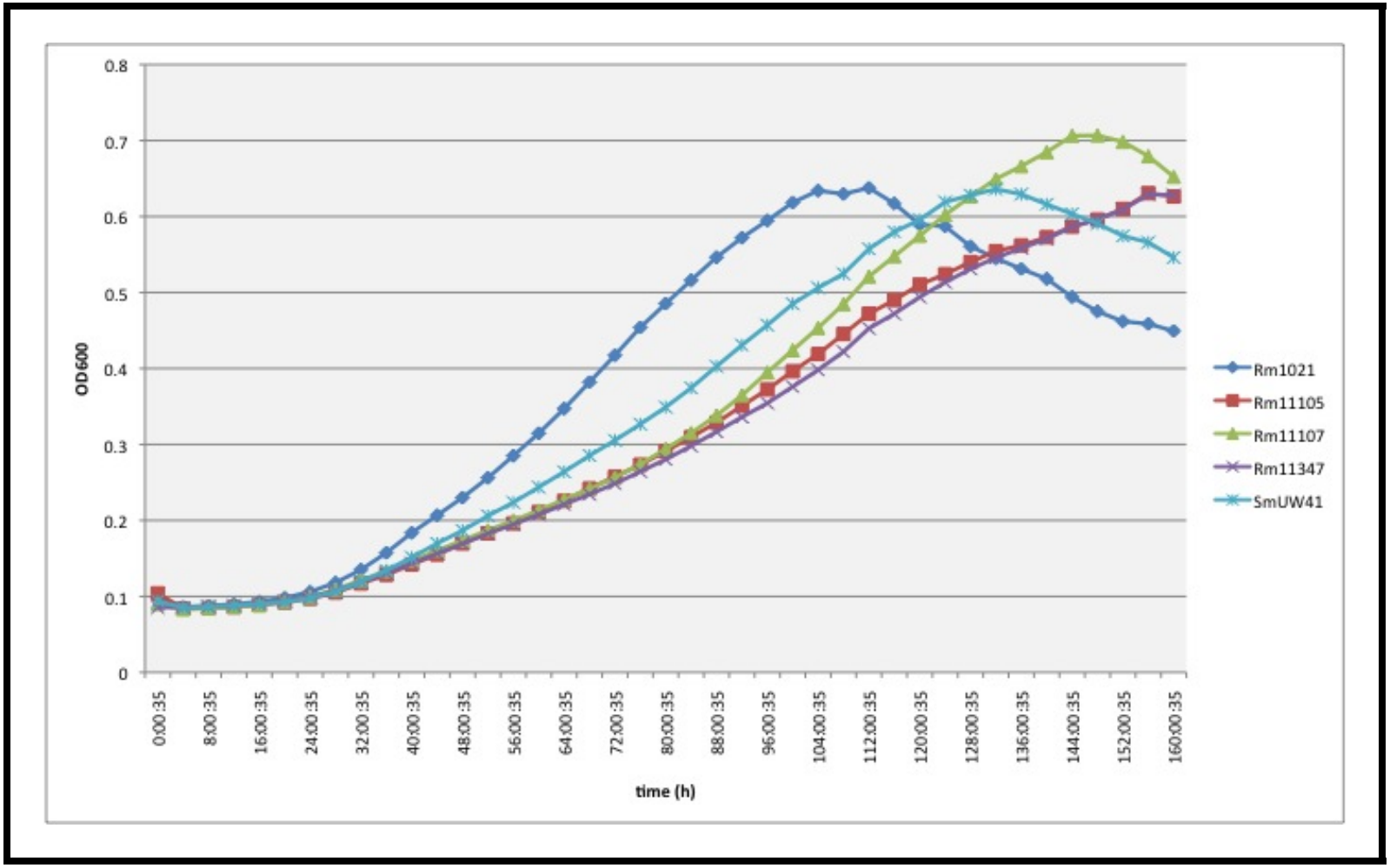

Figure 7.5: Growth curves of the *S. meliloti phbA* mutant SmUW41, and other PHB Cycle mutants, in VMM Acetate medium

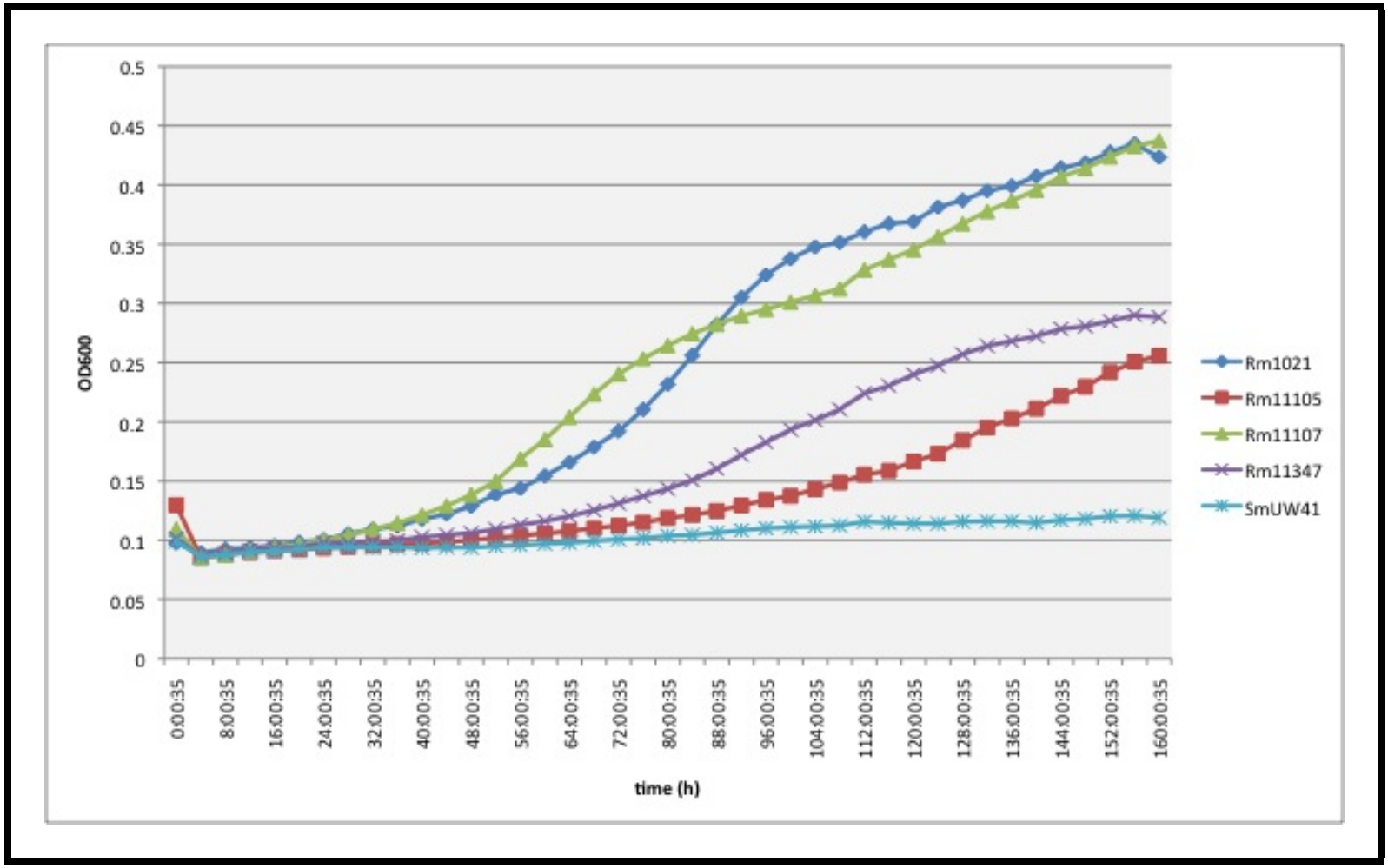

Figure 7.6: Growth curves of the *S. meliloti phbA* mutant SmUW41, and other PHB Cycle mutants, in VMM Acetoacetate medium

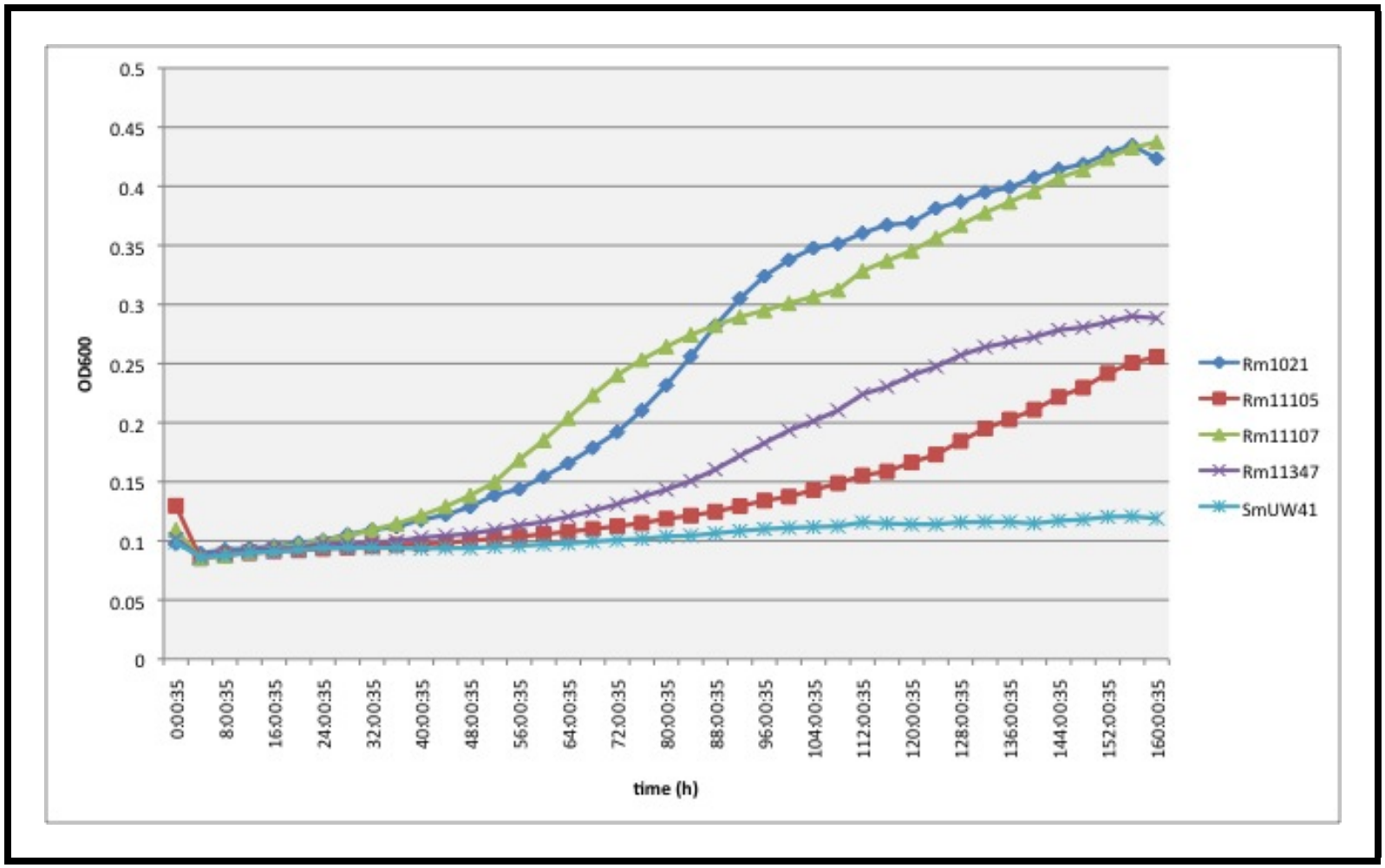

Figure 7.7: Growth curves of the *S. meliloti phbA* mutant SmUW41, and other PHB Cycle mutants, in VMM DL-Hydroxybutyrate medium

7.2.5 β-Ketothiolase Activity in the PHB Synthesis by the *phbA* Mutant of *S. meliloti*

The β-Ketothiolase activity of SmUW41 was tested using a modified version of previously described protocols [184, 249] and is described in Section 2.7.4. This assay monitors the decrease of E_{303} of the Mg^{2+}-Enol complex of acetoacetyl-CoA as it is converted to acetyl-CoA. The chart in Figure 7.8 show the results of this assay and demonstrate the reduction in activity that is evident in the SmUW41 background. It is noteworthy that some β-Ketothiolase activity remains in this strain; an analysis of the *S. meliloti* genome sequence reveals the presence of a second β-Ketothiolase ORF, and it is conceivable that the activity evident in SmUW41 is the result of this second gene.analys

7.3 Conclusions

If the model proposed in Figure 7.2 were correct, it predicts that a *phbA* mutant of *S. meliloti* would be able to grow on acetoacetate as a sole carbon source by channelling carbon out of the PHB cycle via *phbB* and subsequently through an ethylmalonyl-CoA-like pathway. The data presented in Figure 7.6 suggest that this is not the case and that PhbA represents the only exit point for carbon from the PHB cycle. It is interesting to note that, unlike *phbB* and *phbC* mutants, which do exhibit growth (albeit delayed) on acetoacetate, the *phbA* mutant shows absolutely no growth on this substrate even after extended incubation (Figure 7.6). This phenotype represents an interesting twist in the complicated investigation into the role of the PHB metabolism in *S. meliloti*. It also suggests that, although the data in Figure 7.8 indicates an alternative β-ketothiolase may be functional in *S. meliloti*, it is unable to substitute for PhbA in growth on acetoacetate.

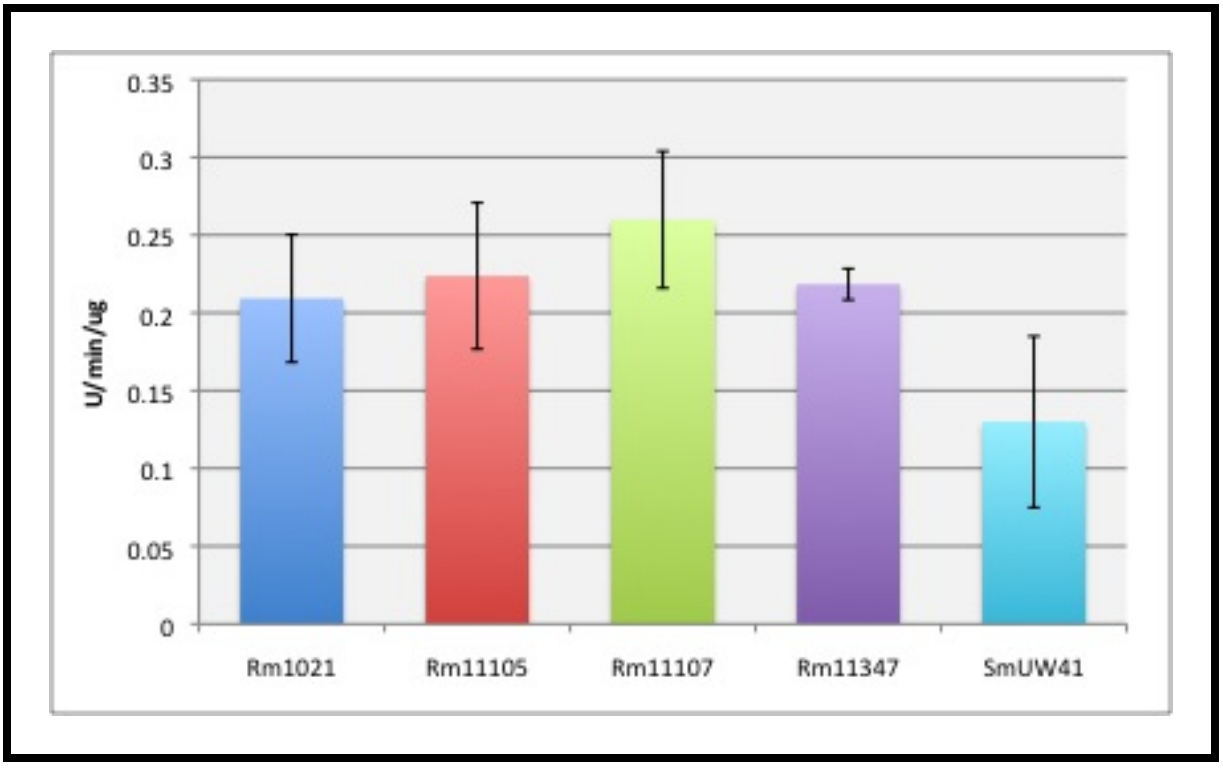

Figure 7.8: Results of the β-Ketothiolase activity assay. *S. meliloti phbA* mutant SmUW41, and other PHB Cycle mutants, were assayed for β-Ketothiolase activity. The results shown indicate the average from two or three independent replicates, assayed using a modified version of standard protocols [184, 249]

Previous studies investigating the interesting carbon utilization phenotypes of PHB synthesis mutants have suggested that the lack of PHB synthesis prevents NADPH consumption, resulting in an accumulation of NADPH or NADH to inhibitory levels [193]. Indeed, a *phaC* mutant of *R. etli* has been shown to accumulate NADH [43], although this mutant also showed reduced growth and organic acid excretion when grown on succinate and glucose; a phenomenon exhibited to a much lesser extent in *S. meliloti phbC* mutants (Figure 7.4). Further analysis of both *S. meliloti* and *R. etli phbC* mutants is needed to determine the significance of this phenomenon.

Chapter 8

Analysis of the Role of Phasins in PHB Synthesis and Rhizosphere Competitiveness in *Sinorhizobium meliloti*

8.1 Introduction

While the enzymology of PHB synthesis and degradation has been well characterized in *S. meliloti*, the regulation of these processes is far less understood. PHB granules within the cytoplasm of the bacterial cell are typically coated in granule-associated proteins known as Phasins. Phasins appear to be ubiquitous among PHA-synthesizing bacteria, including *Ralstonia eutropha*, which has four phasin genes [271, 272], and *Methylobacterium extorquens*, which has two [192].These proteins have low molecular mass, are amphiphilic in nature and can comprise a significant fraction of total cell protein [395]. Although they are not highly conserved

at the sequence level (reviewed in [171]), they do all appear to perform similar regulatory functions.

S. meliloti has two regulatory phasins, encoded by *phaP1* and *phaP2*. A double mutant of *phaP1* and *phaP2* cannot accumulate PHB, has greatly increased levels of glycogen synthesis, and enhanced EPS production relative to Rm1021[379]. Mutants of these phasin genes also have impaired nitrogen fixation capacity on *Medicago truncatula* plants. Here we show that on the host plant *Medicago sativa* (alfalfa), no similar reduction in symbiotic capacity is observed. Furthermore, although previous work has shown that the *phaP1 phaP2* double mutant does not accumulate PHB [379], it has not shown whether it retains the capacity to synthesize it and if so, whether the resultant molecule it is stable or unstable. The *phaP1 phaP2* mutant is also more mucoid than the wild-type Rm1021 but its rhizosphere competitiveness has not been investigated. To address the issue of PHB stability, Phasin-PhaZ mutants were constructed and their resultant PHB synthesis and rhizosphere competitive capacities were investigated.

8.2 Results and Discussion

8.2.1 Analysis of the Symbiotic Phenotype of *S. meliloti* Phasin Mutants on *Medicago sativa*

Alfalfa plants were inoculated with *S. meliloti* cultures as described in Section 2.3. The data shown in Figure 8.1 show that, unlike with the host plant *Medicago truncatula*, *S. meliloti* phasin mutants do not appear to demonstrate a reduced symbiotic capacity.

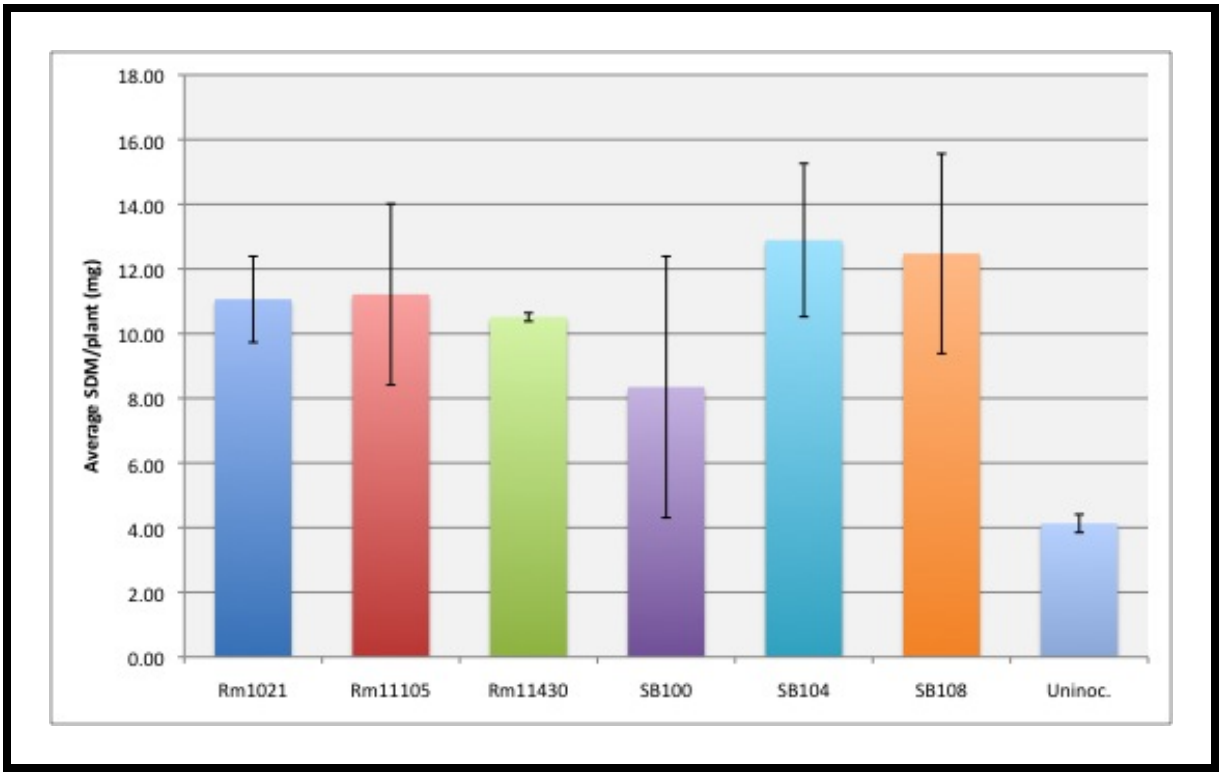

Figure 8.1: Shoot dry masses of alfalfa plants inoculated with *S. meliloti* phasin mutants. Error bars indicate standard deviations

8.2.2 Construction of *S. meliloti phaZ*-Phasin Mutants

A lysate of Rm11430 was prepared as described in Section 2.4.4.8 and transductions into the SB100, SB104 and SM108 backgrounds were carried out as described previously [95]. Transductants were selected on LB containing Sp_{100} and streak purified three times. The resultant strains are described in Table 2.1 and are summarized in Table 8.1 for ease of reading.

8.2.3 Analysis of PHB Synthesis in *S. meliloti* Phasin-*phaZ* Mutants

In order to determine whether the *phaP1 phaP2* double mutant is capable of synthesizing PHB, the PHB content of SmUW85, the *phaP1 phaP2 phaZ* triple mutant was quantitated. Cells were grown to saturation in YMB and PHB extraction and quantitation was carried out as described in Section 2.7.2. The results of this assay are shown in Figure 8.2, and clearly suggest that the lack of PHB accumulation in SB108 is due to a lack of synthesis rather than degradation of an unstable product by means of PhaZ.

8.2.4 Analysis of the Competition Phenotype of *S. meliloti* Phasin-*phaZ* Mutants

The ability of *S. meliloti* SmUW85 to compete for nodule occupancy was assayed by co-inoculating alfalfa plants with different strain combinations. Table 8.2 shows that, when co-inoculated in approximately equal ratios with the wild-type strain, SmUW85 demonstrated a comparable reduction in rhizosphere competitiveness to Rm11105 relative to the wild-type Rm1021.

Table 8.1: Summary of Phasin-*phaZ* mutants constructed in this study

Strain	Relevant Characteristics
SB100	Rm1021 *phaP1*::pK19*mob*
SB104	Rm1021 *phaP2* precise deletion
SB108	Rm1021 *phaP1 phaP2*
SmUW81	SB100 *phaZ*::ΩSmSp
SmUW83	SB104 *phaZ*::ΩSmSp
SmUW85	SB108 *phaZ*::ΩSmSp

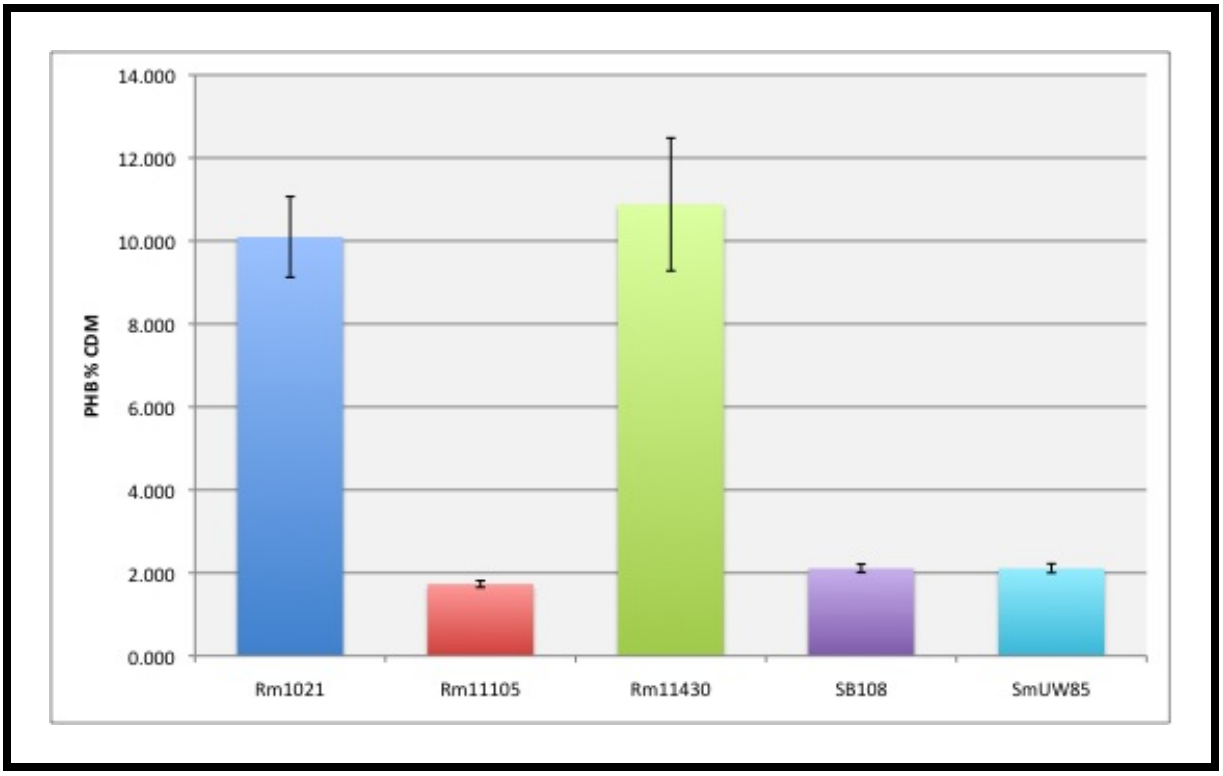

Figure 8.2: PHB accumulation in *S. meliloti* Phasin and Phasin-PhaZ Mutants. Rm1021: wild-type; Rm11105: Rm1021 *phbC*; Rm11430: Rm1021 *phaZ*; SB100: Rm1021 *phaP1*::pK19*mob*; SB104: Rm1021 *phaP2*; SB108: Rm1021 *phaP1 phaP2*.

Table 8.2: Nodulation competitiveness of the *S. meliloti* Rm11105 and SmUW85 strains co-inoculated in the described ratios with the wild-type strain Rm1021 on *M. sativa* plants

Strain (%) in inoculum	No. nodules tested	Nodule occupancy (%)		
		Strain 1	Strain 2	Both
Rm1021 (10) + Rm11105 (90)	19	19	0	0
Rm1021 (51) + Rm11105 (49)	21	20	0	1
Rm1021 (91) + Rm11105 (9)	22	22	0	0
Rm1021 (10) + SmUW85 (90)	15	14	0	1
Rm1021 (51) + SmUW85 (49)	14	14	0	0
Rm1021 (91) + SmUW85 (9)	11	11	0	0

8.3 Conclusions

The PHB synthesis defect demonstrated by SB108 is not due to the degradation of unstable PHB granules; this study shows that in a PHB depolymerase background, the *phaP1 phaP2* mutant does not accumulate PHB (Figure 8.2).

An earlier study demonstrated that the symbiotic phenotype of the phasin mutant strains is host-dependent [379]. This study showed that on the host legume *Medicago truncatula*, the plants exhibited significant reduction in shoot dry mass and acetylene reduction activity [379]. The data presented here demonstrate that this phenotype is host-specific, since *Medicago sativa* plants inoculated with the phasin mutant strains exhibit similar shoot dry masses to those inoculated with wild-type strains.

The competition data shown in Table 8.2 represents an interesting twist in the competition phenotype discussed in Section B.1; it appears that the *phaP1 phaP2 phaZ* triple mutant, which is unable to synthesize PHB but does appear to synthesize succinoglycan, demonstrates a comparable reduction in rhizosphere competitiveness to the *phbC* mutant. The reason for this is unclear and certainly worthy of further investigation.

Chapter 9

Conclusions and Future Directions

9.1 Conclusions and Future Directions

Plants in poor soils routinely suffer nitrogen deprivation; starving in air that is 80% nitrogen. N_2 must be reduced to a biologically available form before it is accessible to the plants that depend on it. Currently most farming operations in the developed world rely on the application of chemical fertilizers to meet the nitrogen needs of the crop plants, resulting in large increases in crop yield, but with concomitant and significant environmental and socioeconomic ramifications. Nitrogen fertilizer has one of the lowest input efficiencies, resulting in considerable environmental damage. Nitrogen fertilizers contaminate surface and groundwater systems, threaten the stability of the ozone layer, present a major threat to the human health, and are prohibitively expensive. The need for integrated management of soil nutrients using biological fertilizer as part of a more sustainable approach to commercial agriculture is needed. For this to happen, biological nitrogen fixation technologies must be accessible, dependable and well understood; more work is needed to understand the intricacies of the intimate nitrogen-fixing relationship between rhizobia and legumes. This study has investigated several aspects of carbon metabolism and

desiccation tolerance in two commercially relevant rhizobial species, *S. meliloti* and *B. japonicum*. This work was undertaken with a view to enhancing current inoculant technologies as a means of augmenting the use of mineral fertilizers with biological alternatives.

The relationship between PHB production and EPS synthesis is indicative of the existence of similar, but thus far uncharacterized, regulatory circuits in both *S. meliloti* and *B. japonicum*. The relationship between EPS synthesis and rhizosphere competitiveness is intriguing and a more detailed analysis of the phenotypes of the PHB cycle mutants in the SmUW3 background might be expected to help decipher these networks. Some preliminary work in this area is outlined in Appendix B.1. In order to facilitate the analysis of EPS synthesis in different Rhizobial strains and species, it will be necessary to develop a quantitative EPS assay that is both internally and externally robust. The isopropanol method used in this study is very effective at comparing multiple samples prepared in the same assay, but there might be value in exploring the possibility of using anthrone as a standard assay in the future [247, 353], as described in Section 2.7.5.3, as a means of improving standardization between studies.

To date, it has not been experimentally demonstrated whether PHB accumulation is modulated by control at the transcriptional level. In order to facilitate an analysis of PHB synthesis throughout the growth curve and under different growth conditions, *lacZ* transcriptional fusions to *S. meliloti phbC* and *phbAB* have been constructed. PCR was used to amplify the *S. meliloti phbC, phbA, phbB* and *phbAB* ORFs, which were then captured in pJET. *phbAB* and *phbC* were then subcloned, in both orientations, into pTH1703 [58] in order to generate *gfp-lacZ* and *gusA* fusions. All of these constructions are recorded in Table 2.1. These constructs were then transferred into *S. meliloti* by triparental conjugation in order to generate functional, choromosomally located fusions. These strains should be used

to monitor the regulation of *phbC* and *phbAB* throughout the growth cycle of the organism in order to determine when, and under which conditions, PHB synthesis is up- and down-regulated.

The carbon utilization phenotypes associated with PHB cycle mutants in *S. meliloti* remain unexplained and certainly warrant further investigation. The observation that a *phbA* mutant is completely unable to utilize acetoacetate as a sole carbon source is somewhat unexpected given the phenotypes of other mutants in this cycle. A more detailed analysis of this mutant, including an assessment of its rhizosphere competitiveness and symbiotic phenotype are needed in order to more fully determine the basis for the observed results documented herein. While the results suggest that an ethylmalonyl-CoA-like pathway is either not present in *S. meliloti*, or does not overlap with the PHB cycle, the phenotypes of the *bhb* mutants, and their overlap with PHB cycle mutants, is certainly an area that warrants further investigation since mutants of *bhb* and *phbC* are unable to utilize either 3-hydroxybutyrate or acetoacetate but are unaffected in their capacity to grow on acetate.

Further analysis of the the role of dicarboxylates, as well as the regulation of *dctA* genes in the *B. japonicum*-soybean symbiosis is needed in order to develop a stronger understanding of bacteroid carbon metabolism in this organism. Analysis of the symbiotic phenotypes of the *dctA* mutants constructed to-date will reveal which, if any, are required for symbiosis. It is conceivable that the redundancy in DctA transporters in *B. japonicum* may be sufficient to prevent any one mutant from having a discernible symbiotic phenotype. To this end it may be necessary to construct multiple *dctA* mutants. An analysis of the transport capacities of each of the mutants may also yield valuable information regarding the roles that each of the individual ORFs play in the physiology of this organism. Radio-label transport assays using different labelled substrates would be a relatively fast and

effective means of analysing this. The reason for the recalcitrance of *B. japonicum dctBD* to mutation remains unclear; further analysis will be necessary given the potential value of this mutant to developing a more comprehensive picture of carbon regulation in symbioses of determinate nodules.

The development of improved inoculant technologies is necessary if we are to reduce our dependence on exogenously applied fertilizers that are synthesized using energy-intensive processes. This aspect of this work was prematurely terminated when our partner Agribiotics was bought by EMD Crop Biosciences, and the operation was moved to the United States. In this study we identify several strains with interesting OSS and ion-tolerance phenotypes. Further analysis of the genetic, physiological and environmental basis for these phenotypes is necessary to start building a more comprehensive understanding of the biochemical factors that influence desiccation tolerance in the Rhizobia. In order to facilitate this, a cosmid library of the Agribiotics commercial inoculant strain of *B. japonicum* was constructed, as described in Section 2.4.5. This library was constructed from a strain with superior OSS to *B. japonicum* USDA110, and may be useful as a tool for identification of genes with a capacity to influence OSS.

As we look at the new century, we are realizing that the road ahead is one unlike that travelled by previous generations. We face unprecedented economic and environmental uncertainty. The development of new paradigms that integrate genomics information with socio-economic and environmental understanding will be key to ensuring a sustainable future for humanity. Symbiotic nitrogen fixation has been an integral component of farming practices for hundreds of years. It is a tried and true technology that is now in a prime position to play a pivotal role in the molecular biotechnology advances of the 21st century; however, in order to fully exploit the potential of biological nitrogen fixation, we must first develop a comprehensive understanding of it in order to ensure we do not repeat the mistakes

of our past in our efforts to repair them.

Appendix A

Media Recipes, Solutions, and Reaction Conditions

A.1 Growth Media and Antibiotics

A.1.1 Bacterial Growth Media Recipes

A.1.1.1 Luria Bertani (LB) Broth

- 5 g Yeast Extract
- 10 g Tryptone
- 5 g NaCl
- 1 l dH_2O
- (15 g Agar)

A.1.1.2 LB-MC Broth

As LB but add $MgCl_2$ and $CaCl_2$ to a final concentration each of 2.5 mM.

A.1.1.3 Typtone Yeast Extract (TY)

- 5 g Tryptone
- 5 g Yeast Extract
- 0.5 g $CaCl_2$
- 1 l dH_2O
- (15 g Agar)

A.1.1.4 Modified M9 Medium for Rhizobia

- 7 g Na_2HPO_4
- 3 g KH_2PO_4
- 1 g NH_4Cl
- 1 g NaCl
- (15 g Agar)

This is autoclaved, cooled to 55°C, and the following are added:

- 1 ml 0.5 M $MgSO_4$
- 0.1 ml 1 M $CaCl_2$

A.1.1.5 Rhizobium Minimal Medium (RMM)

Solutions A, B, C and D are prepared and sterilized separately. RMM is made by adding 1% (v/v) each of RMM A and RMM B and 0.1% (v/v) each of RMM C and RMM D.

RMM A:

- 145 g KH_2PO_4
- 205 g K_2HPO_4
- 15 g NaCl
- 50 g NH_4NO_3
- 1 l dH_2O

RMM B:

- 50 g $MgSO_4.7H_2O$
- 1 l dH_2O

RMM C:

- 10 g $CaCl_2.2H_2O$
- 1 l dH_2O

RMM D:

- 123.3 g $MgSO_4.7H_2O$
- 87 g K_2SO_4
- 0.247 g H_3BO_3
- 0.1 g $CuSO_4.5H_2O$
- 0.338 g $MnSO_4.H_2O$

- 0.288 g $ZnSO_4.7H_2O$
- 0.056 g $CoSO_4.7H_2O$
- 0.048 g $Na_2MoO_4.2H_2O$
- 1 l dH_2O

Prepare the following solutions and filter sterilize. Add to cooled media.

- 0.2 ml Thiamine (1 mg/ml)
- 0.2 ml Ca-pantothenate (1 mg/ml)
- 0.2 ml biotin (1 mg/ml)
- Carbon Source (0.2% succinate: 2 ml 20% succinate in 200 ml final volume)

A.1.1.6 Vincent's Minimal Medium (VMM)

Solutions A, B and C are prepared and sterilized separately. VMM was made by adding 10% (v/v) VMM B and 1% (v/v) VMM C to VMM A. A carbon source was also added to a final concentration of 15 mM.

VMM A:

- 1 g K_2HPO_4
- 1 g KH_2PO_4
- 1 g NH_3Cl (or 0.6 g KNO_3)
- 1 l dH_2O
- (15 g Agar)

VMM B:

- 0.05 g $FeCl_3$
- 0.05 g $MgCl_3$
- 0.5 g $CaCl_2$
- 0.5 l dH_2O

VMM C:

- 0.01 g Biotin
- 0.01 g Thaimin
- 0.01 g Ca-Pantothenate

A.1.1.7 Arabinose Gluconate (AG) Medium

- 1 g Arabinose
- 1 g Gluconate
- 1 g Yeast Extract
- 930 ml dH_2O
- (17 g Agar)

Autoclave the above ingredients then add 10 ml of each of the following autoclaved stock solutions to make one litre of media:

- A. Hepes - Mes Buffer, pH 6.6 - 6.9

  - 65.0 g Hepes (Sigma no. H-3375)
  - 55.0 g Mes (Sigma no. M-8250)
  - pH adjusted to 6.6 - 6.9 with NaOH
  - volume to 500 ml with dH_2O

- B. 0.67 g/l $FeCl_3.6\ H_2O$
- C. 18.0 g/l $MgSO_4.7\ H_2O$
- D. 1.30 g/l $CaCl_2\ .2\ H_2O$
- E. 25.0 g/lNa_2SO_4
- F. 32.0 g/l NH_4Cl
- G. 12.5 g/l Na_2HPO_4

A.1.1.8 Modified Arabinose Gluconate (MAG) Medium

As AG but increase Arabinose and Gluconate content from 1 g/l each to 5 g/l.

A.1.1.9 Yeast Mannitol (YM) Medium

- 0.4 g Yeast Extract
- 10 g Mannitol
- 0.5 g K_2HPO_4
- 0.2 g $MgSO_4.7H_2O$
- 0.1 g NaCl
- 1l dH_2O

- pH to 7.0
- (18 g Agar)

A.1.1.10 Autoinduction Medium

This medium is designed for the over-expression of proteins from genes that are under the control of *lac* repressor (e.g. pET30).

Base Medium

- 6 g Na_2HPO_4
- 3 g KH_2HPO_4
- 20 g Tryptone
- 5 g Yeast Extract
- 5 g NaCl
- 60 ml Glcerol
- 1 l dH_2O
- pH to 7.2 with NaOH

Additives Filter sterilize the following:

- 10% Glucose
- 8% Lactose

Before using, add 25 ml lactose stock and 5 ml glucose stock to the base medium. For an uninduced control, omit the lactose solution.

A.1.1.11 ZYP-5052 Autoinduction Medium

ZY, 20X NPS, 50X 5052, 1 M $MgSO_4$ and 1000X trace metal solution are made up separately. To make 1 l ZYP-5052, the components are added as follows:

- 928 ml ZY
- 1.0 ml 1 M $MgSO_4$
- 1.0 ml Trace Metals solution
- 20 ml 50X 5052
- 50 ml 20X NPS

Note, add 1 M $MgSO_4$ before adding the 20X NPS to avoid precipitation.

Note, Kanamycin must be used in significantly higher concentrations (100 μg/ml) than is typically used.

ZY:

- 10 g Tryptone
- 5 g Yeast Extract
- 925 ml dH_2O

Autoclave to sterilize.

20X NPS:

- 6.6 g NH_4SO_4
- 13.6 g KH_2PO_4

- 14.2 g Na_2HPO_4
- 100 ml dH_2O

pH to 6.75. Autoclave to sterilize.

50X 5052:

- 25 g Glycerol
- 2.5 g Glucose
- 10 g Lactose
- 100 ml dH_2O

1 M $MgSO_4$:

- 24.65 g $MgSO_4.7H_2O$
- 100 ml dH_2O

Trace Metals Solution

- 50 ml 0.1 M $FeCl_3$
- 2.0 ml 1.0 M $CaCl_2.2H_2O$
- 1.0 ml 1.0 M $MnCl_2.4H_2O$
- 1.0 ml 1.0 M $ZnSO_4.7H_2O$
- 1.0 ml 0.2 M $CoCl_2.6H_2O$
- 2.0 ml 0.1 M $CuCl_2.2H_2O$

- 1.0 ml 0.2 M $NiCl_2.6H_2O$
- 2.0 ml 0.1 M $Na_2MoO_4.2H_2O$
- 2.0 ml 0.1 M H_3BO_3

Note, all stock solutions are made up and autoclaved separately (except $FeCl_3$ which is made up in HCl and is not autoclaved). The following volumes of these stock solutions are then added to 36 ml sterile dH_2O and the resultant solution is stored at room temperature.

A.1.2 Antibiotic Concentrations

All antibiotic concentrations listed here are for solid media. Typically these concentrations were halved for growth in liquid culture. Antibiotics were typically prepared at 1000X concentrations and a 1:1000 dilution was used. Stock solutions were stored at 4°C.

A.1.2.1 Antibiotic Concentrations for *E. coli*

- Ampicillin: 100 μg/ml
- Chloramphenicol: 25 μg/ml
- Gentamycin: 10 μg/ml
- Kanamycin: 25 μg/ml (100 μg/ml when using autoinduction medium)
- Naladixic acid: 5 μg/ml
- Tetracycline: 10 μg/ml

A.1.2.2 Antibiotic Concentrations for *S. meliloti*

- Gentamycin: 75 μg/ml
- Neomycin: 200 μg/ml
- Spectinomycin: 100 μg/ml
- Streptomycin: 200 μg/ml
- Tetracycline: 10 μg/ml
- Trimethoprim: 400 μg/ml

A.1.2.3 Antibiotic Concetrations for *B. japonicum*

- Kanamycin: 50 μg/ml
- Streptomycin: 200 μg/ml
- Tetracycline: 200 μg/ml

A.2 Molecular Biology Reagents

A.2.1 Solutions for the Isolation of Genomic DNA

A.2.1.1 Lysozyme Solution

2 mg/ml powdered lysozyme dissolved in $T_{10}E_1$ immediately prior to use

A.2.1.2 SDS-Protease Solution

- 5 mg/mk proteinase K dissolved in $T_{10}E_1$

- incubate 2h at 37°C
- add 0.1 g/ml SDS
- incubate 20 minutes at 45°C to dissolve SDS

A.2.1.3 $\mathbf{T_{10}E_{25}}$

- 10 mM Tris-HCl pH 8.0
- 25 mM EDTA pH 8.0
- store at 4°C

A.2.1.4 $\mathbf{T_{10}E_{1}}$

- 10 mM Tris-HCl pH 8.0
- 1 mM EDTA pH 8.0
- store at room temperature

A.2.2 Solutions I, II and III for Small-Scale Preparation of Plasmid DNA

A.2.2.1 Small-Scale Plasmid Preparation Solution I

- 50 mM glucose
- 25 mM Tris-HCl pH 8.0
- 10 mM EDTA pH 8.0
- autoclaved and stored at 4°C

A.2.2.2 Small-Scale Plasmid Preparation Solution II

- 0.2 N NaOH
- 1% SDS

A.2.2.3 Small-Scale Plasmid Preparation Solution III

- 60 ml 5M potassium acetate
- 11.5 ml glacial acetic acid
- 28.5 ml dH_2O
- stored at 4°C

A.2.2.4 $\mathbf{T_{10}E_{25}}$

- 10 mM Tris-HCl pH 8.0
- 25 mM EDTA pH 8.0

A.2.2.5 $\mathbf{T_{10}E_1}$

- 10 mM Tris-HCl pH 8.0
- 1 mM EDTA pH 8.0

A.2.3 Tris-Acetate-EDTA (TAE) Buffer

A.2.3.1 1X Working Solution

- 40 mM Tris-Acetate
- 1 mM EDTA

A.2.3.2 50 X Stock Solution

- 242 g Tris base
- 57.1 ml Glacial acetic acid
- 100 ml 0.5 M EDTA
- pH 8.0

A.2.4 6X Agarose Gel Loading Dye

- 0.25% Bromophenol Blue
- 40% (w/v) Sucrose in dH_2O

A.2.5 Southern Blot Reagents

A.2.5.1 Transfer buffer

- 0.4 M NaOH
- 0.6 M NaCl

A.2.5.2 20X SSC

- 175.3 g NaCl
- 88.2 g sodium citrate
- 1l dH_2O

A.2.5.3 Hybridization Buffer

- 5X SSC
- 1% w/v blocking reagent (Roche Diagnostics, Basel, Switzerland)
- 0.1% N-lauroyl sarcosine
- 0.02% SDS

A.2.5.4 Stringency Buffer A

- 2X SSC
- 0.1% SDS

A.2.5.5 Stringency Buffer B

- 0.1X SSC
- 0.1% SDS

A.2.5.6 Tris-NaCl Buffer

- 0.1 M Tris-Cl pH 8.0
- 0.15 M NaCl

A.2.5.7 Blocking Buffer

- 1% w/v blocking reagent in Tris-NaCl buffer

A.2.5.8 Detection Buffer

- 0.1 M Tris-HCl pH 9.5
- 0.1 M NaCl

A.2.5.9 Stripping Solution

- 0.2 N NaOH
- 0.1% SDS

A.2.6 Cosmid Library Construction Solutions

A.2.6.1 Phage Dilution Buffer

- 10 mM Tris-HCl (pH 8.3)
- 100 mM NaCl
- 10 mM $MgCl_2$

A.3 Reagents for Protein Work

A.3.1 SDS-PAGE Gel Recipes

A.3.1.1 12% Resolving Gel

- 4 ml Acrylamide/Bis-acylamide (30%)
- 2.5 ml 1.5 M Tris-HCl (pH 8.0)
- 100 μl 10% (w/v) SDS

- 100 μl 0.06% (w/v) APS
- 5 μl (v/v) TEMED
- 3.32 μl dH_2O

A.3.1.2 4% Stacking Gel

- 670 μl Acrylamide/Bis-acylamide (30%)
- 1.25 ml 0.5 M Tris-HCl (pH 6.8)
- 50 μl 10% (w/v) SDS
- 25 μl 0.06% (w/v) APS
- 5 μl (v/v) TEMED
- 3.05 μl dH_2O

A.3.1.3 4X SDS-PAGE Running Buffer

- 12 g Tris-Base
- 57.6 g Glycine
- 1 l dH_2O
- pH 8.3 with HCl

A.3.1.4 1X SDS-PAGE Running Buffer

- 250 ml 4X Stock solution
- 10 ml 10% SDS
- 740 ml dH_2O

A.3.1.5 Coomassie Brilliant Blue Staining Solution

- 0.25 g Coomassie Brilliant Blue R250
- 45 ml Water
- 45 ml Methanol
- 10 ml Glacial Acetic Acid
- Filter through Whatman #1 filter to remove sediment

A.3.1.6 SDS-PAGE Loading Dye

- 5 ml Glycerol
- 2.5 ml β-Mercaptoethanol
- 15 ml 10% SDS
- 25 ml Upper Buffer
- 2.5 ml dH_2O
- Add Bromophenol Blue to colour

A.3.2 Western Blot Reagents

A.3.2.1 Western Transfer Buffer

25X Stock:

- 450 ml dH_2O
- 120 mM Tris Base

- 960 mM Glycine
- dH_2O to 500 ml

1X Working Solution:

- 40 ml 25X stock
- 200 ml EtOH
- 760 ml dH_2O

A.3.2.2 TBS

10X Stock:

- 200 mM Tris
- 5 M NaCl
- pH 7.5

1X Working Solution:

- 100 ml 10X TBS stock
- 900 ml dH_2O

A.3.2.3 TTBS

- 990 ml 1X TBS
- 10 ml Tween-20

A.3.2.4 Blocking Buffer

- 2.5 g non-fat dried milk
- 50 ml 1X TBS

A.3.2.5 Antibody Buffer

- 1 g non-fat dried milk
- 50 ml TTBS

A.3.3 Protein Purification Solutions

A.3.3.1 1X Ni-NTA Bind Buffer

- 300 mM NaCl
- 50 mM sodium phosphate buffer
- 10 mM imidazole
- pH 8.0

A.3.3.2 1X Ni-NTA Wash Buffer

- 300 mM NaCl
- 50 mM sodium phosphate buffer
- 20 mM imidazole
- pH 8.0

A.3.3.3 1X Ni-NTA Elution Buffer

- 300 mM NaCl
- 250 mM imidazole
- 50 mM sodium phosphate buffer
- pH 8.0

A.4 Plant Growth Media

Plant growth medium was prepared by adding 1 ml each of plant growth solutions A, B, C and D to 2 l dH_2O.

A.4.1 Plant Growth Solution A

- 294 g $CaCl_2$
- 1 l dH_2O

A.4.2 Plant Growth Solution B

- 136 g KH_2PO_4
- 1 l dH_2O

A.4.3 Plant Growth Solution C

- 6.7 g $FeCl_3$
- 1 l dH_20

A.4.4 Plant Growth Solution D

- 123 g $MgSO_4$
- 87 g K_2SO_4
- 0.338 g $MnSO_4$
- 0.247 g H_2BO_4
- 0.288 g $ZnSO_4$
- 0.1 g $CuSO_4$
- 0.056 g $CoSO_4$
- 0.048 g Na_2MoO_4
- 1 l dH_2O

A.5 Desiccation Assay Solutions

A.5.1 Phosphate Buffered Saline

- 8 g NaCl
- 0.2 g KCl
- 1.44 g Na_2HPO_4
- 0.24 g KH_2PO_4
- 1 l dH_2O
- pH 7.0

Autoclave to sterilize

A.6 Exopolysaccharide Isolation Reagents

A.6.1 Anthrone Reagent

Note: This reagent must be made fresh daily.

- 500 ml Concentrated H_2SO_4
- 200 ml dH_2O
- 1.4 g Anthrone Reagent

A.7 Typical Reaction Conditions

A.7.1 Polymerase Chain Reaction (PCR) for Cloning

A.7.1.1 KOD HotStart PCR Reaction Mix

- 10 X Reaction buffer: 5 μl
- 2 mM dNTPs: 2.5 μl
- 10 mM Forward primer: 1.5 μl
- 10 mM Reverse primer: 1.5 μl
- Template DNA: 1 μl
- DMSO: As needed up to 5%
- dH_2O to 50 μl

A.7.1.2 Typical KOD HotStart PCR Reaction

- 94°C: 2 mins

1 cycle of:

- 94°C: 15 sec
- 65°C: 30 sec
- 68°C: 90 sec

Repeat cycle 9 times, decreasing annealing temperature by 1°C each cycle 25 cycles of:

- 94°C: 15 sec
- 55°C: 30 sec
- 68°C: 90 sec

1 cycle of:

- 68°C 5 mins
- 4°C: Hold

A.7.2 Cross-Over PCR

A.7.2.1 Typical Initial Reaction Mix

- 10 X Reaction buffer: 5 μl
- 2 mM dNTPs: 2.5 μl

- 10 mM Primer A (or C): 1.5 μl
- 10 mM Primer B (or D): 1.5 μl
- Template DNA: 1 μl
- DMSO: As needed up to 5%
- dH_2O to 50 μl

A.7.2.2 Typical Joining Reaction Mix

- 10 X Reaction buffer: 5 μl
- 2 mM dNTPs: 2.5 μl
- 10 mM Outside primer A: 1.5 μl
- 10 mM Outside primer D: 1.5 μl
- Template DNA AB Reaction: 1 μl
- Template DNA CD Reaction: 1 μl
- DMSO: As needed up to 5%
- dH_2O to 50 μl

A.7.3 Colony PCR

A.7.3.1 Typical Colony PCR Reaction Mix

- 10X Reaction buffer: 2.5 μl
- 10 mM dNTPs: 2.5 μl

- 10 mM Forward primer: 1.5 μl
- 10 mM Reverse primer: 1.5 μl
- Template: 2 μl
- DMSO: as needed
- dH_2O to 25 μl

A.7.3.2 Typical Colony PCR Program

- 94°C: 2 mins

45 cycles of:

- 94°C: 15 sec
- 40°C: 30 sec
- 72°C: 90 sec

1 cycle of:

- 72°C 5 mins
- 4°C: Hold

A.8 Microscopy Reagents

A.8.0.3 Phosphate Buffer

Solution A: 0.2 M Monobasic sodium phosphate Solution B: 0.2 M Dibasic sodium phosphate Add 87.7 ml A to 12.3 ml B. pH 6.0

A.8.0.4 Uranyl Acetate Stain

- 2 g $UO_2(CH_3COO)_22H_2O$
- 1.9 g $H_2C_2O_4$
- 50 ml dH_2O
- Add 25% NH_4OH to pH 7-8

A.8.0.5 Lead Citrate Stain

Note: this stain reacts with CO_2 and carbonate, causing it to precipitate. These contaminants should be avoided during preparation and long-term storage. dH_2O is boiled for 10 minutes to remove any CO_2, then covered and allowed to cool for 30 minutes before use.

- 1.33 g $Pb(NO_3)_2$
- 1.76 g $NaH(C_3H_5O(COO)_3$
- 30 ml prepared dH_2O
- Shake for 60 minutes to allow conversion of lead nitrate to citrate
- Add 8 ml of 1M NaOH; solution should clear
- Store in foil-lined plastic container at 4°C

The stain is stable for up to 6 months; discard if it becomes cloudy.

Appendix B

Analysis of the Role of ExpR in Exopolysaccharide Synthesis and Rhizosphere Competitiveness of *Sinorhizobium meliloti* PHB Cycle Mutants

B.1 Introduction

The *phbC* and *bdhA* mutants of *S. meliloti* both demonstrate a considerable reduction in rhizosphere competitiveness relative to the wild-type strain Rm1021, with the phenotype of the *phbC* mutant being demonstrably more pronounced than that of the *bdhA* strain [9]. Interestingly, neither strain exhibits a reproducible reduction in symbiotic effectiveness when inoculated by itself [275, 9, 390]. The lack of equivalence between the competition phenotypes of the *phbC* and *bdhA* mutants

suggests that the function of PHB as a redox regulator for removal of potential growth inhibitory metabolites [80, 377] may be far more critical than the function of PHB as an internal source of carbon and energy.

The data shown in Chapter 6.1 suggest that, unlike the *bdhA* strain, a *phaZ* mutant of *S. meliloti* does not demonstrate a reduction in rhizosphere competitiveness. Furthermore, although this strain shows higher levels of exopolysaccharide (EPS) production relative to Rm1021, it is not more competitive than the wild-type strain. These data imply that that EPS production is not the sole determinant in the competition phenotype of other PHB cycle mutants. Indeed, it is conceivable that the competition defect observed in *phbC* mutants of *S. meliloti* may be due to extremely low levels of succinoglycan production. Succinoglycan production may be sufficient to permit the establishment of an effective symbiosis but, assuming that the succinoglycan itself is playing a role in signalling during early nodulation, insufficient to facilitate competition with strains producing higher levels of the EPS.

All studies examining the rhizosphere competitiveness of *S. meliloti* PHB cycle mutants, to date, have been conducted in the Rm1021 background. As discussed in Section 1.4, Rm1021 however, carries an insertion element (ISRm2011-1) within the open reading frame of *expR* and only synthesizes EPSII under low phosphate conditions [237, 297, 401]. Earlier work demonstrated that restoration of *expR* expression could restore the production of symbiotically active EPSII, facilitating nodulation in an EPSI mutant background, although the nodulation was less efficient than in the presence of succinoglycan [265].

In this study we report the construction and characterization of PHB cycle mutants in an $expR^+$ $nolR^+$ $pstC^+$ (SmUW3) background. Furthermore, we report the analysis of the rhizosphere competitiveness of strains SmUW1, SmUW24 and SmUW6. These strains possess mutations in *expR*, *exoY* and *nolR pstC* respectively, allowing an analysis of the potential role of these regulatory proteins in

nodulation competitiveness and exopolysaccharide synthesis.

B.2 Results and Discussion

B.2.1 Construction of PHB Cycle Mutants in SmUW3 Background

Lysates of Rm11105, Rm11107, Rm11347 and Rm11430 were prepared as described in Section 2.4.4.8 and transductions into the SmUW3 background were carried out as described previously [95]. Transductants were selected on LB containing either Nm_{200} (*phbC and bdhA*) or Sp_{100} (*phbB and phaZ*) and streak purified three times. The resultant strains are described in Table 2.1 and are summarized in Table B.1 for ease of reading.

B.2.2 Exopolysaccharide Biosynthesis in the SmUW3 Background

Exopolysaccharide biosynthesis was quantitated by isopropanol precipitation of the soluble EPS secreted into the growth medium under EPS-inducing conditions, as described in Section 2.7.5. Although the SmUW3 strain is visibly more mucoid than Rm1021 on YMA, the results shown in Figure B.1 suggest that this increased mucoidy does not translate into significantly higher secretions of EPS when cells are grown in YMB. It would be interesting to compare these data to data generated from cells grown in TY, which is non-EPS-inducing. It is important to remember that EPS is distinct from capsular polysaccharide, and it is conceivable that the increased mucoidy of the SmUW3 strain is entirely due to the production of insoluble capsular polysaccharides that are not isolated in this particular assay. This may

Table B.1: Summary of PHB cycle and exopolysaccharide mutants constructed in SmUW3 background

Strain	Relevant Characteristics
SmUW1	Rm1021 *pstC*$^+$ *nolR*$^+$
SmUW3	Rm1021 *expR*$^+$ *nolR*$^+$ *pstC*$^+$
SmUW6	Rm1021 *expR*$^+$
SmUW24	ϕ-Rm7055 transduced into SmUW6
SmUW33	ϕ-Rm11105 transduced into SmUW3
SmUW34	ϕ-Rm11107 transduced into SmUW3
SmUW35	ϕ-Rm11347 transduced into SmUW3
SmUW36	ϕ-Rm11430 transduced into SmUW3

also explain the interesting phenotype recorded for the *S. meliloti phbA* mutant (Section 7.2.3); SmUW41 also appeared to demonstrate an increase in mucoidy but, when assayed for soluble EPS, did not appear to secrete detectable EPS into the growth medium. Further analysis of the relationship between capsular polysaccharide and soluble EPS in *S. meliloti* is necessary in order to characterize and understand this phenotype more conclusively.

B.2.3 Competition Phenotype of PHB Cycle Mutants in an SmUW3 or SmUW6 Background

The data in Table B.2 show the results of competition assays. In each trial, approximately 15 nodules were crushed and the bacteroids screened for the appropriate antibiotic resistance marker.

The comparison of SmUW1 and SmUW3 suggest that the presence of *expR* does not affect rhizosphere competitiveness; this is corroborated by the data from the comparison of Rm1021 and SmUW6, which also indicated that *expR* does not affect the ability of the cells to compete for nodulation.

The mutation in SmUW24 was recently shown to be within *exoY* and not *exoF* as first thought [207, 244]. The comparison of SmUW24 and SmUW6 suggests that the synthesis of EPSII is not sufficient to restore nodulation competitiveness to the *exoY* strain. Furthermore, the data in Table B.2 suggest that the reduction in competitiveness exhibited by the *phbC* mutant (SmUW33 and Rm11105) is not alleviated by the presence of a functional *expR* however, the phenotype of the *bdhA* mutant is less severe in this background, resulting in an increased competitiveness relative to wild-type.

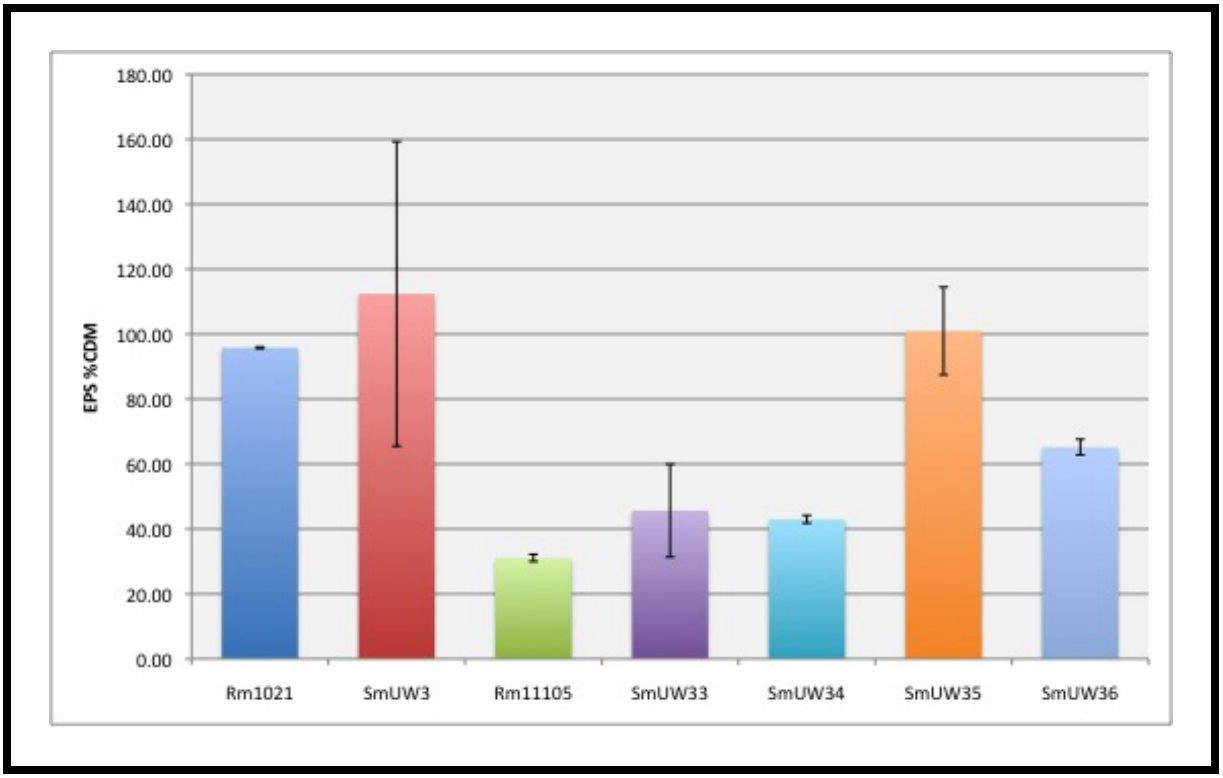

Figure B.1: Results of the isolation and quantitation of soluble exopolysaccharide from Rm1021, SmUW3 and PHB cycle mutants of *S. meliloti*. Rm1021: wild-type; SmUW3: Rm1021 *expR*$^+$ *nolR*$^+$ *pstC*$^+$; Rm11105: Rm1021 *phbC*; SmUW33: SmUW3 *phbC*; SmUW34: SmUW3 *bdhA*; SmUW35: SmUW3 *phbB*; SmUW36: SmUW3 *phaZ*

Table B.2: Nodulation competitiveness of the *S. meliloti* wild-type EPS strains and PHB cycle mutants co-inoculated in the described ratios on *M. sativa* plants

Strain (%) in inoculum	No. nodules tested	Nodule occupancy (%)		
		Strain 1	Strain 2	Both
SmUW1 (7) + SmUW3 (93)	10	2	7	1
SmUW1 (42) + SmUW3 (58)	15	5	6	4
SmUW1 (88) + SmUW3 (12)	16	13	2	1
SmUW3 (11) + SmUW33 (89)	23	12	8	3
SmUW3 (54) + SmUW33 (46)	14	13	0	1
SmUW3 (92) + SmUW33 (8)	16	16	0	0
SmUW3 (5) + SmUW34 (95)	14	0	7	7
SmUW3 (33) + SmUW34 (67)	18	3	4	11
SmUW3 (83) + SmUW34 (17)	17	0	15	2
SmUW33 (4) + SmUW34 (96)	18	1	13	4
SmUW33 (29) + SmUW34 (71)	17	0	17	0
SmUW33 (81) + SmUW34 (19)	15	0	11	4
Rm1021 (2) + Rm11105 (98)	16	11	3	2
Rm1021 (19) + Rm11105 (81)	16	15	1	0
Rm1021 (65) + Rm11105 (35)	20	19	0	1
Rm1021 (6) + Rm11107 (94)	19	19	0	0
Rm1021 (39) + Rm11107 (61)	14	14	0	0
Rm1021 (86) + Rm11107 (14)	18	18	0	0
SmUW24 (9) + SmUW6 (91)	16	0	14	2
SmUW24 (92) + SmUW6 (8)	16	0	15	1
SmUW24 (99) + SmUW6 (1)	17	4	10	3
Rm1021 (30) + SmUW6 (70)	18	3	11	4
Rm1021 (81) + SmUW6 (19)	20	14	5	1
Rm1021 (98) + SmUW6 (2)	19	18	0	1

B.3 Conclusions

The relationship between EPS synthesis, PHB synthesis and rhizosphere competitiveness is undeniable but a comprehensive understanding remains elusive. It is conceivable that *S. meliloti* in the rhizosphere may use a quorum-sensing system to co-ordinate the initiation of plant invasion [265]. *S. meliloti* possesses two QS systems, the first is encoded by the *sinRI locus*, which is responsible for the production of long-chain N-acyl homoserine lactones (AHLs) [219, 220]. Previous work has shown that mutations of the *sinI* locus result in a strain with reduced nodulation efficiency, [220], and mutations in an $expR^{+}$ background completely abolish EPSII synthesis [219].

Bibliography

[1] T. Abe, T. Kobayashi, and T. Saito. Properties of a novel intracellular poly(3-hydroxybutyrate) depolymerase with high specific activity (PhaZd) in *Wautersia eutropha* H16. *J. Bacteriol.*, 187(20):6982–6990, 2005.

[2] E.K. Allen and O.N. Allen. Biochemical and symbiotic properties of the rhizobia. *Bacteriol. Rev.*, 14(4):273–330, 1950.

[3] E.J. Alm, K.H. Huang, M.N. Price, R.P. Koche, K. Keller, I.L. Dubchak, and A.P. Arkin. The microbesonline web site for comparative genomics. *Genome Res.*, 15(7):1015–1022, 2005.

[4] C.R. Amarasingham and B.D. Davis. Regulation of alpha-ketoglutarate dehydrogenase formation in *Escherichia coli*. *J. Biol. Chem.*, 240(9):3664–3668, 1965.

[5] A. Amato, B. Barbour, M. Szatkowski, and D. Attwell. Counter-transport of potassium by the glutamate uptake carrier in glial cells isolated from the tiger salamander retina. *J. Physiol.*, 479(3):371–80, 1994.

[6] P. Aneja and T.C. Charles. Poly-3-hydroxybutyrate degradation in *Rhizobium (Sinorhizobium) meliloti*: isolation and characterization of a gene encoding 3-hydroxybutyrate dehydrogenase. *J. Bacteriol.*, 181(3):849–57, 1999.

[7] P. Aneja, M. Dai, D. A. Lacorre, B. Pillon, and T. C. Charles. Heterologous complementation of the exopolysaccharide synthesis and carbon utilization phenotypes of *Sinorhizobium meliloti* Rm1021 polyhydroxyalkanoate synthesis mutants. *FEMS Microbiol. Lett.*, 239(2):277–83, 2004.

[8] P. Aneja, R. Dziak, G.Q. Cai, and T.C. Charles. Identification of an acetoacetyl coenzyme-A synthetase-dependent pathway for utilization of L-(+)-3-hydroxybutyrate in *Sinorhizobium meliloti*. *J. Bacteriol.*, 184(6):1571–1577, 2002.

[9] P. Aneja, A. Zachertowska, and T.C. Charles. Comparison of the symbiotic and competition phenotypes of *Sinorhizobium meliloti* PHB synthesis and degradation pathway mutants. *Can. J. Microbiol.*, 51(7):599–604, 2005.

[10] J. Antheunisse and L. Arkesteijn-Dijksman. Rate of drying and the survival of microorganisms. *Antonie Van Leeuwenhoek*, 45(2):177–184, 1979.

[11] R. Arwas, J.A. McKay, F.R.P. Rowney, M.J. Dilworth, and A.R. Glenn. Properties of organic acid utilization mutants of *Rhizobium leguminosarum* strain v300. *J. Gen. Microbiol.*, 131:2059–2066, 1985.

[12] K.E. Baker, K.P. Ditullio, J. Neuhard, and R.A. Kelln. Utilization of orotate as a pyrimidine source by *Salmonella typhimurium* and *Escherichia coli* required the dicarboxylate transport protein encoded by *dctA*. *J. Bacteriol.*, 178:7099–7105, 1996.

[13] B. Barbour, H. Brew, and D. Attwell. Electrogenic glutamate uptake in glial cells is activated by intracellular potassium. *Nature*, 335(6189):433–5, 1988.

[14] S. Batista, A.I. Catalan, I. Hernandez-Lucas, E. Martinez-Romero, O.M. Aguilar, and G. Martinez-Drets. Identification of a system that allows a

Rhizobium tropici dctA mutant to grow on succinate, but not on other c_4-dicarboxylates. *Can. J. Microbiol.*, 47(6):509–518, 2001.

[15] M.W. Beijerink. Die bacterien der papilionaceen-knollchen. *Bot. Ztg.*, 46:725–804, 1888.

[16] F.J. Bergersen. The bacterial component of soybean root nodules; changes in respiratory activity, cell dry weight and nucleic acid content with increasing nodule age. *J. Gen. Microbiol.*, 19(2):312–323, 1958.

[17] F.J. Bergersen and G.L. Turner. Bacteriods from soybean root nodules: Respiration and N_2-fixation in flow-chamber reactions with oxyleghaemoglobin. *Proc. R. Soc. Lond. B. Biol. Sci.*, 238(1293):295–320, 1990.

[18] F.J. Bergersen and G.L. Turner. Bacteroids from soybean root nodules: Accumulation of poly-3-hydroxybutyrate during supply of malate and succinate in relation to N_2 fixation in flow-chamber reactions. *Proc. R. Soc. Lond. B. Biol. Sci.*, 240:39–59, 1990.

[19] F.J. Bergersen and G.L. Turner. A role for poly-3-hydroxybutyrate in bacteroids of soybean root nodules. *Proc. R. Soc. Lond. B. Biol. Sci.*, 245:59–64, 1991.

[20] J.E. Beringer. R factor transfer in *Rhizobium leguminosarum*. *J. Gen. Microbiol.*, 84(1):188–198, 1974.

[21] J. Beuerlein. 2004 Ohio soybean inoculation study. Technical report, The Ohio State University, 2004.

[22] A.A. Bhagwat, R.E. Tully, and D.L. Keister. Isolation and characterization of a competition-defective *Bradyrhizobium japonicum* mutant. *Appl. Environ. Microbiol.*, 57(12):3496–3501, 1991.

[23] D. Billi and M. Potts. Life and death of dried prokaryotes. *Res. Microbiol.*, 153(1):7–12, 2002.

[24] K. Birkenhead, S.S. Manian, and F. O'Gara. Dicarboxylic acid transport in *Bradyrhizobium japonicum*: Use of *Rhizobium meliloti dct* gene(s) to enhance nitrogen fixation. *J. Bacteriol.*, 170(1):184–189, 1988.

[25] B. Boesten, J. Batut, and P. Boistard. DctBD-dependent and independent expression of the *Sinorhizobium (Rhizobium) meliloti* C_4-dicarboxylate transport gene (*dctA*) during symbiosis. *Mol. Plant Microbe Interact.*, 11:878–886, 1998.

[26] B.B. Bohlool, J.K. Ladha, D.P. Garrity, and T. George. Biological nitrogen fixation for sustainable agriculture: a perspective. *Plant Soil*, 141(1-2):1–11, 1992.

[27] E. Bolton, B. Higgisson, A. Harrington, and F. O'Gara. Dicarboxylic acid transport in *Rhizobium meliloti*: isolation of mutants and cloning of dicarboxylic acid transport genes. *Arch. Microbiol.*, 144:142–146, 1986.

[28] J.L. Botsford. Osmoregulation in *Rhizobium meliloti*: Inhibition of growth by salts. *Arch. Microbiol.*, 137:124–127, 1984.

[29] M.W. Breedveld, C. Dijkema, L.P.T.M. Zevenhuizen, and A.J.B. Zehnder. Response of intracellular carbohydrates to a NaCl shock in *Rhizobium leguminosarum* bv. *trifolii* and *Rhizobium meliloti* SU-47. *J. Gen. Microbiol.*, 139:3157–3163, 1993.

[30] M.W. Breedveld, L.P.T.M. Zevenhuizen, and A.J.B. Zehnder. Osmotically induced oligo- and polysaccharide synthesis by *Rhizobium meliloti* SU-47. *J. Gen. Microbiol.*, 136:2511–2519, 1990.

[31] E Brinkmann and J Beckwith. Analysis of the regulation of *Escherichia coli* alkaline phosphatase synthesis using deletions and ϕ 80 transducing phages. *J. Mol. Biol.*, 96:307–316, 1975.

[32] J. Brockwell. Studies on seed pelleting as an aid to legume seed inoculation. 1. coating materials, adehesives, and methods of inoculation. *Australian J. Agri. Res.*, 13(4):638–649, 1962.

[33] J. Brockwell and P.J. Bottomley. Recent advances in inoculant technology and prospects for the future. *Soil Biol. Biochem.*, 27(4/5):683–697, 1995.

[34] J. Brockwell, D.F. Herridge, J.A. Roughley, R.J. Thompson, and R.R. Gault. Studies on seed pelleting as an aid to legume seed inoculation. *Aust. J. Exp. Agric. Anim. Husb.*, 15:780–787, 1975.

[35] M. Buck, M.T. Gallegos, D.J. Studholme, Y. Guo, and J.D. Gralla. The bacterial enhancer-dependent σ_{54} (σN) transcription factor. *J. Bacteriol.*, 182(15):4129–36, 2000.

[36] R. C. Burns and R.W.F. Hardy. *Nitrogen Fixation in Bacteria and Higher Plants*. Springer-Verlag, New York, 1975.

[37] H.V.A. Bushby and K.C. Marshall. Dessication-induced damage to the cell-envelope of root nodule bacteria. *Soil Biol. Biochem.*, 9:149–152, 1977.

[38] H.V.A. Bushby and K.C. Marshall. Some factors affecting the survival of root-nodule bacteria on dessication. *Soil Biol. Biochem.*, 9:143–147, 1977.

[39] H.V.A. Bushby and K.C. Marshall. Water stress of rhizobia in relation to their susceptibility to desiccation and to their protection by montmorillonite. *J. Gen. Microbiol.*, 99:19–27, 1977.

[40] G. Cai, B.T. Driscoll, and T.C. Charles. Requirement for the enzymes acetoacetyl coenzyme-A synthetase and poly-3-hydroxybutyrate (PHB) synthase for growth of *Sinorhizobium meliloti* on PHB cycle intermediates. *J. Bacteriol.*, 182(8):2113–2118, 2000.

[41] R. Catoira, C. Galera, F. de Billy, R.V. Penmetsa, E.P. Journet, F. Maillet, C. Rosenberg, D. Cook, C. Gough, and J. Denarie. Four genes of medicago truncatula controlling components of a nod factor transduction pathway. *Plant Cell*, 12:1647–1666, 2000.

[42] G. Catroux, A. Hartmann, and C. Revellin. Trends in rhizobial inoculant production use. *Plant and Soil*, 230:21–30, 2001.

[43] M.A. Cevallos, S. Encarnacion, A. Leija, Y. Mora, and J. Mora. Genetic and physiological characterization of a *Rhizobium etli* mutant strain unable to synthesize poly-β-hydroxybutyrate. *J. Bacteriol.*, 178(6):1646–1654, 1996.

[44] T.C. Charles. *Construction of a genetic linkage map of the Rhizobium meliloti 1600 kilobase megaplasmid pRmeSU47b, generation of defined megaplasmid deletions, and study of megaplasmid-borne genes.* PhD thesis, McMaster University, 1990.

[45] T.C. Charles and P. Aneja. Methylmalonyl-CoA mutase encoding gene of *Sinorhizobium meliloti*. *Gene*, 226(1):121–127, 1999.

[46] T.C. Charles, G.Q. Cai, and P. Aneja. Megaplasmid and chromosomal loci for the PHB degradation pathway in *Rhizobium* (*Sinorhizobium*) *meliloti*. *Genetics*, 146(4):1211–20, 1997.

[47] T.C. Charles and T.M. Finan. Analysis of a 1600-kilobase *Rhizobium meliloti* megaplasmid using defined deletions generated *in vivo*. *Genetics*, 127(1):5–20, 1991.

[48] C.Y. Chen and S.C. Winans. Controlled expression of the transcriptional activator gene *virG* in *Agrobacterium tumefaciens* by using the *Escherichia coli lac* promoter. *J. Bacteriol.*, 173(3):1139–1144, 1991.

[49] F. Chen, Y. Okabe, K. Osano, and S. Tajima. Purification and characterization of an NAD-malic enzyme from *Bradyrhizobium japonicum* A1017. *Appl. Environ. Microbiol.*, 64(10):4073–4075, 1998.

[50] M. Chen and M. Alexander. Survival of soil bacteria during prolonged desiccation. *Soil Biol. Biochem.*, 5:213–221, 1973.

[51] H.P. Cheng and G.C. Walker. Succinoglycan is required for initiation and elongation of infection threads during nodulation of alfalfa by *Rhizobium meliloti*. *J. Bacteriol.*, 180(19):5183–5191, 1998.

[52] S.N. Chohan and L. Copeland. Acetoacetyl coenzyme A reductase and polyhydroxybutyrate synthesis in *Rhizobium (Cicer)* sp. Strain CC 1192. *Appl. Environ. Microbiol.*, 64(8):2859–2863, 1998.

[53] S.R. Clark, I.J. Oresnik, and M.F. Hynes. RpoN of *Rhizobium leguminosarum* bv. *viciae* strain VF39SM plays a central role in FnrN-dependent microaerobic regulation of genes involved in nitrogen fixation. *Mol. Gen. Genet.*, 264(5):623–33, 2001.

[54] S. Cliquet and G. Catroux. Influence of culture medium and growth stage on the survival of *Bradyrhizobium japonicum* during dessciation and storage at two relative humidities. *Symbiosis*, 16:279–287, 1994.

[55] J. Cohn, R.B. Day, and G Stacey. Legume nodule organogenesis. *Trends Plant Sci.*, 3:105–110, 1998.

[56] M.A. Cole and G.H. Elkan. Multiple antibiotic resistance in *Rhizobium japonicum*. *Appl. Environ. Microbiol.*, 37(5):867–870, 1979.

[57] L. Copeland, R.G. Quinnell, and D.A. Day. Malic enzyme activity in bacteroids from soybean nodules. *J. Gen. Microbiol.*, 135:2005–2011, 1989.

[58] A. Cowie, J. Cheng, C.D. Sibley, Y. Fong, R. Zaheer, C.L. Patten, R.M. Morton, G.B. Golding, and T.M. Finan. An integrated approach to functional genomics: Construction of a novel reporter gene fusion library for *Sinorhizobium meliloti*. *Appl. Environ. Microbiol.*, 72(11):7156–7167, 2006.

[59] A.J. Cozzone. Regulation of acetate metabolism by protein phosphorylation in enteric bacteria. *Annu. Rev. Microbiol.*, 52:127–164, 1998.

[60] A.S. Craig and K.L. Williamson. Three inclusions of rhizobial bacteroids and their cytochemical character. *Arch. Microbiol.*, 87:165–171, 1972.

[61] J.H. Crowe and L.M. Crowe. Preservation of membranes in anhydrobiotic organisms: The role of trehalose. *Science*, 223:701–703, 1984.

[62] J.H. Crowe, L.M. Crowe, A.E. Oliver, N. Tsvetkova, W. Wolkers, and F. Tablin. The trehalose myth revisited: Introduction to a symposium on stabilization of cells in the dry state. *Cryobiology*, 43(2):89–105, 2001.

[63] E.J. Cytryn, D.P. Sangurdekar, J.G. Streeter, W.L. Franck, W.S. Chang, G. Stacey, D.W. Emerich, T. Joshi, D. Xu, and M.J. Sadowsky. Transcriptional and physiological responses of *Bradyrhizobium japonicum* to desiccation-induced stress. *J. Bacteriol.*, 189(19):6751–6762, 2007.

[64] P. Davanloo, A.H. Rosenberg, J.J. Dunn, and F.W. Studier. Cloning and expression of the gene for bacteriophage T7 RNA polymerase. *Proc. Natl. Acad. Sci. USA*, 81(7):2035–2039, 1984.

[65] EA Dawes. Microbial energy reserve compounds. In *Microbial energetics*, pages 145–165. Blackie and Son ltd., Glasgow, 1986.

[66] E.A. Dawes and P.J. Senior. The role and regulation of energy reserve polymers in microorganisms. *Adv. Microb. Physiol.*, 10:135–266, 1973.

[67] R. Deaker, R.J. Roughley, and I.R. Kennedy. Legume seed inoculation technology: a review. *Soil Biol. Biochem.*, 36(8):1275–1288, 2004.

[68] F.P. Delafield, M. Doudoroff, N.J. Palleroni, C.J. Lusty, and R. Contopoulos. Decomposition of poly-3-hydroxybutyrate by Pseudomonads. *J. Bacteriol.*, 90(5):1455–1466, 1965.

[69] J. D. F. Denarié and J.C. Promé. Rhizobium lipo-chitooligosaccharide nodulation factors: Signaling molecules mediating recognition and morphogenesis. *Annu. Rev. Biochem.*, 65:503–535, 1996.

[70] R. F. Denison. Legume sanctions and the evolution of symbiotic cooperation by rhizobia. *American Naturalist*, 156:567–576, 2000.

[71] R.F. Denison and T.E. Kiers. Why are most rhizobia beneficial to their plant hosts, rather than parasitic? *Microbes Infect.*, 6(13):1235–9, 2004.

[72] G. Ditta, S. Stanfield, D. Corbin, and D.R. Helsinki. Broad host range DNA cloning system for gram-negative bacteria: construction of a gene bank of *Rhizobium meliloti*. *Proc. Natl. Acad. Sci. USA*, 77:7347–7351, 1980.

[73] R. Dixon. Tandem promoters determine regulation of the *Klebsiella pneumoniae* glutamine synthetase (*glnA*) gene. *Nucleic Acids Res.*, 12(20):7811–30, 1984.

[74] R.O.D. Dixon. The origin of the membrane envelope surrounding the bacteria and bacteroids and the presence of glycogen in clover root nodules. *Arch. Microbiol.*, 56:156–166, 1967.

[75] A. Dominguez-Ferreras, R. Perez-Arnedo, A. Becker, J. Olivares, M.J. Soto, and J. Sanjuan. Transcriptome profiling reveals the importance of plasmid psymb for osmoadaptation of *Sinorhizobium meliloti*. *J. Bacteriol.*, 188(21):7617–7625, 2006.

[76] D.N. Dowling, U. Samrey, J. Stanley, and W.J. Broughton. Cloning of *Rhizobium leguminosarum* genes for competitive nodulation blocking on peas. *J. Bacteriol.*, 169:1345–1348, 1987.

[77] B.T. Driscoll and T.M. Finan. NAD^+-dependent malic enzyme of *Rhizobium meliloti* is required for symbiotic nitrogen fixation. *Mol. Microbiol.*, 7(6):865–873, 1993.

[78] B.T. Driscoll and T.M. Finan. Properties of NAD^+- and $NADP^+$-dependent malic enzymes of *Rhizobium* (*Sinorhizobium*) *meliloti* and differential expression of their genes in nitrogen-fixing bacteroids. *Microbiology*, 143(2):489–498, 1997.

[79] M.J. Duncan and D.G. Fraenkel. α-ketoglutarate dehydrogenase mutant of *Rhizobium meliloti*. *J. Bacteriol.*, 137(1):415–419, 1979.

[80] M.F. Dunn. Tricarboxylic acid cycle and anaplerotic enzymes in rhizobia. *FEMS Microbiol. Rev.*, 22(2):105–123, 1998.

[81] M.F. Dunn, G. Araiza, S. Encarnacion, M. del Carmen Vargas, and J. Mora. Effect of *aniA* (carbon flux regulator) and *phaC* (poly-3-hydroxybutyrate synthase) mutations on pyruvate metabolism in *Rhizobium etli*. *J. Bacteriol.*, 184(8):2296–2299, 2002.

[82] S.I. Dymov, D.J.J. Meek, B. Steven, and B.T. Driscoll. Insertion of transposon Tn*5tac1* in the *Sinorhizobium meliloti* malate dehydrogenase (*mdh*) gene results in conditional polar effects on downstream TCA cycle genes. *Mol. Plant Microbe Interact.*, 17(12):1318–1327, 2004.

[83] B.D. Eardly, L.A. Materon, N.H. Smith, D.A. Johnson, M.D. Rumbaugh, and R.K. Selander. Genetic structure of natural populations of the nitrogen-fixing bacterium *Rhizobium meliloti*. *Appl. Environ. Microbiol.*, 56(1):187–194, 1990.

[84] A.K. El Din. A succinate transport mutant of *Bradyrhizobium japonicum* forms ineffective nodules on soybean. *Can. J. Microbiol.*, 38:230–234, 1992.

[85] G.H. Elkan. The taxonomy of the *Rhizobiaceae*. *Int. Rev. Cytology Suppl.*, 13:1–14, 1981.

[86] T.A. Else, C.R. Pantle, and P.S. Amy. Boundaries for biofilm formation: humidity and temperature. *Appl. Environ. Microbiol.*, 69(8):5006–5010, 2003.

[87] S. Encarnacion, del Carmen V.M., M.F. Dunn, G. Davalos, A.cand Mendoza, Y. Mora, and J. Mora. AniA regulates reserve polymer accumulation and global protein expression in *Rhizobium etli*. *J. Bacteriol.*, 184(8):2287–2295, 2002.

[88] M. Engelhard. *Trehalose and the nitrogen fixing nodule symbiosis of legumes: studies on rhizobia deficient in the trehalose-6-phosphate synthase gene otsA*. Doctoral, Universitat Basel, 2004.

[89] T. Engelke, M.N. Jagadish, and A. Puhler. Biochemical and genetical analysis of *Rhizobium meliloti* mutants defective in C_4-dicarboxylate transport. *J. Gen. Microbiol.*, 133:3019–29, 1987.

[90] T. Engelke, D. Jording, D. Kapp, and A. Puhler. Identification and sequence analysis of the *Rhizobium meliloti dctA* gene encoding the c_4-dicarboxylate carrier. *J. Bacteriol.*, 171(10):5551–60, 1989.

[91] T.J. Erb, I.A. Berg, V. Brecht, M. Muller, G. Fuchs, and B.E. Alber. Synthesis of C_5-dicarboxylic acids from C_2-units involving crotonyl-CoA carboxylase/reductase: the ethylmalonyl-CoA pathway. *Proc. Natl. Acad. Sci. USA*, 104(25):10631–10636, 2007.

[92] J. Felsenstein. PHYLIP – phylogeny inference package (version 3.2). *Cladistics*, 5:164–166, 1989.

[93] L. Feng, R.J. Roughley, and L. Copeland. Morphological changes of rhizobia in peat cultures. *Appl. Environ. Microbiol.*, 68(3):1064–1070, 2002.

[94] D.H. Figurski and D.R. Helsinki. Replication of an origin-containing derivative of plasmid RK2 dependent on a plasmid function provided in trans. *Proc. Natl. Acad. Sci. USA*, 76:1648–1652, 1979.

[95] T.M. Finan, E. Hartwieg, K. LeMieux, K. Bergman, G.C. Walker, and E.R. Signer. General transduction in *Rhizobium meliloti. J. Bacteriol.*, 159(1):120–124, 1984.

[96] T.M. Finan, B. Kunkel, G.F. De Vos, and E.R. Signer. Second symbiotic megaplasmid in *Rhizobium meliloti* carrying exopolysaccharide and thiamine synthesis genes. *J. Bacteriol.*, 167(1):66–72, 1986.

[97] T.M. Finan, I. Oresnik, and A. Bottacin. Mutants of *Rhizobium meliloti* defective in succinate metabolism. *J. Bacteriol.*, 170(8):3396–403, 1988.

[98] T.M. Finan, J.M. Wood, and D.C. Jordan. Succinate transport in *Rhizobium leguminosarum. J. Bacteriol.*, 148(1):193–202, 1981.

[99] T.M. Finan, J.M. Wood, and D.C. Jordan. Symbiotic properties of c_4-dicarboxylic acid transport mutants of *Rhizobium leguminosarum*. *J. Bacteriol.*, 154:1403–1413, 1983.

[100] T. Forrai, E. Vincze, Z. Banfalvi, G.B. Kiss, G.S. Randhawa, and A. Konderosi. Localization of symbiotic mutations in *Rhizobium meliloti*. *J. Bacteriol.*, 153:635–643, 1983.

[101] P.F. Fottrell and P. Mooney. The regulation of some enzymes involved in ammonia assimilation by *Rhizobium japonicum*. *J. Gen. Microbiol.*, 59(2):211–214, 1969.

[102] N. Fraysse, F. Couderc, and V. Poinsot. Surface polysaccharide involvement in establishing the rhizobium-legume symbiosis. *Eur. J. Biochem.*, 270(7):1365–1380, 2003.

[103] D.J. Gage, T. Bobo, and S.R. Long. Use of green fluorescent protein to visualize the early events of symbiosis between *Rhizobium meliloti* and alfalfa (*Medicago sativa*). *J. Bacteriol.*, 178(24):7159–7166, 1996.

[104] F. Galibert, T.M. Finan, S.R. Long, A. Puhler, P. Abola, F. Ampe, F. Barloy-Hubler, M.J. Barnett, A. Becker, P. Boistard, G. Bothe, M. Boutry, L. Bowser, J. Buhrmester, E. Cadieu, D. Capela, P. Chain, A. Cowie, R.W. Davis, S. Dreano, N.A. Federspiel, R.F. Fisher, S. Gloux, T. Godrie, A. Goffeau, B. Golding, J. Gouzy, M. Gurjal, I. Hernandez-Lucas, A. Hong, L. Huizar, R.W. Hyman, T. Jones, D. Kahn, M.L. Kahn, S. Kalman, D.H. Keating, E. Kiss, C. Komp, V. Lelaure, D. Masuy, C. Palm, M.C. Peck, T.M. Pohl, D. Portetelle, B. Purnelle, U. Ramsperger, R. Surzycki, P. Thebault, M. Vandenbol, F.J. Vorholter, S. Weidner, D.H. Wells, K. Wong, K.C. Yeh,

and J. Batut. The composite genome of the legume symbiont *Sinorhizobium meliloti*. *Science*, 293(5530):668–72, 2001.

[105] J.N. Galloway and E.B. Cowling. Reactive nitrogen and the world: 200 years of change. *Ambio*, 31(2):64–71, 2002.

[106] D Gao, A Maehara, T Yamane, and S Ueda. Identification of the intracellular polyhydroxyalkanoate depolymerase gene of *Paracoccus denitrificans* and some properties of the gene product. *FEMS Microbiol. Lett.*, 196(2):159–164, 2001.

[107] A. Gardiol, A. Arias, C. Cervenansky, and G. Martinez-Drets. Succinate dehydrogenase mutant of *Rhizobium meliloti*. *J. Bacteriol.*, 151(3):1621–1623, 1982.

[108] B. Gebauer and D. Jendrossek. Assay of poly (3-hydroxybutyrate) depolymerase activity and product determination. *Appl. Environ. Microbiol.*, 72(9):6094–6100, 2006.

[109] P. Gepts, W.D. Beavis, E.C. Brummer, R.C. Shoemaker, H.T Stalker, N.F. Weeden, and N.D. Young. Legumes as a model plant family. genomics for food and feed report of the cross-legume advances through genomics conference. *Plant Physiol.*, 137(4):1228–1235, 2005.

[110] T. Gerson, J.J. Patel, and M.N. Wong. The effects of age, darkness, and nitrate on poly-2-hydroxybutyrate levels and nitrogen-fixing ability of rhizobium in lupinus angustifoli. *Physiologia Plantarum*, 42:420–424, 1978.

[111] L. Giblin, J. Archdeacon, and F. O'Gara. Modular structure of the *Rhizobium meliloti* dctb protein. *FEMS Microbiol. Lett.*, 139(1):19–25, 1996.

[112] L. Giblin, B. Boesten, S. Turk, P. Hooykaas, and F. O'Gara. Signal transduction in the *Rhizobium meliloti* dicarboxylic acid transport system. *FEMS Microbiol. Lett.*, 126(1):25–30, 1995.

[113] J. Glazebrook and G.C. Walker. A novel exopolysaccharide can function in place of the calcofluor-binding exopolysaccharide in nodulation of alfalfa by *Rhizobium meliloti*. *Cell*, 56(4):661–672, 1989.

[114] A.R. Glenn and N.J. Brewin. Succinate-resistant mutants of *Rhizobium leguminosarum*. *J. Gen. Microbiol.*, 126:237–241, 1981.

[115] A.R. Glenn and M.J. Dilworth. Oxidation of substrates by isolated bacteroids and free-living cells of *Rhizobium leguminosarum* 3841. *J. Gen. Microbiol.*, 126:243–247, 1981.

[116] A.R. Glenn and M.J. Dilworth. The uptake and hydrolysis of disaccharides by fast- and slow-growing species of *Rhizobium*. *Arch. Microbiol.*, 129:233–239, 1981.

[117] A.R. Glenn and M.J. Dilworth. Methylamine and ammonium transport systems in *Rhizobium leguminosarum*. *J. Gen. Microbiol.*, 103:1961–1968, 1984.

[118] S.A. Glenn, N. Gurich, M.A. Feeney, and J.E. Gonzalez. The ExpR/Sin quorum-sensing system controls succinoglycan production in *Sinorhizobium meliloti*. *J. Bacteriol.*, 189(19):7077–7088, 2007.

[119] J.E. Gonzalez, B.L. Reuhs, and G.C. Walker. Low molecular weight EPS II of *Rhizobium meliloti* allows nodule invasion in *Medicago sativa*. *Proc. Natl. Acad. Sci. USA*, 93(16):8636–8641, 1996.

[120] J.E. Gonzalez, G.M. York, and G.C. Walker. *Rhizobium meliloti* exopolysaccharides: synthesis and symbiotic function. *Gene*, 179(1):141–146, 1996.

[121] V. Gonzalez, R.I. Santamaria, P. Bustos, I. Hernandez-Gonzalez, A. Medrano-Soto, G. Moreno-Hagelsieb, S.C. Janga, M.A. Ramirez, V. Jimenez-Jacinto, J. Collado-Vides, and G. Davila. The partitioned *Rhizobium etli* genome: Genetic and metabolic redundancy in seven interacting replicons. *Proc. Natl. Acad. Sci. USA*, 103(10):3834–3839, 2006.

[122] D.J. Goodchild and F.J. Bergersen. Electron microscopy of the infection and subsequent development of soybean nodule cells. *J. Bacteriol.*, 92(1):204–213, 1966.

[123] M. Gottfert, S. Rothlisberger, C. Kundig, C. Beck, R. Marty, and H. Hennecke. Potential symbiosis-specific genes uncovered by sequencing a 410-kilobase DNA region of the *Bradyrhizobium japonicum* chromosome. *J. Bacteriol.*, 183(4):1405–1412, 2001.

[124] K. Gouffi, N. Pica, V. Pichereau, and C. Blanco. Disaccharides as a new class of nonaccumulated osmoprotectants for *Sinorhizobium meliloti*. *Appl. Environ. Microbiol.*, 65(4):1491–500, 1999.

[125] P.H. Graham and C.A. Parker. Diagnostic features in the characterization of the root-nodule bacteria of legumes. *Plant Soil*, 20:383–396, 1964.

[126] P.H. Graham and C.P. Vance. Legumes: Importance and constraints to greater use. *Plant Physiol.*, 131(3):872–877, 2003.

[127] C.T. Gray, J.W. Wimpenny, and M.R. Mossman. Regulation of metabolism in facultative bacteria. II. Effects of aerobiosis, anaerobiosis and nutrition on the formation of Krebs cycle enzymes in *Escherichia coli*. *Biochim. Biophys. Acta.*, 117(1):33–41, 1966.

[128] L.S. Green and D.W. Emerich. The formation of Nitrogen-fixing bacteroids is delayed but not abolished in soybean infected by an α-Ketoglutarate

dehydrogenase-deficient mutant of *Bradyrhizobium japonicum*. *Plant Physiol.*, 114(4):1359–1368, 1997.

[129] L.S. Green and D.W. Emerich. *Bradyrhizobium japonicum* does not require α-ketoglutarate dehydrogenase for growth on succinate or malate. *J. Bacteriol.*, 179(1):194–201, 1997.

[130] L.S. Green, D.B. Karr, and D.W. Emerich. Isocitrate dehydrogenase and glyoxylate cycle enzyme activities in *Bradyrhizobium japonicum* under various growth conditions. *Arch. Microbiol.*, 169(5):445–451, 1998.

[131] L.S. Green, Y. Li, D.W. Emerich, F.J. Bergersen, and D.A. Day. Catabolism of α-ketoglutarate by a *sucA* mutant of *Bradyrhizobium japonicum*: evidence for an alternative tricarboxylic acid cycle. *J. Bacteriol.*, 182(10):2838–2844, 2000.

[132] P. M. Gresshoff and B.G. Rolfe. Viability of Rhizobium bacteroids isolated from soybean nodule protoplasts. *Planta*, 142:329–333, 1978.

[133] B. Gu, J.H. Lee, T.R. Hoover, D. Scholl, and B.T. Nixon. *Rhizobium meliloti* DctD, a σ_{54}-dependent transcriptional activator, may be negatively controlled by a subdomain in the c-terminal end of its two-component receiver module. *Mol. Microbiol.*, 13(1):51–66, 1994.

[134] A. Hadri, H.P. Spaink, T. Bisseling, and N.J. Brewin. Diversity of root nodulation and rhizobial infection processes. In H.P. Spaink, A. Kopndorosi, and P.J.J. Hooykaas, editors, *The Rhizobiaceae: molecular biology of model plant-associated bacteria*. Kluwer Academic Publishers, Dordrecht, Boston, London, 1998.

[135] M.L. Hahn, D. Meyer, B. Studer, B. Regensburger, and H. Hennecke. Insertion and deletion mutations within the *nif* region of *Rhizobium japonicum*. *Plant Mol. Bio.*, 3:159–168, 1984.

[136] D. Hanahan. Studies on transformation of *Escherichia coli* with plasmids. *J. Mol. Biol.*, 166(4):557–80, 1983.

[137] G. Hardason. Methods for measuring biological nitrogen fixation in grain legumes. *Plant Soil*, 152(1):1–17, 1993.

[138] R.W.F. Hardy and U.D. Havelka. Photosynthase as a major limitation to N_2-fixation by field-grown legumes with an emphasis on soybeans. In P.S. Nutman, editor, *International biological programme, symbiotic nitrogen fixation in plants*. Cambridge University Press, 1975.

[139] P.G. Hartel and M. Alexander. Role of extracellular polysaccharide production and clays in the desiccation tolerance of cowpea *Bradyrhizobia*. *Soil Sci. Soc. Am. J.*, 50:1193–1198, 1986.

[140] J.L. Hatfield and J.H. Prueger. Nitrogen over-use, under-use, and efficiency. In *New directions for a diverse planet: Proceedings of the 4th International Crop Science Congress*, 2004.

[141] U.D. Havelka and R.W.F. Hardy. Legume N_2 fixation as a problem of carbon nutrition. In *Proceedings of the first international symposium on nitrogen fixation*. Washington State University Press, 1976.

[142] G.W. Haywood, A.J. Anderson, L. Chu, and E.A. Dawes. The role of NADH- and NADPH-linked acetoacetyl-CoA reductases in the poly-3-hydroxybutyrate synthesizing organism *Alcaligenes eutrophus*. *FEMS Microbiol. Lett.*, 52:259–264, 1988.

[143] G.W. Haywood, A.J. Anderson, and E.A. Dawes. The importance of PHB-synthase substrate specificity in polyhydroxyalkanoate synthesis by *Alcaligenes eutrophus*. *FEMS Microbiol. Lett.*, 57:1–6, 1989.

[144] H. Hellriegel and H. Wilfarth. Untersuchungen uber die stickstoffnahrung der gramineen und leguminosen. *Rubenzucker-Ind., Dtsh. Reichs.*, page 234, 1888.

[145] F.W. Hely. Survival studies with *Rhizobium trifolii* on seed of *Trifolium incartum* l. inoculated for aerial sowing. *Australian J. Agri. Res.*, 16(4):575–589, 1965.

[146] G.R. Her, J. Glazebrook, G.C. Walker, and V.N. Reinhold. Structural studies of a novel exopolysaccharide produced by a mutant of *Rhizobium meliloti* strain Rm1021. *Carbohydr. Res.*, 198(2):305–312, 1990.

[147] I. Hernandez-Lucas, M.A. Pardo, L. Segovia, J. Miranda, and E. Martinez-Romero. *Rhizobium tropici* chromosomal citrate synthase gene. *Appl. Environ. Microbiol.*, 61(11):3992–3997, 1995.

[148] A.M. Hirsch, M. Bang, and F.M. Ausubel. Ultrastructural analysis of ineffective alfalfa nodules formed by *nif*::Tn*5* mutants of *Rhizobium meliloti*. *J. Bacteriol.*, 155(1):367–380, 1983.

[149] A.M. Hirsch, S.R. Long, M. Bang, N. Haskins, and F.M. Ausubel. Structural studies of alfalfa roots infected with nodulation mutants of *Rhizobium meliloti*. *J. Bacteriol.*, 151(1):411–419, 1982.

[150] H.H. Hoang, A. Becker, and J.E. Gonzalez. The LuxR homolog ExpR, in combination with the Sin quorum sensing system, plays a central role in *Sinorhizobium meliloti* gene expression. *J. Bacteriol.*, 186(16):5460–5472, 2004.

[151] R.G. Hoeft and E.D. Nafziger. Getting the most from your 2001 nitrogen dollars, January 2001 2001.

[152] I. Hoelzle and J.G. Streeter. Increased accumulation of trehalose in rhizobia cultured under 1% oxygen. *Appl. Environ. Microbiol.*, 56:3213–3215, 1990.

[153] K. Hofmann, E.B. Heinz, T.C. Charles, M. Hoppert, W. Liebl, and W.R. Streit. *Sinorhizobium meliloti* strain 1021 *bioS* and *bdhA* gene transcriptions are both affected by biotin available in defined medium. *FEMS Microbiol. Lett.*, 182(1):41–44, 2000.

[154] R.M. Horton, H.D. Hunt, S.N. Ho, J.K. Pullen, and L.R. Pease. Engineering hybrid genes without the use of restriction enzymes: Gene splicing by overlap extension. *Gene*, 77(1):61–68, 1989.

[155] R.W. Howarth, E.W. Boyer, W.J. Pabich, and J.N. Galloway. Nitrogen use in the united states from 1961–2000 and potential future trends. *Ambio*, 31(2):88–96, 2002.

[156] E.R. Hull and P.D.J. Weitzman. Evidence for allosteric NADH regulation of *Acinetobacter* α-oxoglutarate dehydrogenase from multiple inhibition studies. *Biochem. Biophys. Res. Comm.*, 74:1613–1617, 1977.

[157] C. Humbeck and D. Werner. Delayed nodule development in a succinate transport mutants of *Bradyrhizobium japonicum*. *J. Plant Physiol.*, 134:276–283, 1989.

[158] T.P. Hunt and B. Magasanik. Transcription of *glnA* by purified *Escherichia coli* components: Core RNA polymerase and the products of *glnF, glnG*, and *glnL*. *Proc. Natl. Acad. Sci. USA*, 82(24):8453–7, 1985.

[159] W. Huth, C. Dierich, V. von Oeynhausen, and W Seubert. Multiple mitochondrial forms of acetoacetyl-CoA thiolase in rat liver: Possible regulatory role in ketogenesis. *Biochem. Biophys. Res. Commun.*, 56(4):1069–1077, 1974.

[160] F.A. Jackson and E.A. Dawes. Regulation of the tricarboxylic acid cycle and poly-3-hydroxybutyrate metabolism in *Azotobacter beijerinckii* grown under nitrogen and oxygen limitation. *J. Gen. Microbiol.*, 97:303–312, 1976.

[161] A.I. Jacob, S.A.I. Adham, D.S. Capstick, S.R.D. Clark, T. Spence, and T.C. Charles. Mutational analysis of the *Sinorhizobium meliloti* short-chain dehydrogenase/reductase family reveals substantial contribution to symbiosis and catabolic diversity. *Mol. Plant Microbe Interact.*, 21(7):979–987, 2008.

[162] K.E. Jaeger, S. Ransac, B.W. Dijkstra, C. Colson, M. van Heuvel, and O. Misset. Bacterial lipases. *FEMS Microbiol. Rev.*, 15(1):29–63, 1994.

[163] I.G. Janausch, E. Zientz, Q.H. Tran, A. Kroger, and G. Unden. C_4-dicarboxylate carriers and sensors in bacteria. *Biochim. Biophys. Acta.*, 1553(1-2):39–56, 2002 Jan 17.

[164] D. Jendrossek and R. Handrick. Microbial degradation of polyhydroxyalkanoates. *Annu. Rev. Microbiol.*, 56:403–432, 2002.

[165] L.S. Jenkins and W.D. Nunn. Genetic and molecular characterization of the genes involved in short-chain fatty acid degradation in *Escherichia coli*: the *ato* system. *J. Bacteriol.*, 169(1):42–52, 1987.

[166] J.B. Jensen, N.K. Peters, and T.V. Bhuvaneswari. Redundancy in periplasmic binding protein-dependent transport systems for trehalose, sucrose, and maltose in *Sinorhizobium meliloti*. *J. Bacteriol.*, 184(11):2978–86, 2002.

[167] J.Q. Jiang, W. Wei, B.H. Du, X.H. Li, L. Wang, and S.S. Yang. Salt-tolerance genes involved in cation efflux and osmoregulation of *Sinorhizobium fredii* RT19 detected by isolation and characterization of Tn*5* mutants. *FEMS Microbiol. Lett.*, 239(1):139–146, 2004.

[168] G.V. Johnson, J. Evans, and T. Ching. Enzymes of the glyoxylate cycle in Rhizobia and nodules of legumes. *Plant Physiol.*, 41:1330–1336, 1966.

[169] J.D. Jones and N. Gutterson. An efficient mobilizable cosmid vector, pRK7813, and its use in a rapid method for marker exchange in *Pseudomonas fluorescens* strain HV37a. *Gene*, 61(3):299–306, 1987.

[170] D.C. Jordan, I. Grinyer, and W.H. Coulter. Electron microscopy of infection threads and bacteria in young root nodules of medicago sativa. *J. Bacteriol.*, 86(1):125–137, 1963.

[171] L. Jurasek and R.H. Marchessault. The role of phasins in the morphogenesis of poly(3)-hydroxybutyrate) granules. *Biomacromol.*, 3(2):256–261, 2002.

[172] D. Kadouri, S. Burdman, E. Jurkevitch, and Y. Okon. Identification and isolation of genes involved in poly-3-hydroxybutyrate biosynthesis in *Azospirillum brasilense* and characterization of a *phbC* mutant. *Appl. Environ. Microbiol.*, 68(6):2943–2949, 2002.

[173] D. Kadouri, E. Jurkevitch, and Y. Okon. Involvement of the reserve material poly-β-hydroxybutyrate in *Azospirillum brasilense* stress endurance and root colonization. *Appl. Environ. Microbiol.*, 69:3244–3250, 2003.

[174] D. Kadouri, E. Jurkevitch, and Y. Okon. Poly-β-hydroxybutyrate depolymerase (PhaZ) in *Azospirillum brasilense* and characterization of a *phaZ* mutant. *Arch. Microbiol.*, 180(5):309–318, 2003.

[175] M.L. Kahn, J. Kraus, and J.E. Sommerville. A model of nutrient exchange in the Rhizobium-legume symbiosis. In H.J. Evans, P.J. Bottomley, and W.E. Newton, editors, *Nitrogen Fixation Research Progress*, pages 193–199. Martinus Nijhoff, Dordrecht, 1985.

[176] T. Kaneko, Y. Nakamura, S. Sato, E. Asamizu, T. Kato, S. Sasamoto, A. Watanabe, K. Idesawa, A. Ishikawa, K. Kawashima, T. Kimura, Y. Kishida, C. Kiyokawa, M. Kohara, M. Matsumoto, A. Matsuno, Y. Mochizuki, S. Nakayama, N. Nakazaki, S. Shimpo, M. Sugimoto, C. Takeuchi, M. Yamada, and S. Tabata. Complete genome structure of the nitrogen-fixing symbiotic bacterium *Mesorhizobium loti* (supplement). *DNA Res.*, 7(6):381–406, 2000.

[177] T. Kaneko, Y. Nakamura, S. Sato, E. Asamizu, T. Kato, S. Sasamoto, A. Watanabe, K. Idesawa, A. Ishikawa, K. Kawashima, T. Kimura, Y. Kishida, C. Kiyokawa, M. Kohara, M. Matsumoto, A. Matsuno, Y. Mochizuki, S. Nakayama, N. Nakazaki, S. Shimpo, M. Sugimoto, C. Takeuchi, M. Yamada, and S. Tabata. Complete genome structure of the nitrogen-fixing symbiotic bacterium *Mesorhizobium loti*. *DNA Res.*, 7(6):331–338, 2000.

[178] T. Kaneko, Y. Nakamura, S. Sato, K. Minamisawa, T. Uchiumi, S. Sasamoto, A. Watanabe, K. Idesawa, M. Iriguchi, K. Kawashima, M. Kohara, M. Matsumoto, S. Shimpo, H. Tsuruoka, T. Wada, M. Yamada, and S. Tabata. Complete genomic sequence of nitrogen-fixing symbiotic bacterium *Bradyrhizobium japonicum* USDA110. *DNA Res.*, 9(6):189–97, 2002.

[179] T. Kaneko, Y. Nakamura, S. Sato, K. Minamisawa, T. Uchiumi, S. Sasamoto, A. Watanabe, K. Idesawa, M. Iriguchi, K. Kawashima, M. Kohara, M. Matsumoto, S. Shimpo, H. Tsuruoka, T. Wada, M. Yamada, and S. Tabata.

Complete genomic sequence of nitrogen-fixing symbiotic bacterium *Bradyrhizobium japonicum* USDA110 (supplement). *DNA Res.*, 9(6):225–256, 2002.

[180] B.I. Kanner and I. Sharon. Active transport of l-glutamate by membrane vesicles isolated from rat brain. *Biochemistry*, 17(19):3949–53, 1978.

[181] D.B. Karr, J.K. Waters, and D.W. Emerich. Analysis of poly-3-hydroxybutyrate in *Rhizobium japonicum* bacteroids by ion-exclusion high-pressure liquid chromatography and UV detection. *Appl. Environ. Microbiol.*, 46(6):1339–1344, 1983.

[182] D.B. Karr, J.K. Waters, F. Suzuki, and D.W. Emerich. Enzymes of the poly-3-hydroxybutyrate and citric acid cycles of *Rhizobium japonicum* bacteroids. *Plant Physiol.*, 75(4):1158–1162, 1984.

[183] M. Keller, A. Roxlau, W.M. Weng, M. Schmidt, J. Quandt, K. Niehaus, D. Jording, W. Arnold, and A. Puhler. Molecular analysis of the *Rhizobium meliloti mucR* gene regulating the biosynthesis of the exopolysaccharides succinoglycan and galactoglucan. *Mol. Plant Microbe Interact.*, 8(2):267–277, 1995.

[184] J. Kidwell, H.E. Valentin, and D. Dennis. Regulated expression of the *Alcaligenes eutrophus* PHA biosynthesis genes in *Escherichia coli*. *Appl. Environ. Microbiol.*, 61(4):1391–1398, 1995.

[185] E.T. Kiers, R.A. Rousseau, S.A. West, and R.F. Denison. Host sanctions and the legume–rhizobium mutualism. *Nature*, 425:78–81, 2003.

[186] S.A. Kim and L. Copeland. Enzymes of poly-(beta)-hydroxybutyrate metabolism in soybean and chickpea bacteroids. *Appl. Environ. Microbiol.*, 62:4186–4190, 1996.

[187] A.H. Klein, A. Shulla, S.A. Reimann, D.H. Keating, and A.J. Wolfe. The intracellular concentration of acetyl phosphate in *Escherichia coli* is sufficient for direct phosphorylation of two-component response regulators. *J. Bacteriol.*, 189(15):5574–5581, 2007.

[188] R.V. Klucas and H.J. Evans. An electron donor system for nitrogenase-dependent acetylene reduction by extracts of soybean nodules. *Plant Physiol.*, 43(9):1458–1460, 1968.

[189] T. Kobayashi, K. Nishikori, and T. Saito. Properties of an intracellular poly(3-hydroxybutyrate) depolymerase (PhaZ1) from *Rhodobacter spheroides*. *Curr. Microbiol.*, 49(3):199–202, 2004.

[190] H.L. Kornberg. The role and control of the glyoxylate cycle in *Escherichia coli*. *Biochem. J.*, 99(1):1–11, 1966.

[191] S. Kornfeld, M. Benziman, and Y. Milner. α-ketoglutarate dehydrogenase complex of *Acetobacter xylinum*. *J. Biol. Chem.*, 252:2940–2947, 1977.

[192] N. Korotkova, L. Chistoserdova, and M.E. Lidstrom. Poly-β-hydroxybutyrate biosynthesis in the facultative methylotroph *Methylobacterium extorquens* AM1: Identification and mutation of *gap11, gap20,* and *phaR*. *J. Bacteriol.*, 184(22):6174–6181, 2002.

[193] N. Korotkova and M.E. Lidstrom. Connection between poly-β-hydroxybutyrate biosynthesis and growth on C_1 and C_2 compounds in the methylotroph *Methylobacterium extorquens* AM1. *J. Bacteriol.*, 183(3):1038–1046, 2001.

[194] J.W. Kosanke, R.M. Osburn, G.I. Shuppe, and R.S. Smith. Slow rehydration improves the recovery of dried bacterial populations. *Can. J. Microbiol.*, 38(6):520–525, 1992.

[195] H. Kouchi, K. Fukai, H. Katagiri, K. Minamisawa, and S. Tajima. Isolation and enzymological characterization of infected and uninfected cell protoplasts from root nodules of *Glycine max*. *Physiologia Plantarum*, 73(3):327–334, 2006.

[196] M.E. Kovach, P.H. Elzer, D.S. Hill, G.T. Robertson, M.A. Farris, R.M. Roop, and K.M. Peterson. Four new derivatives of the broad-host-range cloning vector pBBR1MCS, carrying different antibiotic-resistance cassettes. *Gene*, 166:175–176, 1995.

[197] I. Kullik, S. Fritsche, H. Knobel, J. Sanjuan, H. Hennecke, and H.M. Fischer. *Bradyrhizobium japonicum* has two differentially regulated, functional homologs of the sigma 54 gene (*rpoN*). *J. Bacteriol.*, 173(3):1125–1138, 1991.

[198] C. Kundig, H. Hennecke, and M. Gottfert. Correlated physical and genetic map of the *Bradyrhizobium japonicum* 110 genome. *J. Bacteriol.*, 175(3):613–622, 1993.

[199] M. Labes and T. M. Finan. Negative regulation of σ_{54}-dependent *dctA* expression by the transcriptional activator DctD. *J. Bacteriol.*, 175(9):2674–81, 1993.

[200] JH Law and RA Slepecky. Assay of poly-3-hydroxybutyric acid. *J. Bacteriol.*, 82:33–36, 1961.

[201] D.B. Layzell. Oxygen and the control of nodule metabolism and N_2 fixation. *In "Biological Nitrogen Fixation for the 21st Century" Elmerich, C. et al., eds.*, pages 4435–440, 1998.

[202] D.B. Layzell, S. Hunt, and G.R. Palmer. Mechanism of nitrogenase inhibition in soybean nodules. pulse-modulated spectroscopy indicates that nitrogenase activity is limited by O_2. *Plant Physiol.*, 92:1101–1107, 1990.

[203] H. Ledebur, B. Gu, J. Sojda, and B.T. Nixon. *Rhizobium meliloti* and *Rhizobium leguminosarum dctD* gene products bind to tandem sites in an activation sequence located upstream of sigma 54-dependent *dctA* promoters. *J. Bacteriol.*, 172(7):3888–97, 1990.

[204] H. Ledebur and B.T. Nixon. Tandem DctD-binding sites of the *Rhizobium meliloti dctA* upstream activating sequence are essential for optimal function despite a 50- to 100-fold difference in affinity for DctD. *Mol. Microbiol.*, 6(23):3479–92, 1992.

[205] J.H. Lee and T.R. Hoover. Protein crosslinking studies suggest that *Rhizobium meliloti* C_4-dicarboxylic acid transport protein D, a sigma 54-dependent transcriptional activator, interacts with σ54 and the β-subunit of RNA polymerase. *Proc. Natl. Acad. Sci. USA*, 92(21):9702–6, 1995.

[206] J.H. Lee, D. Scholl, B.T. Nixon, and T.R. Hoover. Constitutive ATP hydrolysis and transcription activation by a stable, truncated form of *Rhizobium meliloti* DctD, a σ_{54}-dependent transcriptional activator. *J. Biol. Chem.*, 269(32):20401–20409, 1994.

[207] J.A. Leigh, E.R. Signer, and G.C. Walker. Exopolysaccharide-deficient mutants of *Rhizobium meliloti* that form ineffective nodules. *Proc. Natl. Acad. Sci. USA*, 82(18):6231–5, 1985.

[208] R.D. Lins, C.S. Pereira, and P.H. Hunenberger. Trehalose-protein interaction in aqueous solution. *Proteins*, 55(1):177–86, 2004.

[209] J. Lloret, L. Bolanos, M.M. Lucas, J.M. Peart, N.J. Brewin, I. Bonilla, and R. Rivilla. Ionic stress and osmotic pressure induce different alterations in the lipopolysaccharide of a *Rhizobium meliloti* strain. *Appl. Environ. Microbiol.*, 61(10):3701–3704, 1995.

[210] J. Lloret, B.B. Wulff, J.M. Rubio, J.A. Downie, I. Bonilla, and R. Rivilla. Exopolysaccharide II production is regulated by salt in the halotolerant strain *Rhizobium meliloti* EFB1. *Appl. Environ. Microbiol.*, 64(3):1024–1028, 1998.

[211] E.M. Lodwig, A.H.F. Hosie, A. Bourdes, K. Findlay, D. Allaway, R. Karunakaran, J.A. Downie, and P.S. Poole. Amino-acid cycling drives nitrogen fixation in the legume-rhizobium symbiosis. *Nature*, 422:722–726, 2003.

[212] E.M. Lodwig, M. Leonard, S. Marroqui, T.R. Wheeler, K. Findlay, J.A. Downie, and P.S. Poole. Role of polyhydroxybutyrate and glycogen as carbon storage compounds in pea and bean bacteroids. *Mol. Plant Microbe Interact.*, 18(1):67–74, 2005.

[213] E.M. Lodwig and P.S. Poole. Metabolism of Rhizobium bacteroids. *Crit. Rev. Plant Sci.*, 22(1):37–78, 2003.

[214] S.R. Long, S. McCune, and G.C. Walker. Symbiotic loci of *Rhizobium meliloti* identified by random Tn*phoA* mutagenesis. *J. Bacteriol.*, 170(9):4257–65, 1988.

[215] S.R. Long, J.W. Reed, J. Himawan, and G.C. Walker. Genetic analysis of a cluster of genes required for synthesis of the calcofluor-binding exopolysaccharide of *Rhizobium meliloti*. *J. Bacteriol.*, 170(9):4239–48, 1988.

[216] N.I. Lopez, M.E. Floccari, A.F. Garcia, A. Steinbuchel, and B.S. Mendez. Effect of poly(3-hydroxybutyrate) (PHB) content on the starvation survival of bacteria in natural waters. *FEMS Microbiol. Ecol.*, 16:95–102, 1995.

[217] L.L. Madison and G.W. Huisman. Metabolic engineering of poly(3-hydroxyalkanoates): from dna to plastic. *Microbiol. Mol. Biol. Rev.*, 63(1):21–53, 1999.

[218] N.C. Mandal and P.K. Chakrabartty. Enzymes of carbohydrate metabolism in fast-growing Rhizobium grown on hexoses or succinate. *Indian J. Biochem. Biophys.*, 26(2):120–122, 1989.

[219] M.M. Marketon, S.A. Glenn, A. Eberhard, and J.E. Gonzalez. Quorum sensing controls exopolysaccharide production in *Sinorhizobium meliloti*. *J. Bacteriol.*, 185(1):325–31, 2003.

[220] M.M. Marketon and J.E. Gonzalez. Identification of two quorum-sensing systems in *Sinorhizobium meliloti*. *J. Bacteriol.*, 184(13):3466–3475, 2002.

[221] S. Marroqui, A. Zorreguieta, C. Santamaria, F.J. Temprano, M. Soberon, M. Megias, and J.A. Downie. Enhanced symbiotic performance by *Rhizobium tropici* glycogen synthase mutants. *J. Bacteriol.*, 183:854–864, 2001.

[222] P. Mary, N. Dupuy, C. Dolhem-Biremon, C. Defives, and R. Taillez. Differences among *Rhizobium meliloti* and *Bradyrhizobium japonicum* strains in tolerance to dessication and storage at different relative humidities. *Soil Biol. Biochem.*, 26:1125–1132, 1994.

[223] P. Mary, N. Moschetto, and R. Tailliez. Production and survival during storage of spray-dried *Bradyrhizobium japonicum* cell concentrates. *J. Appl. Bacteriol.*, 74:340–344, 1993.

[224] P. Mary, D. Ochin, and R. Tailliez. Rates of drying and survival of *Rhizobium meliloti* strains during storage at different relative humidities. *Appl. Environ. Microbiol.*, 50(2):207–211, 1985.

[225] P. Mary, D. Ochin, and R. Tailliez. Growth status of rhizobia in relation to their tolerance to low water activities and desiccation stress. *Soil Biol. Biochem.*, 18:179–184, 1986.

[226] L.A. Materon and R.W. Weaver. Inoculant maturity influences survival of rhizobia on seed. *Appl. Environ. Microbiol.*, 49(2):465–467, 1985.

[227] P. Matson, K. Lohse, and S.J. Hall. The globalization of nitrogen: consequences for terrestrial ecosystems. *Ambio*, 31:113–119, 2002.

[228] H. Matsubara, E.R. Liman, P. Hess, and G. Koren. Pretranslational mechanisms determine the type of potassium channels expressed in the rat skeletal and cardiac muscles. *J. Biol. Chem.*, 266(20):13324–8, 1991.

[229] C.F. McAllister and J.E. Lepo. Succinate transport by free-living forms of *Rhizobium japonicum*. *J. Bacteriol.*, 153(3):1155–1162, 1983.

[230] W.R. McCleary, J.B. Stock, and A.J. Ninfa. Is acetyl phosphate a global signal in *Escherichia coli*? *J. Bacteriol.*, 175(10):2793–2798, 1993.

[231] T. R. McDermott, P.H. Graham, and D.H. Brandwein. Viability of *Bradyrhizobium japonicum* bacteroids. *Arch. Microbiol.*, 148(100-106), 1987.

[232] T.R. McDermott, S.M. Griffith, C.P. Vance, and P.H. Graham. Carbon metabolism in *Bradyrhizobium japonicum* bacteroids. *FEMS Microbiol. Rev.*, 63(327-340), 1989.

[233] T.R. McDermott and M.L. Kahn. Cloning and mutagenesis of the *Rhizobium meliloti* isocitrate dehydrogenase gene. *J. Bacteriol.*, 174(14):4790–4797, 1992.

[234] I.A. McKay, M.J. Dilworth, and A.R. Glenn. C_2-dicarboxylate metabolism in free-living and bacteroid forms of *Rhizobium leguminosarum* MNF3841. *J. Gen. Microbiol.*, 134:1433–1440, 1988.

[235] D.G. McRae, R.W. Miller, and W.B. Berndt. Viability of alfalfa nodule bacteroids isolated by density gradient centrifugation. *Symbiosis*, 7:67–80, 1989.

[236] H.M. Meade, S.R. Long, G.B. Ruvkun, S.E. Brown, and F.M. Ausubel. Physical and genetic characterization of symbiotic and auxotrophic mutants of *Rhizobium meliloti* induced by transposon Tn*5* mutagenesis. *J. Bacteriol.*, 149(1):114–22, 1982.

[237] K.E. Mendrygal and J.E. Gonzalez. Environmental regulation of exopolysaccharide production in *Sinorhizobium meliloti*. *J. Bacteriol.*, 182(3):599–606, 2000.

[238] N. Mercam. Production of polyhydroxybutyrate (PHB) by some rhizobium bacteria. *Turk. J. Biol.*, 26:215–219, 2002.

[239] P. Mergaert, T. Uchiumi, B. Alunni, G. Evanno, A. Cheron, O. Catrice, A. Mausset, F. Barloy-Hubler, F. Galibert, A. Kondorosi, and E. Kondorosi. Eukaryotic control on bacterial cell cycle and differentiation in the rhizobium-legume symbiosis. *Proc. Natl. Acad. Sci. USA*, 103(13):5230–5235, 2006.

[240] J. M. Merrick and M. Doudoroff. Depolymerization of poly-3-hydroxybutyrate by an intracellular enzyme system. *J. Bacteriol.*, 88(1):72–80, 1964.

[241] M.J. Merrick. In a class of its own–the RNA polymerase sigma factor σ_{54} (σN). *Mol. Microbiol.*, 10(5):903–9, 1993.

[242] J. Michiels, M. Moris, B. Dombrecht, C. Verreth, and J. Vanderleyden. Differential regulation of *Rhizobium etli rpoN2* gene expression during symbiosis and free-living growth. *J. Bacteriol.*, 180(14):3620–8, 1998.

[243] J.H. Miller. *Experiments in molecular genetics*. Cold Spring Harbor Laboratory. Cold Spring Harbor, NY. USA, 1972.

[244] M. Miller-Williams, P.C. Loewen, and I.J. Oresnik. Isolation of salt-sensitive mutants of *Sinorhizobium meliloti* strain Rm1021. *Microbiology*, 152(7):2049–2059, 2006.

[245] M. Miyake, K. Kataoka, M. Shirai, and Y. Asada. Control of poly-β-hydroxybutyrate synthase mediated by acetyl phosphate in cyanobacteria. *J. Bacteriol.*, 179(16):5009–13, 1997.

[246] R.M. Mohammad, M. Akhavan-Khara, W.F. Campbell, and M.D. Rumbaugh. Identification of salt- and drought-tolerant *Rhizobium meliloti* l. strains. *Plant Soil*, 134:271–276, 1991.

[247] D.L. Morris. Quantitative determination of carbohydrates with dreywood's anthrone reagent. *Science*, 107(2775):254–255, 1948.

[248] National Research Council. Biological nitrogen fixation research challenges - a review of research grants funded by the U.S. Agency for International Development, 1994.

[249] T. Nishimura, T. Saito, and K. Tomita. Purification and properties of β-ketothiolase from *Zoogloea ramigera*. *Arch. Microbiol.*, 116(1):21–27, 1978.

[250] H. Odame. Biofertilizer in Kenya: Research, production and extension dilemmas. *Biotechnology and Development Monitor*, 30:2023, 1997.

[251] G. O'Hara, R. Yates, and J. Howieson. Selection of strains of root nodule bacteria to improve inoculant performance and increase legume productivity in stressful environments. In D. Herridge, editor, *Inoculants and nitrogen*

fixation of legumes in Vietnam, volume 109e, pages 75–80, Hanoi, Vietnam, 2001. ACIAR Proceedings.

[252] Y. Okon and R. Itzigsohn. Poly-β-hydroxybutyrate metabolism in *Azospirillum brasilense* and the ecological role of PHB in the rhizosphere. *FEMS Microbiol. Lett.*, 103:131–139, 1992.

[253] G.E.D. Oldroyd and J.A. Downie. Calcium, kinases and nodulation signalling in legumes. *Nat. Rev. Mol. Cell Biol.*, 5(7):566–576, 2004.

[254] T. Ophir and D.L. Gutnick. A role for exopolysaccharides in the protection of microorganisms from desiccation. *Appl. Environ. Microbiol.*, 60(2):740–745, 1994.

[255] I.J. Oresnik, T.C. Charles, and T.M. Finan. Second site mutations specifically suppress the fix$^-$ phenotype of *Rhizobium meliloti ndvF* mutations on alfalfa: Identification of a conditional *ndvF*-dependent mucoid colony phenotype. *Genetics*, 136(4):1233–1243, 1994.

[256] I.J. Oresnik, S.L. Liu, C.K. Yost, and M.F. Hynes. Megaplasmid pRme2011a of *Sinorhizobium meliloti* is not required for viability. *J. Bacteriol.*, 182(12):3582–3586, 2000.

[257] L.N. Ornston and M.K. Ornston. Regulation of glyoxylate metabolism in *Escherichia coli* K-12. *J. Bacteriol.*, 98(3):1098–1108, 1969.

[258] L.O. Osa-Afiana and M. Alexander. Effect of moisture on the survival of *Rhizobium* in soil. *Soil Sci. Soc. Am. J.*, 43:925–930, 1979.

[259] L.O. Osa-Afiana and M. Alexander. Differences among cowpea Rhizobia in tolerance to high temperature and desiccation in soil. *Appl Environ Microbiol*, 43(2):435–439, 1982.

[260] A.S. Paau, W.T. Leps, and W.J. Brill. Agglutinin from alfalfa necessary for binding and nodulation by *Rhizobium meliloti*. *Science*, 213(4515):1513–1515, 1981.

[261] W.J. Page and O. Knosp. Hyperproduction of poly-3-hydroxybutyrate during exponential growth of *Azotobacter vinelandii* UWD. *Appl. Environ. Microbiol.*, 55(6):1334–1339, 1989.

[262] W.J. Page, A. Tindale, M. Chandra, and E. Kwon. Alginate formation in I UWD during stationary phase and the turnover of poly-3-hydroxybutyrate. *Microbiology*, 147(2):483–490, 2001.

[263] S Park. *Structural studies on Sinorhizobium meliloti DctD related to ATP binding and activation*. Ph.D. Thesis, The Pennsylvania State University, 2002.

[264] D. Parke and L.N. Ornston. Nutritional diversity of *Rhizobiaceae* revealed by auxanography. *J. Gen. Microbiol.*, 130:1743–1750, 1984.

[265] B.J. Pellock, M. Teplitski, R.P. Boinay, W.D. Bauer, and G.C. Walker. A luxr homolog controls production of symbiotically active extracellular polysaccharide II by *Sinorhizobium meliloti*. *J. Bacteriol.*, 184(18):5067–5076, 2002.

[266] J.J. Pena-Cabriales and M. Alexander. Survival of Rhizobium in soils undergoing drying. *Soil Sci. Soc. Am. J.*, 43:962–966, 1979.

[267] O.P. Peoples, S. Masamune, C.T. Walsh, and A.J. Sinskey. Biosynthetic thiolase from *Zoogloea ramigera*. iii. isolation and characterization of the structural gene. *J. Biol. Chem.*, 262(1):97–102, 1987.

[268] O.P. Peoples and A.J. Sinskey. Poly-β-hydroxybutyrate biosynthesis in *Alcaligenes eutrophus* H16. characterization of the genes encoding β-ketothiolase and acetoacetyl-CoA reductase. *J. Biol. Chem.*, 264(26):15293–15297, 1989.

[269] M. Peralta-Gil, D. Segura, J. Guzman, L. Servin-Gonzalez, and G. Espin. Expression of the *Azotobacter vinelandii* poly-3-hydroxybutyrate biosynthetic *phbBAC* operon is driven by two overlapping promoters and is dependent on the transcriptional activator PhbR. *J. Bacteriol.*, 184(20):5672–5677, 2002.

[270] C.S. Pereira, R.D. Lins, I. Chandrasekhar, L.C.G. Freitas, and P.H. Hunenberger. Interaction of the disaccharide trehalose with a phospholipid bilayer: A molecular dynamics study. *Biophys. J.*, 86(4):2273–2285, 2004.

[271] M. Potter, H. Muller, F. Reinecke, R. Wieczorek, F. Fricke, B. Bowien, B. Friedrich, and A. Steinbuchel. The complex structure of polyhydroxybutyrate (PHB) granules: Four orthologous and paralogous phasins occur in *Ralstonia eutropha*. *Microbiology*, 150(7):2301–2311, 2004.

[272] M. Potter, H. Muller, and A. Steinbuchel. Influence of homologous phasins (PhaP) on PHA accumulation and regulation of their expression by the transcriptional repressor PhaR in *Ralstonia eutropha* H16. *Microbiology*, 151(3):825–833, 2005.

[273] M. Potts. Desiccation tolerance of prokaryotes. *Microbiol. Rev.*, 58(4):755–805, 1994.

[274] S. Povolo and S. Casella. A critical role for *aniA* in energy-carbon flux and symbiotic nitrogen fixation in *Sinorhizobium meliloti*. *Arch. Microbiol.*, 174(1 - 2):42–49, 2000.

[275] S. Povolo, R. Tombolini, A. Morea, A.J. Anderson, S. Casella, and M.P. Nuti. Isolation and characterization of mutants of *Rhizobium meliloti* unable

to synthesize poly-3-hydroxybutyrate (phb). *Can. J. Microbiol*, 40:823–829, 1994.

[276] PRB. World population data sheet. Technical report, Population Reference Bureau, Washington DC, http://www.prb.org, 2008.

[277] H. Preusting, J. Kingma, G. Huisman, A. Steinbuchel, and B. Witholt. Formation of polyester blends by a recombinant strain of *Pseudomonas oleovorans*: Different poly(3-hydroxyalkanoates) formation of polyester blends by a recombinant strain of *Pseudomonas oleovorans*: Different poly(3-hydroxyalkanoates) are stored in separate granules. *J. Env. Polym. Degrad.*, 1(1):11–21, 1993.

[278] M. Prud'homme and P. Heffer. World agriculture and fertilizer demand, global fertilizer supply and trade 2008 – 2009. summary report. Technical report, International Fertlizer Association, 34th IFA Enlarged Council Meeting, Ho Chi Minh City, Viet Nam, 2008.

[279] H.N. Pryor, W.L. Lowther, H.J. McIntyre, and C.W. Ronson. An inoculant Rhizobium strain for improved establishment and growth of hexaploid caucasian clover (*Trifolium ambiguum*). *N.Z. J. Agric. Res.*, 41:179–189, 1998.

[280] S.J. Pueppke and W.J. Broughton. *Rhizobium* sp. NGR234 and *R. fredii* USDA257 share exceptionally broad, nested host range. *Mol. Plant Microbe Interact.*, 12:293–318, 1999.

[281] P. Putnoky, G. Petrovics, A. Kereszt, E. Grosskopf, D.T. Ha, Z. Banfalvi, and A. Kondorosi. *Rhizobium meliloti* lipopolysaccharide and exopolysaccharide can have the same function in the plant-bacterium interaction. *J. Bacteriol.*, 172(9):5450–5458, 1990.

[282] J.A. Ramirez-Trujillo, S. Encarnacion, E. Salazar, A. Garcia de los Santos, M.F. Dunn, D.W. Emerich, E. Calva, and I. Hernandez-Lucas. Functional characterization of the *Sinorhizobium meliloti* acetate metabolism genes *aceA*, SMc00767, and *glcB*. *J. Bacteriol.*, 189(16):5875–5884, 2007.

[283] J.L. Ramos, M.T. Gallegos, S. Marques, M.I. Ramos-Gonzalez, M. Espinosa-Urgel, and A. Segura. Responses of gram-negative bacteria to certain environmental stressors. *Curr. Opin. Microbiol.*, 4(2):166–171, 2001.

[284] M.C. Rayner. Trees and toadstools. Technical report, Journey to Forever, http://journeytoforever.org, 2009.

[285] B.H.A. Rehm. Polyester synthases: Natural catalysts for plastics. *Biochem. J.*, 376(1):15–33, 2003.

[286] B.H.A. Rehm and A. Steinbüchel. Biochemical and genetic analysis of PHA synthases and other proteins required for PHA synthesis. *Int. J. Biol. Macromol.*, 25(3):3–19, 1999.

[287] C.J. Reid and P.S. Poole. Roles of DctA and DctB in signal detection by the dicarboxylic acid transport system of *Rhizobium leguminosarum*. *J. Bacteriol.*, 180(10):2660–9, 1998.

[288] B.B. Reinhold, S.Y. Chan, T.L. Reuber, A. Marra, G.C. Walker, and V.N. Reinhold. Detailed structural characterization of succinoglycan, the major exopolysaccharide of *Rhizobium meliloti* Rm1021. *J. Bacteriol.*, 176(7):1997–2002, 1994.

[289] O. Resendis-Antonio, J.L. Reed, S. Encarnacion, J. Collado-Vides, and B.O. Palsson. Metabolic reconstruction and modeling of nitrogen fixation in *Rhizobium etli*. *PLoS Comput. Biol.*, 3(10):1887–1895, 2007.

[290] T.L. Reuber and G.C. Walker. Biosynthesis of succinoglycan, a symbiotically important exopolysaccharide of *Rhizobium meliloti*. *Cell*, 74(2):269–80, 1993.

[291] E.B. Roberson and M.K. Firestone. Relationship between desiccation and exopolysaccharide production in a soil *Pseudomonas* sp. *Appl. Environ. Microbiol.*, 58(4):1284–1291, 1992.

[292] C.W. Ronson, P.M. Astwood, and J.A. Downie. Molecular cloning and genetic organization of c_4-dicarboxylate transport genes from *Rhizobium leguminosarum*. *J. Bacteriol.*, 160(3):903–909, 1984.

[293] C.W. Ronson, P. Lyttleton, and J.G. Robertson. C_4-dicarboxylate transport mutants of *Rhizobium trifolii* form ineffective nodules of *Trifolium repens*. *Proc. Natl. Acad. Sci. USA*, 78(7):4284–4288, 1981.

[294] C.W. Ronson, B.T. Nixon, L.M. Albright, and F.M. Ausubel. *Rhizobium meliloti ntrA* (*rpoN*) gene is required for diverse metabolic functions. *J. Bacteriol.*, 169(6):2424–31, 1987.

[295] R.L. Ronson and J.R. Postgate. Oxygen and hydrogen in biological nitrogen fixation. *Annu. Rev. Microbiol.*, 34:183–207, 1980.

[296] R.J. Roughley, L.G. Gemell, J.A. Thompson, and J. Brockwell. The number of *Bradyrhizobium* sp (*lupinus*) applied to seed and its effect on rhizosphere colonization, nodulation and yield of lupin. *Soil Biol. Biochem.*, 25(10):1453–1458, 1993.

[297] S. Ruberg, A. Puhler, and A. Becker. Biosynthesis of the exopolysaccharide galactoglucan in *Sinorhizobium meliloti* is subject to a complex control by the phosphate-dependent regulator PhoB and the proteins ExpG and MucR. *Microbiology*, 145(3):603–611, 1999.

[298] J. A. Ruiz, N. I. Lopez, R. O. Fernandez, and B. S. Mendez. Polyhydroxyalkanoate degradation is associated with nucleotide accumulation and enhances stress resistance and survival of *Pseudomonas oleovorans* in natural water microcosms. *Appl. Environ. Microbiol.*, 67(1):225–30, 2001.

[299] G.J.A. Ryle, C.E. Powell, and A.J. Gordon. The respiratory costs of nitrogen fixation in soybean, cowpea, and white clover. i. nitrogen fixation and the respiration of the nodulated root. *J. Exp. Bot.*, 30:135–144, 1979.

[300] M.J. Sadowsky, H.H. Keyser, and B.B. Bohlool. Biochemical characterization of fast- and slow-growing rhizobia that nodulate soybeans. *Int. J. Syst. Bacteriol.*, 33:716–722, 1983.

[301] H. Saegusa, M. Shiraki, C. Kanai, and T. Saito. Cloning of an intracellular poly d(-)-3-hydroxybutyrate depolymerase gene from *Ralstonia eutropha* H16 and characterization of the gene product. *J. Bacteriol.*, 183(1):94–100, 2001.

[302] H. Saegusa, M. Shiraki, and T. Saito. Cloning of an intracellular d(-)-3-hydroxybutyrate-oligomer hydrolase gene from *Ralstonia eutropha* H16 and identification of the active site serine residue by site-directed mutagenesis. *J. Biosci. Bioeng.*, 94(2):106–112, 2002.

[303] M.P. Salema, C.A. Parker, D.K. Kidby, and D.L. Chatel. Death of rhizobia on inoculated seed. *Soil Biol. Biochem.*, 14:13–14, 1982.

[304] M.P. Salema, C.A. Parker, D.K. Kidby, D.L. Chatel, and T.M. Armitage. Rupture of nodule bacteria on drying and rehydration. *Soil Biol. Biochem.*, 14:15–22, 1981.

[305] S.O. Salminen and Streeter J.G. Involvement of glutamate in the respiratory metabolism of *Bradyrhizobium japonicum* bacteroids. *J. Bacteriol.*, 169:495–499, 1987.

[306] S.O. Salminen and J.G. Streeter. Labeling of carbon pools in *Bradyrhizobium japonicum* and *Rhizobium leguminosarum* bv. *viciae* bacteroids following incubation of intact nodules with $^{14}CO_2$. *Plant Physiol.*, 100:597–604, 1992.

[307] J. Sambrook and D.W. Russell. *Molecular Cloning: a laboratory manual.* Cold Spring Harbor Laboratory, Cold Spring Harbor, NY, 3rd edition, 2001.

[308] A.D. Sarma and D.W. Emerich. Global protein expression pattern of *Bradyrhizobium japonicum* bacteroids: A prelude to functional proteomics. *Proteomics*, 5(16):4170–4184, 2005.

[309] A.D. Sarma and D.W. Emerich. A comparative proteomic evaluation of culture-grown vs nodule-isolated *Bradyrhizobium japonicum*. *Proteomics*, 6(10):3008–28, 2006.

[310] A. Schafer, A. Tauch, W. Jager, J. Kalinowski, G. Thierbach, and A. Puhler. Small mobilizable multi-purpose cloning vectors derived from the *Escherichia coli* plasmids pK18 and pK19: Selection of defined deletions in the chromosome of *Corynebacterium glutamicum*. *Gene*, 145(1):69–73, 1994.

[311] B.K. Schroeder, B.L. House, M.W. Mortimer, S.N. Yurgel, S.C. Maloney, K.L. Ward, and M.L. Kahn. Development of a functional genomics platform for *Sinorhizobium meliloti*: Construction of an ORFeome. *Appl. Environ. Microbiol.*, 71(10):5858–5864, 2005.

[312] P. Schubert, A. Steinbüchel, and H.G. Schlegel. Cloning of the *Alcaligenes eutrophus* genes for synthesis of poly-β-hydroxybutyric acid (PHB) and synthesis of PHB in *Escherichia coli*. *J. Bacteriol.*, 170(12):5837–5847, 1988.

[313] P.J. Senior, G.A. Beech, G.A.F. Ritchie, and E.A. Dawes. The role of oxygen limitation in the formation of poly-3-hydroxybutyrate during batch and

continuous culture of *Azotobacter beijerinckii*. *Biochem. J.*, 128:1193–1201, 1972.

[314] P.J. Senior and E.A. Dawes. Poly-3-hydroxybutyrate biosynthesis and the regulation of glucose metabolism in *Azotobacter beijinkereii*. *Biochem. J.*, 125:55–66, 1971.

[315] R. Shah and D.W. Emerich. Isocitrate dehydrogenase of *Bradyrhizobium japonicum* is not required for symbiotic nitrogen fixation with soybean. *J. Bacteriol.*, 188(21):7600–7608, 2006 Nov.

[316] P. Singleton, H. Keyser, and E. Sande. Development and evaluation of liquid inoculants. In D. Herridge, editor, *Inoculants and Nitrogen Fixation of Legumes in Vietnam*, Hanoi, Vietnam, 2001. ACIAR Proceedings.

[317] A. Skorupska, M. Janczarek, M. Marczak, A. Mazur, and J. Krol. Rhizobial exopolysaccharides: Genetic control and symbiotic functions. *Microb. Cell Fact.*, 5:7, 2006.

[318] S.C. Slater, W.H. Voige, and D.E. Dennis. Cloning and expression in *Escherichia coli* of the *Alcaligenes eutrophus* H16 poly-β-hydroxybutyrate biosynthetic pathway. *J. Bacteriol.*, 170(10):4431–4436, 1988.

[319] D. J. Slotboom, W. N. Konings, and J. S. Lolkema. Structural features of the glutamate transporter family. *Microbiol. Mol. Biol. Rev.*, 63(2):293–307, 1999.

[320] D. J. Slotboom, W. N. Konings, and J. S. Lolkema. The structure of glutamate transporters shows channel-like features. *FEBS Lett.*, 492(3):183–6, 2001.

[321] D.J. Slotboom, J.S. Lolkema, and W.N. Konings. Membrane topology of the C-terminal half of the neuronal, glial, and bacterial glutamate transporter family. *J. Biol. Chem.*, 271(49):31317–21, 1996.

[322] J.E. Somerville and M.L. Kahn. Cloning of the glutamine synthetase I gene from *Rhizobium meliloti*. *J. Bacteriol.*, 156:168–176, 1983.

[323] P. Spiekermann, B.H. Rehm, R. Kalscheuer, D. Baumeister, and A. Steinbuchel. A sensitive, viable-colony staining method using nile red for direct screening of bacteria that accumulate polyhydroxyalkanoic acids and other lipid storage compounds. *Arch. Microbiol.*, 171(2):73–80, 1999.

[324] H. Stam, H.W. van Verseveld, W. de Vries, and A.H. Stouhamer. Utilization of poly-β-hydroxybutyrate in free-living cultures of *Rhizobium* ORS571. *FEMS Microbiol. Lett.*, 35:215–220, 1986.

[325] Statistics-Canada. Field and specialty crops, 2005-01-11 2004.

[326] A. Steinbüchel and H.E. Valentin. Diversity of bacterial polyhydroxyalkanoic acids. *FEMS Microbiol. Lett.*, 128(3):219–228, 1995.

[327] J. Stigter, M. Schneider, and F.J. de Bruijn. *Azorhizobium caulinodans* nitrogen fixation (*nif/fix*) gene regulation: Mutagenesis of the *nifA* -24/-12 promoter element, characterization of a *ntrA*(*rpoN*) gene, and derivation of a model. *Mol. Plant Microbe Interact.*, 6(2):238–52, 1993.

[328] H. Stockdale, D.W. Ribbons, and E.A. Dawes. Occurence of poly-3-hydroxybutyrate in the *Azotobacteriaceae*. *J. Bacteriol.*, 95(5):1798–1803, 1968.

[329] I. Stovall and M. Cole. Organic acid metabolism by isolated *Rhizobium japonicum* bacteroids. *Plant Physiol.*, 61(5):787–790, 1978.

[330] M.D. Stowers. Carbon metabolism in rhizobium species. *Ann. Rev. Microbiol.*, 39:89–108, 1985.

[331] J.G. Streeter. Carbohydrates in soybean nodules: II distribution of compounds in seedlings during the onset of nitrogen fixation. *Plant Physiol.*, 66(3):471–476, 1980.

[332] J.G. Streeter. Effect of trehalose on survival of *Bradyrhizobium japonicum* during desiccation. *J. Appl. Microbiol.*, 95(3):484–91, 2003.

[333] J.G. Streeter and A. Bhagwat. Biosynthesis of trehalose from maltooligosaccharides in rhizobia. *Can. J. Microbiol.*, 45(8):716–21, 1999.

[334] F.W. Studier and B.A. Moffatt. Use of bacteriophage T7 RNA polymerase to direct selective high-level expression of cloned genes. *J. Mol. Biol.*, 189(1):113–130, 1986.

[335] N. Suganuma and Y. Yamamoto. Carbon metabolism related to nitrogen fixation in sobean root nodules. *Soil Sci. and Plant Nutr.*, 33:79–91, 1987.

[336] N. Sukdeo and T. C. Charles. Application of crossover-PCR-mediated deletion-insertion mutagenesis to analysis of the *bdhA-xdhA2-xdhB2* mixed-function operon of *Sinorhizobium meliloti*. *Arch. Microbiol.*, 179(4):301–4, 2003.

[337] W.D. Sutton and A.D. Paterson. Effects of the host plant on the detergent sensitivity and viability of Rhizobium bacteroids. *Planta*, 148:287–292, 1980.

[338] F. Suzuki, W.L. Zahler, and D. W. Emerich. Acetoacetyl-CoA thiolase of *Bradyrhizobium japonicum* bacteroids: Purification and properties. *Arch. Biochem. Biophys.*, 254:272–281, 1987.

[339] S. Tal and Y. Okon. Production of the reserve material poly-3-hydroxybutyrate and its function in *Azospirillum brasilense*. *Can. J. Microbiol*, 31:608–613, 1985.

[340] R. Talibart, M. Jebbar, G. Gouesbet, S. Himdi-Kabbab, H. Wroblewski, C. Blanco, and T. Bernard. Osmoadaptation in rhizobia: ectoine-induced salt tolerance. *J. Bacteriol.*, 176(17):5210–7, 1994.

[341] T. Tanio, T. Fukui, Y. Shirakura, T. Saito, K. Tomita, T. Kaiho, and S. Masamune. An extracellular poly(3-hydroxybutyrate) depolymerase from *Alcaligenes faecalis*. *Eur. J. Biochem.*, 124(1):71–11, 1982.

[342] F.J. Temprano, M. Albareda, M. Camacho, A. Daza, C. Santamaria, and D.N. Rodriguez-Navarro. Survival of several *Rhizobium/Bradyrhizobium* strains on different inoculant formulations and inoculated seeds. *Int. Microbiol.*, 5(2):81–6, 2002.

[343] J.D. Thompson, T.J. Gibson, and D.G. Higgins. Multiple sequence alignment using clustalw and clustalx. *Curr. Protoc. Bioinformatics*, 2002.

[344] L. Thony-Meyer and P. Kunzler. The *Bradyrhizobium japonicum* aconitase gene (*acnA*) is important for free-living growth but not for an effective root nodule symbiosis. *J. Bacteriol.*, 178(21):6166–6172, 1996.

[345] P. Tittabutr, W. Payakapong, N. Teaumroong, N. Boonkerd, P.W. Singleton, and D. Borthakur. The alternative sigma factor RpoH2 is required for salt tolerance in *Sinorhizobium sp.* strain BL3. *Res. Microbiol.*, 157(9):811–818, 2006.

[346] B. Tolner, B. Poolman, and W.N. Konings. Characterization and functional expression in *Escherichia coli* of the sodium/proton/glutamate symport pro-

teins of *Bacillus stearothermophilus* and *Bacillus caldotenax*. *Mol. Microbiol.*, 6(19):2845–56, 1992.

[347] B. Tolner, T. Ubbink-Kok, B. Poolman, and W. N. Konings. Characterization of the proton/glutamate symport protein of *Bacillus subtilis* and its functional expression in *Escherichia coli*. *J. Bacteriol.*, 177(10):2863–9, 1995.

[348] B. Tolner, T. Ubbink-Kok, B. Poolman, and W.N. Konings. Cation-selectivity of the l-glutamate transporters of *Escherichia coli, Bacillus stearothermophilus* and *Bacillus caldotenax*: dependence on the environment in which the proteins are expressed. *Mol. Microbiol.*, 18(1):123–33, 1995.

[349] R. Tombolini, S. Povolo, A. Buson, A. Squartini, and M.P. Nuti. Poly-3-hydroxybutyrate (phb) biosynthetic genes in *Rhizobium meliloti* 41. *Microbiology*, 141:2553–2559, 1995.

[350] J.P. Tomkins, T.C. Wood, M.G. Stacey, J.T Loh, A. Judd, J.L. Goicoechea, G. Stacey, M.J. Sadowsky, and R.A. Wing. A marker-dense physical map of the *Bradyrhizobium japonicum* genome. *Genome Res.*, 11(8):1434–1440, 2001.

[351] M. A. Trainer and T. C. Charles. The role of PHB metabolism in the symbiosis of rhizobia with legumes. *Appl. Microbiol. Biotechnol.*, 71(4):377–86, 2006.

[352] M.A. Trainer, S.N. Yurgel, and M.L. Kahn. Role of a conserved membrane glycine residue in a dicarboxylate transporter from *Sinorhizobium meliloti*. *J. Bacteriol.*, 189(5):2160–2163, 2007.

[353] W.E. Trevelyan and J.S. Harrison. Studies on yeast metabolism: Fractionation and microdetermination of cell carbohydrates. *Biochem. J.*, 50:298–303, 1952.

[354] M.J. Trinick. Relationships among the fast-growing rhizobia of *Lablab purpureus, Leucaena leucocephala, Mimosa* spp., *Acacia farnesiana* and *Sesbania grandiflora*. *J. Appl. Bacteriol.*, 49:39–53, 1980.

[355] A.P. Trotman and R.W. Weaver. Survival of rhizobia on arrowleaf clover seeds under stresses of seed-coat toxins, heat and desiccation. *Plant Soil*, 218(1-2):43–47, 2000.

[356] C.L. Tseng, H.J. Chen, and G.C. Shaw. Identification and characterization of the *Bacillus thuringiensis phaZ* gene, encoding new intracellular poly-3-hydroxybutyrate depolymerase. *J. Bacteriol.*, 188(21):7592–7599, 2006.

[357] H.C. Tsien, P.S. Cain, and E.L. Schmidt. Viability of Rhizobium bacteroids. *Appl. Environ. Microbiol.*, 34(6):854–856, 1977.

[358] UCS. The hidden cost of fossil fuels. Technical report, Union of Concerned Scientists, http://www.ucsusa.org, 2002.

[359] M.K. Udvardi and D.A. Day. Metabolite transport across symbiotic membranes of legume nodules. *Ann. Rev. Plant Physiol. Plant Mol. Biol.*, 48:493–523, 1997.

[360] M.K. Udvardi, G.D. Price, P.M. Gresshoff, and D.A. Day. A dicarboxylate transporter on the peribacteroid membrane of soybean nodules. *FEBS Letters*, 231(1):36–40, 1988.

[361] UN-FAO. The state of food insecurity in the world. Technical report, Food and Agriculture Organization of the United Nations, ftp://ftp.fao.org/docrep/fao/009/a0750e/a0750e00.pdf, 2006.

[362] USDA. Crop production: Annual summary. Technical report, United States Department of Agriculture, National Agricultural Statistics Service, http://www.nass.usda.gov/index.asp, 2004.

[363] USDA. Average U.S. farm prices of selected fertilizers. Technical report, Economic Research Service. United States Department of Agriculture, June 2005.

[364] USDA. Agricultural statistics. Technical report, United States Department of Agriculture, National Agricultural Statistics Service, http://usda.mannlib.cornell.edu, 2009.

[365] J. Van Elsas and L.S. van Overbeek. Bacterial responses to soil stimuli. In S. Kejelleberg, editor, *Starvation in bacteria*, pages 55–79. Plenum Press, New York, 1993.

[366] J.C. van Slooten, T.V. Bhuvanasvari, S. Bardin, and J. Stanley. Two c_4-dicarboxylate transport systems in *Rhizobium* sp. NGR234: rhizobial dicarboxylate transport is essential for nitrogen fixation in tropical legume symbioses. *Mol. Plant Microbe Interact.*, 5(2):179–186, 1992 Mar-Apr.

[367] J.C. van Slooten, E. Cervantes, W.J. Broughton, C.H. Wong, and J. Stanley. Sequence and analysis of the *rpoN* sigma factor gene of *Rhizobium* sp. strain NGR234, a primary coregulator of symbiosis. *J. Bacteriol.*, 172(10):5563–5574, 1990.

[368] J.A. van Veen, L.S. van Overbeek, and J.D. van Elsas. Fate and activity of microorganisms introduced into soil. *Microbiol. Mol. Biol. Rev.*, 61(2):121–135, 1997.

[369] C.P. Vance and P.H. Graham. Nitrogen fixation in agriculture: applcation and perspective. In I.A. Tikhonovich, N.A. Provorov, V.I. Romanov, and

W.E. Newton, editors, *Nitrogen Fixation: Fundamentals and Applications*, pages 77–86. Kluwer Academic Publishers, Dordrecht, 1995.

[370] J. Vasse, F. de Billy, S. Camut, and G. Truchet. Correlation between ultrastructural differentiation of bacteroids and nitrogen fixation in alfalfa nodules. *J. Bacteriol.*, 172(8):4295–4306, 1990.

[371] V. Vassileva and G. Ignatov. Relationship between bacteroid poly-β-hydroxybutyrate accumulation and nodule functioning in the *Galega orientalis-Rhizobium galegae* symbiosis under diamine treatment. *Physiologia Plantarum*, 114:27–32, 2002.

[372] J.H. Venable and R. Coggeshall. A simplified lead citrate stain for use in electron microscopy. *J. Cell Biol.*, 25:407–8, 1965.

[373] J.M. Vincent. Serological properties of the root-nodule bacteria. i. strains of *Rhizobium meliloti*. *Proc. Linn. Soc. N.S.W.*, 66(145-154), 1941.

[374] J.M. Vincent, J.A. Thompson, and K.O. Donovan. Death of root-nodule bacteria on drying. *Australian J. Agri. Res.*, 13:258–270, 1962.

[375] J.A.C. Vriezen, F.J. de Bruijn, and K. Nusslein. Desiccation responses and survival of *Sinorhizobium meliloti* USDA 1021 in relation to growth phase, temperature, chloride and sulfate availability. *Lett. Appl. Microbiol.*, 42(2):172–178, 2006.

[376] J.A.C. Vriezen, F.J. de Bruijn, and K. Nusslein. Responses of rhizobia to desiccation in relation to osmotic stress, oxygen, and temperature. *Appl. Environ. Microbiol.*, 73(11):3451–3459, 2007.

[377] D.L. Walshaw, A. Wilkinson, M. Mundy, M. Smith, and P.S. Poole. Regulation of the TCA cycle and the general amino acid permease by overflow

metabolism in *Rhizobium leguminosarum*. *Microbiology*, 143(7):2209–2221, 1997.

[378] C. Wang, M. Saldanha, X. Sheng, K.J. Shelswell, K.T. Walsh, B.W.S. Sobral, and T.C. Charles. Roles of poly-3-hydroxybutyrate (PHB) and glycogen in symbiosis of *Sinorhizobium meliloti* with *Medicago sp. Microbiology*, 153(2):388–398, 2007.

[379] C. Wang, X. Sheng, R.C. Equi, M.A. Trainer, T.C. Charles, and B.W.S Sobral. Influence of the poly-3-hydroxybutyrate (PHB) granule-associated proteins (PhaP1 and PhaP2) on PHB accumulation and symbiotic nitrogen fixation in *Sinorhizobium meliloti* Rm1021. *J. Bacteriol.*, 189(24):9050–9056, 2007.

[380] Y.P. Wang, K. Birkenhead, B. Boesten, S. Manian, and F. O'Gara. Genetic analysis and regulation of the *Rhizobium meliloti* genes controlling C_4-dicarboxylic acid transport. *Gene*, 85(1):135–144, 1989.

[381] R.J. Watson. Analysis of the C_4-dicarboxylate transport genes of *Rhizobium meliloti*: Nucleotide sequence and deduced products of *dctA, dctB*, and *dctD*. *Mol. Plant Microbe Interact.*, 3(3):174–81, 1990.

[382] R.J. Watson, Y.K. Chan, R. Wheatcroft, A.F. Yang, and S.H. Han. *Rhizobium meliloti* genes required for c_4-dicarboxylate transport and symbiotic nitrogen fixation are located on a megaplasmid. *J. Bacteriol.*, 170(2):927–34, 1988.

[383] W. Wei, X.L. Jiang, L. Wang, and S.S. Yang. Isolation of salt-sensitive mutants from *Sinorhizobium meliloti* and characterization of genes involved in salt tolerance. *Lett. Appl. Microbiol.*, 39:278–283, 2004.

[384] P.D.F. Weitzman. Regulation of α-ketoglutarate dehydrogenase activity in *Acinetobacter*. *FEBS Lett.*, 22:323–326, 1972.

[385] D T Welsh. Ecological significance of compatible solute accumulation by micro-organisms: from single cells to global climate. *FEMS Microbiol. Rev.*, 24(3):263–290, 2000.

[386] D. Werner and R. Stripf. Differentiation of *Rhizobium japonicum*. i. Enzymatic comparison of nitrogenase repressed and derepressed free living cells and of bacteroids. *Z Naturforsch*, 33c(3-4):245–252, 1978.

[387] J. White, J. Prell, E.K. James, and P. Poole. Nutrient sharing between symbionts. *Plant Physiol.*, 144(2):604–614, 2007.

[388] WHO. Malnutrition worldwide. Technical report, World Health Organization, http://www.mikeschoice.com, 2005.

[389] J.F. Wilkinson. The extracellular polysaccharides of bacteria. *Bacteriol. Rev.*, 22:788–794, 1958.

[390] L.B. Willis and G.C. Walker. The *phbC* (poly-β-hydroxybutyrate synthase) gene of *Rhizobium* (*Sinorhizobium*) *meliloti* and characterization of *phbC* mutants. *Can. J. Microbiol.*, 44(6):554–564, 1998.

[391] P.P. Wong and H.J. Evans. Poly-3-hydroxybutyrate utilization by soybean (*Glycine max* merr.) nodules and assessment of its role in maintenance of nitrogenase activity. *Plant Physiol.*, 47:750–755, 1971.

[392] E.A. Yakobson and D.G. Guiney. Conjugal transfer of bacterial chromosomes mediated by the RK2 plasmid transfer origin cloned into transposon tn*5*. *J. Bacteriol.*, 160(1):451–453, 1984.

[393] L.J.O. Yang, M.K. Udvardi, and D.A. Day. Specificity and regulation of the dicarboxylate carrier on the peribacteroid membrane of soybean nodules. *Planta*, 182:437–444, 1990.

[394] O.K. Yarosh, T.C. Charles, and T.M. Finan. Analysis of c_4-dicarboxylate transport genes in *Rhizobium meliloti*. *Mol. Microbiol.*, 3(6):813–23, 1989.

[395] G.M. York, J. Stubbe, and A.J. Sinskey. New insight into the role of the PhaP phasin of *Ralstonia eutropha* in promoting synthesis of polyhydroxybutyrate. *J. Bacteriol.*, 183(7):2394–2397, 2001.

[396] S.N. Yurgel and M.L. Kahn. Dicarboxylate transport by Rhizobia. *FEMS Microbiol. Rev.*, 28(4):489–501, 2004.

[397] S.N. Yurgel and M.L. Kahn. *Sinorhizobium meliloti dctA* mutants with partial ability to transport dicarboxylic acids. *J. Bacteriol.*, 187(3):1161–1172, 2005.

[398] S.N. Yurgel, M.W. Mortimer, K.N. Rogers, and M.L. Kahn. New substrates for the dicarboxylate transport system of *Sinorhizobium meliloti*. *J. Bacteriol.*, 182:4216–21, 2000.

[399] N. Zerangue and M. P. Kavanaugh. Flux coupling in a neuronal glutamate transporter. *Nature*, 383(6601):634–7, 1996.

[400] L.P.T.M. Zevenhuizen. Cellular glycogen, β-1,2-glucan, poly-3-hydroxybutyic acid and extracellular polysaccharides in fast-growing species of rhizobium. *Antonie van Leeuwenhoek*, 47:481–497, 1981.

[401] H.J. Zhan, C.C. Lee, and J.A. Leigh. Induction of the second exopolysaccharide (EPSb) in *Rhizobium meliloti* SU47 by low phosphate concentrations. *J. Bacteriol.*, 173(22):7391–7394, 1991.

[402] H.J. Zhan, S.B. Levery, C.C. Lee, and J.A. Leigh. A second exopolysaccharide of *Rhizobium meliloti* strain SU47 that can function in root nodule invasion. *Proc. Natl. Acad. Sci. USA*, 86(9):3055–3059, 1989.

[403] L.I. Zon, D.M. Dorfman, and S.H. Orkin. The polymerase chain reaction colony miniprep. *Biotechniques*, 7(696-698), 1989.